Geophysical Monitoring for Climatic Change

No. 15

Summary Report 1986

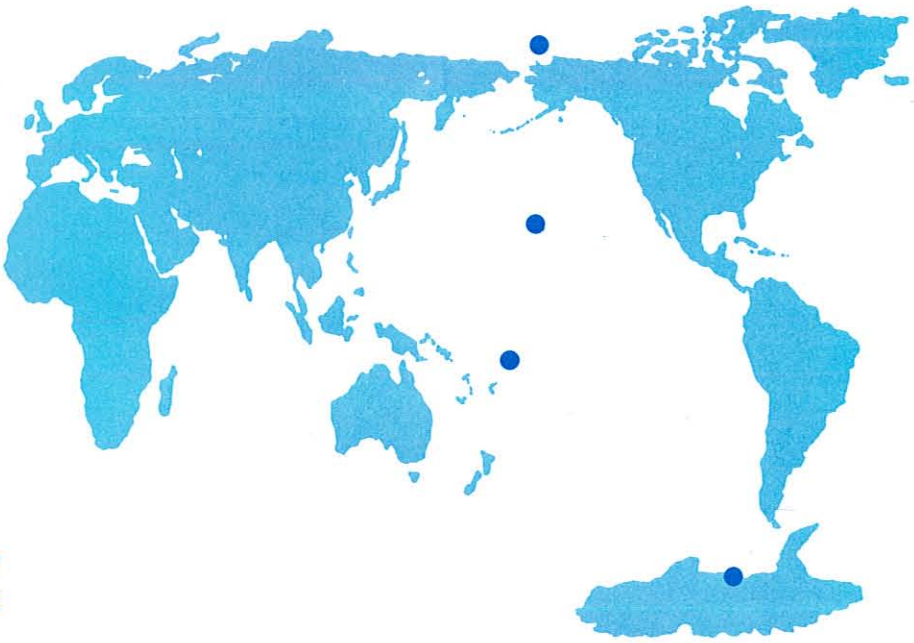

U.S. DEPARTMENT OF COMMERCE

NATIONAL OCEANIC AND ATMOSPHERIC ADMINISTRATION

ENVIRONMENTAL RESEARCH LABORATORIES

Geophysical Monitoring for Climatic Change No. 15

Summary Report 1986

Russell C. Schnell, Editor
Rita M. Rosson, Assistant Editor

Air Resources Laboratory
Geophysical Monitoring for Climatic Change

Boulder, Colorado

December 1987

U.S. DEPARTMENT OF COMMERCE
C. William Verity, Secretary

National Oceanic and Atmospheric Administration

Environmental Research Laboratories
Vernon E. Derr, Director

NOTICE

Mention of a commercial company or product does not constitute an endorsement by NOAA Environmental Research Laboratories. Use for publicity or advertising purposes of information from this publication concerning proprietary products or the tests of such products is not authorized.

For sale by the National Technical Information Service, 5285 Port Royal Road
Springfield, VA 22161

CONTENTS

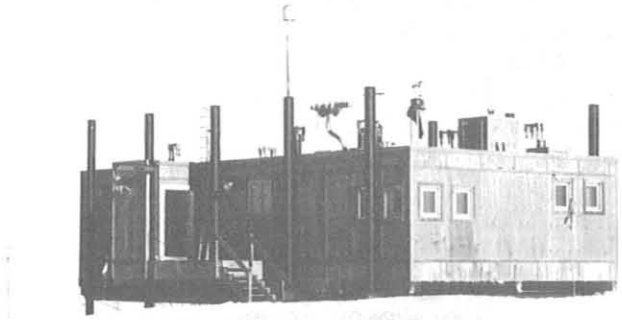

November 1986

December 1986

The National Science Foundation's Clean Air Facility at Amundsen-Scott Base South Pole, Antarctica. The facility was raised 12 feet above the Antarctic polar ice field during the austral sumer of 1986-1987. The building is located upwind of the central dome and adjacent to the clear air sector at

GMCC Staff, 1986

Director's Office

James Peterson, Director
Bernard Mendonca, Deputy Director
Jeanne Kelsey, Secretary
Ellen Hardman, Secretary
Howard Bridgman, Guest Worker
Dale Gillette, Physical Scientist
Lori Neff, Scientific Data Clerk
Everett C. Nickerson, Meteorologist
Rita Rosson, Clerk-Typist
Russell Schnell, CIRES
Elizabeth Shuey, Scientific Data Clerk
L. Paul Steele, CIRES
Paul Stockton, Physical Science Tech.
Thomas Watson, Physical Science Aid

Acquisition and Data Management Group

Gary Herbert, Chief
Dee Dee Giebelhaus, Secretary
Richard Clark, Computer Programmer
Richard Cook, Physical Science Aid
Joyce Harris, Computer Specialist
Steve Roughton, Computer Assistant
Kenneth Thaut, Electronic Technician

Aerosols and Radiation Monitoring Group

John DeLuisi, Chief
Marilyn Van Asche, Secretary
Christa Anderson, Physical Science Aid
Barry Bodhaine, Meteorologist
Ellsworth Dutton, Meteorologist
Rudy Haas, Mathematician
David Kanzer, Physical Science Aid
Michael Konyak, Physical Science Aid
David Longenecker, CIRES
David Massey, Physical Science Aid
Donald Nelson, Meteorologist
Timothy Quakenbush, Physical Science Aid
Patrick Reddy, CIRES
Lois Stearns, Meteorologist

Air Quality Group

Joseph Boatman, Chief
Dee Dee Giebelhaus, Secretary
Mark Cichy, CO-OP
Laureen Gunter, Meteorologist
Helmut Horvath, CIRES
Menachem Luria, NRC, Post Doctorate
Herman Sievering, Guest Worker
Karen Stamminger, Physical Science Aid
Charles Van Valin, Research Chemist
Dennis Wellman, Engineer
Stan Wilkinson, Meteorologist

Carbon Cycle Group

Pieter Tans, CIRES
Lee Prendergast, Secretary
Craig Averman, CO-OP
Teresa Bals, CO-OP
Thomas Conway, Research Chemist
Ellen DeMoney, CIRES
Tom Greaney, CIRES
Duane Kitzis, CIRES
Bradley Halter, Meteorologist
Patricia Lang, CIRES
Kenneth Masarie, CIRES
John Parker, CO-OP
Kirk Thoning, CIRES
Lee Waterman, Chemist
Glen Weiler, Physical Science Aid

Monitoring Trace Gases Group

Walter Komhyr, Chief
Lee Prendergast, Secretary
Mark Anderson, Physical Science Aid
Sean Coleman, Physical Science Aid
Robert Evans, CIRES
Leigh Fanning, Physical Science Aid
Paul Franchois, CIRES
Robert Grass, Physicist
Gloria Koenig, Computer Programmer
Kent Leonard, CIRES
Samuel Oltmans, Physicist
Frank Polacek, III, Meteorological Technician
Ronald Thorne, Engineering Technician

Nitrous Oxide and Halocarbons Group

James Elkins, Chief
Marilyn Van Asche, Secretary
James Butler, CIRES
Keith Egan, CIRES
Brad Hall, Physical Science Tech.
Michael Lavilla, Physical Science Aid
Thayne Thompson, Physicist

Barrow Observatory

Daniel Endres, Station Chief
James Wendell, Electronic Technician

Mauna Loa Observatory

Elmer Robinson, Director
Judith Pereira, Secretary
Lynne Ashman, Physical Science Aid
Arne Austring, Physical Scientist
John Chin, Physicist
Thomas DeFoor, Electronic Engineer
Thomas Garcia, Meteorological Technician
Barbara Kerecman, Data Clerk
Darryl Kuniyuki, NOAA Jr. Fellow
Mamoru Shibata, Electronic Technician
Alan Yoshinaga, Chemist

Samoa Observatory

Steve Ryan, Station Chief
Meredith E. Wilson, Electronic Technician

South Pole Observatory

Clifford Wilson, NOAA Corps, Station Chief
Bradley Halter, Electronic Technician
Scott Kuester, NOAA Corps, Station Chief
Patrick Reitelbach, Electronic Technician

GMCC Station Information

Name:	Barrow (BRW)	Mauna Loa (MLO)
Latitude:	71.3233	19.533
Longitude:	156.6067	155.578
Elevation:	0 km	3.4 km
Time Zone:	GMT -9	GMT -10
Office Hours:	8:00am-5:00pm	8:00am-5:00pm
Telephone		
Office hours:	(907) 852-6500	(808) 961-3788
After hours:	(907) 852-6500	(808) 961-3788
Postal Address:	Officer in Charge NOAA/ERL/ARL/GMCC Pouch 8888 Barrow, AL 99723	US Dept. of Commerce NOAA - Mauna Loa Observatory P.O. Box 275 Hilo, HI 96720
Freight Address:		US Dept. of Commerce NOAA - Mauna Loa Observatory 154 Waianuenue Ave. Hilo, HI 96720

Name:	Samoa (SMO)	South Pole (SPO)
Latitute:	-14.2522	-90.000
Longitude:	170.5628	0.000
Elevation:	0 km	2.8 km
Time Zone:	GMT -11	GMT +12
Office Hours:	8:00am-5:00 pm	8:00am-5:00pm
Telephone:		
Office hours:	011-(684) 622-7455	Relayed through GMCC Boulder
After hours:	011-(684) 699-9953	
Postal Address:	US Dept. of Commerce NOAA - GMCC Samoa Observatory P.O. Box 2568 Pago Pago, American Samoa 96799	Officer in Charge, GMCC Program Box 400 USARP C/O NAVSUPPFORANTARCTICA FPO San Fransciso, CA 96692 ATTN: South Pole #S-257 R. Poston

GEOPHYSICAL MONITORING FOR CLIMATIC CHANGE

NO. 15

SUMMARY REPORT 1986

1. SUMMARY

At MLO, a major addition was construction of a 40-m walk-up tower to be used to increase the height of certain air sampling intakes and as a platform for special experiments. An astronomical dome and associated observation building were installed for the University of Arizona solar monitoring program. At BRW, new programs included weekly ozonesondes and gas chromatographs for in situ monitoring of CH_4, CFC-11, CFC-12, N_2O, CH_3CCl_3 and CCl_4. The Dobson spectrophotometer used for total column ozone observations was reinstalled. Special efforts were made to support the AGASP-II field program and for monitoring the radioactive cloud from the Chernobyl nuclear accident.

At SMO, operations were interrupted following a lightning strike and when island power lost generating capacity. Most programs continued, however, without significant downtime. New measurements included weekly ozonesondes and installation of gas chromatographs for in situ determinations of CFC-11, CFC-12, N_2O, CH_3CCl_3 and CCl_4. At SPO, a program of regular ozonesonde flights was initiated for study of the Antarctic ozone hole. Data flow from the Pole to BRW improved markedly with initiation of regular data transmissions via ATS-3 satellite. Efforts to raise the CAF failed, but valuable experience was gained for a planned second attempt next year.

The ongoing GMCC core measurement programs continued. They include CO_2 and CH_4 from the flask network and observatories, total column ozone, ozone vertical distribution by ECC sonde and Umkehr technique, surface ozone, stratospheric water vapor by balloon soundings at Boulder, CFC-11, CFC-12, and N_2O from flask samples, stratospheric aerosols at MLO using lidar, aerosol light scattering and CN concentration, direct and diffuse solar and infrared radiation, meteorological variables, and chemistry of precipitation.

In the Aerosols and Radiation Group, CN concentrations at SPO the last 2 years have been below average and the long-term change with time is now (not statistically significant) negative. Shortwave and longwave radiation components are measured at three sites. Mauna Loa lidar and turbidity data, in combination with other data, give detailed information on the transport of the El Chichon volcanic cloud and its decay over several years. Cooperation with NWS to operate the U.S. solar radiation network continued with addition of new solar trackers and PC-based data acquisition systems. Research on stratospheric aerosol effects on Umkehr ozone profiles yielded improved data quality. An assessment was completed of wind flow structure in the Grand Canyon and changes in visibility due to annual controlled forest burns.

The Carbon Cycle Group continued in situ CO_2 measurements at the observatories and flask analyses of CO_2 and CH_4 at 26 cooperative sites. An improved statistical treatment of our historical data yielded a mean CO_2 increase over the past decade of nearly 1.4 ppm/year. The global increase of methane averaged about 13 ppb/year from 1983-1986. A gas chromatograph was installed at BRW for in situ methane measurements. Special CO_2 and CH_4 measurements

included vertical profiles by aircraft near south Florida, north-south Pacific Ocean transects on cargo ships, and participation in EPOCS and AGASP-II expeditions. A two-dimensional global transport-diffusion model was developed to estimate large-scale CO_2 sources and sinks.

The Trace Gases Group continued Dobson total ozone measurements at 15 sites and international calibration work, including participation with the world standard Dobson at a regional intercomparison in Switzerland. Vertical ozone profiles were obtained regularly by balloon-borne ozonesonde and by Umkehr (six sites each), partially for NESDIS-supported SBUV/2 data validation. Data from SPO gave clear definition of the depth and duration of the "ozone hole" during austral spring. Surface ozone measurements at SPO show increasing annual amplitude during the past decade, a change postulated due to altered large-scale atmospheric transport processes. Regular balloon soundings from Boulder of stratospheric water vapor continued.

The Acquisition and Data Management Group continued responsibility for regular meteorological measurements at the observatories. Wind, temperature, and pressure data for the year generally were not anomalous, although wind speed at SMO was 23% greater than average. The SPO station continued to have the most well defined and most frequent wind flow representative of background conditions. Numerous air mass trajectories were calculated for NOAA researchers and affiliates at other institutions. Comparisons of trajectories based on U.S. and European Center global wind field analysis were underway.

The Air Quality Group continued involvement in the National Acid Precipitation Assessment Program (NAPAP) with the NOAA King Air research aircraft. Their participation in WATOX involved quantifying the flux of nitrogen and sulfur species from the U.S. east coast via aircraft measurements of SO_2, dimethyl sulfide and aerosol size distributions. Following Chernobyl, they measured radioactivity along the northwest North American coast. They completed analysis of the characteristics of aerosols and clouds in polluted and non-polluted air at Whiteface Mountain, NY. Finally, they further improved the King Air for atmospheric chemistry research.

The Nitrous Oxide and Halocarbons Group was formed in response to new GMCC responsibilities under the RITS initiative for additional trace species monitoring. They continued the historical flask sampling for CFC-11, CFC-12, and N_2O at the observatories. They installed automated gas chromatographs at SMO and BRW for continuous, in situ monitoring of CFC-11, CFC-12, N_2O, CCl_4, and $CH_3\ CCl_3$. They began planning for regular monitoring of CFC-22, CFC-113, Halon-1211 and Halon-1301, for preparation by gravimetric techniques of absolute gas calibration standards of the trace species we monitor, and for participation in the US-USSR Pacific Ocean research cruise.

Within the Director's Office, research continued on the effects of natural alkaline materials (wind-blown soil aerosol and road dust) on precipitation chemistry. AGASP-II, a multi-institution research program to determine the distribution, transport, chemistry, and radiative effect of Arctic haze, was conducted during March-April from the Alaskan and Canadian Arctic. Initial data analysis, a case study of one event, is reported. Many scientists from universities and other institutions used the observatories for cooperative research; several projects are summarized.

2. OBSERVATORY REPORTS

2.1 Mauna Loa

FACILITIES

The GMCC core program of monitoring and observations was maintained in operation throughout the year, although the dew point temperature sensor and the Dasibi ozone monitor began to have problems late in the year. A special aerosol and precipitation sampling program was carried out for DOE in the spring in conjunction with the study of the global dispersion of the atmospheric plume from the Soviet nuclear accident in Chernobyl.

Construction was an important part of 1986 operations. In the fall a 40-m (126-ft) walk-up tower was installed. This construction required an extensive concerete pad and guy-anchor installations. In addition, a 12 × 14 ft solar observational operational building and an 11-ft-diameter observation dome were constructed for the University of Arizona solar photometer program.

Lidar operations continued on an approximately weekly schedule. The lidar upgrade program moved into the assembly and construction phase. A stratospheric plume from the eruption of the Columbian volcano Nevado del Ruiz in November 1985 continued to be observed by the lidar; the stratospheric effects persisted into 1986, probably at least through June.

The ozonesonde program, begun in December 1984 with NOAA NESDIS support, was continued on approximately a weekly schedule through the year using the NWS radiosonde facility at the Hilo airport.

The Pu'u O'o vent of Kilauea volcano erupted periodically on an almost regular 27-day schedule through June. In July a new fissure opened and began a continuous emission of lava estimated at 500,000 m^3 per day. This caused an extensive new lava flow that moved about 7 mi to enter the ocean in November. More than 30 homes were destroyed, and there were periodic forest fires during the 1986 phase of this continuous eruption identified as phase 48 in the 4-yr-long eruption on the east rift of Kilauea.

PROGRAMS

The principal programs conducted at MLO during the year are listed in table 1. Those instruments recorded continuously by the CAMS are indicated by an asterisk. Brief comments on some of the individual programs follow.

Carbon Dioxide

The GMCC URAS-2T and the SIO Applied Physics infrared analyzers were operated in parallel without problems throughout the year. Preliminary results indicate that the average CO_2 concentration for the year was about 346.7 ppm and the rate of CO_2 increase for 1986 was approximately 1.2 ppm.

The weekly CO_2 flask sampling programs at MLO and Cape Kumukahi were continued without problems during the year.

Table 1.--Summary of sampling programs at MLO in 1986

Program	Instrument	Sampling frequency	Remarks
Gases			
CO_2	URAS-2T infrared analyzer*	Continuous	MLO
	3-L glass flasks	1 pair wk^{-1}	MLO and Kumukahi (seacoast)
	0.5-L glass flasks, P'	1 pair wk^{-1}	MLO and Kumukahi
	0.5-L glass flasks, through analyzer	1 pair wk^{-1}	MLO
	5-L evacuated glass flasks	1 pair wk^{-1}	MLO and Kumukahi
CO_2 and CH_4	Gas chromatograph	Continuous	MLO
Surface ozone	Dasibi ozone meter*	Continuous	MLO
Total ozone	Dobson spectrophotometer no. 76	3 day^{-1}	Weekdays
Ozone profile	Dobson spectrophotometer no. 76	2 day^{-1}	Umkehr
	Balloonborne ECC sonde	1 wk^{-1}	From Hilo Airport
CFC-11, CFC-12, and N_2O	300-mL stainless steel flasks	1 pair wk^{-1}	MLO
Aerosols			
Condensation nuclei	Pollak CNC	Discrete	Weekdays
	G.E. CNC*	Continuous	
Optical properties	Four-wavelength nephelometer*	Continuous	450, 550, 700, 850 nm
Stratospheric aerosols	Lidar	Discrete	694.3 nm; average 1 profile wk^{-1}
Solar Radiation			
Global irradiance	Eppley pyranometers (3) with Q, OG1, and RG8 filters*	Continuous	Weekdays
Direct irradiance	Eppley pyrheliometers (2) with Q filter*	Continuous	Weekdays
	Eppley pyrheliometer with Q, OG1, RG2, and RG8 filters	3 day^{-1}	Weekdays
	Eppley/Kendall active cavity radiometer	Discrete	Weekdays
Diffuse irradiance	Eppley pyranometer with shading disk and Q filter*	Continuous	
Turbidity	J-series 1982 sunphotometers	3 day^{-1}	380, 500, 778, 862 nm; narrowband
	PMOD three-wavelength sunphotometer*	Continuous	380, 500, 778 nm; narrowband
Meteorology			
Air temperature	Thermistor (aspirated)*	Continuous	2-m height
	Max.-min. thermometers	1 day^{-1}	Standard shelter
	Hygrothermograph	Continuous	MLO and Kulani Mauka
Dewpoint temperature	Dewpoint hygrometer*	Continuous	2-m height
Relative humidity	Hygrothermograph	Continuous	MLO and Kulani Mauka (8300 ft)
Pressure	Capacitance transducer*	Continuous	
	Microbarograph	Continuous	
	Mercurial barometer	1 day^{-1}	
Wind (speed and direction)	Bendix Aerovane*	Continuous	6-m height
Precipitation	Rain gauge, 8-in	1 day^{-1}	
	Rain gauge, 8-in	1 wk^{-1}	Kulani Mauka
	Rain gauge, weighing bucket	Continuous	Weekly chart record
	Rain gauge, tipping bucket*	Continuous	Program began Oct.
Total precipitable water	Foskett infrared hygrometer*	Continuous	
	HAO infrared hygrometer*	Continuous	
Precipitation Chemistry			
pH	pH meter--Hilo lab.	Weekly	Rainwater collections, 3 sites
Conductivity	Conductivity bridge--Hilo lab.	Weekly	Rainwater collections, 3 sites
Chemical components	Ion chromatograph--Hilo lab.	Weekly	Rainwater collections, 3 sites
Cooperative Programs			
CO_2 (SIO)	Infrared analyzer (Applied Physics)	Continuous	
CO_2, ^{13}C, N_2O (SIO)	5-L evacuated glass flasks	1 pair wk^{-1}	MLO and Kumukahi
Surface SO_2 (EPA)	Chemical bubbler system	Every 12 days	24-h (0000-2400) sample
CO_2, CO, CH_4, $^{13}C/^{12}C$ (CSIRO)	Pressurized glass flask sample	1 mo^{-1}	MLO
CO_2, CH_4 and other trace gases (NCAR)	Evacuated stainless steel flasks	1 pair wk^{-1}	MLO and Kumukahi
HNO_3 and HCl vapor (SRI International)	Special sampling system	4 periods yr^{-1}	2-wk periods
Total suspended particles (DOE)	High-volume sampler	Continuous	1 filter wk^{-1}

Table 1.-- Summary of sampling programs at MLO in 1986--Continued

Programs	Instrument	Sampling frequency	Remarks
Cooperative Programs--Cont.			
Total suspended particles (EPA)	High-volume sampler	Every 12 days	24-h (0000-2400) sample
Ultraviolet radiation (Temple Univ.)	Ultraviolet radiometer (erythema)	Continuous	Radiation responsible for sunburning of skin
Ultraviolet radiation (Smithsonian)	7-wavelength UV radiometer	Continuous	295-325 nm, narrowband
Solar variability (Univ. of Arizona)	Solar spectroradiometer	Discrete	Program began Sept. 1985
Solar aureole intensity (CSU)	Multi-aperture tracking photometer	Continuous	Program began Jan. 1985
Precipitation collection (DOE)	Exposed collection pails	Continuous	
Precipitation collection (ISWS)	Aerochemetric automatic collector	Continuous	Analysis for ^{7}Be and ^{10}Be
Precipitation collection (Univ. of Virginia)	Aerochemetric automatic collector	Continuous	Organic acid analysis
Wet-dry deposition (ISWS)	Aerochemetric automatic collector	Continuous	NADP
Aerosol chemistry (Univ. of Washington)	Nuclepore filters	Continuous	Upslope-downslope discrimination
^{13}C (USGS, Denver)	10-L stainless steel flasks	Biweekly	
Various trace gases (OGC)	Stainless steel flasks	1 set wk^{-1} (3 flasks)	MLO and Kumukahi

*Indicates program recorded by CAMS.

The continuous measurements of CO_2 along with Aitken nuclei observations were used to monitor and define the beginning and end of short-term (usually 1 h or less) disturbances in the record, which are caused by local contamination. In most cases the disturbances are caused by volcanic outgassings from Mauna Loa and Kilauea. Table 2 summarizes the incidences detected from Mauna Loa.

Table 2. Monthly occurrences of outgassing from the volcanic caldera on Mauna Loa during 1986

	Jan	Feb	Mar	Apr	May	Jun	Jul	Aug	Sep	Oct	Nov	Dec	Year
No. of days	10	4	20	15	24	12	12	10	17	8	14	14	160
Percent of days	32	14	65	50	77	40	39	32	57	26	47	45	44

The low percentage of observed disturbances in February was probably due to an unusually high frequency of westerly winds. The 1986 frequency of outgassing events, 44%, is a small decrease from the 48% frequency that occurred in 1985. Both values are greater than the 5-yr average frequency of 27% observed prior to 1984. It should be noted that these frequencies relate to the number of days of occurrence and not to the number of hours of data that are affected; most events last only about an hour or so per day.

The air-sampling intakes of the GMCC and SIO 80-ft-high tower were remounted at the 80-ft level of the new 40-m (126-ft) walk-up tower in December. The intakes were installed side by side and put back to daily, normal operation. In addition, two new aluminum air intake lines for the two analyzers were installed side by side at the 40-m elevation for future uses.

Ozone

The ozonesonde program was carried out with the support of the NWS Hilo radiosonde facility. A total of 51 successful flights were made in 1986; of these, 47 or 92% were flown with the large 40-km plastic balloon. The remainder were flown using 3000-g rubber balloons when rainy weather precluded launching a plastic balloon. For the plastic balloons, 70% reached or exceeded an altitude of 40 km and the median altitude was 40.9 km. The maximum altitude reached was 42.6 km. The four rubber balloons reached altitudes ranging from 28.3 to 35.0 km.

The MLO ozone program also continued to include the continuous monitoring of surface ozone using the Dasibi monitor. Stratospheric ozone measurements were taken throughout the year using the automated Dobson instrument no. 76. Umkehr profiles were made daily by the automated system, and total ozone measurements were initiated manually three or more times a day when weather permitted. A short program of calibration of the WMO world standard Dobson no. 83 was carried out in June and July.

Surface Aerosol Measurements

Three instruments were used to characterize the surface aerosol particles: the G.E. CNC, the Pollak CNC, and the nephelometer.

The G.E. CNC operated continuously with only occasional maintenance or mechanical problems. The Pollak counter was operated in the normal manner during the year as a convenient calibration check for the G.E. CNC system. The nephelometer was in operation on essentially a continuous basis.

Stratospheric Aerosols--Lidar

Lidar observations were carried out, sky conditions permitting, on approximately a weekly schedule. When possible, lidar observations were correlated with SAGE II satellite overpasses so that the lidar profiles could be coordinated with the SAGE aerosol experiments. A total of 47 observations were made during the year. As noted earlier, the stratospheric aerosol loading from the winter 1985 Ruiz eruption continued to be observed into the summer of 1986.

Solar Radiation

No major changes were made in the MLO solar radiation program. There are several components in this system: continuous solar and total-sky measurements using both stationary and tracking instruments; discrete broadband and narrowband observations on a routine, weather-permitting basis; discrete, manual, high-precision observations; and calibrations and intercomparisons of instruments using MLO facilities and instruments as working standards. All of these activities continued in 1986.

Two normal incidence pyrheliometers with Q filters, three global pyranometers with Q, OG1, and RG8 cutoff filters, and a diffuse Q pyranometer with shading disk and Q filter were operated throughout the year to obtain continuous radiation measurements. A filter-wheel pyrheliometer with Q, OG1, RG2, and RG8 cutoff filters was operated to obtain 3-day^{-1} broadband radiation measurements. Turbidity measurements were obtained with hand-held sunphotometers J202 (380 and 500 nm) and J314 (778 and 862 nm) throughout the year.

The active solar tracker and the 32-channel CAMS operated the whole year with only minor problems in the automated solar dome. The dome and shutter controllers operated reasonably well, although there were some problems with the dome positioning motor and controller. Instruments mounted in the solar dome included a normal incidence pyrheliometer, an infrared water vapor meter, a three-wavelength PMOD sunphotometer, and an active cavity radiometer.

The MLO solar radiation program was augmented by a number of cooperative programs.

Meteorology

Meteorological measurements were continued without major problems during 1986. Wind and temperature sensors were located at the top of the new 40-m tower to provide gradient data to compare with the surface data.

Precipitation Chemistry

The GMCC precipitation chemistry program continued without difficulties at about the same level of activity as in prior years. The usual MLO program consists of the collection and analysis of precipitation from three local sites; the coastal site at Cape Kumukahi was discontinued because of repeated vandalism. MLO also carries out the analysis of precipitation samples collected on the Island of Kauai and at the GMCC observatories at Barrow, Samoa, and South Pole. Weekly snow or rain samples are collected at these GMCC sites. Samples are analyzed in the MLO Hilo laboratory for pH and conductivity. In addition, both anions and cations are determined in these samples using ion chromatography. Several cooperative programs in precipitation and deposition chemistry augment the GMCC program.

Cooperative Programs

The large number of cooperative programs at MLO continued in normal operation and with little change through 1986. These are listed in table 1, and a brief summary of some of these activities follows.

The program of high-precision BUV radiation measurements at seven wavelengths (295-325 nm) was continued at MLO by the Smithsonian Institution Radiation Biology Laboratory as was the program of erythema (sunburn) radiation measurements by Temple University. These two sets of data are important in assessing the potential impact of changes in the ozone layer. The CSU program of measurements with a five-element tracking solar photometer begun in 1985 was continued through the year.

Precipitation collection for chemical analysis continued to be important, and there were several cooperative investigator programs in this research area. Collections of precipitation for organic acid analysis for the University of Virginia and for beryllium 7 and 10 analyses for ISWS continued, as did sample collections for DOE and NADP. Following the Soviet Chernobyl nuclear accident, special precipitation collections were made for DOE.

Aerosol particle samples were collected for the University of Washington with filters changed on a continuous schedule using Nuclepore filters. This program used a sampler-controller discriminating on the basis of time of day, wind speed, wind direction, and Aitken nucleus count. The purpose of this controller is to separate sample collections according to upslope and downslope air trajectories and to exclude calm conditions. Downslope air should be representative of midtropospheric conditions whereas upslope air parcels may contain various amounts of material with a recent origin at the earth's surface. Total particle samples were also collected on filters on a weekly basis for DOE. High-volume filter samples were collected for EPA using standard EPA methods with one 24-h filter sample being taken every 12 days. The DOE program was augmented to include daily filter changes during the Chernobyl nuclear incident.

The CO analyzer of the Max Planck Institut, Mainz, Germany, operated during several previous years, was taken out of service early in the year.

The SIO Applied Physics infrared CO_2 analyzer operated without major problems during 1986 in parallel with the GMCC CO_2 analyzer. Flask samples of air from MLO and Cape Kumukahi continued to be supplied to SIO on a weekly basis.

Flask sample collections were made both at MLO and at the seacoast at Cape Kumukahi for several investigators interested in a variety of constituents. Flask collections were made at MLO for the Australian CSIRO who is analyzing the samples for the $^{13}C/^{12}C$ ratio as well as for CO, CO_2, and CH_4. Other flask sample programs include those of the OGC, NCAR, and SIO. Colorado College continued its periodic sampling at MLO for nitric acid and hydrochloric acid vapors over 2-wk periods every 3 mo by SRI International investigators.

The University of Arizona solar photometry program, supported by a NOAA ARL grant that includes the installation of a multiwavelength solar spectroradiometer and its long-term operation at MLO, was in preliminary operation during the year. The overall goal of the program is to determine the long-term variability of solar spectral irradiance, i.e., the solar "constant." Measurements over a solar cycle are contemplated. A permanent facility to house this program was completed at the close of the year.

2.2 Barrow

FACILITIES

The third-party support agreement between the U.S. Air Force DEW Line contractor and GMCC was reviewed and updated. Besides provisions for electricity, arrangements for road clearance, vehicles, and lodging are now included. The agreement has been beneficial to the GMCC operation at BRW.

The observatory obtained a new Ski-Doo snow machine in January; Paperwork was started to excess two snow machines and the Bombadier Bombi. None of these machines have value, so they will be excessed as scrap. The Dodge truck continued to be a source of constant trouble; and Boulder is working to have it replaced by a GSA vehicle next year. The Chevy Suburban was sold as excess in 1986.

The roof of the observatory was rewired in the summer and can now handle 110 V ac or 220 V ac. Plans were being worked on to upgrade the mechanical systems in the observatory. With the increased projects we have an overheating problem in the station.

A modem was connected to the IBM PC and used this year to send data to and from Boulder at any time of the night or day. A BBS named FIDO is used on a regular basis to communicate with the message service provided by Boulder. BRW also used the PC to transfer data from the CAMS to the disk drive, in preparation for the day when Boulder uses this feature.

The North Slope Borough (NSB) and NSF cosponsored a meeting in BRW for the review of U.S. Arctic Science Policy. GMCC/BRW personnel attended these meetings and were asked for their opinions. Personnel from GMCC were also called on several times, by the NSB, for technical help and input. The BRW personnel were named in a proposal to NSF to increase funding for training NSB science teachers.

PROGRAMS

Table 3 lists the 1986 programs; some of the programs are further described below.

Carbon Dioxide

A new program was installed in the CAMS package in May to take care of a bug that was found in the old program. There has been no trouble since. The coolant in the CryoCool water vapor freezeout trap was changed to bring the temperature back down to -70°C. New CO_2 standards were put online in November. Flask samples continued as before, with the exception of the 5-L flasks that were discontinued in March.

Ozone

The Dasibi surface ozone meter ran fine all year except for two burned-out pumps.

Table 3.--Summary of sampling programs at BRW in 1986

Program	Instrument	Sampling frequency
Gases		
CO_2	URAS-2T infrared analyzer	Continuous
	0.5-L glass flasks, P[3]	1 pair wk^{-1}
	0.5-L glass flasks, through analyzer	1 pair wk^{-1}
	3-L glass flasks	1 pair wk^{-1}
Surface ozone	Dasibi ozone meter	Continuous
Methane	0.5-L glass flasks	1 pair wk^{-1}
	Carle GC with HP acquisition	Continuous
CFC-11, CFC-12, CCl_4, CH_3CCl_3, and N_2	300-mL stainless steel flasks HP-GC with HP acquisition	1 pair wk^{-1}
Total ozone	Ozone balloons	1 wk^{-1}
	Dobson ozone spectrophotometer no 91	Discrete
Aerosols		
Condensation nuclei	Pollak CNC	Discrete
	G.E. CNC	Continuous
Optical properties	Four-wavelength nephelometer	Continuous
Solar Radiation		
Albedo	Eppley pyranomter	Continuous
Global irradiance	Eppley pyranometers with Q and RG8 filters	Continuous
Direct irradiance	Tracking NIP	Continuous
Direct irradiance	Eppley pyrheliometer with Q, OG1, RG2, and RG8 filters	Discrete
Terrestrial (IR) radiation	Eppley pyrgeometer	Continuous
Turbidity	Sunphotometers with 380-, 500-, 778-, and 862-nm narrowband filters	Discrete
Meteorology		
Air temperature	Thermistor-2 levels	Continuous
	Max.-min. thermometers	1 day^{-1}
Dewpoint temperature	Dewpoint hygrometer	Continuous
Pressure	Capacitance transducer	Continuous
	Mercurial barometer	Discrete
Wind (speed and direction)	Bendix Aerovane	Continuous
Precipitation Chemistry		
pH	pH meter (samples analyzed at MLO)	Discrete
Conductivity	Conductivity bridge (samples analyzed at MLO)	2 mo^{-1}
Cooperative Programs		
Total surface particulates (DOE)	High-volume sampler	Continuous (1 filter wk^{-1})
Aerosol chemistry (URI)	High-volume sampler	Continuous (2 filters wk^{-1})
Aerosol chemistry (Univ. of Alaska)	Hi-Vol filters	Continuous 3 filters wk^{-1}
Ultraviolet radiation (Temple Univ.)	Ultraviolet radiometer	Continuous
Precipitation gauge (ASCS)	Wyoming shielded precipitation gauge	2 mo^{-1}
Magnetic fields (USGS)	Magnetometer	1 station check wk^{-1})
^{13}C (USGS)	10-L stainless steel flasks	1 pair mo^{-1}
Various trace gases (OGC)	Stainless steel flasks	1 set wk^{-1} (3 flasks set^{-1})
Various trace gases (NCAR)	3-L stainless steel flasks	1 pair wk^{-1}
$^{13}C/^{12}C$ (CSIRO)	5-L glass flasks	1 pair $(2\ wk)^{-1}$
CO_2, ^{13}C, N_2O (SIO)	5-L evacuated glass flasks	1 pair wk^{-1}
$^{12}C/^{13}C$ (Univ. of Washington)	35-L stainless steel flasks	1 $(2\ wk)^{-1}$
Halocarbon monitoring (Univ. of Calif., Irvine)	Various stainless steel flasks	1 set $(3\ mo)^{-1}$
Earthquake detection (Univ. of Alaska)	Seismograph	Continuous Check site wk^{-1} Change tape mo^{-1}
Correlation of metal signatures with position of Arctic front & radioisotope (Univ. of Alaska)	Hi-Vol sampler	Continuous 3 filters wk^{-1}
Elemental aerosol collection, PIXE Univ. of Florida	Streaker sampler impactor sampler	Discrete March-April
Aerosol composition/size distribution (Univ. of Hawaii)	Knollenberg counter	Discrete March-April
$^{13}CH_4$($^{13}C/^{12}C$) (Univ. of Washington)	35-L stainless steel flasks	Discrete

A Dobson spectrophotometer, no 91, was installed by station personnel in June, and routine readings were begun. There has not been a Dobson instrument in BRW for several years because the observing conditions are poor with very few clear-sky conditions.

Regular ozone balloon flights were begun in February, starting with two to three flights per week and dropping to one per week after the spring. Several cold-weather problems made the first year trying, but still successful. The small, 1600, 2000, and 3000 g balloons were used as little as possible; the majority of flights used the 19,000 and 146,000 ft^3 balloons.

Methane

In January Boulder staff installed a methane GC system. The installation was quick and had few problems. During the year, two methanizer catalysts were replaced. High methane values were measured in winds that were outside the designated clear-air sector. These high values are believed to be from local sources.

Halocarbons

In October, Boulder personnel installed a GC system to measure N_2O, CFC-11, CFC-12, CCl_4, and CH_3CCl_3. Except for a problem with the interface, everything went smoothly. The system ran fine the rest of the year. Flask samples will be taken weekly as a comparison, to ensure high-quality data intercomparabilities between the two measurement methods. Larger sample loops will be installed in the GC to improve the precision of the measurements as they arrive from the factory.

Aerosols

The G.E. CNC and the four-channel nephelometer ran fine all year. A TSI CNC with a size selector was sent to the observatory for AGASP observations. Boulder personnel setup the equipment for AGASP.

Solar Radiation

The solar radiation program ran with few problems all year. Turbidity and filter wheel NIP readings were taken as conditions permitted. The box on the tracking NIP was not water tight. This was repaired in July. Early in the year it was discovered that, during the normal migration of the caribou, the albedo rack was being used as a scratching post. The lines were tightened and the poles set upright again.

Meteorology

The meteorology instruments ran fine all year. This year a storm hit on September 20 that had 65 mi h^{-1} winds, the highest measured on record. Several roads in town were washed out, including the one to the GMCC observatory, and several houses were in danger of being washed out. There was also damage to the 300-400 yr old burial site in town. This was all during the first 2 h of the storm, the worst in 23 yr. This winter also had one of the highest snowfalls on record.

Precipitation Chemistry

ARL personnel visited BRW and reviewed the acid precipitation sampling program. A new protocol was established to continue rain and snow sampling.

Cooperative Programs

The last of the LBL instruments were returned to LBL this year as the project came to a close. The Hi-Vol pump was left here and was used by the University of Alaska, Fairbanks.

The GMCC/BRW observatory proved to be a focal point for measurements after the Chernobyl nuclear reactor accident. The GMCC staff were pressed into special observational programs to monitor fallout from Chernobyl. Small amounts of fallout were detected from measurements made at BRW. Special Chernobyl monitoring measurements were made for the state of Alaska, the University of Alaska, the Department of Health for the University of Maryland, and DOE.

The BRW observatory also participated in the second AGASP experiment during March and April. Special aerosol measurements for AGASP-II were made by the University of Florida; the University of Hawaii; and GMCC Boulder. All GMCC measurements were intensified and tied into NOAA's WP-3D research aircraft flights in and around Barrow during AGASP.

Other cooperative experiments started in 1986 included methane sampling for the University of Washington, He^4 sampling for the Department of Interior, and navigational beacon setups for two offshore navigation companies.

2.3 Samoa

FACILITIES

The SMO GMCC observatory continued with another year of successful operation in 1986. Observations were interrupted for a short time by a lightning strike in April and massive island utility blackouts in May and June. Weekly ozonesonde flights were added to the program in April and continued throughout the year.

The lightning strike occurred on April 22 in the early afternoon. The bolt struck a tree 10 m from the observatory and entered a cable buried nearby to gain access to both the main and EKTO buildings. All the MO3 CAMS boards were destroyed, along with several ASR CAMS boards, the photovoltaic system controller, the Dasibi ozone monitor and communications board, the telephones, and the standby generator control relay. Both of the station personnel were in the building but were unhurt. During the ensuing 1 h downpour, the skies became so dark that all solar radiation channels read zero. A 6-in-deep crater was later found where the lightning entered the ground.

A power crisis lasting throughout May and June led to a failure of the standby generator at the station. The island utility company lost 70% of its generating capacity and was forced to put the territory on a schedule of rotating blackouts totalling 16 to 20 h per day. Businesses and schools closed, water systems lost pressure, and television and radio shut down for over a month. The observatory continued fairly normal operation until June 16, when the standby generator suffered a ruptured radiator and cracked head. Repairs were complete in 3 days because luckily the proper parts were on the island. By July, the utility power was restored.

Long-standing grounding problems were solved in 1986. In February the EKTO building was rewired; more outlets and breakers were added, electronic and motor/pump grounds were isolated, a UPS was hardwired in, and a grounding rod was established. In August a heavy copper cable was used to connect the EKTO and observatory grounding rods, reducing signal noise between the two buildings and eliminating the Dasibi-CAMS communication problem.

A new van was delivered in October and the old van excessed.

PROGRAMS

All 1986 programs are summarized in table 4; some are further described below.

Carbon Dioxide

The URAS-2T continuous analyzer monitored CO_2 concentrations throughout the year. Failure of a Cincinatti Sub-Zero freezer in July led to its temporary replacement by a CryoCool unit with alcohol bath. An upgraded water trap based on a small home refrigerator was put in place on the Matatula Point in August.

Table 4.--Summary of sampling programs at SMO in 1986

Program	Instrument	Sampling frequency
Gases		
CO_2	URAS-2T infrared analyzer	Continuous
	0.5-L glass flasks P^3	1 pair wk^{-1}
	0.5-L glass flasks, through analyzer	1 pair wk^{-1}
	3-L evacuated glass flasks	1 pair wk^{-1}
Surface ozone	Dasibi ozone meter	Continuous
Total ozone	Dobson spectrophotometer no. 42 or 65	3 day^{-1}
Ozone profile	Balloon borne ECC sonde	1 wk^{-1}
Methane	0.5-L glass flasks	1 pair wk^{-1}
CFC-11, CFC-12, and N_2O	300-mL stainless steel flasks	1 pair wk^{-1}
CFC-11, CFC-12, N_2O, CCl_4, and CH_3CCl_3	HP5890 automated gas chromatograph	1 h^{-1}
Aerosols		
Condensation nuclei	Pollak CNC	Discrete
	G.E. CNC	Continuous
Optical properties	Four-wavelength nephelometer	Continuous
Solar Radiation		
Global irradiance	Eppley pyranometers with Q and RG8 filters	Continuous
	Eppley pyranometers with Q filters on tilted mounts	Continuous
Direct irradiance	Eppley pyrheliometer with Q filter	Continuous
Direct irradiance	Eppley pyrheliometer with Q, OG1, RG2, and RG8 filters	Discrete
Turbidity	Sunphotometers with 380-, 500-, 778-, and 862-nm narrowband filters	Discrete
Meteorology		
Air Temperature	Thermistors (3)	Continuous
	Max.-min. thermometers	1 day^{-1}
	Hygrothermograph	Discrete
Dewpoint temperature	Dewpoint hygrometer	Continuous
Relative humidity	Hygrothermograph	Discrete
	Sling psychrometer	Discrete
Pressure	Capacitance transducer	Continuous
	Microbarograph	Discrete
	Mercurial barometer	1 wk^{-1}
Wind (speed and direction)	Bendix Aerovane	Continuous
Precipitation	Rain gauge, weighing bucket	Continuous
	Tipping rain guage	Continuous
	Plastic bulk rain guage	1 day^{-1}
Precipitation Chemistry		
pH	Fisher model 805 meter	1 day^{-1} (GMCC); 1 wk^{-1} (NADP)
Conductivity	Beckman model RC-16C meter	1 day^{-1} (GMCC); 1 wk^{-1} (NADP)
Cooperative Programs		
CO_2, ^{13}C, N_2O (SIO)	5-L evacuated glass flasks	3 flasks wk^{-1}
ALE project: CFC-11, CFC-12, N_2O, CH_3CCl_3, CCl_4 (OGC)	HP5880 gas chromatograph	1 h^{-1}
Various trace gases (OGC)	Stainless steel flasks	3 flasks wk^{-1} (3 flasks set^{-1})
^{13}C, ^{18}O, CO_2 (CSIRO)	5-L glass flasks	1 pair mo^{-1}
^{13}C (USGS)	10-L stainless steel flasks	2 pair mo^{-1}
Wet-dry deposition (NADP)	HASL wet-dry collector Chemetrics	1 wk^{-1}, wet; 2 mo^{-1}, dry
Bulk deposition (EML)	Plastic bucket	1 mo^{-1}
Hi-Vol sampler (EML)	Hi-Vol pump and filter	1 wk^{-1}
Hi-Vol sampler (SEASPAN Project)	Hi-Vol pump and filter with clean	1 wk^{-1}
CO_2, CH_4, trace gases (NCAR)	Evacuated stainless steel flasks	1 pair wk^{-1}
^{13}C, $^{13}CH_4$ (Argonne Lab.)	30-L evacuated steel cylinders	1 pair wk^{-1}

Five-liter flask collections were discontinued in March. Samples from 3-L flasks and pairs of 0.5-L P[3] and through-analyzer flasks continued to be taken in 1986. At year's end, tests were begun to determine the extent to which CO_2 was absorbed by the O-rings of the 0.5-L flasks, and a change was made to flasks with greased stopcocks.

Surface Ozone

The Dasibi UV ozone meter operated continuously except for a 1-mo repair period in Boulder after the April lightning strike damaged it.

Total Ozone

Dobson ozone spectrophotometer no. 42 was replaced by instrument no. 65 in June and returned to Boulder for calibration. Both instruments provided an uninterrupted record of 3 day^{-1} total ozone observations in 1986.

Ozonesondes

Beginning on April 1, weekly ozonesonde flights were conducted by GMCC SMO personnel at the NWS station at the Tafuna Airport. Rubber balloons weighing 1600, 2000, or 3000 g were used; flights to 5-10 mb altitude were routinely achieved. In the first year of operation, 53 flights were made with a 72% success rate.

A series of ozonesonde and water-vapor balloon flights was conducted by GMCC Boulder in July.

Halocarbons

In June the GMCC/NOAH group installed a GC to measure concentrations of N_2, CFC-11, CFC-12, CCl_4, and CH_3CCl_3. Although it is a new and major program, the equipment operated virtually trouble-free for the remainder of the year. Weekly stainless steel flask samples continued to be taken for the GMCC/NOAH group.

Surface Aerosols

The G.E. CNC operated continuously except for a 2-wk period in April when the instrument was in Boulder for repair. The four-wavelength nephelometer was in Boulder in June and July, but operated well during the remainder of the year.

Solar Radiation

A new chart recorder went on line in February, and the pyrheliometer was replaced in May following the lightning strike. The program of global irradiance, direct irradiance, and turbidity measurements continued in 1986 as before.

Meteorology

Beginning in July, a tipping rain gauge measuring in 0.01-in increments connected to the MO3 CAMS was put on line. The complement of meteorology instruments in Samoa remained the same in 1986.

Precipitation Chemistry

The Corning model 125 pH meter was replaced with a Fisher model 805 in March. During a visit by an ARL/Silver Spring staff member in September, plans were made to upgrade the program for 1987.

Cooperative Programs

OGC discontinued operation of its HP5840 gas chromatograph in May and installed an IBM PC-based data acquisition system for the present HP5880 gas chromatograph in June. The present configuration has evolved into a user-friendly and trouble-free system with virtually no downtime.

In June the SMO electronic technician attended a training session for the NADP program in Illinois. As a result, the layout of precipitation collectors on the observatory roof was revised in September.

A new program of flask sampling for Argonne National Laboratory was initiated in September. The samples are analyzed for the isotopic carbon composition of atmospheric methane.

2.4 South Pole

FACILITIES

Amundsen-Scott South Pole station is located about 150 m from the geographical South Pole. Located on the Polar Plateau, the station's elevation is about 9301 ft. According to SPO data for the year, the temperatures ranged from -22°C to -80°C for the 1985-1986 season. Because of the intense cold and darkness, the U.S. Navy's Operation Deep Freeze squadron, VXE-6, can operate on the continent only during the austral summer months with its LC-130 ski-equipped aircraft. This year the station opened on November 1, 1985, and closed on February 17, 1986. This was the only period when supplies and mail could be delivered to the pole, with the exception of an Air Force airdrop of approximately 12,000 lbs of supplies on June 22, 1986.

The GMCC SPO program is located in NSF's CAF building. It is positioned such that about 99% of the winds come from the Clean-Air Sector. Several major building projects were planned for this year. The raising of the CAF building onto its 10 steel I-beam supports was attempted throughout the summer. However, because of lack of the proper lifting equipment, along with concerns for the safety of the workers, it was determined to postpone the lift for another year. Grooming of the snow surface was sufficient to allow another year in the CAF without serious impairment from drifting snow. Another major project for the year, replacing the power cable to the CAF, was accomplished with considerable difficulty. The new cable is positioned deeply enough and out of the way enough that there should not be any more power problems associated with broken cables. Additionally, a computer cable from the IBM PC in the CAF to the station PDP 11/73 was installed while the trench was open for the power cable. The installation of a UPS was not completed because the batteries to run the unit never arrived. A railing around the roof of the CAF was completed. It is solidly made of 2-in-diameter steel pipe. A steel fire escape ladder out the back door of the CAF, complete with a small porch and iron railings was installed. A replacement manifold for the trace gas stack was installed in January and has worked very well. The support provided by NSF for the joint NOAA-NSF research effort in Antarctica was excellent.

The station's science computer, a DEC PDP 11/23, was upgraded to an 11/73 in January 1986. This allowed us to connect CAF's IBM PC to the station computer, which was the first step to getting GMCC data to Boulder on a monthly basis via satellite transmission.

Electric power this year was exceptionally clean. Frequency fluctuations as previously seen on the CO_2 trace were virtually nonexistent. This was due to an excellent power plant operator as well as the installation of Woodward governors on all three generators last summer. At the same time, two of the three generator engines were overhauled and the alternators replaced.

GMCC had a very good year at the pole, and had two major additions to the program. These were the successful implementation of regular monthly data transmissions via satellite to the home facility in Boulder, and the start of a program to launch ozonesondes to 3 mb altitude by means of large plastic balloons, in an effort to monitor the decrease in ozone over the Antarctic

continent in the austral spring. In addition, a cooperative project with NZARP to measure NO_2 through the atmospheric column was initiated. All long-term GMCC projects and cooperative programs were successfully run throughout the season. All electronic and electrical failures were successfully repaired by the instrument specialist quickly, with the bare minimum of downtime.

PROGRAMS

Table 5 lists the sampling programs carried out during the 1985-1986 season. Comments on some of the programs follow.

Satellite Data Transmissions

For the first time, GMCC SPO data was sent via ATS-3 satellite to Boulder on a monthly basis during the austral winter. The system starts with an IBM PC in CAF, using a tape reader, in-house written software, and KERMIT, to prepare the data from all the CAMS units, and also Dobson ozone data. The CAMS data are all in an hourly average format. The data are then transferred to the station PDP 11 computer using the shielded cable and line drivers. Once the data are on hard disk in the station computer, the staff transfers the data to Malabar, Florida via the ATS satellite, where it is available for retrieval by the Boulder computer staff. The system, though cumbersome at this point, works extremely well.

Control and Monitoring System (CAMS)

The CAMS systems have worked extremely well all year. There have been no BRAM losses except for ones caused by maintenance or by swapping boards. Problems have been very few, and on almost all occasions the CAMS successfully restarted automatically after power outages. The ZRAM boards received in December may have been a large reason for the success of the program.

Carbon Dioxide

There were some relatively minor problems with the CO_2 CAMS, which caused the unit to restart automatically often during printouts, but they were solved by the end of the season. The cleaner power to the building resulted in a much better analyzer trace than in previous years.

Surface Ozone

The surface ozone had a few problems this year, but little data were lost because of fast repairs by the instrument technician. Most of these problems were related to the ozone generator, but the Dasibi meter also required a little maintenance.

Total Ozone

During November 1985, Dobson ozone spectrophotometer no. 80 was replaced with Dobson no. 82 without difficulty. Dobson no. 82 was used all year, including moon observations during the winter, without any problems besides replacing the photomultiplier step switch, thus providing total ozone data for SPO.

Table 5.- Summary of sampling programs at SPO in 1986

Program	Instrument	Sampling frequency
Gases		
CO_2	URAS-2T infrared analyzer	Continuous
	0.5-L glass flasks P[3]	1 pair $(2\ wk)^{-1}$
	0.5-L glass flasks, through analyzer	1 pair twice mo^{-1}
Surface ozone	Dasibi ozone meter	Continuous
Total ozone	Dobson spectrophotometer no. 80 or no 82	3 day^{-1}
Ozone profile	Balloonborne ozonesondes	Twice mo^{-1} summer Three times mo^{-1} winter
CFC-11, CFC-12, and N_2O	300-mL stainless steel flasks	1 pair wk^{-1} summer
	Gas chromatograph	2 analyses wk^{-1}
O_2N_2 (NOAA/ARL)	Flasks	1 flask mo^{-1} present
Aerosols		
Condensation nuclei	Pollak CNC	Discrete
	G.E. CNC	Continuous
Optical properties	Four-wavelength nephelometer	Continuous
Solar Radiation		
Global spectral irradiance	Eppley pyranometers with Q and RG8 filters	Continuous
	Eppley pyrheliometer with Q, OG1, RG2, and RG8 filters	Discrete, summer
Turbidity	Sunphotometers with 380-, 500-, 778-, and 862-nm narrowband filters	Discrete, summer
Albedo	Eppley pyranometers with Q and RG8 filters, downward-facing	Continuous
Terrestrial (IR) radiation	Eppley pyrgeometers, upward- and downward-facing	Continuous
Meteorology		
Air Temperature	Platinum resistor	Continuous
Snow temperature	Platinum resistor 0.5 cm	Continuous
Pressure	Capacitance transducer	Continuous
	Mercurial barometer	1 time day^{-1}
Wind speed/direction	Bendix Aerovane recorder	Continuous
Cooperative Programs		
CO_2, ^{13}C, N_2O (SIO)	5-L evacuated glass flasks	2 mo^{-1} (3 flasks $sample^{-1}$)
Total surface particulates (DOE)	High-volume sampler	Continuous (1 filter wk^{-1})
Aerosol physical properites (SUNYA)	Pollak CNC with diffusion battery Nuclepore filters	Discrete Continuous
Various trace gases (OGC)	Stainless steel flasks	Twice mo^{-1} (3 flasks set^{-1})
$^{13}C/^{12}C$, CH_4 (USGS)	10-L stainless steel cylinder	1 mo^{-1} (2 cylinders $sample^{-1}$)
^{14}C (NOAA/ARL)	3,000 psi spheres	500 psi day^{-1}
Snow acidity (NOAA/ARL)	125-mL Nalgene flasks	1 $(2\ wk)^{-1}$
Various trace gases	Aluminum flasks	Weekly
Cosmic Dust Collection (Univ. of Pittsburgh)	Cosmic dust collector	Continuous
Interhemispheric $^{13}C/^{14}C$ (CSIRO)	Flasks	2 flasks mo^{-1}
NO_2 (NZARP)	Spectrophotometer, data logger	2 day^{-1} for 6 wk at sunrise & sunset

Ozonesondes

The first ozonesonde launch with the large (142,000 ft^3) balloons took place in late January. Since the inflation took place outdoors, the very slight breeze was sufficient to destroy the balloon. A 3000-g rubber balloon was then launched without problems. Considerable difficulties with the

intense cold, winds, drifting snow, and some poor-quality (diluted) helium caused an approximately 50% failure rate in the ozonesonde attempts, especially when the very large (225,000 ft^3) balloons were used. However, on airdrop, a supply of 19,000 ft^3 balloons arrived, which allowed continuance of the program using the balloon inflation tower as a facility for launching. This reduced the failure rate to about 20%, and allowed the program to continue during the austral Spring, when the ozone decrease reached a seasonal low. A total of 51 launch attempts were made, 34 successful, reaching to 2.0 mb pressure altitude.

Halocarbons

The halocarbon program with the Shimadzu GC and summer flask sampling continued throughout the year with some problems.

Aerosols

The Pollak CNC performed well all year. It compared with the G.E. CNC's fairly well throughout the year. The G.E.'s needed the usual frequent maintenance, but nevertheless produce a very good data set for the year. The nephelometer performed very well all year, except for channels occasionally dropping to zero because of the low ambient levels.

Solar Radiation

This year an HP-71-based system was installed to augment the CAMS data acquisition system with backup tapes and to provide a chart output. All instruments and maintenance routines were continued as in previous years. There were a few problems associated with bad pre-amps and cable connections, but system downtime was minimal. It was discovered that certain combinations of frequencies and antennas from the station HF radio transmissions would cause erratic traces on the solar radiation instruments, but communications with the radio operators minimized this.

Meteorology

This program generally ran fairly well. During the visit by the GMCC SMO Station Chief, it was discovered that the connections to T_d were not compatible with the specifications, and were changed. The difference between GMCC SPO temperatures and NWS temperatures was also investigated. No conclusions were made, but it was noted that the average difference between T_a and the NWS temperature was about 0.5°C. This compares more favorably than the discrepancies reported in previous years.

Cooperative Programs

The majority of the cooperative projects listed in table 5 continued with few problems. The USGS gas bubbler experiment for carbon 14/carbon 12 was discontinued in mid-1985. The LBL carbon aerosol program was discontinued in July 1986. A new project for the NZARP was initiated to measure NO_2 using solar scattering in the 4500 Angstrom region. There were a few initial problems with this program, but experience solved them all. Finally, the pumps for the NOAA/ARL carbon 14 program and the DOE Hi-Volume sampler were both replaced during the austral summer.

3. AEROSOLS AND RADIATION MONITORING GROUP

3.1 Continuing Programs

SURFACE AEROSOLS

The GMCC aerosol monitoring program continued during 1986 in the same mode as in previous years. Condensation nucleus (CN) concentration and aerosol scattering extinction coefficient (σ_{sp}) were measured continuously at BRW, MLO, SMO, and SPO. A G.E. automatic CN counter operated continuously and a Pollak CN counter provided daily calibration points for the automatic CN counter at each station. A four-wavelength nephelometer at each station continuously measured σ_{sp} at 450-, 550-, 700-, and 850-nm wavelengths. The MLO nephelometer exhibited low sensitivity on channel four (850 nm); therefore, only 450-, 550-, and 700-nm scattering extinction data for MLO are shown in this report. The SMO and SPO aerosol monitoring programs operated essentially trouble free.

Figure 1 shows daily geometric means of CN concentration (lower portion of each plot), σ_{sp} (middle portion of each plot), and Angstrom exponent (upper portion of each plot) at the GMCC stations for 1986. Three independent values of Angstrom exponent were calculated from the σ_{sp} data. Monthly geometric means of the entire data record for each station are shown in fig. 2. Monthly geometric means of the data for 1986 are listed in table 1.

Table 1.--Monthly geometric means of CN concentration (cm^{-3}) and σ_{sp} (m^{-1}) at 450, 550, 700, and 850 nm, for BRW, MLO, SMO, and SPO during 1986

	Jan	Feb	Mar	Apr	May	Jun	Jul	Aug	Sep	Oct	Nov	Dec
BRW												
CN	121	342	790	474	158	292	434	361	222	159	145	113
σ_{sp}(450)	1.13-5	1.07-5	2.16-5	1.73-5	5.63-6	3.36-6	3.65-6	3.26-6	4.03-6	5.92-6	5.72-6	1.02-5
σ_{sp}(550)	9.88-6	9.78-6	1.88-5	1.46-5	4.53-6	2.74-6	3.00-6	3.15-6	3.77-6	5.09-6	4.88-6	9.68-6
σ_{sp}(700)	6.52-6	6.88-6	1.23-5	9.10-6	2.76-6	1.80-6	1.96-6	2.42-6	2.88-6	3.50-6	3.23-6	7.26-6
σ_{sp}(850)	4.65-6	5.02-6	8.27-6	5.91-6	1.72-6	1.23-6	1.51-6	2.09-6	2.22-6	2.53-6	2.27-6	5.51-6
MLO												
CN	258	205	315	191	299	227	279	297	287	198	234	363
σ_{sp}(450)	8.15-7	9.13-7	1.57-6	1.45-6	2.13-6	1.39-6	7.17-7	1.15-6	1.54-6	7.79-7	9.67-7	6.86-7
σ_{sp}(550)	6.31-7	7.15-7	1.17-6	1.07-6	1.66-6	1.09-6	6.02-7	8.24-7	1.16-6	5.21-7	6.94-7	4.62-7
σ_{sp}(700)	4.73-7	5.43-7	8.86-7	8.16-7	1.39-6	9.04-7	4.65-7	6.05-7	8.32-7	4.08-7	5.69-7	4.04-7
σ_{sp}(850)	--	--	--	--	--	--	--	--	--	--	--	--
SMO												
CN	329	477	483	535	286	231	287	271	182	276	274	286
σ_{sp}(450)	1.89-5	1.70-5	1.61-5	1.41-5	--	--	--	2.04-5	1.57-5	9.87-6	1.05-5	1.33-5
σ_{sp}(550)	1.82-5	1.58-5	1.47-5	1.31-5	--	--	--	2.03-5	1.53-5	9.27-6	1.01-5	1.31-5
σ_{sp}(700)	1.92-5	1.56-5	1.46-5	1.34-5	--	--	--	2.12-5	1.56-5	9.63-6	1.01-5	1.36-5
σ_{sp}(850)	2.02-5	1.59-5	1.49-5	1.42-5	--	--	--	2.25-5	1.63-5	1.05-5	9.74-6	1.47-5
SPO												
CN	76	80	53	24	12	9	10	10	21	43	85	106
σ_{sp}(450)	3.71-7	3.64-7	2.61-7	1.93-7	3.30-7	3.81-7	6.77-7	6.73-7	8.11-7	1.11-6	4.51-7	4.25-7
σ_{sp}(550)	2.43-7	2.20-7	1.49-7	1.54-7	2.28-7	2.95-7	4.88-7	5.62-7	6.15-7	8.87-7	3.05-7	2.71-7
σ_{sp}(700)	1.13-7	1.02-7	8.46-8	9.30-8	1.28-7	1.72-7	2.70-7	3.62-7	3.77-7	5.90-7	1.78-7	1.36-7
σ_{sp}(850)	5.40-8	5.91-8	4.95-8	5.25-8	8.06-8	1.00-7	1.68-7	2.49-7	2.58-7	4.15-7	1.14-7	8.19-8

A compact exponential format is used for σ_{sp} such that 1.13-5 = 1.13×10^{-5}.

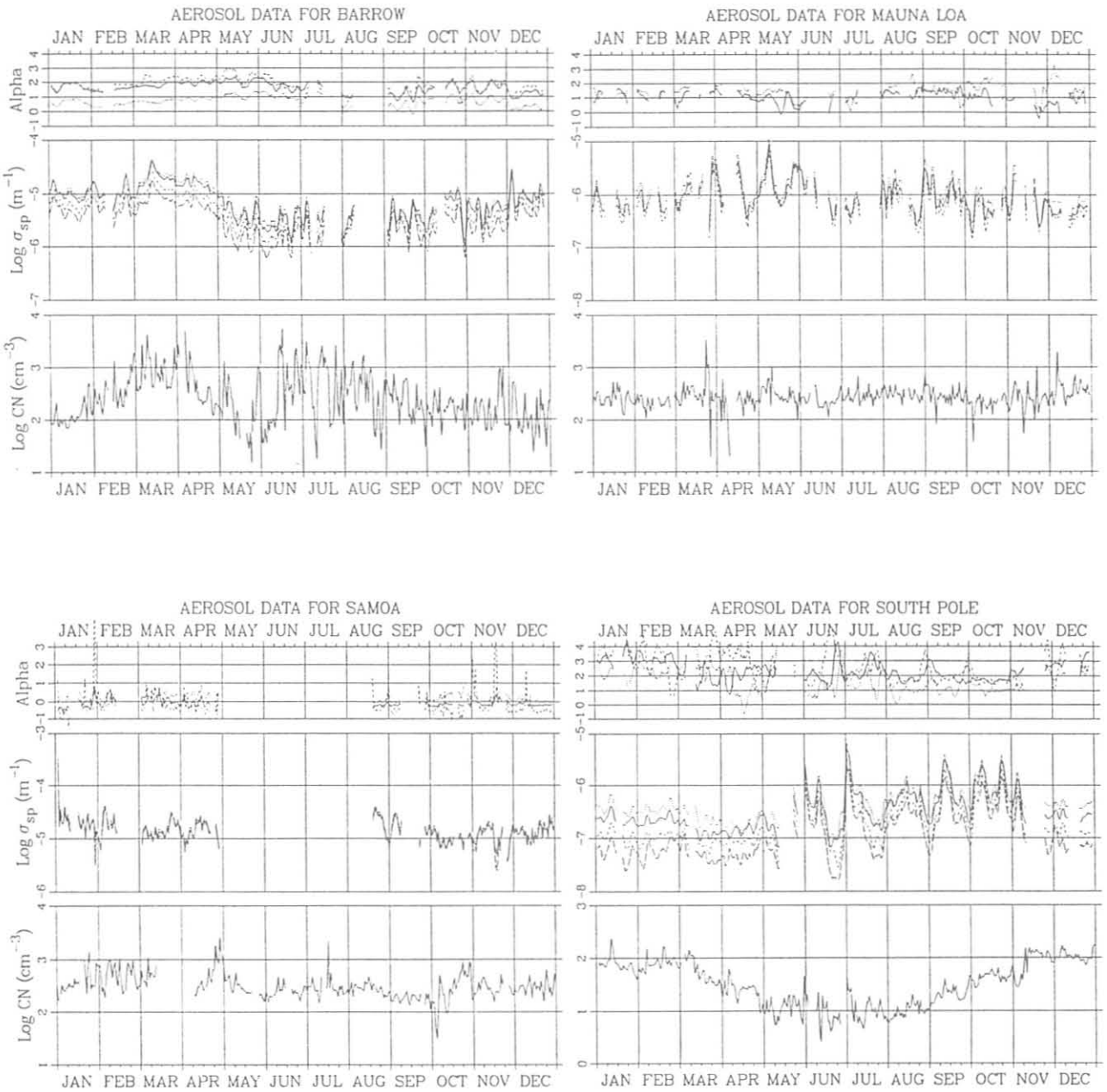

Figure 1.--Daily geometric means of σ_{sp}, CN, and alpha data at BRW, MLO, SMO, and SPO for 1986. Data for MLO are included only for 0000-0800 LST. For each station, CN concentration (lower) is shown as a solid line; σ_{sp} data (middle) are shown for 450 (dotted), 550 (solid), 700 (dashed), and 850 nm (long-dashed); Angstrom exponents were calculated from 450- and 550-nm (dotted), 550- and 700-nm (solid), and 700- and 850-nm (dashed) σ_{sp} data. σ_{sp} data for 850 nm and Angstrom exponent (alpha) data for 700-850 nm are not shown for MLO.

The BRW data in fig. 1 show a maximum in σ_{sp} of about 10^{-5} m^{-1} on 14 March, typical of the well-known springtime Arctic haze. The first 2 weeks of April 1986, when the flights of AGASP-II took place near BRW, show significant variations in the intensity of the Arctic haze. The high springtime values of σ_{sp} decrease rapidly in May, reaching values well below 10^{-6} m^{-1} in June. This regular annual cycle is apparent in the BRW long-term record shown in fig. 2; monthly means are above 10^{-5} m^{-1} in the spring or occasionally below 10^{-6} in the summer. The BRW CN record shows a more variable semiannual cycle; maxima usually occur in March and August, and minima usually occur in June and November. The entire BRW aerosol data record was recently presented by Quakenbush and Bodhaine (1987).

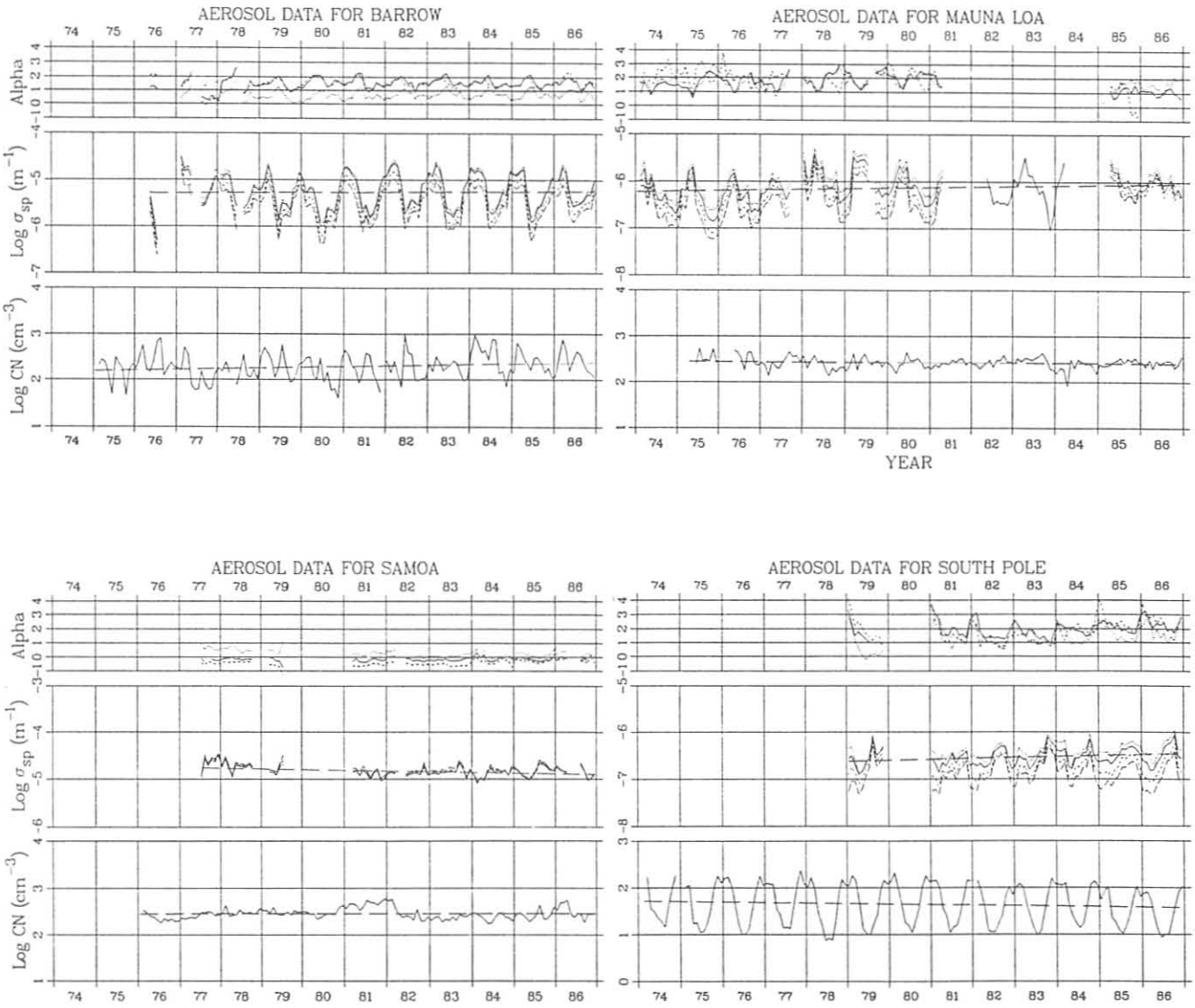

Figure 2.--Monthly geometric means of σ_{sp}, CN, and alpha data for the entire data record. Details of the trend lines are given in table 2.

The surface aerosol data and the meteorological situation during AGASP-II were discussed by Bodhaine et al. (1988). Three aircraft flights were conducted in the vicinity of BRW on 2, 8, and 9 April 1986. Prior to 7 April the top of the surface temperature inversion above BRW was near 850 mb and the tropopause was near 350 mb. On 7 April a high-pressure system moved into the vicinity of BRW; the height of the temperature inversion was at about 950 mb, the tropopause was at about 250 mb, and the surface temperature inversion was strengthened. The series of aerosol events during 8-11 April was probably caused by horizontal transport as the high-pressure system moved into the area. As a low-pressure system perturbed the area, an aerosol event during 13-15 April was accompanied by a weakening of the surface inversion. This aerosol event was probably caused by vertical transport from above the inversion to the surface. During this time period, surface winds were from the clean-air sector. Large-scale back trajectories show slow transport originating over the Arctic basin.

In the 1983 AGASP experiment (Bodhaine et al., 1984), BRW surface data showed aerosol events associated with direct, rapid transport originating over Asia. Also, aerosol optical depth data correlated strongly with surface aerosol data, suggesting increased vertical mixing. In the 1986 AGASP experiment, aerosol optical depth measurements did not correlate with surface aerosol measurements and no direct, rapid, large-scale transport was observed. As part of AGASP 1986 at BRW, a Nuclepore-filter diffusion battery apparatus for the measurement of particle size distribution in the Aitken size range, a Thermal Systems, Inc. alcohol-based CN counter, an aethalometer for the measurement of soot carbon, and an HP data acquisition system were installed in the observatory building.

The MLO σ_{sp} data shown in fig. 1 are typical for MLO and show a maximum in April-May that is caused by the long-range transport of Asian desert dust in the upper troposphere to the vicinity of Hawaii. Of particular interest is the large event that occurred during the first 2 weeks of May. Note that σ_{sp} data for 850 nm are not shown on this plot. The MLO CN data shown in fig. 1 average about 250-300 cm^{-3} and are probably representative of the background troposphere in this region.

The SMO σ_{sp} and CN data continue as in previous years with no significant annual cycle or long-term trend. The SMO aerosol is representative of a background marine boundary layer. Bodhaine and DeLuisi (1985) presented a detailed analysis of the entire SMO data record. The long-term mean at SMO is about 1.5×10^{-5} m^{-1} for σ_{sp} and about 270 cm^{-3} for CN concentration.

The SPO CN data show a strong annual cycle reaching a maximum of about 200 cm^{-3} in the austral summer and a minimum of about 10 cm^{-3} in the winter. The σ_{sp} data, being dominated by large events in the austral winter, show a cycle strikingly different from the CN cycle. These large aerosol events are caused by the transport of sea salt in the middle troposphere from stormy regions near the coast to the interior of the continent, and then vertical transport down to the surface. The largest σ_{sp} (550 nm) event recorded at SPO occurred in August 1979 and exceeded 1.5×10^{-5} m^{-1}, compared with a long-term mean of about 2.8×10^{-7} m^{-1}. Note that the long-term mean of σ_{sp} in the marine boundary layer at SMO is about 1.5×10^{-5} m^{-1}. Analyses of the SPO data were presented by Bodhaine et al. (1986, 1987).

The least-squares trend lines shown in fig. 2 were calculated using the common logarithms of the monthly means of the entire data record, and the results are given in table 2. Similar trend lines have been calculated and presented in previous GMCC Summary Reports. The long-term trends are still not statistically significant compared with the standard error (S.E.) about the regression line, suggesting that there is no long-term trend in the background aerosol measured at these four stations. Samson et al. (1987) studied the long-term CN concentration record for SPO and found a downward trend related to recent reduced concentrations in the austral spring.

Table 2.--Least-squares trend analysis of the common logarithms of the data shown in fig. 2*

	Parameter	Slope	Intercept	S.E.	Trend (% yr^{-1})
BRW	CN	0.0160	-29.4	0.296	3.8
	σ_{sp}	0.00394	-13.1	0.377	0.91
MLO	CN	-0.00587	14.1	0.132	-1.3
	σ_{sp}	0.0149	-35.7	0.326	3.5
SMO	CN	0.000548	1.36	0.118	0.13
	σ_{sp}	-0.0153	25.5	0.120	-3.5
SPO	CN	-0.0107	22.9	0.435	-2.4
	σ_{sp}	0.0213	-48.8	0.189	4.8

*The time axis is in fractional years, with a data point centered at the middle of a month; e.g., Jan 1974 =1974.042, Feb 1974 = 1974.125, etc.

RADIATION

The surface radiation budget is an important factor in global climate. Surface radiation budget measurements are currently being made at three sites by GMCC. These sites include SPO, BRW, and Erie, CO. The sites were selected so that the resulting data would be representative of a large, radiatively uniform surface area, thus permitting comparisons with satellite surface radiation budget observations.

At SPO, upwelling radiation measurements have been made 3-6 ft above the surface at a location upwind of the station. The surface at that location is essentially undisturbed and is representative of a large region on the Antarctic plateau.

At BRW the radiation budget measurements are made 6 ft above the tundra surface. Although there is a large area of tundra around BRW, in the summer months there are also many areas of standing melt water. The BRW surface radiation measurements should be representative of large portion of the land area, particularly during the time of year when the tundra is frozen and snow-covered.

Radiation budget measurements at the Erie, CO, site are made from the top of the 1000-ft BAO tower, which is surrounded by agricultural terrain. The reflected shortwave and upwelling longwave radiation measured at this height is integrated over a variety of surface types. The radiation budget observed from the tower is affected by the 1000 ft of atmosphere between the instruments and the ground and therefore cannot be considered a totally representative measurement of the surface budget. In the absence of clouds, the tower height has only slight influence on the shortwave budget, but it can have significant and variable effect on the longwave calculations.

At each of the three sites an array of four radiometers is operated to separately measure the upward and downward fluxes of shortwave (solar) and longwave (thermal) radiation. Eppley pyranometers and pyrgeometers are used to measure shortwave and longwave components respectively. The downward-facing instruments, which measure the upwelling radiation, were compared side by side with the upward-facing instruments. Any corrections, if needed, were applied so that biases between the two instruments could be made to cancel in the budget calculations within each wavelength regime. There is, however, no simple method to check the absolute response (and hence a bias) between the longwave and shortwave instruments, and therefore, the measured values are dependent on the absolute calibration in each wavelength regime. The calibration of the shortwave instruments is quite accurate and based on an absolute cavity radiometer. The longwave instruments were calibrated by the manufacturer. Calibration of infrared instruments is more difficult because of the problem in obtaining an accurate absolute radiation source.

Figures 3 and 4 show the components of the net radiation budget for approximately 1 year from SPO and Erie (BAO). One point is plotted for each day. The units on the left are energy per area integrated over the day and the units on the right are power per area averaged over the day. The differences in latitude and surface types between the two locations is apparent in the net shortwave and albedo plots. Major variations in albedo at BAO are due to intermittent snow cover. At SPO the albedo variations are caused by changes in solar zenith angle and clouds that block the direct solar beam.

STRATOSPHERIC AEROSOL LIDAR OBSERVATIONS

The GMCC MLO lidar record, starting in the fall of 1974, continues to the present. During this period, two major volcanic events had been observed: De Fuego (14.5°N, 90.9°W), 14 October 1974; and El Chichon (17.3°N, 93.2°W), 28 March and 3-4 April 1982. These two events have been studied for characteristics of stratospheric aerosols during perturbed conditions. In addition, the quiescent periods have been studied, and it appears that a lower threshold aerosol optical thickness over Mauna Loa can be obtained from the data.

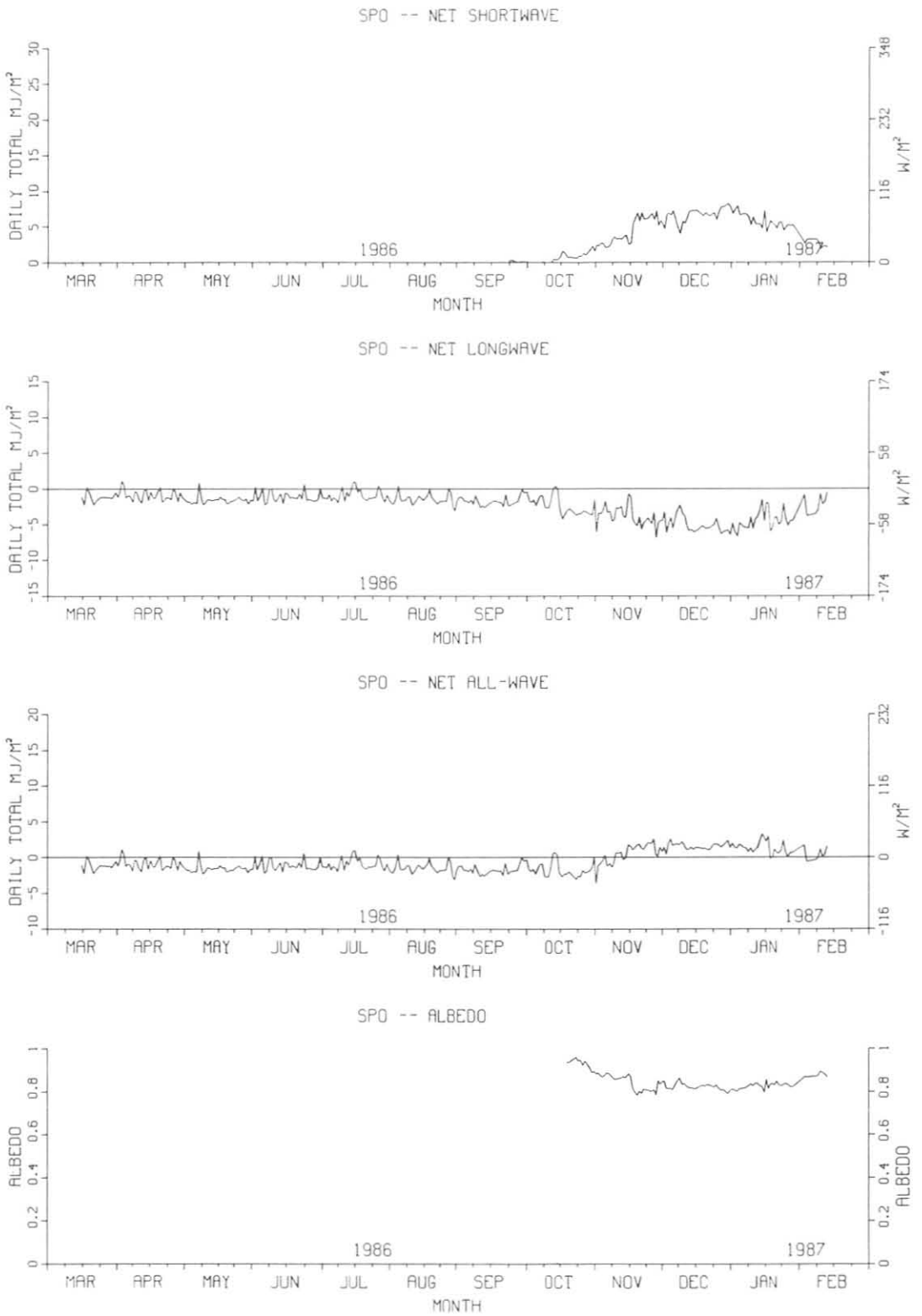

Figure 3.--Components of the daily total radiation budget as measured over a 1-yr period at SPO. The bottom panel is the daily average surface albedo.

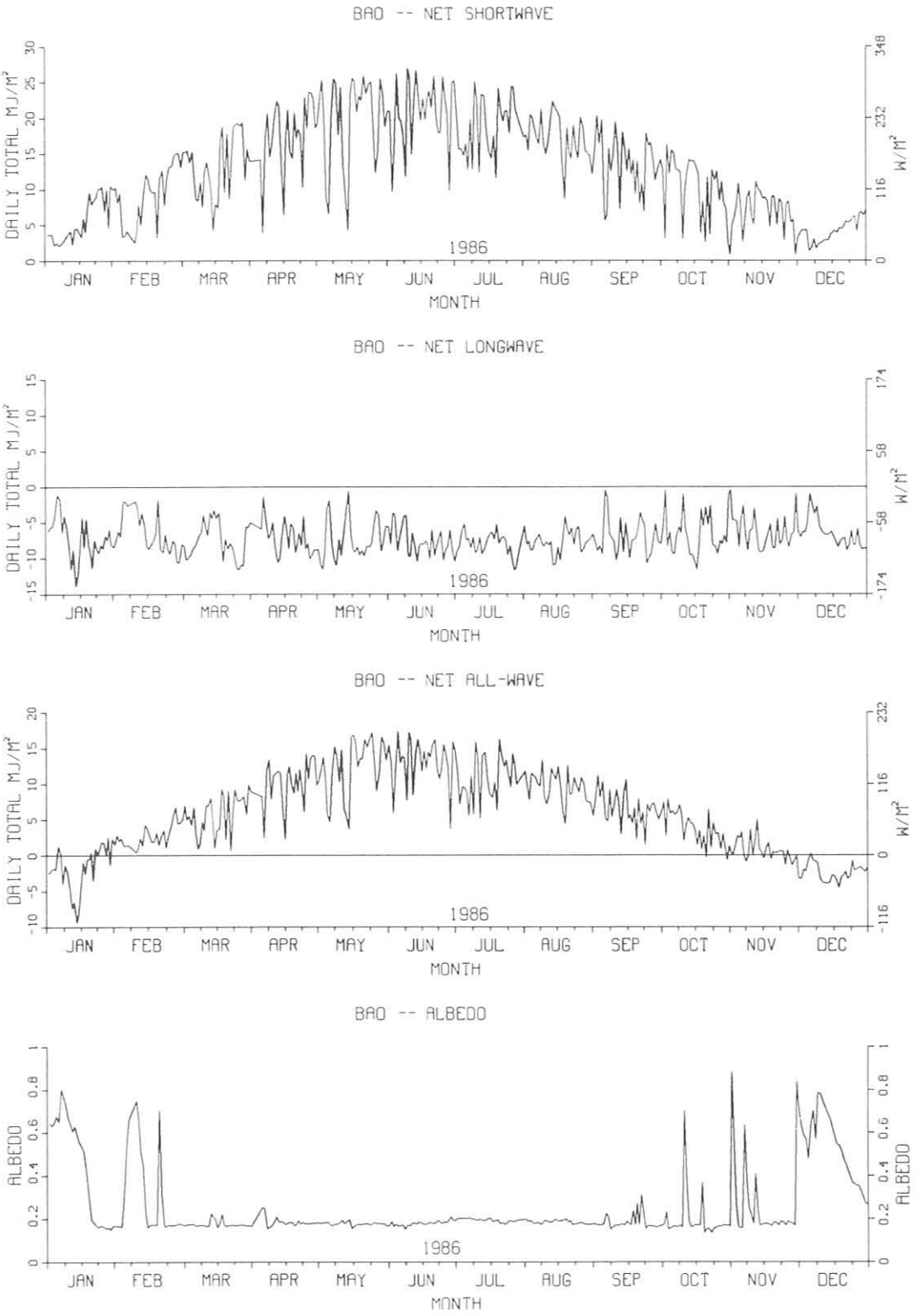

Figure 4.--Components of the daily total radiation budget as measured over a 1-yr period at the BAO. The bottom om panel is the daily average surface albedo.

When lidar data from MLO are compared with lidar data from other latitudes, the representativeness of Mauna Loa's observations as a measure of stratospheric aerosols at higher latitudes can be investigated. This is an important issue that has been raised from a trend analysis of middle-latitude Umkehr ozone profile data, which were corrected by MLO transmission measurements. Preliminary results of a study based on a rather limited data set indicates that MLO observations are reasonably representative of higher latitude stratospheric aerosols for eruptions occurring at the lower latitudes.

Figure 5 is a comparison of lidar observations made at four stations and one set of sunphotometer optical thickness data made at Vancouver, B.C. The two stations having the largest record are MLO and Langley. The figure shows that the data from these two stations agree reasonably well on the long term. Nevertheless, a rather marked departure occurred after the eruption of El Chichon in April 1982. The volcanic cloud from this eruption was detected over MLO almost immediately after the eruption, and a downward trend began shortly after, whereas at Langley, the optical thickness did not reach a maximum until January 1983. Thereafter, the diminution rates of each do not differ by much. Although, on the long term, observations of stratospheric aerosol effects at MLO seem to be representative of aerosols at higher latitudes, it is much more informative to have lidar stations at the higher latitudes if we wish to provide a more accurate picture of the stratospheric aerosol over the Northern Hemisphere.

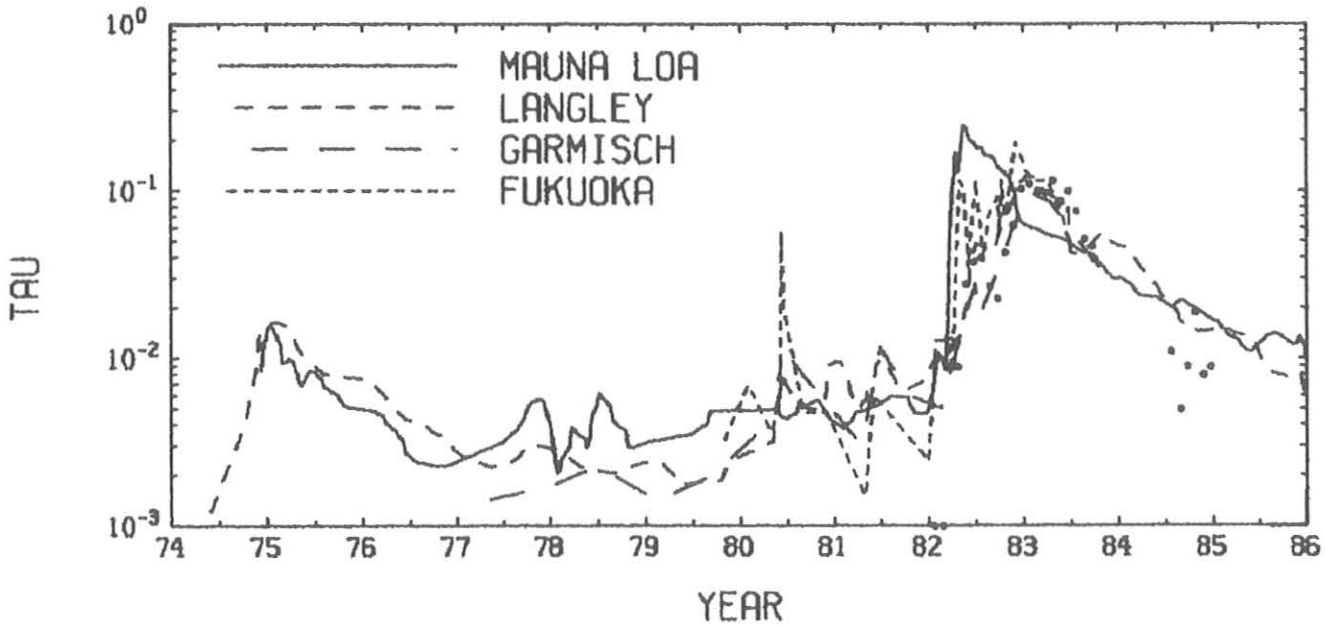

Figure 5.--Stratospheric aerosol optical thickness lidar data (tau) vs. time from Mauna Loa (19°N), Langley (37°N) (McCormick et al., 1984), Garmisch-Partenkirchen (47°N) (Jager et al., 1984), and Fukuoka (30°N) (Hirono et al., 1984). The unconnected data points are from ground-based sunphotometer measurements made at Vancouver, B.C. (Hay and Darby, 1984).

Another interesting feature of this figure is the minimum optical thickness during the period 1977-1979 inclusive seen by lidar at higher latitudes. The data of this period imply an optical thickness of 0.002-0.003 for the stratosphere starting at 15 km. The uncertainty of this estimate of "background" aerosol is quite large (perhaps as much as ±100%) because of the difficulty in accurately adjusting the relative lidar measurement to an estimate of the lidar backscatter for a molecular atmosphere, and assumptions concerning the optical properties of the stratospheric aerosol.

A more complete set of lidar and some sunphotometer data was used to track the poleward progression of the El Chichon stratospheric aerosol maximum. An analysis of aerosol optical thickness observations at nine stations for the time when the aerosol optical thickness was a maximum over each station is shown in fig. 6. A straight line drawn through the data suggests an average northward progression rate of 0.33° day^{-1}. The point for MLO is an exception to the analysis; here, the data show an optical depth step decrease of approximately 0.05 that occurred sometime in the interval of the last week of November and first week of December 1982. This is most likely the aerosol that disappeared over MLO then moved northward and appeared as a maximum over the higher latitude stations.

One other point of interest with the lidar data of fig. 6 is that the maximum optical thickness observed at each station was approximately the same, 0.12-0.13. This is a rather unexpected result that might provide additional information for further understanding of stratospheric transport processes. On the basis of these results, preliminary conclusions concerning low-latitude injections are the following:

(1) Low-latitude injections are transported to both poles in a wavelike fashion.

(2) Transport to high latitudes appears to be linear with time.

(3) Maximum optical thickness at mid-latitudes in the northern hemisphere occurs during January.

(4) The maximum optical thickness of the transport wave is constant with latitude, to a first approximation.

(5) The wave begins to build up in higher latitudes almost immediately after an eruption.

GMCC SOLAR RADIATION FACILITY

Activities of the SRF during 1986 were concentrated in the following areas: (1) analysis of the 1985 New River Intercomparison of active cavity radiometers (NRIP7); (2) contracting activities required by procurement of new solar trackers for the NOAA national network; (3) installation and operation of an initial version of a new IBM-PC based data acquisition system to be used at the 31 solar radiation monitoring sites in the U.S. network; (4) purchase and installation of a new SRF computer and data acquisition system; (5) design, purchase, fabrication, and installation of new SRF sensor platforms on the roof of building RL-3 in Boulder.

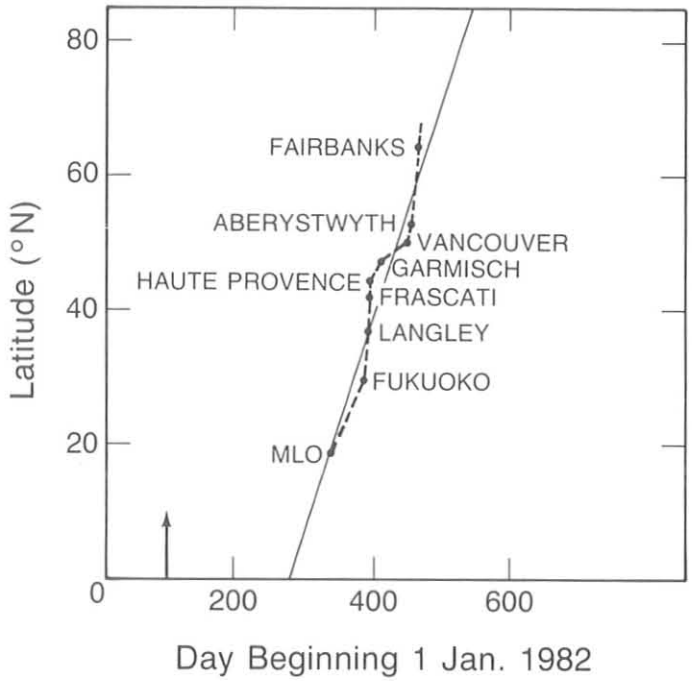

Figure 6.--Time of the maximum stratospheric aerosol optical thickness over a station, at its latitude. The straight solid line is for the northward linear transport rate of the maximum, which is 0.33° latitude day^{-1}. All stations are lidar except Vancouver and Fairbanks, which are sunphotometer.

NRIP7 Analysis

The New River Intercomparisons of active cavity radiometers were begun in 1978 for the purpose of allowing participants to verify the operation of their sensors. A primary reference for these comparisons has been the NOAA active cavity radiometer TMI no. 67502. Historical ratios of various other sensors to sensor no. 67502 provide a basis for establishing confidence and the stability of these types of sensors, and also serve as periodic checks on potential instrument drift. Analysis of the NRIP7 data was performed by the NOAA/SRF and will be published in a report. A departure from earlier NRIP reports was implemented in the NRIP7 analysis. Earlier NRIP reports summarized participant cavity performance by ratioing to the reference, no. 67502. The NRIP7 report differs from that method. Instead of one reference cavity on which to base all ratios, a ratio to a group mean was employed. The sensors chosen to be the reference group were those that had participated in the Sixth International Pyrheliometer Comparison held in Davos, Switzerland, in October 1985. Eight NRIP7 participants satisfied this criterion, and their data were used to establish a reference against which all participating sensors could be compared. Additionally, the results of IPC6 are also incorporated in the NRIP7 report for the eight IPC6 participants. Specifically, the results used were the derived ratios to the World Radiometric Reference of each of the eight active cavity radiometers. By incorporating these ratios in the NRIP7 analysis, effectively using all eight IPC6 participants as transfer standards with equal weight in the analysis, a derived ratio of any NRIP7 participant to the World Radiometric Reference was obtained. Note that the use of the eight active cavity radiometers as transfer standards has no official sanction by WMO, but nevertheless, the results were encouraging and may be useful in future discussions concerning active cavity radiometer performance.

Solar Tracker Contract

Efforts begun in 1985 to purchase replacement trackers for the NOAA network continued in 1986. After evaluation of proposals, the Eppley Laboratory was awarded a contract to produce prototype units for tests and evaluation. The Eppley prototype units were delivered in September and evaluated throughout the fall months for compliance with specifications required by the proposal. One of the units was loaned to SERI in Golden, CO, where it was fitted with position sensors to monitor its tracking accuracy. The SERI tests, using two different types of position sensors, verified compliance with required tracking specifications. Other compliance checks were completed in Boulder by SRF.

The tracker is an altitude azimuth design that is strong enough to carry a load equal to two Eppley active cavity radiometers (model HF), or approximately 20 pounds. The NOAA network versions are configured with two mounts made to hold an Eppley-style pyrheliometer.

Prototype Data Acquisition System

A two-pronged effort, begun in 1985 by NOAA, to modernize the solar radiation monitoring network has been associated with solar tracker replacement, discussed in the previous section, and data acquisition system replacement. The new data acquisition system is IBM-PC based. A software package for gathering data from one global and one direct-beam sensor, processing measurements into hourly totals, and comparing these with a site-specific clear-sky model, was developed by ARL. Site personnel will be able to run the model each day after sunset, examine measured hourly values versus expected hourly values, and flag days on which sensor or data acquisition malfunction might have occurred. The model also has menu options for incorporating daily turbidity data if available, and also cloudiness. The Boulder prototype unit and software were first used in mid-March and ran until roof construction activity in late May necessitated removal of sensors and data lines. The system was restarted later in the fall and has been operational to date.

SRF Computer/Data Acquisition System

A significant SRF upgrade during 1986 was the purchase and installation of a new 100-channel digitizer and the purchase of a new computer system to process data and control the digitizer. The computer is shared among other users in the GMCC/ARM Group. Installation was completed in October, and preliminary versions of data-gathering software were being developed by the end of the year.

New SRF Sensor Platforms

As a result of major RL-3 roof reconstruction, which lasted over 5 months, SRF rooftop activities were severely curtailed during 1986. However, the complete removal of all SRF rooftop tables and equipment created an opportunity to design and install new replacements. SRF tables were designed, constructed, and finally installed in November after completion of the roof work. Existing signal lines from the roof into the SRF laboratory were retained and reused. Channel capacity of the new SRF data acquisition system

is identical to the older setup, so significant cable modifications were not required.

The SRF platforms were fabricated using industrial fiberglass reinforced grating supported on a custom-designed framework built from aluminum structural members. For each platform, 3 × 9 ft gratings were used to replace the former SRF wooden platforms. The primary pyranometer table consists of two gratings set end to end on an aluminum framework, creating a level, very rigid platform 3 × 18 ft. It was configured to accommodate 45 pyranometers. Two other platforms of similar design are used for support of solar trackers carrying direct-beam sensors, additional pyranometer locations, and shading disk calibrations. Each pyranometer location consists of a circular aluminum base of 7.5-in diameter and 0.25-in thickness. The disks are attached to the grating, and individual pyranometers are positioned on the disks, leveled, and then bolted solidly to the disk. Advantages of the grated platforms are the structural rigidity, self-ventilating action to reduce the daily temperature variation of the sensors, and a design that provides for ease of cleaning the sensors after precipitation events, especially snow.

SRF Calibration Activity

Limited access to the new RL-3 roof became available in late summer 1986, and calibration activities were resumed but were restricted to comparisons of pyrheliometers and active cavity radiometers. Pyranometer calibrations are scheduled to begin early in 1987 after software is developed for the new data acquisition system and after the new pyranometer platforms become functional. The calibration activities of the SRF will be limited to instruments in the U.S. solar radiation network, instruments participating in government-sponsored field experiments such as FIRE, and instruments owned by noncommercial institutions, such as universities, that do not have regularly funded solar research programs.

TURBIDITY

GMCC's network of turbidity monitoring sites within the contiguous United States was expanded from 10 to 17 during 1986. The stations that were added are Ely, NV; Las Vegas, NV; Salt Lake City, UT; Sterling, VA; Madison, WI; Raleigh, NC; and Lander, WY. Sunphotometers at Sterling, Madison, Raleigh, and Lander have only been used to provide turbidity observations at 500 nm for input into an IBM-PC program for quality control of the solar radiation data at these stations. These locations are not yet reporting sunphotometer observations as part of the turbidity network. Turbidity measurements also continued at the four GMCC baseline stations during 1986. Table 3 lists the 21 stations and the wavelengths at which turbidity was measured.

The working instrument at most of the 21 stations is the NOAA J-series sunphotometer. New methods for quick and accurate calibration of these instruments continued to be tested during 1986. It was determined in 1984 that Langley plot calibrations made from observations at Boulder are unreliable. Intercomparisons with a precision standard instrument that was calibrated by the Langley plot method at MLO were substituted for Boulder Langley plot calibrations. Langley plot calibrations were also obtained from observations made in small aircraft flying over Colorado at 12,500 ft above

Table 3.--GMCC turbidity monitoring sites and filter wavelengths for sunphotometers used at each site

Station	Sunphotometer wavelength (nm)
Barrow, AK*	380, 500, 778, 862
Mauna Loa, HI*	380, 500, 778, 862
Samoa*	380, 500, 778, 862
South Pole*	380, 500, 778, 862
Alamosa, CO*	380, 500
Atlantic City, NJ	380, 500
Boulder, CO	380, 500, 778, 862
Bismarck, ND	380, 500
Caribou, ME*	380, 500
Ely, NV	380, 500
Huron, SD	380, 500
Lander, WY†	380, 500
Las Vegas, NV	380, 500
Madison, WI	380, 500
Meridian, MS*	380, 500
Raleigh, NC†	380, 500
Salem, IL	380, 500
Salt Lake City, UT	380, 500
Sterling, VA†	380, 500
Tallahassee, FL	380, 500
Victoria, TX*	380, 500

*BAPMoN stations.
†Not yet reporting data as part of the turbidity network.

sea level. Calibrations obtained from these flights appear to be comparable in repeatability and accuracy to calibrations made at MLO.

Turbidity project staff also initiated routine Langley plot calibrations at mountain sites west of Boulder at elevations of 9,500-10,300 ft above sea level. These calibrations also compare well with calibrations made at MLO. Calibrations in the mountains by the Langley plot method or in Boulder by the intercomparison method, have been chosen as the principal means for calibrating the J-series sunphotometers. In 1986, 118 instrument calibrations were completed.

Nine precision Mainz II sunphotometers were received from a manufacturer in West Germany in 1986. A circuit defect was discovered during calibrations at MLO, and the sunphotometers were returned to the manufacturer for repair. The manufacturer substantially redesigned the instruments and returned them in the fall of 1986. Recalibration was started late in the year. These sunphotometers will be used at Automated Dobson Network (ADN) sites to provide information on the climatology of aerosols and the potential effects of aerosols on Umkehr and total ozone measurements.

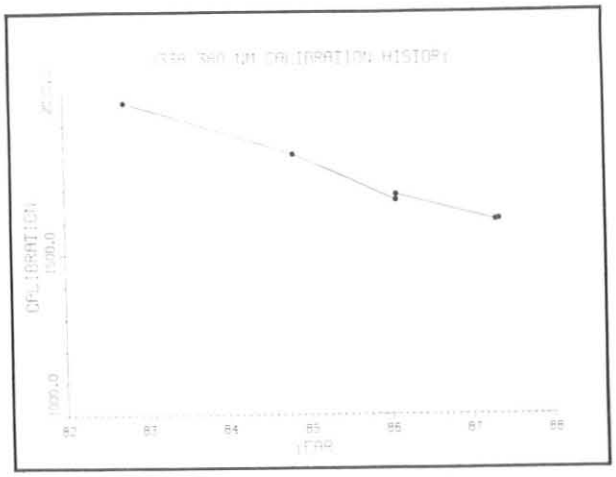

Figure 7.--Drift in J-series sunphotometer calibration.

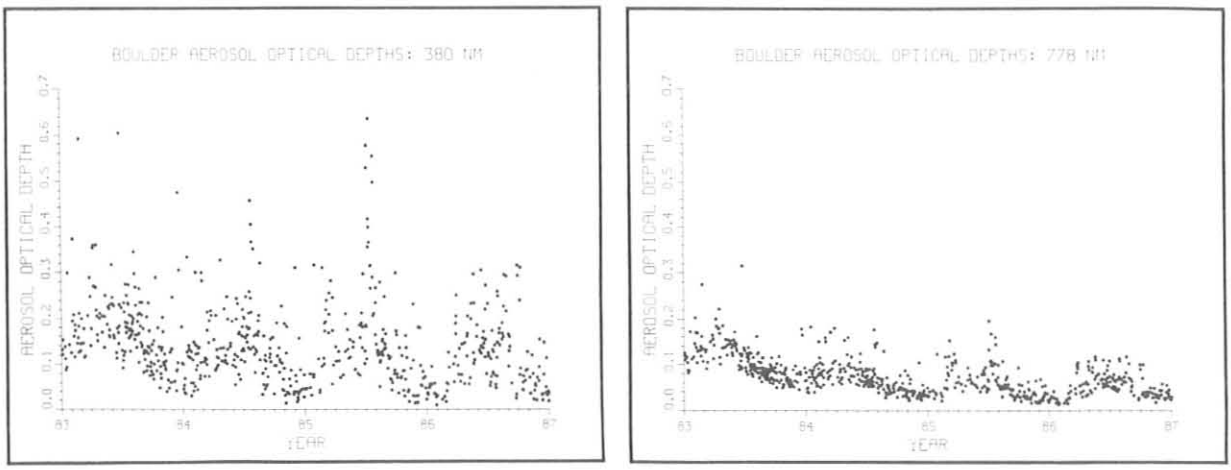

Figure 8.--Daily average aerosol optical depths at Boulder for 380 nm and 778 nm.

The calibration constants of the J-series sunphotometers drift with time. Additional calibration points in 1986 greatly improved the estimates of drift for these sunphotometers. Fortunately, as illustrated by fig. 7, the drift for many of the sunphotometers is nearly linear.

The availability of improved calibration histories made it necessary to revise the processed data for the turbidity network. In some cases, improved calibration data resulted in substantial changes in the turbidity record computed for 1983-1986.

Data processed to date include those from 1983 through the end of 1986 for Boulder, (see fig. 8) and 1983 through June 1986 for Bismarck, Huron,

Salem, Tallahassee, Alamosa, Meridian, Atlantic City, and Caribou. Victoria is complete for 1983 through November 1986. Data for 1986 for Las Vegas, Ely, and Salt Lake City have been processed.

Data for Boulder and other continental U.S. stations continue to show a clear annual cycle having maxima in the spring or summer months and minima during November, December, or January. The impact of El Chichon is evident at many stations and appears as a slow downward trend in optical depths since the beginning of the record in early 1983.

Data for the MLO baseline station (fig. 9) show the El Chichon perturbation and its exponential decay more clearly. The 1982-1985 record encompasses both the initial influx of volcanic aerosols and recovery to conditions approaching background. The annual springtime maximum, which is caused by advection of Asian dust, is also visible in the record. Figure 10 shows aerosol optical depths measured by the precision PMOD-type sunphotometer at MLO.

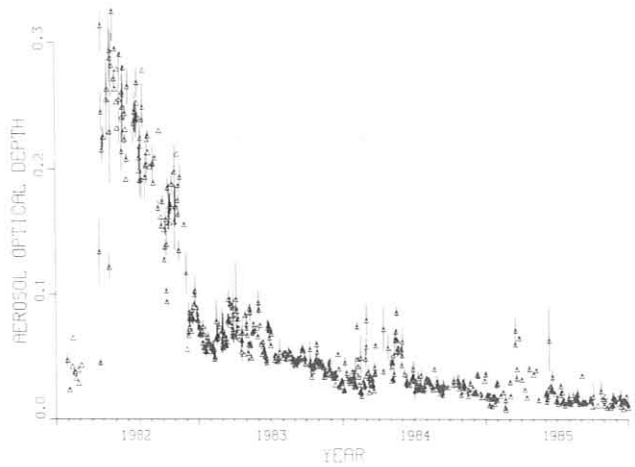

Figure 9.--Daily average aerosol optical depths at MLO for 500 nm, as measured with a NOAA J-series sunphotometer.

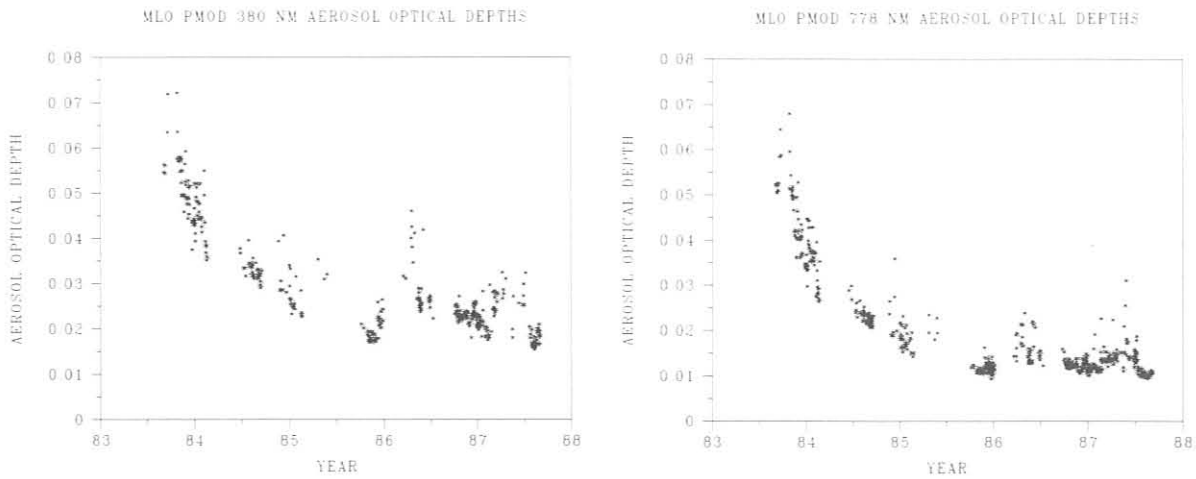

Figure 10.--Daily morning average aerosol optical depths at MLO for 380 nm and 778 nm, as measured with a precision PMOD-type sunphotometer.

UMKEHR RESEARCH

This year there were four separate research activities aimed at improving the Umkehr measurement and improving data analysis:

(1) Acquiring multiwavelength sunphotometers to measure aerosol optical depth at the automated Dobson sites.

(2) Designing and constructing zenith-sky cloud detectors to observe zenith-sky conditions during operation of the automated Dobson system.

(3) Continuing an analysis of the El Chichon stratospheric aerosol error to the Umkehr measurements for global-scale corrections. Data from the World Lidar Network are being used in this activity.

(4) Making a preliminary analysis of automated Dobson Umkehr ozone profiles for special features and comparison with ozonesonde data.

Items 1 and 2 are concerned with quality control of ADN Umkehr measurements. A nonobjective quality control procedure was established for a first look at the inverted ADN raw Umkehr data (inverted at Boulder) before they are submitted to the WODC at Toronto for reduction and publication in the Redbooks. This is a first-step procedure for quality control beyond the initial data processing procedure for converting R readings to N values. Procedures for items 1 and 2 are not finalized. However, when they are, they will be used in an operational mode. From the data acquired by items 1 and 2, estimated monthly errors (or corrections) to the Umkehr measurement will be constructed and issued for each ADN station. At ADN stations where lidar observations of stratospheric aerosol are not available, some delay in providing error estimates should be expected because it will be necessary to extrapolate stratospheric aerosol data from a variety of sources to the Umkehr stations lacking lidar data.

Stratospheric aerosol data are now derived from the following sources; however, because the missions of the institutions that provide these data are not dedicated to providing long-term data, a uniform flow of data cannot be anticipated:

(1) World Lidar Network, 11-12 stations. See International Activities (sec. 9) for more information.

(2) SAGE II satellite measurements provided by NASA Langley.

(3) Ground-based sunphotometer measurements provided by publications and the ADN sunphotometers.

(4) In situ, high-altitude aircraft measurements provided by NASA Ames.

(5) Balloon soundings of aerosol properties provided by the University of Wyoming.

The ARM Group has become an unofficial repository of stratospheric aerosol data because of the Umkehr correction problem. As a result, greater involvement with outside research activities concerned with the correction of remote sensing of ozone has ensued.

The stratospheric aerosol properties that provide necessary information for estimating errors to remote sensing systems are (1) vertical profile; (2) optical depth; (3) size distribution; (4) transport; (5) optical properties such as phase function, absorption, and extinction; (6) origin; and (7) the global distribution of the above properties and their changes with time.

3.2 Special Projects

POTENTIAL TEMPERATURE IN THE GRAND CANYON

The terrain near both the south and north rims of the Grand Canyon is heavily forested; therefore, controlled burning has become necessary along the rims to meet resource management objectives. Burning is done during the spring and fall of the year when the forest is dry and cool. A significant amount of smoke is produced, thus reducing visibility and enjoyment of the Canyon's scenic splendor.

A CESSNA T207 instrumented aircraft was flown over and within the eastern canyon at four altitudes in the same pattern. The two highest flight levels were flown above the south and east rims whereas the lowest two flights (2195 and 1981 m) were flown entirely within the canyon. Details of the flight path and geographic location can be found in Stearns (1987a).

Two days in June, a clear day and a cloudy day, were selected to illustrate the potential temperature structure within the canyon. Morning and afternoon analyses of cross sections of the canyon from the south to the north rim are given in fig. 11 for both days. On the clear day (9 June), data were obtained 3.5 hours after sunrise and before sunset. A cooler tongue of air present in the morning over the south rim at 2750 m extends almost across the canyon (fig. 11a). Cold pockets are noted below the south rim at 1981 m and near the north rim at 2195 m. These features create an unstable layer (shaded area) that extends across the canyon. In the afternoon of 9 June (fig. 11b), the cool tongue extends farther across the canyon, and now has an almost wave-like form consisting of two warm troughs between the crests and a small, closed cold pocket north of the center of the canyon at 2195 m. The unstable layers are at a higher elevation than in the morning. Two warmer tongues are found next to the two rims.

The sky was mostly cloudy all day on 11 June having 0.8 sky cover with cloud bases at 6100 m in the morning and two levels of clouds with bases at 3000 and 6100 m in the afternoon. The data flights were made 3 hours after sunrise and 2.5 hours before sunset. The only outstanding features of the morning analysis (fig. 11c) are a small warm tongue under the north rim and its associated instability, and a small area of instability above the south rim. In the afternoon (fig. 11d), a warm tongue extends from the south rim nearly across the canyon and a cold pool is in the center of the canyon. The unstable areas have deepened throughout most of the canyon.

The analyses of potential temperatures and thermal stability indicate that in the eastern portion of the Grand Canyon stable layers are common in the early morning. Downslope winds from the south rim do not regularly appear nightly nor are they observed very often (Schnell, 1986). A possible explanation of this absence of observed downslope winds is that the canyon walls and floor retain some of the solar radiation heat because of the complex geometry of the surfaces, as discussed in Stearns (1987b). This may reduce the total sensible heat lost to the atmosphere. The cooling of the surfaces is reduced, and therefore the gravity flow is reduced. Further study of the nightly infrared cooling is recommended to clarify this feature.

The potential temperature of dry air changes when heat is added or removed. This can be caused by frontal systems, warm or cold advection, radiational cooling or warming, conduction, and sometimes condensation. Cool air tends to move toward warm air, but this may be altered by broad-scale pressure patterns, stability, terrain constraints, and radiational cooling or warming. Therefore, because of the complexity of the problem, the reasons for cool pools of air in the canyon cannot be given simply. However, it is likely that density-induced flow is primarily responsible for local winds within the canyon.

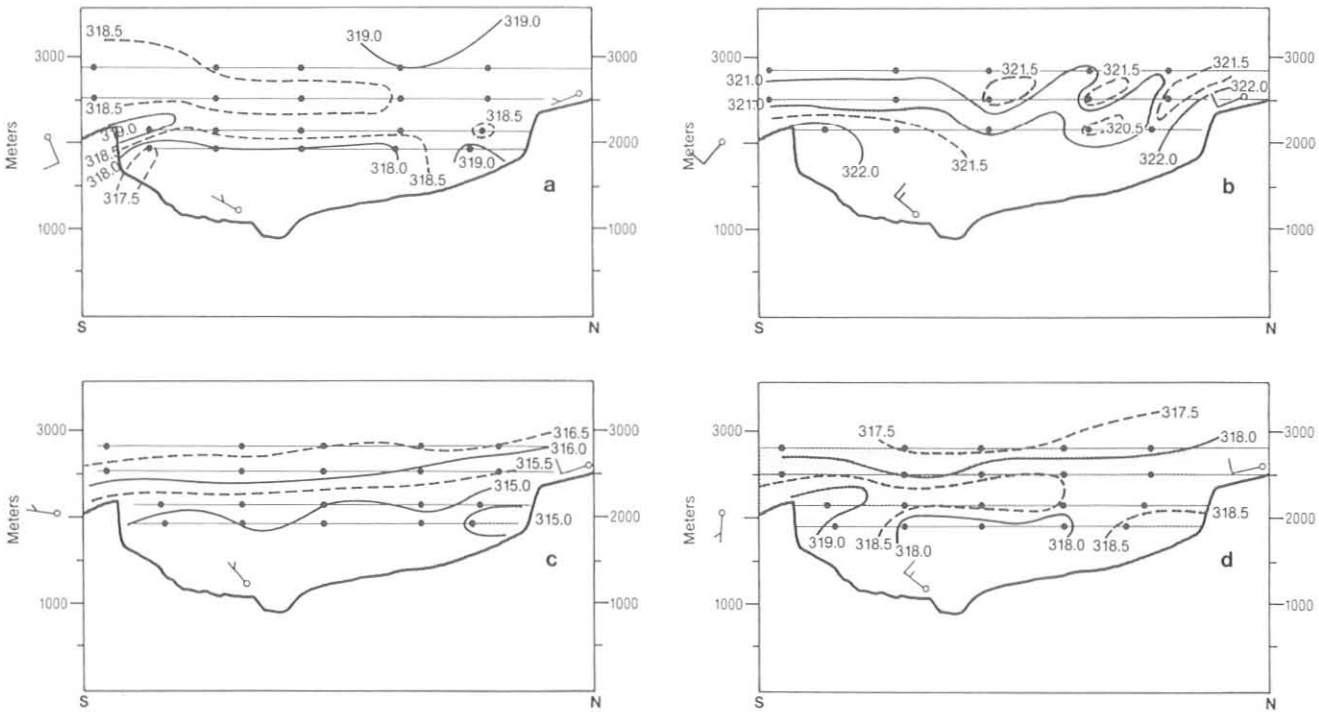

Figure 11.--Potential temperature isolines in the Grand Canyon. (a) 9 June 1985, morning; (b) 9 June, afternoon; (c) 11 June, morning; (d) 11 June, afternoon. Unstable areas are shaded. Wind barbs represent the airport on the left, Tonto Plateau Station near the center, and North Rim Station on the right; an upright flag denotes wind from the north. The heavy line represents the canyon floor. The horizontal lines show flight levels and the dots show data points used to draw the contour lines.

3.3 References

Bodhaine, B. A., and J. J. DeLuisi, 1985. An aerosol climatology of Samoa. Journal of Atmospheric Chemistry 3:107-122.

Bodhaine, B. A., E. G. Dutton, and J. J. DeLuisi, 1984. Surface aerosol measurements during AGASP. Geophysical Research Letters 11:377-380.

Bodhaine, B. A., J. J. DeLuisi, J. M. Harris, P. Houmere, and S. Bauman, 1986. Aerosol measurements at the South Pole. Tellus 38B:223-235.

Bodhaine, B. A., J. J. DeLuisi, J. M. Harris, P. Houmere, and S. Bauman, 1987. PIXE analysis of South Pole aerosol. Nuclear Instrument Methods B22:241-247.

Bodhaine, B. A., E. G. Dutton, J. J. DeLuisi, G. A. Herbert, G. E. Shaw, and A. D. A. Hansen, 1988. Aerosol measurements at Barrow. Journal of Atmospheric Chemistry, submitted.

Hay, J. E., and R. Darby, 1984. El Chichon, influence on aerosol optical depth and direct, diffuse and total solar irradiances at Vancouver, B.C. Atmospheres and Oceans 22:354-368.

Hirono, M. T., T. Shibata, M. Fujiewara, and N. Fujiewara, 1984. Enormous increase of volcanic clouds in the stratosphere over Fukuoka after April 1982. Geofisica Internacional 23:259-276.

Jager, R., R. Reiter, W. Carnuth, and W. Funk, 1984. El Chichon cloud over central Europe. Geofisica Internacional 23:243-258.

McCormick, M. P., T. J. Swissler, W. H. Fuller, W. H. Hunt, and M. T. Osborn, 1984. Airborne and ground-based lidar measurements of the El Chichon stratospheric aerosol from 90°N to 56°S. Geofisica Internacional 23:187-222.

Quakenbush, T. K., and B. A. Bodhaine, 1987. Surface aerosols at the Barrow GMCC Observatory: Data from 1976 through 1985. NOAA Data Rep. ERL ARL-10, NOAA Environmental Research Laboratories, Boulder, CO, 230 pp.

Samson, J. A., S. C. Barnard, J. S. Obremski, D. C. Riley, J. J. Black, B. B. Murphey, and A. W. Hogan, 1987. On the recent diminution of surface aerosol concentrations at the South Pole. Atmospheric Environment, submitted.

Schnell, R. C. (ed.), 1986. Geophysical Monitoring for Climatic Change, No. 13: Summary Report 1985. NOAA Environmental Research Laboratories, Boulder, CO, 146 pp.

Stearns, L. P., 1987a. Aspects of the local circulation at the Grand Canyon in the fall season. Journal of Climate and Applied Meteorology., in press.

Stearns, L. P., 1987b. Meteorological studies in the Grand Canyon. Boundary Layer Meteorology, submitted.

4. CARBON CYCLE GROUP

4.1 Continuing Programs

CONTINUOUS ANALYZERS

The in situ NDIR CO_2 analyzers at the four GMCC observatories continued to operate in 1986. Preliminary monthly and annual means for 1986 are shown in table 1, expressed in the WMO 1985 mole fraction scale (X85). The complete record for each station is shown in fig. 1. Data acquisition procedures remained the same as in 1985. The location of the air intake line at MLO was moved to the new walkup tower at an elevation of 80 ft in late December. Also at MLO, a new Siemens Ultramat-3 NDIR analyzer was ordered for eventual replacement of the URAS-2 analyzer, which has been in use at the station since May 1974.

Table 1.--Provisional monthly and annual mean CO_2 concentrations (ppm relative to dry air--X85 mole fraction scale) from the continuous CO_2 analyzers for 1986

	BRW	MLO	SMO	SPO
January	350.28	346.03	344.14	344.53
February	351.78	346.71	344.19	344.41
March	353.60	347.28	344.06	344.39
April	353.09	349.35	344.14	344.47
May	353.43	349.92	345.53	344.60
June	351.49	349.30	346.24	344.89
July	344.75	347.39	346.27	345.37
August	339.47	345.51	345.88	345.77
September	342.26	344.20	345.95	346.03
October	345.11	343.70	346.03	346.23
November	348.61	345.04	346.02	345.98
December	350.96	346.29	346.16	345.76
Annual	348.73	346.73	345.38	345.20

A digital-filtering technique involving the fast Fourier transform and low-pass filters was developed in 1986 for analysis of the continuous CO_2 data. This technique was used to smooth the data and to separate the seasonal cycle and long-term trend signals. The long-term trend, or secular increase, is defined in this method by the curve that results from a low-pass filter with the cutoff frequency at 0.55 cycles yr^{-1}. For the seasonal cycle the cutoff frequency is set at 7.3 cycles yr^{-1}, after the secular increase has been subtracted from the data. The resulting long-term trend curves are shown in fig 1. The average rate of increase was 1.27 ppm yr^{-1} for BRW, 1.42 ppm yr^{-1} for MLO, 1.32 ppm yr^{-1} for SMO, and 1.42 ppm yr^{-1} for SPO. The differences in the rates of increase are due mainly to the different starting

dates of the records for each station. The differences of the preliminary annual means between 1986 and 1985 are 1.73 ppm (BRW), 0.88 ppm (MLO), 1.02 ppm (SMO), and 1.35 ppm (SPO).

The calibrations of CO_2-in-air reference gas tanks continued in 1986; a Siemens Ultramat-3 NDIR analyzer replaced the URAS-2T analyzer. The precision of the Ultramat-3 is about four times better than that of the URAS-2T. On 139 days in 1986, 278 tanks were calibrated. A program for filling cylinders with natural air from Niwot Ridge, CO, was started. If this program is successful, these tanks may replace some of the synthetically prepared CO_2 reference gases that are now purchased from compressed gas suppliers.

FLASK SAMPLE CO_2 MEASUREMENTS

Measurements of the global distribution of atmospheric CO_2 continued during 1986. Whole air samples were collected in glass flasks at the sites of the NOAA/GMCC cooperative flask sampling network. The network consisted of the same 26 sites as in 1985 (Schnell, 1986). An analysis of the 1981-1984 flask data, spanning the 1982-1983 ENSO event, was completed (Conway et al., 1988).

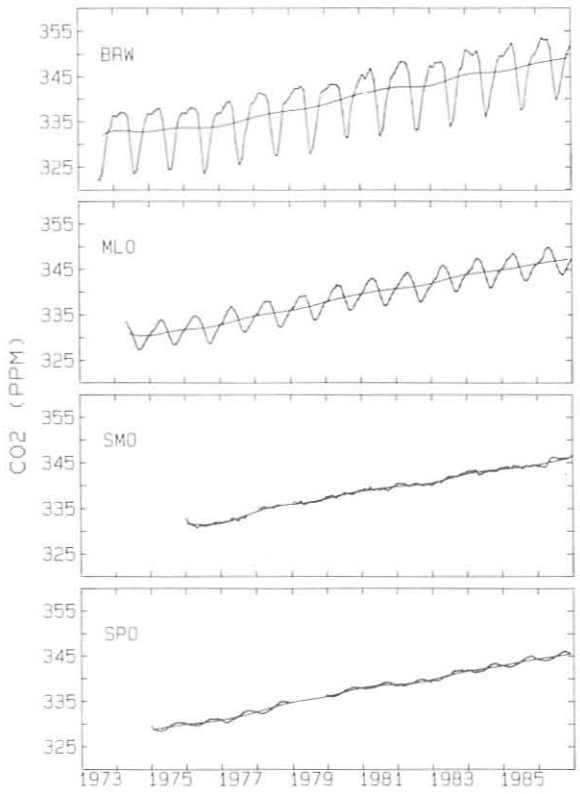

Figure 1.--Monthly mean CO_2 concentrations at the four GMCC observatories. The smooth curves represent the long-term trend (see text).

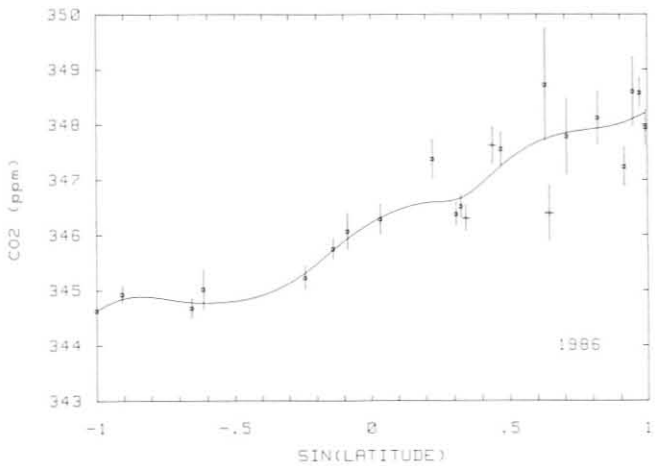

Figure 2.--Annual mean CO_2 concentrations vs. sin(latitude) for the GMCC flask sampling network. Data plotted with the symbol (+) have not been included in the curve fit (smooth curve).

The annual mean CO_2 concentrations for 1984-1986 are given in table 2. The annual mean CO_2 concentrations for 1986 are plotted vs. sin (latitude) in fig. 2. This figure extends the series of CO_2 vs. latitude plots given in Schnell (1986).

In 1986, the first full year of data was obtained for four sites at which sampling began in 1985: Alert, N.W.T., Canada; Shemya Island, Alaska; Midway Island; and South Georgia Island (the flasks from South Georgia Island had not been received at the time of this writing). In addition, samples were collected once per month at the Japanese Antarctic Research Program site at Syowa Station, Antarctica (69.0°S, 39.6°E). The Syowa Station flask data will be compared with the Japanese in situ data, providing the first intercomparison of the Japanese CO_2 program with GMCC. The 1986 CO_2 data for Alert and Syowa are shown in fig. 3.

Table 2. -- Provisional annual mean atmospheric CO_2 concentrations (ppm relative to dry air--X85 mole fraction scale) from the flask network sites

Code	Station	1984	1985	1986
ALT	Alert, N.W.T., Canada	--	--	348.0
AMS	Amsterdam I.	342.4	344.1	[ ]
ASC	Ascension I.	343.9	345.0	345.8
AVI	St. Croix, VI	343.4	345.4	346.4
AZR	Terceira I., Azores	344.5	346.0	349.2
BRW	Barrow, AK	345.4	346.5	348.5
CBA	Cold Bay, AK	345.5	347.2	348.1
CGO	Cape Grim, Tasmania	342.0	343.7	344.6
CHR	Christmas I.	344.8	345.9	346.3
CMO	Cape Meares, OR	344.9	347.4	347.8
COS	Cosmos, Peru	[ ]	[ ]	[ ]
GMI	Guam, Mariana I.	344.6	346.2	347.3
HBA	Halley Bay, Ant.	342.8	344.2	[ ]
KEY	Key Biscayne, FL	345.3	346.7	347.7
KUM	Cape Kumukahi, HI	344.3	345.6	346.5
MBC	Mould Bay, Canada	345.6	346.7	348.6
MID	Midway I.	--	--	347.5
MLO	Mauna Loa, HI	344.2	345.3	346.3
NWR	Niwot Ridge, CO	344.7	346.1	346.4
PSA	Palmer Station, Ant.	342.7	343.9	344.7
SEY	Mahé I., Seychelles	343.8	344.8	346.0
SGI	South Georgia I.	--	--	[ ]
SHM	Shemya I.	--	--	348.9
SMO	Cape Matatula, Am. Samoa	343.6	344.7	345.2
SPO	South Pole, Ant.	342.3	343.6	344.6
STM	Station M	344.7	346.0	347.2

[ ] No flasks received
-- No ongoing program

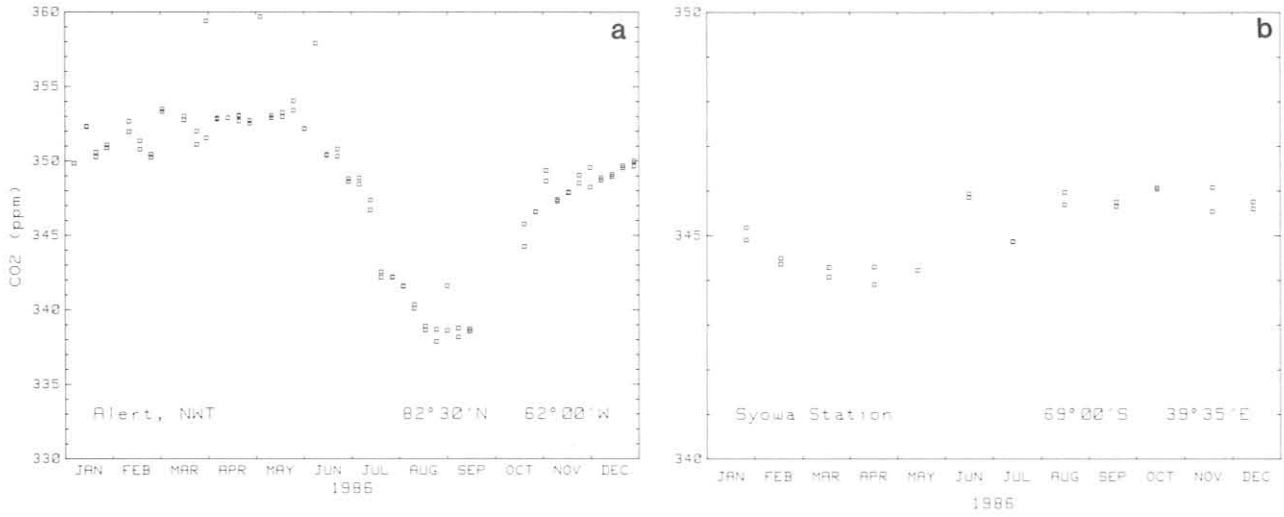

Figure 3.--Provisional 1986 flask data for (a) Alert and (b) Syowa Station. Note the different scales of a and b.

An analysis was made of the statistical uncertainties and some of the biases of results obtained from weekly flask samples. We constructed many artificial flask records by picking, using certain random procedures, hourly averages from the continuous records at BRW, MLO, and SMO. These hourly averages were then designated as flask measurements and treated as such (Conway et al., 1988) for data rejection and time series analysis. The "best fit" curves obtained for parallel artificial flask series differed from each other by amounts depending on the site and time of year. The summer drawdown is determined by flasks at BRW to about 1 ppm (one sigma), whereas at MLO the uncertainty is 0.3 ppm. This uncertainty is solely due to the sparsity of weekly samples combined with the atmospheric variability. There were also systematic biases of up to 0.5 ppm. The selection criteria for flasks are necessarily less stringent than those for continuous data. As a result, some of the diurnal variability at the site is evident in the flask records.

The following three new projects involving flask sample measurements were begun in 1986.

Aircraft Measurements

The purpose of this project is to determine the vertical distributions of several radiatively important trace species and the variation of these distributions over time. Samples are collected in stainless steel flasks during monthly flights of the NOAA OAO King Air aircraft based in Miami, FL. Concentrations of CH_4, CO_2, CO, and H_2 are measured in each sample. The concentrations of CFC-11, CFC-12, and N_2O are measured in a subset of samples from each flight. An example of the CH_4 and CO_2 concentration profiles is shown in fig. 4. These measurements will provide important constraints on two- and three-dimensional models used to study the sources, sinks, and transport of these species.

Shipboard Flask Sampling: Operation Pacific Air

This project is intended to provide higher resolution data than is available from our network of land-based sampling sites, to determine the spatial and temporal variations of the CO_2 and CH_4 distributions over the Pacific Ocean. The project is operated by the deck officers of the SOUTHLAND STAR, a container-carrying British merchant ship operated by Blue Star Lines, Ltd., London. Pairs of flask samples are collected at 5°-latitude intervals from 40°N to 40°S on scheduled voyages between Los Angeles, CA, and Auckland, New Zealand (fig. 5). Each round trip takes 6 weeks. This project will add about 15 regularly sampled floating stations in the Pacific Ocean and will triple the number of sites in this sector of the network.

Two-Dimensional Model

GMCC flask data are used in this project for one of the purposes for which they were originally intended: to deduce the globally significant sources and sinks of atmospheric CO_2. A two-dimensional (latitude and altitude) advective-diffusive atmospheric transport model based on the two-dimensional transport fields of Plumb and Mahlman (1987) was constructed. At each time step in the model, transport of the existing CO_2 concentrations occurs, and CO_2 sources and sinks are calculated as necessary to account for the discrepancy between the measured CO_2 distribution and the distribution resulting from transport alone. Preliminary results for the annual mean distribution and time variation of sources and sinks are encouraging and indicate that CO_2 measurements in continental regions are needed to deduce the source/sink distribution accurately.

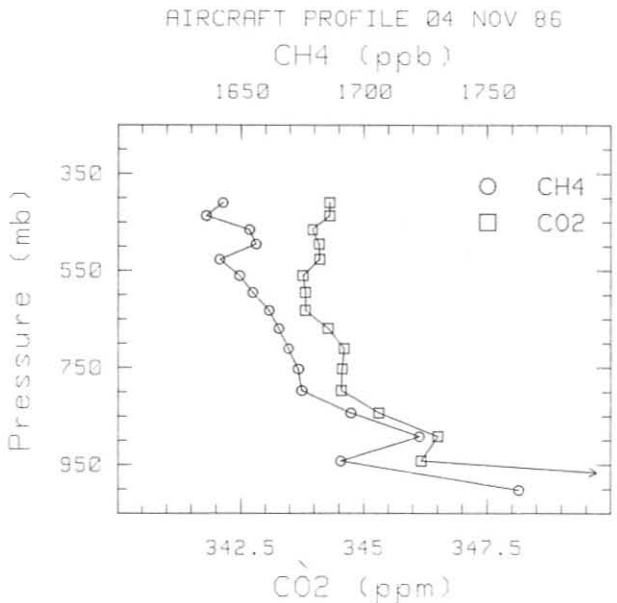

Figure 4.--Distribution of CH_4 and CO_2 concentrations determined from flask samples collected over the Gulf of Mexico off the coast of Ft. Myers, FL, 4 November 1986.

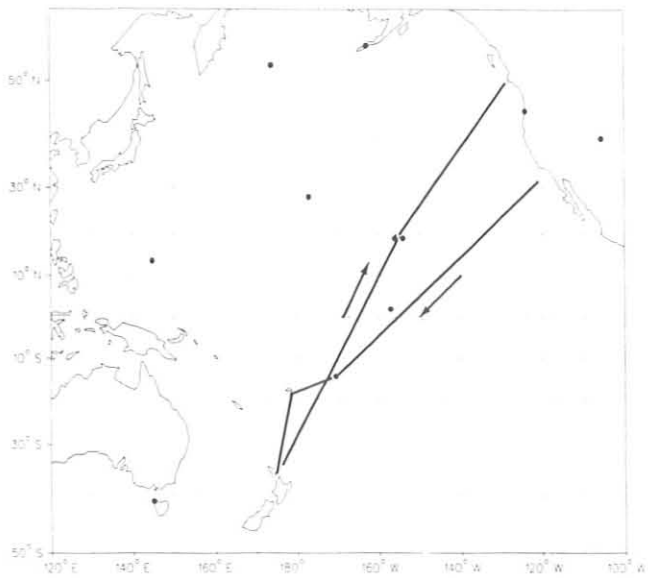

Figure 5.--Schematic representation of SOUTHLAND STAR cruise track for "Operation Pacific Air." Flask sampling sites of the flask network are indicated with dots.

FLASK SAMPLE METHANE MEASUREMENTS

As in previous years, the measurement of methane in air samples collected from the NOAA/GMCC cooperative flask sampling network continued in 1986. A global representation of the methane concentrations measured from the network sites in the remote marine boundary layer is shown in fig. 6. It covers the period from the beginning of this program in May 1983 through to the end of 1986. The procedures used in the construction of this type of figure are described in Steele et al. (1987). It should be noted that data from the high-altitude sites of Mauna Loa, Niwot Ridge, and Cosmos are not used in this global representation.

The globally averaged growth rate of methane derived from the results shown in fig. 6 is 12.96 ± 0.05 ppb yr^{-1}. This growth rate is calculated from a least-squares linear fit to the globally averaged 12-mo running mean methane concentrations (see Steele et al., 1987), and has a r^2 (correlation coefficient squared) value of 0.9996. This growth rate compares very closely with that of 12.8 ± 0.1 ppb yr^{-1} reported by Steele et al. (1987) for the globally averaged growth rate from the first 2 years of data from the flask network.

IN SITU METHANE MEASUREMENTS

An automated gas chromatographic system for the in situ measurement of atmospheric methane was installed at BRW in January 1986. The system is based upon a Hach-Carle series 400 gas chromatograph (model 04270-A) with a flame ionization detector. It provides real-time, hardcopy printouts of methane concentrations at the site, and writes the raw data onto magnetic data cassettes that are returned to Boulder for processing. Ambient air samples are analyzed every 24 minutes (60 samples per day), and each ambient sample analysis is bracketed by the analysis of samples of calibration gas. All air samples are dried before being injected onto the columns of the chromatograph.

The unselected methane data for 1986 are shown in fig. 7. From the start of regular operation on 29 January 1986 until the end of December 1986, 88% of the maximum possible methane data was obtained; the major loss occurred in July. During the year ambient methane concentrations frequently exceeded 2000 ppb, and sometimes even exceeded 3000 ppb. By constrast, the lower boundary of the data shown in fig. 7 is relatively well-defined, and clearly shows the seasonal variation in methane concentration. Agreement between these in situ measurements and the weekly flask air samples taken at BRW and analyzed in Boulder is very good.

In order to begin to understand the causes of the large variability of methane at BRW, a powerful, but flexible interactive software package named MUSIC was developed for use on the HP computers attached to the Shared Resources Management network system. This package operates on up to 1 month of hourly average data and can accept all of the surface meteorological, aerosol, and trace gas measurements currently made at the GMCC observatories. Time series plots can be generated, as can scatter plots of any variable against any other variable. The effects of various data selection criteria can be easily evaluated by plotting only those data that meet the

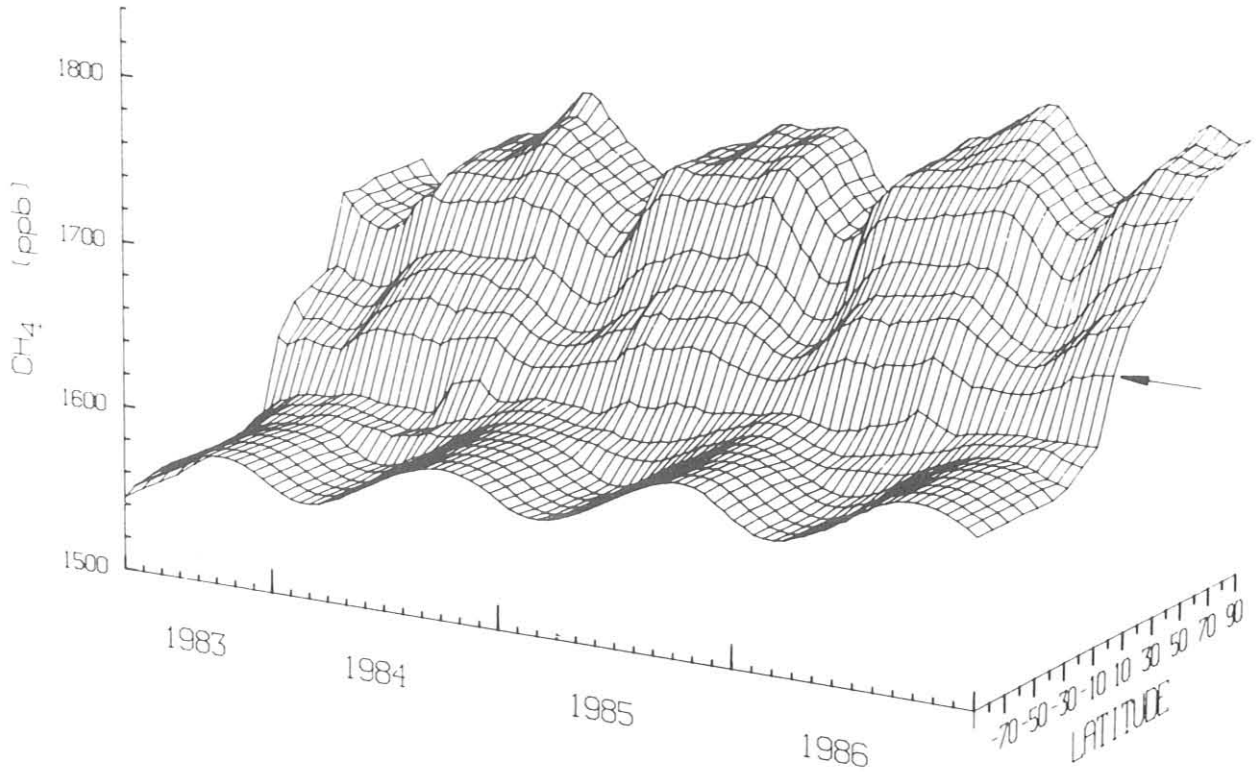

Figure 6.--Three-dimensional representation of atmospheric methane in the marine boundary layer from May 1983 to December 1986 inclusive. Grid spacing is 10° in latitude and 0.5 month in time. The arrow indicates the position of the equator.

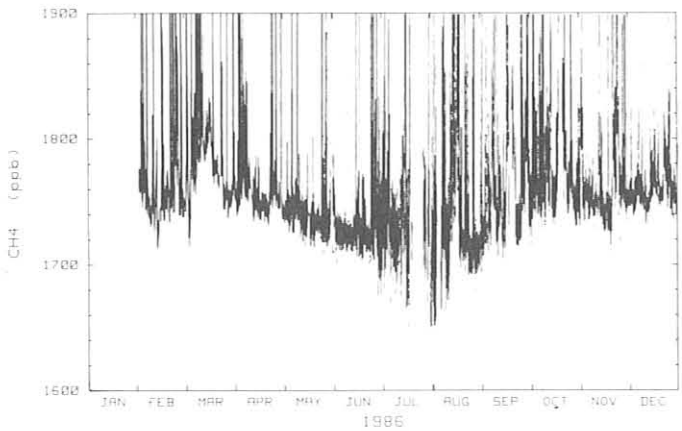

Figure 7.--Unselected record of in situ methane measurements at Barrow during 1986. Some concentrations exceed 1900 ppb.

specified restrictions. For example, the methane data obtained from only the clean air sector can be plotted simply by specifying the limits of the sector (in degrees). An example of the output of the MUSIC package is shown in fig. 8, the variation of methane concentrations with local wind direction at BRW during April 1986. The highest methane concentrations occur in a relatively narrow wind sector that corresponds to the location of the nearby Distant Early Warning line facility. Significantly elevated concentrations also occur sometimes when the winds are blowing from the direction of the township of BRW and the town dump.

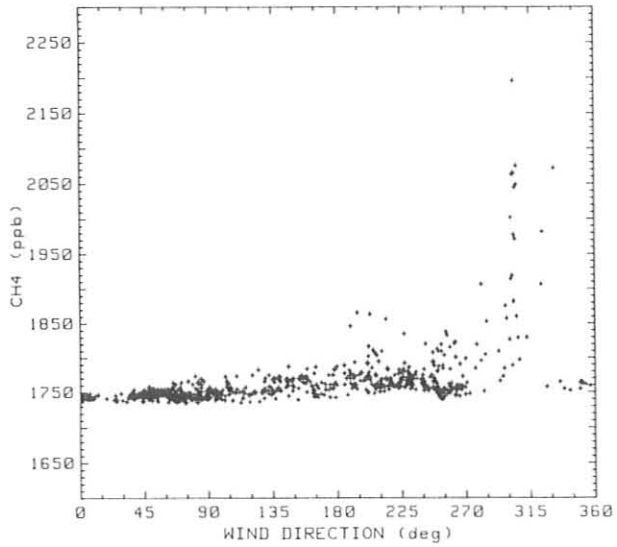

Figure 8.--Variation of hourly average in situ methane concentrations with hourly average wind direction at BRW during April 1986.

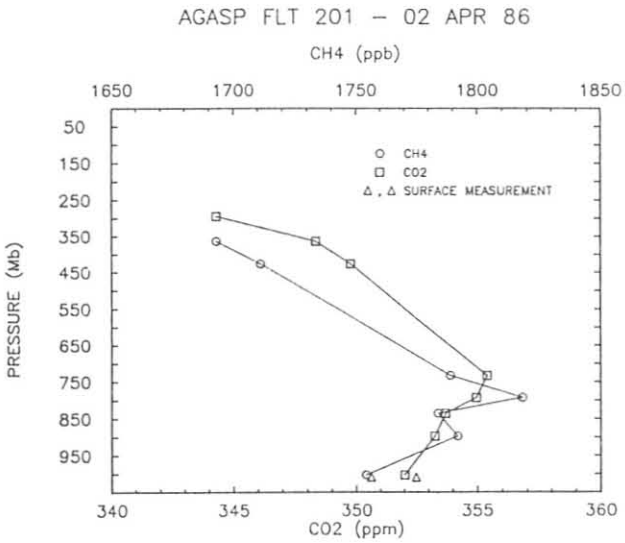

Figure 9.--CO_2 and CH_4 concentration vs. altitude for flight 201 during AGASP-II.

4.2 Special Projects

1986 EPOCS/CO_2 CRUISES

The CO_2 Group participated in the spring EPOCS and the annual PMEL carbon dioxide cruises aboard the NOAA Ship OCEANOGRAPHER during 1986.

The Weiss-design, custom-built gas chromatograph was set up aboard the ship by GMCC personnel in April prior to departure from Seattle on leg 1. The equipment was activated in May at Rodman Naval Station, Republic of Panama, prior to sailing on EPOCS leg 2. The monitoring program was operated by GMCC personnel until July when it was shut down at Kodiak, AK, and the equipment dismantled and stored aboard ship.

The OCEANOGRAPHER returned to Seattle in September and the equipment was reactivated by GMCC personnel in early October for the autumn EPOCS cruise. The monitoring program was operated on the autumn EPOCS cruise by PMEL personnel.

AGASP-II

During the second Arctic Gas and Aerosol Sampling Program in March and April 1986, 50 flask samples were collected on six flights of the NOAA WP-3D Orion aircraft. The purpose was to determine the horizontal and vertical distribution of CO_2 and CH_4 in the Arctic. For samples taken in the background troposphere we found negative vertical gradients (lower concentrations aloft) for both gases. The vertical profile measured on flight 201 (2 April 1986) is shown as an example in fig. 9. The strong correlation of CO_2 and CH_4 is apparent and is consistent throughout the entire data set.

Furthermore, elevated concentrations of CO_2 and CH_4 were found to be associated with haze layers. This correlation between the two gases seen in the aircraft samples was corroborated by in situ surface measurements of these gases made at the BRW observatory during March and April 1986. The strong correlation between the methane and carbon dioxide concentrations suggest a common source region for both, with subsequent long-range transport of the polluted air to the Arctic. These results were presented in detail by Conway and Steele (1987).

JOINT U.S.-MEXICO CRUISE

In July-August 1986, 12 pairs of flasks were collected aboard the Mexican research vessel H-02 during a joint U.S.-Mexico cruise in the Gulf of Mexico. These samples were collected in support of the more extensive measurements made by ESG of NOAA/ERL. The lowest measured concentrations of CO_2 and CH_4 were similar to measurements at flask network sites at comparable latitudes. The remainder of the samples showed high and variable CO_2 and CH_4 concentrations, reflecting the influence of nearby anthropogenic or biological sources of these gases.

4.3 References

Conway, T.J., and L.P. Steele, 1987. Carbon dioxide and methane in the Arctic atmosphere. Journal of Atmospheric Chemistry (submitted).

Conway, T.J., P. Tans, L.S. Waterman, K.W. Thoning, K.A. Masarie, and R.H. Gammon, 1988. Atmospheric carbon dioxide measurements in the remote global troposphere, 1981-1984. Tellus (in press).

Plumb, R.A., and J.D. Mahlman, 1987. The zonally averaged transport characteristics of the GFDL general circulation/transport model. Journal of the Atmospheric Sciences 44:298-327.

Schnell, R.C. (ed.), 1986. Geophysical Monitoring for Climatic Change, No. 14: Summary Report 1985. NOAA Environmental Research Laboratories, Boulder, CO, 146 pp.

Steele, L.P., P.J. Fraser, R.A. Rasmussen, M.A.K. Khalil, T.J. Conway, A.J. Crawford, R.H. Gammon, K.A. Masarie, and K.W. Thoning, 1987. The global distribution of methane in the troposphere. Journal of Atmospheric Chemistry 5:125-171.

5. MONITORING TRACE GASES GROUP

5.1 Continuing Programs

TOTAL OZONE

Routine total ozone observations were made with Dobson spectrophotometers during 1986 at 15 stations that constitute the U.S. total ozone station network (table 1). Of the 15 stations, 5 are operated by GMCC personnel, 3 are foreign cooperative stations, 3 are domestic cooperative stations, and 4 are operated by NWS.

Table 1. U. S. Dobson ozone spectrophotomer station network for 1986

Station	Period of record	Inst. no.	Agency
Bismarck, ND	1 Jan 1963-present	33	NOAA
Caribou, ME	1 Jan 1963-present	34	NOAA
SMO	19 Dec 1975-present	42	NOAA
Tallahassee, FL	2 May 1964-present	58	NOAA; Fla. State Univ.
Nashville, TN	2 Jan 1963-present	79	NOAA
SPO	17 Nov 1961-present	82	NOAA
Wallops Is., VA	1 Jul 1967-present	86	NOAA; NASA
Huancayo, Peru	14 Feb 1964-present	87	NOAA; Huancayo Obs.
Fresno, CA	22 Jun 1983-present	94	NOAA
Boulder, CO	1 Sep 1966-present	61	NOAA
Poker Flat, AK	6 Mar 1984-present	63	NOAA; Univ. of Alaska
MLO	2 Jan 1964-present	76	NOAA
Perth, Australia	30 Jul 1984-present	81	NOAA; Australian Meteorol. Dept.
Haute Provence, France	2 Sep 1983-present	85	NOAA; Obs. Haute Prov.
Barrow, AK	6 Jun 1986-present	91	NOAA

Daily 1986 total ozone amounts applicable to local apparent noon for stations in the U.S. Dobson instrument network have been archived by the World Ozone Data Centre, 4905 Dufferin Street, Downsview, Ontario M3H5TH, Canada, in Ozone Data for the World. Table 2 lists provisional monthly mean total ozone amounts for 1986 for the NOAA observatories and cooperative stations.

WMO International Dobson Spectrophotometer Comparison

In a continuing program within the WMO Global Ozone Monitoring and Research Project to upgrade the quality of worldwide total ozone observations, a comparison of Dobson ozone spectrophotometers was held in Arosa, Switzerland, 11-29 August 1986 at the Laboratory for Atmospheric Physics. A total of 16 Dobson instruments and 3 Brewer instruments participated in the intercomparison. Participants in the comparison are listed in table 3.

Table 2.--Provisional 1986 mean total ozone amounts (milli-atm-cm)

	Jan	Feb	Mar	Apr	May	Jun	Jul	Aug	Sep	Oct	Nov	Dec
Bismarck, ND	366	295	368	358	341	308	316	302	306	287	308	322
Caribou, ME	380	400	404	379	374	352	339	--	293	302	324	323
SMO	255	257	256	255	260	258	253	250	257	263	243	--
Tallahassee, FL	312	312	323	344	337	332	311	322	301	296	271	277
Nashville, TN	329	334	337	340	325	321	314	309	286	293	305	302
SPO	280	262	227	221	230	243	240	250	--	184	313	321
Wallops Is., VA	347	352	345	386	356	331	324	316	295	295	312	294
Huancayo, Peru	254	252	252	245	--	249	--	--	--	--	--	--
Fresno, CA	309	326	326	344	341	322	313	307	308	297	278	299
Boulder, CO	319	313	342	326	334	310	300	299	288	279	278	305
Poker Flat, AK	--	--	--	--	--	394	338	329	336	293	280	--
MLO	243	263	269	292	281	279	266	259	258	261	248	251
Perth, Australia	270	267	266	261	273	292	307	305	314	329	305	297
Haute Provence, France	365	392	370	409	365	349	323	308	299	289	312	315
BRW	--	--	--	--	--	--	348	296	308	--	--	--

Table 3.--Arosa intercomparison participants

Country	Instrument	Participants
	Dobson Instrument	
United States	83	W. Komhyr, R. Grass, R. Evans, and K. Leonard
Portugal	13	No participant
Switzerland	15	H. Dütsch
Belgium	40	D. DeMuer
Switzerland	51	K. Aeschbacker
Norway	56	S. Larsen
German Democratic Republic	64	U. Feister
German Democratic Republic	71	P. Plessing
Czechoslovakia	74	V. Vanicek
Poland	84	M. Vegorska, B. Rojewska-Wiech
France	85	A. Bekaddour
Denmark	92	P. Christensen, J. Bjerglind
Egypt	96	G. K. Y. Hassan
Switzerland	101	A. Rösch
Federal Republic of Germany	104	R. Hartmannsgruber, H. Claude, and U. Köhler
El Arenosillo, Spain	120	J. Cacho
	Brewer Instrument	
Federal Republic of Germany	10	U. Köler
Canada	17	J. Kerr, K. Lamb
Greece	5	I. Ziomas, A. Bais

Work was performed on several other Dobson instruments during 1986. A new air wedge was installed in Bismarck, ND, Dobson no. 33, because the old air wedge had deteriorated. An air wedge was also installed in Nashville, TN, Dobson no. 79. The Bismarck and Nashville instruments were optically aligned and recalibrated by means of direct comparison with the World Standard Dobson no. 83.

Dobson no. 93 on loan to INPE at Natal, Brazil, was recalled for recalibration. After installing an air wedge, the instrument was optically aligned and then recalibrated by means of direct comparison with Dobson no. 83. Instrument no. 93 was returned to Natal in May 1986.

A calibration check was made on automated Dobson no. 72 by directly comparing it with World Standard Dobson no. 83 on 1 May 1986. This instrument was shipped to Lauder, New Zealand, in late 1986 for initiation of the automated Dobson program in early 1987.

OZONE VERTICAL DISTRIBUTION

Ozonesonde Observations

With funding from NESDIS, weekly high-altitude ozonesonde balloon flights were continued at Boulder, CO (60); Hilo, HI (48); and Edmonton, Alberta, Canada (in cooperation with AES, Canada). These data will be used by NESDIS to validate SBUV ozone retrievals from the NOAA F satellite. In addition, weekly ECC ozonesonde flight programs at GMCC baseline stations SMO and BRW were begun in April and February 1986, respectively. An increased number of flights from BRW in April coincided with the AGASP-II.

A cooperative project with DSIR, New Zealand (with funding from CMA and NOAA), began in August 1986 to complement Southern Hemisphere ozone information from SPO and SMO. From a total of 37 balloon flights made in 1986 from Lauder, New Zealand, 26 flights were made from August through September, the period of ozone hole activity in Antarctica.

A program of ozone soundings at Amundsen-Scott base, South Pole, was conducted throughout 1986 with support from NOAA and NSF. Twice-monthly flights were launched from January through July, twice-weekly flights from August through mid-November, and once-weekly flights the remainder of the year. The total of 51 South Pole ozone profiles for 1986 has been published in NOAA Data Report ERL ARL-11 (Komhyr et al., 1987b).

Averaged Dobson correction factors for the year at stations where total ozone readings are rountinely taken on days of balloon flights were Boulder, 1.020 ± .058; Hilo, 1.009 ± .056; and Lauder, 1.020 ± .055. These mean differences in Dobson versus ECC sonde values for integrated ozone come mainly from uncertainties in pump efficiency corrections above 10 mb and differences in sampling times and locations between the Dobson and sonde observations. Mean seasonal ECC sonde data for mandatory atmospheric pressure levels are presented in table 4.

Table 4.--Seasonal partial pressure data (nb) for mandatory atmospheric pressure levels obtained from soundings in 1986*

Pressure (mb)	Jan-Mar	Apr-Jun	Jul-Sep	Oct-Dec
		Barrow		
sfc	16 (23.3) 10.1	7 (16.7) 12.7	4 (22.0) 6.9	7 (28.9) 5.0
1000	16 (28.1) 9.1	7 (20.9) 14.6	4 (22.8) 6.2	7 (28.7) 4.4
700	16 (33.4) 4.5	7 (35.7) 15.5	4 (31.5) 9.5	7 (30.3) 3.5
500	16 (26.6) 3.0	7 (32.3) 10.6	4 (31.5) 9.5	7 (24.3) 3.5
300	16 (34.9) 19.3	7 (46.4) 36.6	4 (41.5) 18.5	7 (27.0) 18.8
200	16 (104.4) 39.8	7 (108.9) 37.1	4 (64.8) 6.9	7 (68.4) 27.8
150	16 (130.1) 41.2	6 (124.3) 56.0	4 (74.3) 14.1	7 (93.0) 36.3
100	16 (161.0) 59.4	6 (139.3) 40.8	3 (105.0) 24.0	6 (116.3) 31.1
70	16 (204.4) 35.8	6 (183.8) 40.8	3 (131.0) 11.1	6 (141.3) 24.2
50	15 (211.5) 27.8	6 (173.2) 31.2	3 (113.7) 0.6	5 (132.8) 12.8
30	13 (173.9) 33.9	6 (131.2) 23.8	3 (113.3) 10.2	3 (109.3) 22.2
20	8 (118.5) 57.7	5 (99.2) 12.3	3 (96.7) 14.2	3 (71.3) 37.0
10	5 (73.0) 26.4	5 (61.0) 6.2	--	2 (38.0) 9.9
7	4 (53.5) 23.8	4 (38.8) 5.7	--	1 (22.0) 0.0
5	4 (35.5) 18.4	3 (23.7) 4.9	--	1 (15.0) 0.0
3	--	--	--	1 (5.0) 0.0
		Boulder		
sfc	13 (32.0) 6.5	18 (39.3) 14.4	11 (38.8) 11.1	15 (26.6) 7.3
700	13 (34.5) 5.4	18 (43.1) 8.7	11 (40.8) 9.3	15 (31.3) 3.6
500	13 (26.8) 3.7	18 (30.9) 6.4	11 (27.1) 8.5	15 (23.3) 2.6
300	13 (25.3) 16.2	18 (26.0) 15.0	11 (16.2) 6.1	15 (16.6) 7.6
200	13 (42.8) 42.3	18 (51.9) 38.2	11 (15.6) 5.2	15 (26.5) 12.7
150	13 (50.8) 36.8	18 (61.7) 26.9	11 (21.2) 8.9	15 (25.3) 11.1
100	13 (59.9) 38.4	18 (61.4) 32.2	11 (39.5) 8.7	15 (40.4) 25.6
70	13 (100.9) 30.4	18 (93.1) 21.0	11 (76.4) 9.5	15 (81.9) 17.5
50	13 (162.5) 15.0	18 (109.6) 15.2	11 (110.8) 5.9	15 (118.7) 17.9
30	13 (154.5) 9.1	18 (137.8) 8.6	11 (136.4) 7.5	14 (139.1) 11.5
20	13 (120.7) 10.4	18 (120.7) 8.9	11 (130.7) 3.8	14 (118.6) 8.1
10	13 (62.7) 9.2	18 (78.7) 4.8	11 (78.2) 4.3	14 (66.5) 7.6
7	12 (41.0) 5.2	13 (50.7) 7.2	11 (51.0) 2.9	14 (43.9) 5.3
5	12 (27.2) 2.9	12 (31.7) 3.7	10 (31.7) 2.1	14 (28.2) 4.1
3	3 (9.3) 0.6	5 (9.2) 1.9	3 (14.0) 1.0	7 (12.0) 3.1

Table 4.--Seasonal partial pressure data (nb) for mandatory atmospheric pressure levels obtained from soundings in 1986*--continued

Pressure (mb)	Jan-Mar			Apr-Jun			Jul-Sep			Oct-Dec		
					Hilo							
sfc	11	(17.0)	13.2	11	(25.5)	13.6	11	(15.2)	9.0	12	(24.0)	11.4
1000	11	(18.6)	12.8	11	(24.1)	12.6	11	(14.2)	8.7	12	(27.2)	10.0
700	11	(34.9)	9.3	11	(39.5)	11.5	11	(18.8)	11.3	12	(26.1)	6.9
500	11	(24.9)	6.8	11	(23.5)	8.6	11	(13.5)	4.9	12	(20.6)	3.2
300	11	(13.4)	4.5	11	(13.6)	6.4	11	(5.8)	3.5	12	(13.8)	5.4
200	11	(10.5)	4.2	11	(13.7)	5.4	11	(4.5)	2.0	12	(9.2)	4.9
150	11	(9.5)	3.9	11	(15.6)	7.3	11	(3.6)	1.5	12	(7.9)	3.2
100	11	(9.8)	4.4	11	(28.3)	10.4	11	(16.1)	4.3	12	(10.8)	3.0
70	11	(32.5)	15.3	11	(52.5)	13.6	11	(41.8)	3.9	12	(39.3)	11.7
50	11	(70.8)	14.0	11	(89.3)	15.5	11	(79.1)	5.2	12	(77.6)	7.1
30	11	(138.5)	10.4	11	(131.8)	5.1	11	(129.3)	8.4	12	(124.3)	8.7
20	11	(124.1)	4.3	11	(135.6)	6.0	11	(136.7)	7.4	12	(131.8)	7.3
10	11	(89.0)	9.7	11	(92.9)	3.4	11	(89.5)	5.0	11	(89.7)	7.9
7	11	(54.4)	5.7	11	(56.8)	5.8	11	(59.1)	6.7	11	(53.0)	3.8
5	11	(31.4)	5.5	10	(32.4)	3.4	11	(35.3)	6.3	11	(30.3)	2.5
3	1	(7.0)	0.0	4	(8.5)	4.4	8	(11.1)	7.2	2	(7.5)	3.5
					South Pole							
sfc	6	(13.2)	4.0	7	(18.6)	2.4	14	(18.4)	2.5	23	(14.5)	4.4
500	6	(11.7)	1.9	7	(16.6)	2.2	14	(17.2)	1.6	23	(13.8)	1.9
300	6	(35.0)	20.0	7	(24.3)	17.1	14	(13.5)	2.7	23	(15.3)	6.7
200	6	(54.0)	7.9	7	(45.7)	9.2	14	(34.1)	9.2	22	(46.5)	18.2
150	6	(59.2)	6.4	6	(57.2)	9.1	14	(57.9)	7.0	21	(58.6)	10.2
100	6	(107.8)	15.4	4	(83.3)	29.1	14	(95.2)	23.6	21	(60.4)	23.0
70	6	(139.5)	4.2	4	(129.8)	37.7	14	(119.9)	35.4	21	(87.5)	67.4
50	6	(122.2)	14.0	4	(134.3)	12.8	13	(106.6)	35.9	20	(99.2)	71.7
30	6	(94.2)	25.4	4	(84.3)	10.2	13	(81.0)	11.0	18	(114.0)	34.1
20	6	(64.3)	10.4	4	(56.0)	3.5	13	(71.8)	5.7	16	(85.1)	18.8
10	6	(30.5)	7.6	3	(34.0)	5.3	10	(43.3)	4.9	8	(43.3)	2.7
7	3	(20.7)	3.2	2	(25.0)	9.9	1	(32.0)	0.0		--	
5	2	(14.5)	3.5	2	(15.0)	8.5		--			--	
3	1	(8.0)	0.0	1	(14.0)	0.0		--			--	

Table 4.--Seasonal partial pressure data (nb) for mandatory atmospheric pressure levels obtained from soundings in 1986*--continued

Pressure (mb)	Jan-Mar	Apr-Jun	Jul-Sep	Oct-Dec
		Lauder		
sfc	--	--	14 (20.4) 5.3	19 (17.3) 4.4
700	--	--	14 (26.0) 3.4	19 (24.4) 5.7
500	--	--	14 (22.5) 4.9	19 (21.7) 5.7
300	--	--	14 (22.3) 8.7	19 (22.5) 15.1
200	--	--	14 (65.8) 20.1	19 (50.7) 19.2
150	--	--	14 (66.4) 27.3	19 (52.5) 20.0
100	--	--	14 (103.6) 28.0	19 (71.3) 19.0
70	--	--	14 (146.9) 36.0	19 (127.5) 26.2
50	--	--	13 (178.2) 21.1	19 (158.7) 23.6
30	--	--	13 (152.2) 8.9	19 (142.4) 14.3
20	--	--	12 (123.8) 8.2	19 (118.2) 9.5
10	--	--	5 (66.4) 7.2	--
7	--	--	4 (44.8) 4.6	--
5	--	--	2 (30.5) 0.7	--
		Samoa		
sfc	--	12 (15.6) 7.2	10 (20.9) 7.0	10 (17.5) 5.9
1000	--	12 (15.7) 7.2	10 (20.9) 7.0	10 (17.7) 5.7
700	--	12 (20.9) 7.5	10 (22.8) 9.3	10 (25.0) 9.7
500	--	12 (16.1) 4.9	10 (15.4) 4.0	10 (22.2) 9.3
300	--	12 (10.9) 6.2	10 (9.9) 2.2	10 (12.7) 4.9
200	--	12 (8.3) 3.4	10 (8.6) 3.7	10 (7.0) 2.5
150	--	12 (7.9) 3.2	10 (8.4) 4.1	10 (6.0) 1.8
100	--	12 (10.2) 2.8	10 (10.7) 3.7	9 (7.3) 3.1
70	--	11 (30.7) 4.5	10 (32.9) 8.5	9 (32.6) 9.0
50	--	10 (74.2) 9.1	10 (86.8) 11.8	9 (76.7) 12.2
30	--	10 (127.9) 14.1	10 (120.2) 8.1	9 (121.7) 12.4
20	--	10 (136.5) 6.7	7 (129.1) 9.3	9 (131.0) 11.0
10	--	5 (87.0) 9.3	5 (83.8) 9.3	4 (105.5) 22.5
7	--	3 (58.3) 6.1	4 (60.3) 5.3	2 (110.0) 2.8
5	--	2 (39.0) 1.4	2 (33.5) 2.1	1 (90.0) 0.0

*Values in parentheses are the ozone partial pressures. Values preceding and following each value in parentheses are the number of observations per season and the standard deviation of the seasonal mean value, respectively.

Vertical profiles of ozone partial pressure for each season are plotted in fig. 1; the data from each station for each hemisphere are plotted together. The strong latitudinal gradient in the lower stratosphere during the winter and spring is readily apparent in the Northern Hemisphere but is much less pronounced in the Southern Hemisphere. In the Southern Hemisphere during October-December there is less ozone at South Pole than at Lauder, reflecting the influence of the hole phenomenon.

Umkehr Observations

Umkehr observations were made in 1986 at six stations: Boulder (BDR), CO, 40°N, 105°W; Mauna Loa Observatory (MLO), HI, 20°N, 156°W; l'Observatoire de Haute Provence (OHP), France, 44°N, 6°E; Poker Flat Research Range (PKF), AL, 65°N, 148°W; Perth Airport, Australia, 32°S, 116°E; and Huancayo Observatory, Peru, 12°S, 75°E. Table 5 shows the number of conventional and short Umkehr observations made and reduced for each station.

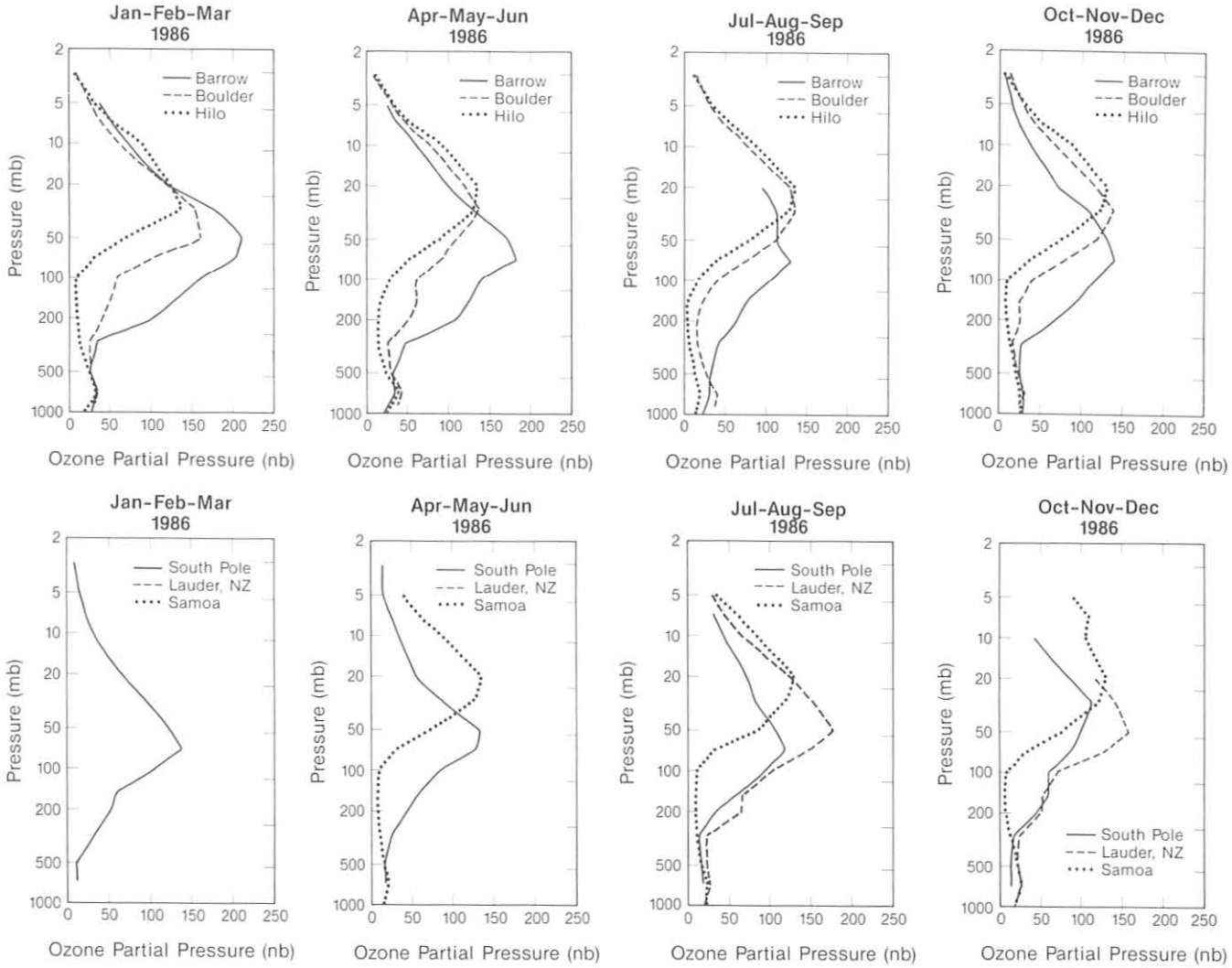

Figure 1.--Mean seasonal ECC ozonesonde vertical distributions for the Northern Hemisphere (top) and the Southern Hemisphere (bottom), from the six-station GMCC sonde network.

Table 5.--The numbers of conventional/short Umkehr observations made at the automated Dobson spectrophotometer stations in 1986

Station	Jan	Feb	Mar	Apr	May	Jun	Jul	Aug	Sep	Oct	Nov	Dec
BDR	22/22	5/5	12/14	8/8	17/17	9/9	16/16	14/16	17/17	12/12	15/16	28/30
MLO	45/45	41/41	28/28	23/23	35/35	40/40	22/23	27/28	12/13	29/29	23/23	41/41
OHP	14/16	9/8	21/20	11/10	22/21	19/19	21/23	17/17	28/29	21/20	17/18	21/22
PKF	--	--	--	--	12/11	14/14	7/7	6/8	7/7	8/13	--	--
PTH	28/28	19/19	29/30	36/37	16/17	16/18	13/14	15/15	5/5	17/17	27/27	29/29
HUA	5/5	2/2	2/2	1/1	--	11/11	--	--	--	--	--	--

Disk drives were added to the stations early in 1986, and the operating system rewritten. There was less down time at the stations in 1986, except for Huancayo Observatory. This station stopped making observations in late June, and remained down for the rest of the year. The reason had not been determined by the end of the year. At the end of October, equipment was shipped to New Zealand for installation of a seventh site at Lauder, 45°S, 169°E.

Ozone vertical distributions at five sites, derived from conventional Umkehr observations, are plotted in fig. 2. Mean annual ozone partial pressures for the various Umkehr layers are indicated on the plots, together with standard deviations of the layer annual mean values.

OZONE HOLE AT SOUTH POLE

The ozone vertical profile measurement program at Amundsen-Scott (Komhyr et al., 1987a), 51 vertical profiles (see Ozonesonde Observations). In addition to providing detailed ozone profiles to altitudes of 30-35 km, the ozonesonde data were integrated to give a clearer picture of the seasonal march of total ozone.

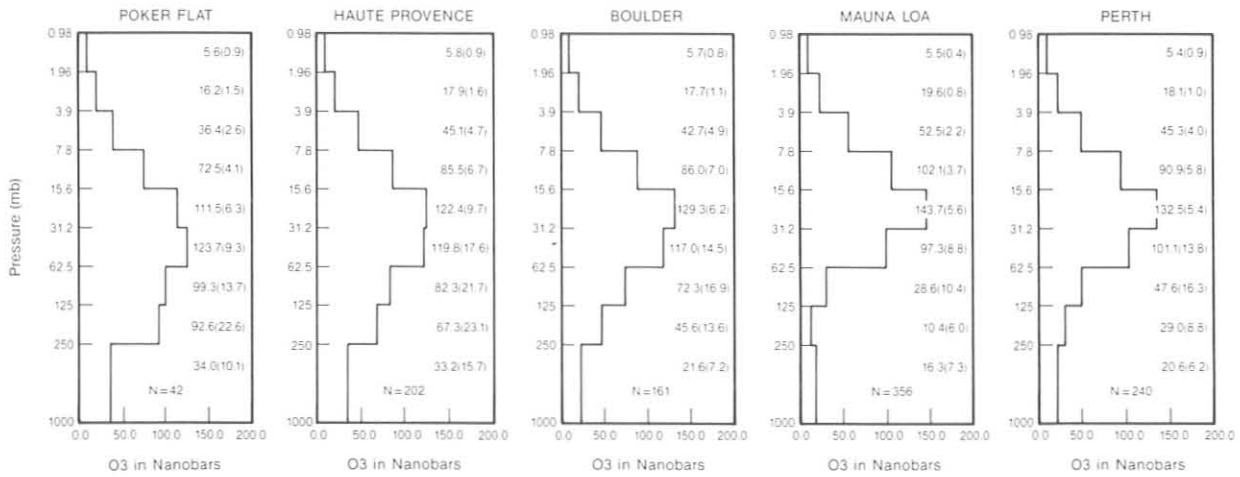

Figure 2.--Mean 1986 ozone vertical distribution profiles obstained from conventional Umkehr observations at the NOAA/GMCC automated Dobson spectrophotometer network. Values in parentheses are standard deviation of the layer around mean values.

Daily total ozone measurements from both the Dobson spectrophotometer and integrated ECC ozonesonde profiles for 1986 are shown in fig. 3. Total ozone gradually decreased from near 300 D.U. (D.U. = Dobson unit = 1 milli-atm cm ozone) in January to about 220 D.U. in late April. Ozone column amounts increased during the polar night, again achieving a value near 300 D.U. in August. Following this, the value dropped precipitously to a low value of 160 D.U. in early October. With the stratospheric warming in late October, and more rapid warming by mid-November, total ozone values rose to over 400 D.U. This was the first reading above 400 D.U. since 1980. The October-December total ozone average in 1986 was about 40 D.U. units higher than the corresponding 1985 value, representing a modest recovery. The 1986 amounts are still, however, far below the 1962-1979 average for this time of year of about 330 D.U. (Komhyr et al., 1986).

The formation of the 1986 ozone hole at South Pole is detailed in fig. 4, which compares six profiles in September and October with a profile obtained in August prior to the hole formation. Although minimum column ozone amounts occurred in early October, ozone concentrations in the hole region continued to decrease into mid-October. During the period of most rapid ozone decrease,

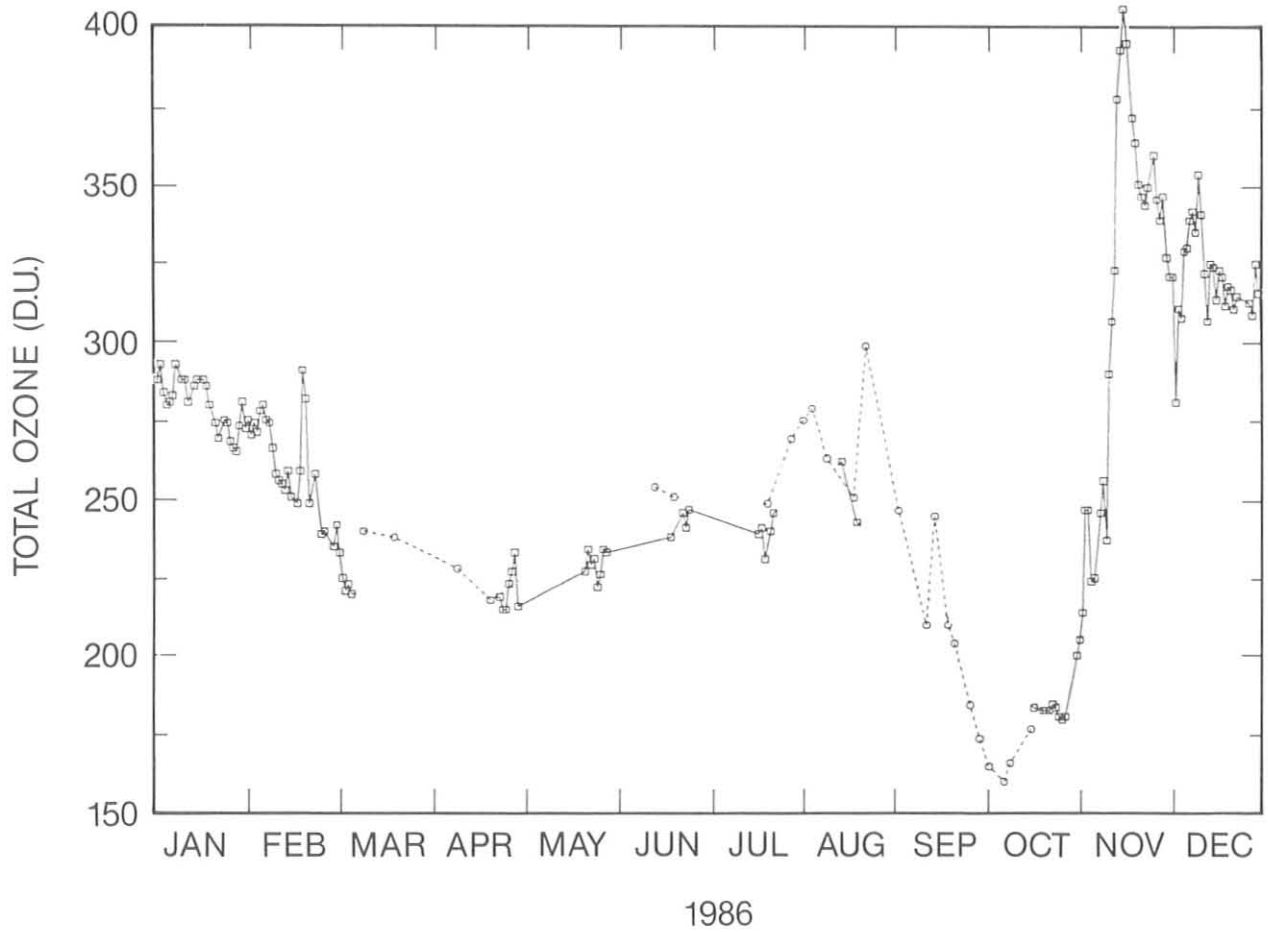

Figure 3.--Daily total ozone amounts (Dobson units) at South Pole, Antarctica, in 1986 derived from Dobson spectrophotometer observations (□) and ECC ozonesonde observations (o).

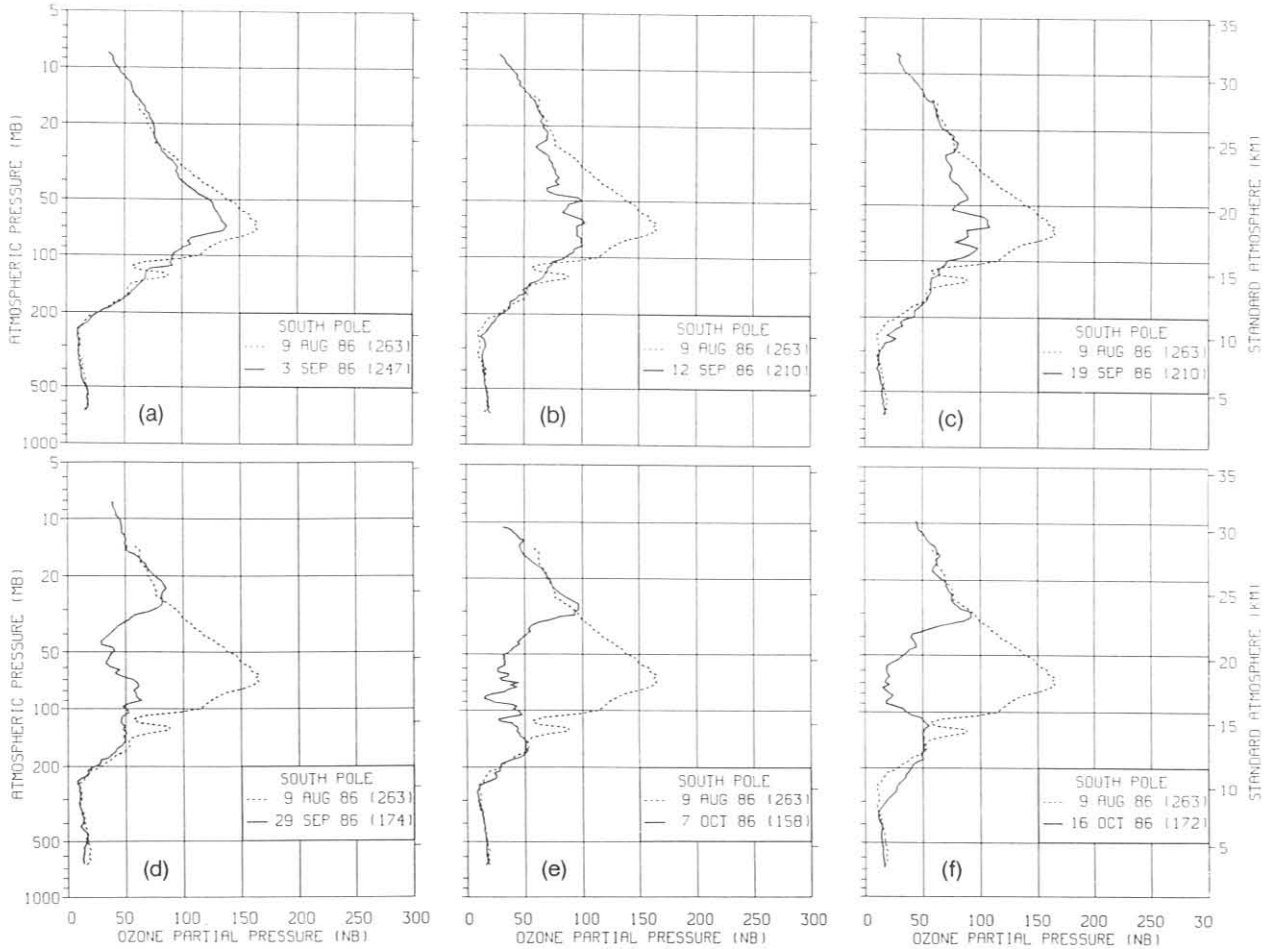

Figure 4.--ECC ozonesonde vertical profiles showing the development of the ozone hole in September and October 1986, compared with a profile taken in August 1986 prior to hole formation.

from 20 September to 15 October, the mixing ratio decreased by 78% in the region of maximum ozone depletion (16 ± 1 km). The exponential ozone decay rate half-life was 11 days. ECC ozonesonde soundings made at South Pole in 1971 suggest that at that time ozone began to be transported into Antarctica above the 25-km level by mid-September, 1.5 months earlier than in 1986. Transport processes appear to be significantly altered in recent years compared with years prior to 1980. Associated delays in times of breakdown of the Antarctica circumpolar vortex most likely augment conditions that accelerate ozone loss through photochemical reactions involving natural and anthropogenic pollutants.

SURFACE OZONE

The four-station GMCC surface ozone network continued operation in 1986 in the same manner as in recent years. Although both BRW and MLO had annual mean surface ozone concentrations in 1986 that were slightly below normal (fig. 5), the 13-yr linear trends at these stations remain significantly posi-

tive. The magnitude of this trend, however, continues to decline from the peak values found in 1983 after 10 years of observations (Schnell and Rosson, 1986).

At SMO, a statistically significant trend in the monthly anomalies is apparent for the first time. This negative linear trend (significant at the 95% level) appears in 9 of the 12 months, although the largest trend is in the month of January, which is the only individual month where the trend is significant.

At SPO, where the overall trend for the 12-y period of measurements is near zero, there has in fact been a very significant change in the character of the seasonal cycle (fig. 6) with a twofold increase in the amplitude during the period 1975-1986. It appears that altered transport processes are responsible for this marked change. These processes, including horizontal advection of tropospheric ozone from lower latitudes and downward mixing of ozone from the stratosphere, give rise to the annual cycle (Oltmans and Komhyr, 1986). Evidence from particle measurements at the South Pole (Samson et al., 1987) point to a retarded tropospheric transport into the pole during the summer months, suggesting this is the cause of the decreasing ozone values during these months. The aerosol data on the other hand show no statistically significant long-term changes during the austral winter, suggesting that the increase in ozone at the surface seen during this time of the year is from enhanced downward fluxes of ozone from the stratosphere.

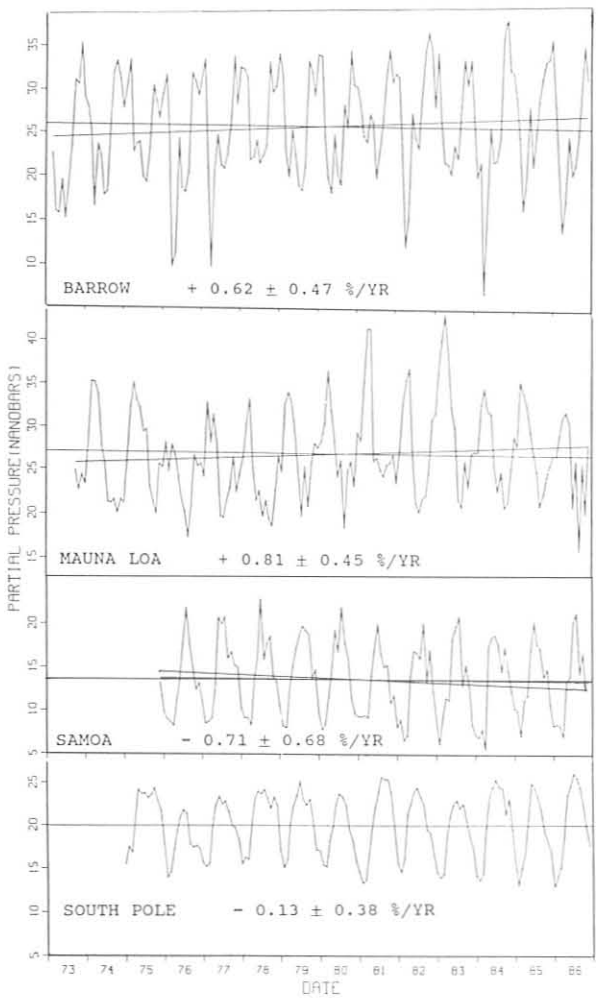

Figure 5.--Monthly mean surface ozone values at the NOAA/GMCC baseline stations for 1973-1986. Also shown is the linear trend and 95% confidence interval in percent per year.

It is also worth noting that the two lowest seasonal maximum values in 1976 and 1983 (fig. 6) were in years immediately following ENSO events, again indicative of the role of transport in the long-term variations in surface ozone.

STRATOSPHERIC WATER VAPOR

Regular monthly soundings of the water vapor content of the upper troposphere and stratosphere to about 25 km were continued in Boulder. In addition, a sounding was made in July 1986 from Pago Pago, American Samoa, in support of the SAGE II satellite validation effort. Water vapor mixing ratio vertical profiles from Boulder and Samoa for the stratosphere are shown in fig. 7. In the October and November soundings at Boulder enhanced water vapor concentrations appear above the 30 mb level. By 1987 more normal values are seen at this level.

The seasonal trend in water vapor in the lower stratosphere is apparent in the time-height cross section shown in fig. 8. The deep minimum. which reaches its lowest values in March at about the 130-mb level, gradually fills and moves upward through the summer and autumn. Above about the 70-mb level, the changes throughout the year are small, while below 150 mb, a very strong gradient reflecting the transition region in the vicinity of the tropopause dominates the distribution.

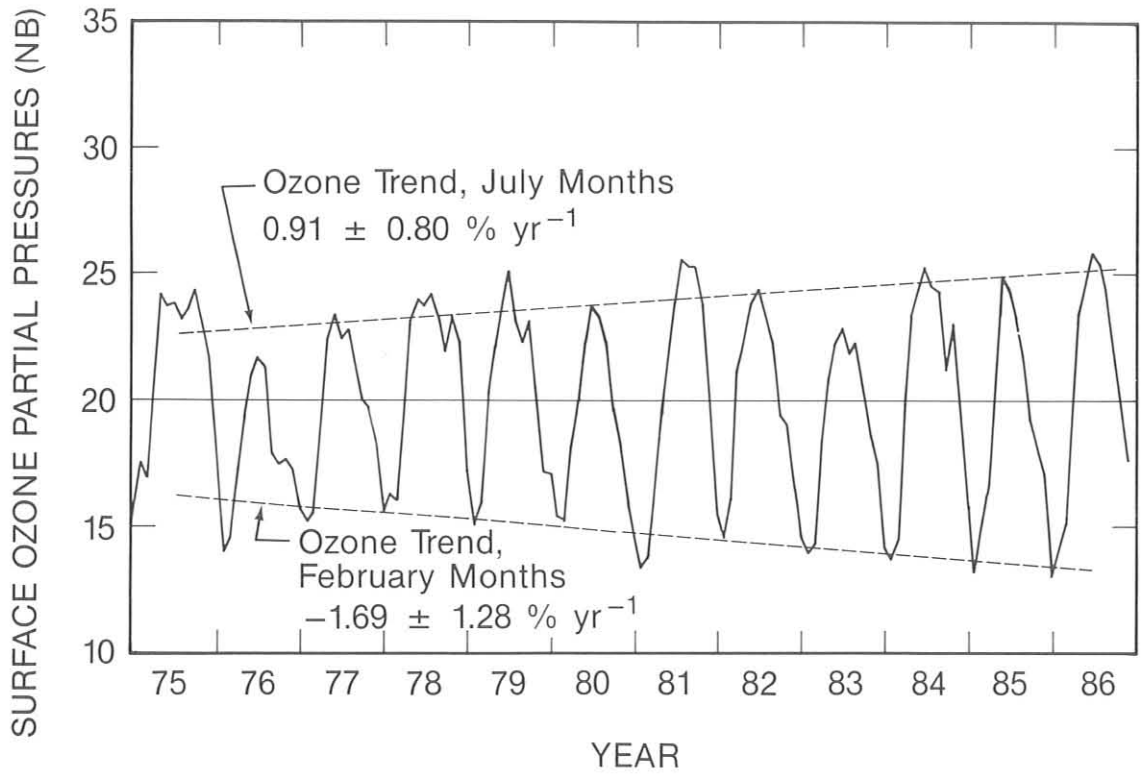

Figure 6.--Plots of 1975-1986 South Pole surface ozone monthly means (solid curve) and secular trends for February and July months (dashed lines), which are times of minima and maxima, respectively, in the surface ozone annual cycle.

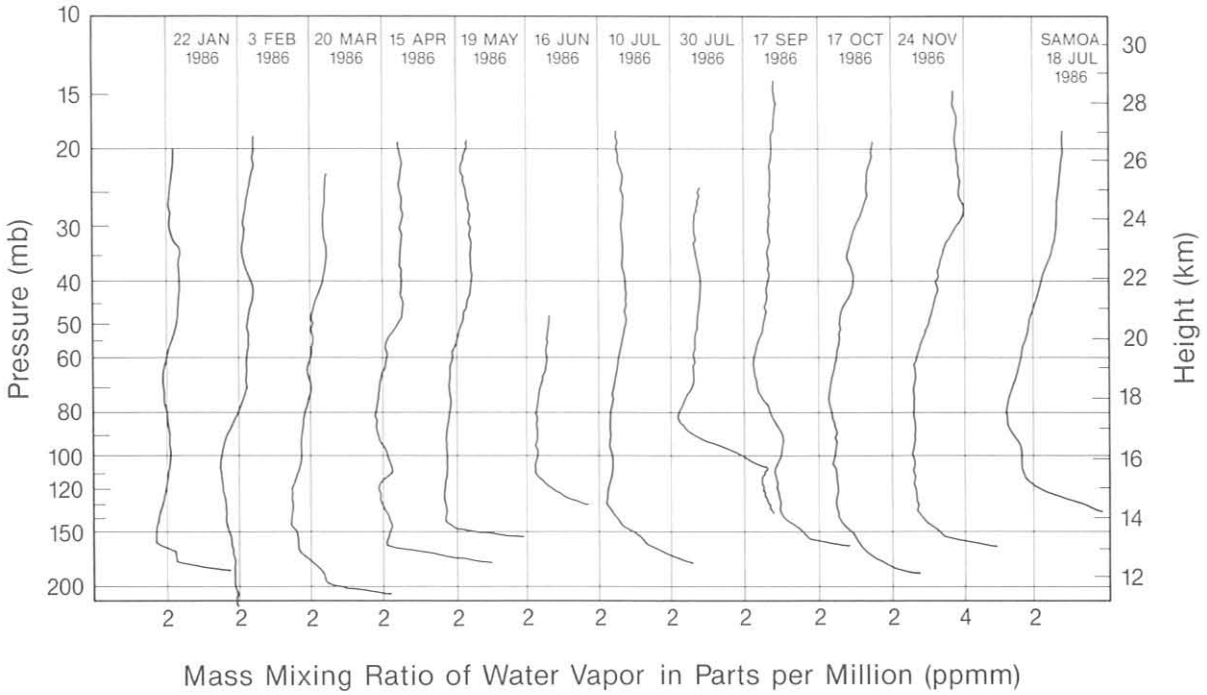

Figure 7.--Profiles of stratospheric water vapor mass mixing ratio (ppm) at Boulder, CO for 1986, at Pago Pago, American Samoa for 18 July 1986.

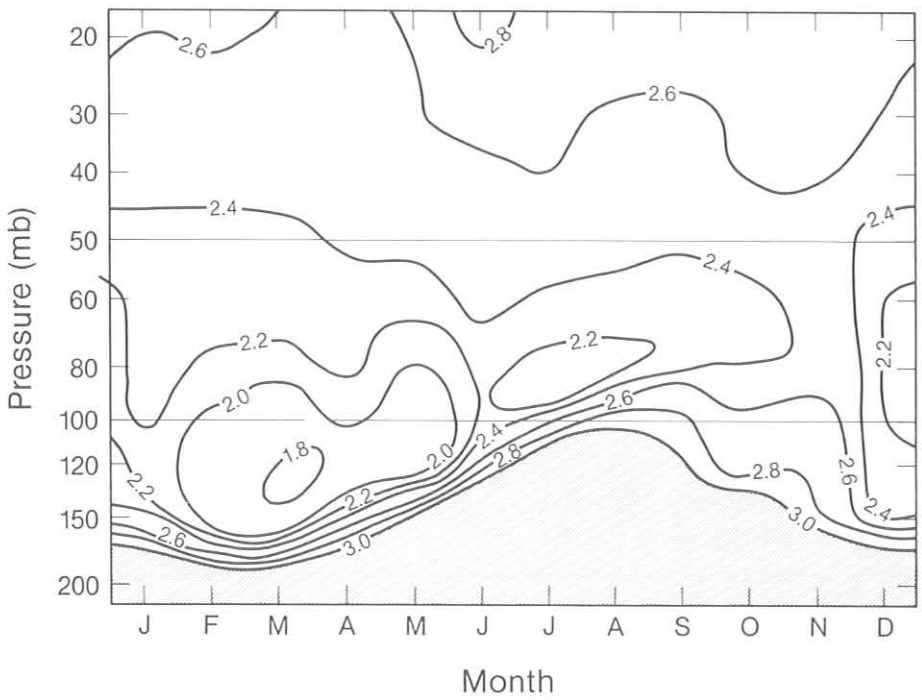

Figure 8.--Time-height cross section of water vapor mass mixing ratio (ppm) for the stratosphere showing the average seasonal behavior from 1981 to 1986. In the stippled area the mixing ratio lines on the scale shown are closely spaced.

5.2 References

Komhyr, W. D., R. D. Grass, and R. K. Leonard, 1986. Total ozone decrease at South Pole, Antarctica, 1964-1985. Geophysical Research Letters 13: 1248-1251.

Komhyr, W. D., S. J. Oltmans, and R. D. Grass, 1987a. Atmospheric ozone at South Pole, Antarctica in 1986. Journal of Geophysical Research (submitted).

Komhyr, W. D., P. R. Franchois, B. C. Halter, C. C. Wilson, 1987b. ECC ozonesonde observations at South Pole, Antarctica during 1986. NOAA Data Report ERL ARL-11, NOAA Environmental Research Laboratories, Boulder, CO, 213 pp.

Oltmans, S. J., and W. D. Komhyr, 1986. Surface ozone distributions and variations from 1973-1984 measurements at the NOAA Geophysical Monitoring for Climatic Change Baseline Observatories. Journal of Geophysical Research, 91: 5229-5239.

Samson, J. A., S. C. Barnard, J. S. Obremski, D. C. Riley, J. J. Black, B. B. Murphey, M. D. Loizeaux, and A. W. Hogan, 1987. On the recent diminution of surface aerosol concentrations at the South Pole. Atmospheric Environment (in press).

Schnell, R. C., and R. M. Rosson, 1986. Geophysical Monitoring for Climatic Change, No. 14: Summary Report 1985. NOAA Environmental Research Laboratories, Boulder, CO, 146 pp.

6. ACQUISITION AND DATA MANAGEMENT GROUP

6.1 Continuing Programs

STATION CLIMATOLOGY

The interpretation of measured values of aerosols, trace gases, and turbidity requires the measurement of meteorological variables to adjust gas measurements to standard conditions and to assess the influence of local pollution sources. These variables include wind direction, wind speed, station pressure, air and dewpoint temperature, and a determination of boundary layer stability. The main criterion used in selecting sensors for these measurements was ruggedness, considering the stress of the polar environment at two of the stations. Where appropriate, commercially available instrumentation was chosen and WMO-recommended exposure standards were followed. With the exception of sensors for temperature measurements at the South Pole, the same sensors are used at all four stations. A complete list of the sensors, model numbers, and heights appear in Nickerson (1986).

With the installation of CAMS units at all stations during the latter half of 1984, the increased reliability of the data acquisition hardware significantly reduced the quantity of missing data. Also, the quality of the data improved as a result of the new daily routine of printing hourly averages and comparing them with observed conditions. The printout known as the Daily Weather Report (DWR) was used for this purpose. It contains hourly average values for the individual meteorological variables for a 24-h period. Herbert et al. (1986a, b) present a detailed discussion of the individual elements in the DWR and other printouts from CAMS. The DWR's are sent to Boulder, checked, and stored on microfiche for future reference. The numerical values, from which tables 1-4 are generated, are also stored on tape.

Barrow

A description of the BRW site, its surroundings, and climate can be found in previous GMCC Summary Reports (e.g., DeLuisi, 1981). Wind roses of the hourly average resultant wind direction and speed are presented in 16 direction classes and 4 speed classes. The distribution of the wind by direction for 1986 is consistent in general distribution with the average for the 1977-1985 period (fig. 1). The predominant wind direction is again from the "representative sampling sector," NE-SE, and all other directions, except westerly, are less than 5%. In 1985, the wind rose showed 15.5% of the wind equal to or greater than 10 m s^{-1}, and in 1986 the value was 18% as contrasted to 9% for the long-term average. New maximum wind speeds were observed for the months of May and September, and for the year (table 1). The new maximum of 24.1 m s^{-1} replaces the previous value 21.7 m s^{-1}.

Meteorologically speaking, the most significant event of the year was the storm that passed BRW on the autumnal equinox. A frontal passage occurred at 2300 GMT 20 September, at which time the wind direction shifted from southeasterly to southwesterly. The hourly average wind speed increased from 8 to > 20 m s^{-1} in the next hour. The hourly average maximum wind speed of 24 m s^{-1} (54 mi h^{-1}) was measured at 0100 GMT 21 September. During this hour, the 10-min average peak wind velocity was 26 m s^{-1} (57.8 mi h^{-1}) and the peak instantaneous gust recorded was 29 m s^{-1} (66 mi h^{-1}). NWS also reported a peak

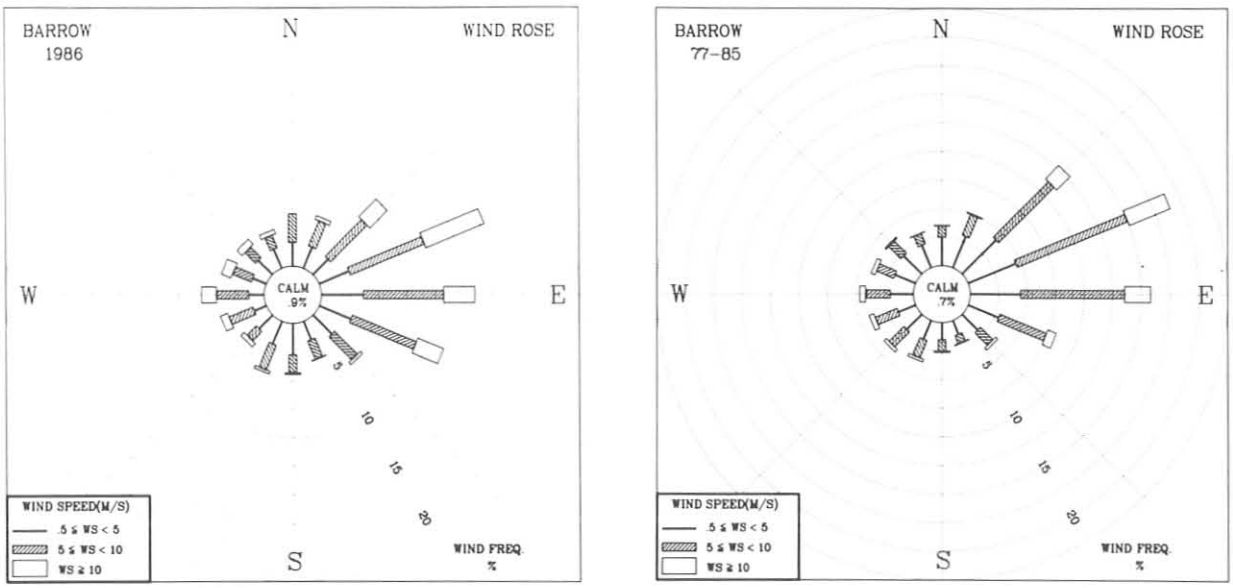

Figure 1.--Wind rose of surface winds for BRW for 1986 (left) and 1977-1985 (right). The distribution of the resultant wind direction and speed are in units of percent occurrence for the year and 9-yr period, respectively. Wind speed is displayed as a function of direction in three speed classes.

Table 1.--BRW 1986 monthly climate summary*

	Jan	Feb	Mar	Apr	May	Jun	Jul	Aug	Sep	Oct	Nov	Dec	1986
Prevailing wind direction	ENE	ESE	N	ENE	E	E	ESE	E	S	SSW	E	ENE	ENE
Average wind speed ($m\ s^{-1}$)	9.9	6.9	5.7	5.8	5.2	6.0	6.2	7.0	7.6	6.6	6.4	7.9	6.8
Maximum wind speed† ($m\ s^{-1}$)	17	16	18	13	14	12	13	17	24	15	17	19	24
Direction of max. wind† (deg.)	55	95	270	55	70	75	100	335	265	235	75	260	265
Average station pressure (mb)	1018.7	1017.3	1019.3	1020.7	1016.9	1011.7	1012.2	1009.5	1009.6	1013.8	1017.2	1009.5	1014.7
Maximum pressure† (mb)	1034	1033	1041	1036	1032	1024	1021	1019	1027	1026	1042	1035	1042
Minimum pressure† (mb)	1005	1000	1005	1005	1003	996	997	999	987	987	997	986	986
Average air temperature (°C)	-27.1	-23.8	-29.1	-23.4	-7.3	.3	3.6	3.7	2.1	-9.0	-17.6	-21.6	-12.4
Maximum temperature† (°C)	-14	-7	-8	-12	-2	14	14	15	13	-.6	-4.9	-5.2	15
Minimum temperature† (°C)	-35	-43	-44	-42	-17	-7	-3	-2	-11	-23	-32	-33	-44
Average dewpoint temperature (°C)	-30.8	-27.1	-33.0	-27.0	-10.4	-2.2	1.4	.7	-.8	-12.2	-20.5	-24.9	-15.6
Maximum dewpoint† temperature (°C)	-17.7	-8.8	-9.9	-14.9	-.9	8.5	9.0	8.4	9.3	3.4	-6.6	-7.5	9.3
Minimum dewpoint† temperature (°C)	-38.4	-47.0	-48.3	-45.7	-19.4	-12.1	-4.2	-6.3	-13.0	-26.0	-35.9	-37.3	-48.3

*Instrument heights: wind, 17 m; pressure, 9.5 m (MSL); air and dewpoint temperature, 3 m. Wind and temperature instruments are on a tower located 25 m northeast of the main building.
†Maximum and minimum values are hourly averages.

gust of 66 mi h^{-1} in Barrow village. This is a new maximum wind speed for the BRW NWS as well. The storm and associated high waves caused considerable erosion and damage along the coast.

The pressure and temperatures in 1986 were generally close to long-term averages. The average pressure for the year was 0.9 mb above the average for the previous 9 years. The average temperature was only 0.6°C cooler than normal. Record high pressure and minimum temperature were reported for March, and a record high temperature was reported for June. All frost-point measurements were converted to dewpoint.

Mauna Loa

A description of the MLO site and its general climatology can be found in previous GMCC Summary Reports. The MLO 1986 monthly climate summary is shown in table 2. Note that, for most variables, the average values are not representative of median values because of the bimodal distribution of the wind direction based on the time of day. The effect of Mauna Loa is to redirect stronger, predominantly easterly or westerly winds aloft down the slope with a more southerly component. The winds were again predominantly from the south in 1986 as in earlier years (fig. 2). A typical number of spring storms were reported in March and April, but the number of storms and days with above-normal wind speeds in December was unusual. The maximum wind speed and the minimum pressure observed in December set new records for that month. New maximum wind speeds were also observed in April and July as well. Both air and dewpoint temperatures were within normal ranges for the year.

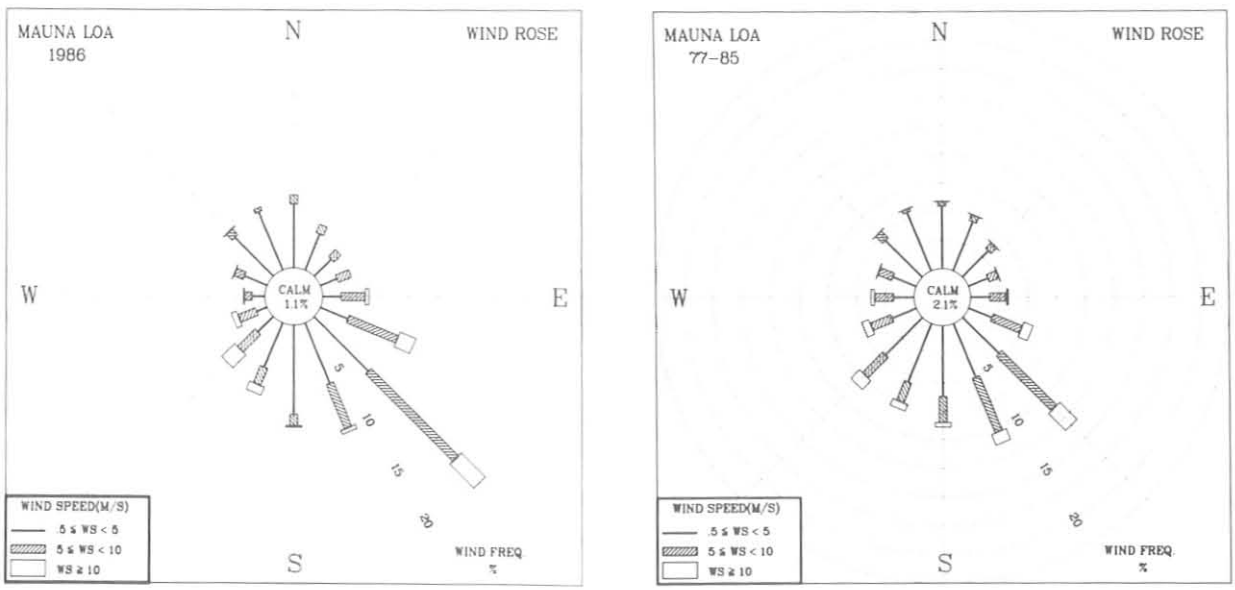

Figure 2.--Wind rose of surface winds for MLO for 1986 (left) and 1977-1985 (right). The distribution of the resultant wind direction and speed are in units of percent occurrence for the year and 9-yr period, respectively. Wind speed is displayed as a function of direction in three speed classes.

Table 2.--MLO 1986 monthly climate summary*

	Jan	Feb	Mar	Apr	May	Jun	Jul	Aug	Sep	Oct	Nov	Dec	1986
Prevailing wind direction	SW	SW	SSE	SE	SE	SE	SE	SE	SE	SE	SE	SE	SE
Average wind speed ($m\ s^{-1}$)	5.3	7.4	4.2	5.7	4.0	5.2	5.0	5.6	3.4	4.6	5.4	6.0	5.1
Maximum wind speed† ($m\ s^{-1}$)	13	17	14	17	12	12	20	15	12	11	15	20	20
Direction of max. wind† (deg.)	245	220	215	115	145	145	120	110	140	145	135	1854	120
Average station pressure (mb)	679.1	678.0	680.7	679.3	680.1	680.7	681.1	681.9	680.3	680.9	679.7	680.0	680.1
Maximum pressure† (mb)	683	682	686	683	683	683	683	684	683	684	683	683	686
Minimum pressure† (mb)	674	673	677	675	677	678	677	678	678	678	675	670	670
Average air temperature (°C)	7.4	6.6	6.7	5.2	7.9	9.1	8.4	9.2	7.8	7.9	7.1	7.1	7.5
Maximum temperature† (°C)	15	14	15	13	18	18	18	18	15	16	14	18	18
Minimum temperature† (°C)	-1	-3	0	-1	0	3	2	3	3	1	2	0	-3
Average dewpoint temperature (°C)	-16.8	-12.0	-8.4	-5.9	-6.7	-10.7	-7.2	-5.9	-1.7	-8.6	--	--	-8.6
Maximum dewpoint† temperature (°C)	7	6	6	7	7	7	8	8	7	7	--	--	8
Minimum dewpoint† temperature (°C)	-35	-33	-29	-26	-31	-32	-32	-29	-21	-24	--	--	-35
Precipitation (mm)	0	18	19	301	40	T	43	79	91	6	66	10	673

*Instrument heights: wind, 17 m; pressure, 3399 m (MSL); air and dewpoint temperature, 3 m. Wind and temperature instruments are on a tower located 25 m northeast of the main building.
†Maximum and minimum values are hourly averages.

The average pressure for 1986 was 0.8 mb below the 9-yr average for the period 1977-1985. Furthermore 11 of the 12 individual monthly averages were below the comparable monthly averages for this period. One explanation is that there were a large number of storms at MLO in 1986 (the precipitation amount of 673 mm for the year was 40% more than the 13-yr average reported by Chin et al., 1971). However, the average pressure for 1985 was below (1.3 mb) the long-term average as well. Therefore, another explanation is measured error. The pressure sensor is checked against the mercurial barometer at the station twice weekly and the two are in good agreement. Thus a recheck of the mercurial barometer is necessary before this difference can be resolved.

Samoa

A comparison of the wind rose for 1986 with that for the preceding 9 years shows a very similar distribution except for the shift in the predominant wind direction toward SSW and the higher percentage of wind equal to or greater than 10 $m\ s^{-1}$ (fig. 3). In 1986, wind speeds were reported in the highest class 6.5% of the time in contrast to a long-term average of 2.8%, and as compared with 8% in 1985. The average wind speed for the year was 5.4 $m\ s^{-1}$, which was 1.0 $m\ s^{-1}$ above the long-term average. Table 3 shows that new maximum wind speeds were observed for the months of January, February, May, and September. In September wind speeds of 10 $m\ s^{-1}$ or greater were reported 13% of the time as compared with a normal of 1%. The higher winds from the northwest early in the year were associated with stormy periods accompanied by precipitation. Relatively large precipitation amounts were reported for January, February, April, and May. In September, the strong southeasterlies were associated with a well-developed trade wind regime.

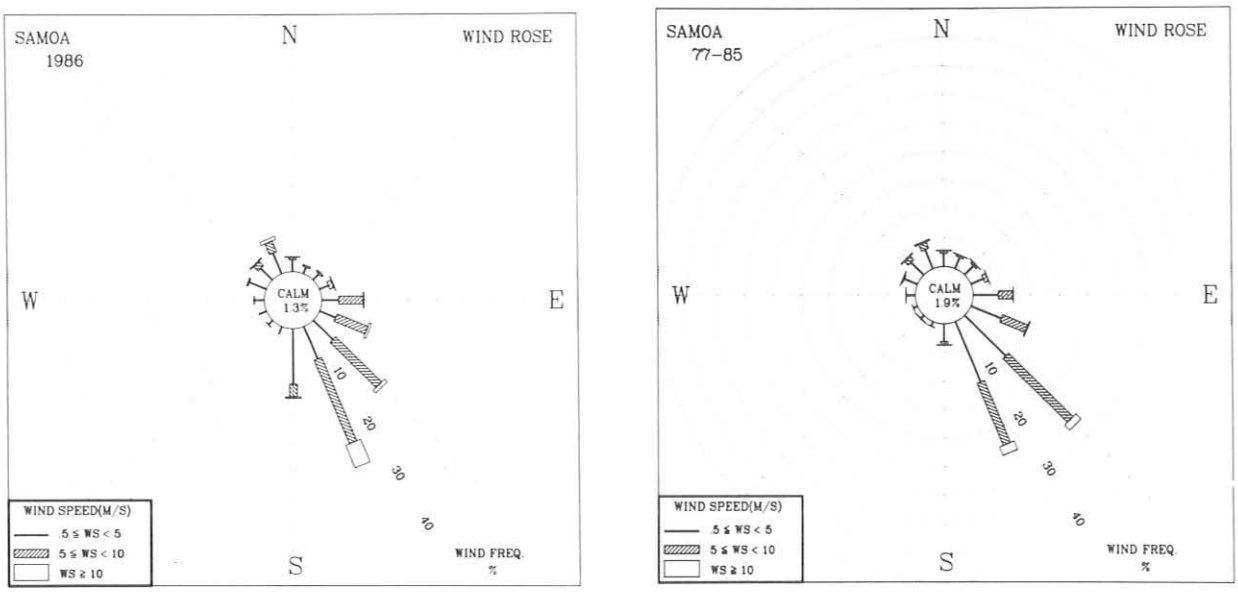

Figure 3.--Wind roses of surface wind for SMO for 1986 (left) and 1977-1985 (right). The distribution of the resultant wind direction and speed are in units of percent occurrence for the year and 9-yr period, respectively. Wind speed is displayed as a function of direction in three speed classes.

Table 3.--SMO 1986 monthly climate summary*

	Jan	Feb	Mar	Apr	May	Jun	Jul	Aug	Sep	Oct	Nov	Dec	1986
Prevailing wind direction	NNW	WNW	ESE	SE	SSE	SSE	SSE	S	SSE	SSE	SSE	SSE	SSE
Average wind speed ($m\ s^{-1}$)	5.0	3.1	4.5	4.2	6.1	5.7	6.3	6.0	6.5	5.2	5.6	5.6	5.4
Maximum wind speed† ($m\ s^{-1}$)	16	16	9	12	17	12	11	16	15	13	11	14	17
Direction of max. wind† (deg.)	340	325	95	335	160	110	165	160	160	150	160	150	160
Average station pressure (mb)	997.3	998.4	1000.3	999.3	1001.2	1000.9	1001.5	1001.0	1001.1	1002.3	999.4	997.9	1000.1
Maximum pressure† (mb)	1002	1003	1004	1004	1006	1005	1006	1006	1005	1005	1003	1002	1006
Minimum pressure† (mb)	993	993	996	994	995	996	997	995	998	999	995	993	993
Average air temperature (°C)	27.2	27.6	28.2	27.6	26.4	26.9	25.7	25.3	26.0	26.4	26.8	27.0	26.7
Maximum temperature† (°C)	31	32	31	32	29	33	32	31	30	30	31	31	33
Minimum temperature† (°C)	24	23	24	24	22	22	22	21	23	21	24	23	21
Average dewpoint temperature (°C)	26.0	26.4	26.9	26.3	25.4	--	--	--	--	--	--	--	--
Maximum dewpoint† temperature (°C)	30	31	30	31	27	--	--	--	--	--	--	--	--
Minimum dewpoint† temperature (°C)	21	21	22	20	24	--	--	--	--	--	--	--	--
Precipitation (mm)	357	336	165	437	353	147	141	66	80	268	211	--	(2562)

*Instrument heights: wind, 14 m; pressure, 30 m (MSL); air and dewpoint temperature, 9 m. Wind and temperature sensors located atop Lauagae Ridge, a distance 110 m northeast of the station. Pressure sensors are located in the station.
†Maximum and minimum values are hourly averages.

The remainder of the meteorological variables measured in 1986 were reasonably close to seasonal and annual norms (table 3). The average station pressure of 1000.1 mb was only 0.5 mb above the long-term average. The average air temperature, measured at a height of 9 m above the level section on the east end of Lauagae Ridge, was 26.7°C, just 0.4°C below normal. In the case of both pressure and temperature, the extreme values are within normal limits. The dewpoint hygrometer was returned to service in September 1985 after being sent to the manufacturer for repair and recalibration. Nonetheless, problems developed in June 1986 and much of the data taken after this time is questionable. The average monthly precipitation for the year of 233 mm is only 20 mm above normal.

South Pole

The most distinguishing feature of the distribution of the surface wind directions at SPO is the large percentage (81%) of wind flow from the NE quadrant (N-E). As shown in fig. 4, the distribution of surface wind speed with direction is very similar to the distribution for the preceding 9 years. The main difference in 1986 is that the predominant wind direction was grid northerly. For five of the months, the prevailing wind direction was also northerly (table 4). A second feature of the 1986 wind rose is the relatively large number of occurrences of wind speeds equal to or greater than 10 m s^{-1}: 7% as compared with 3% in the preceding 9 years. Nonetheless, the average wind speed for the year of 6.0 m s^{-1} was only 0.7 m s^{-1} greater than the long-term average. New maximum wind speeds were observed for the months of January and March.

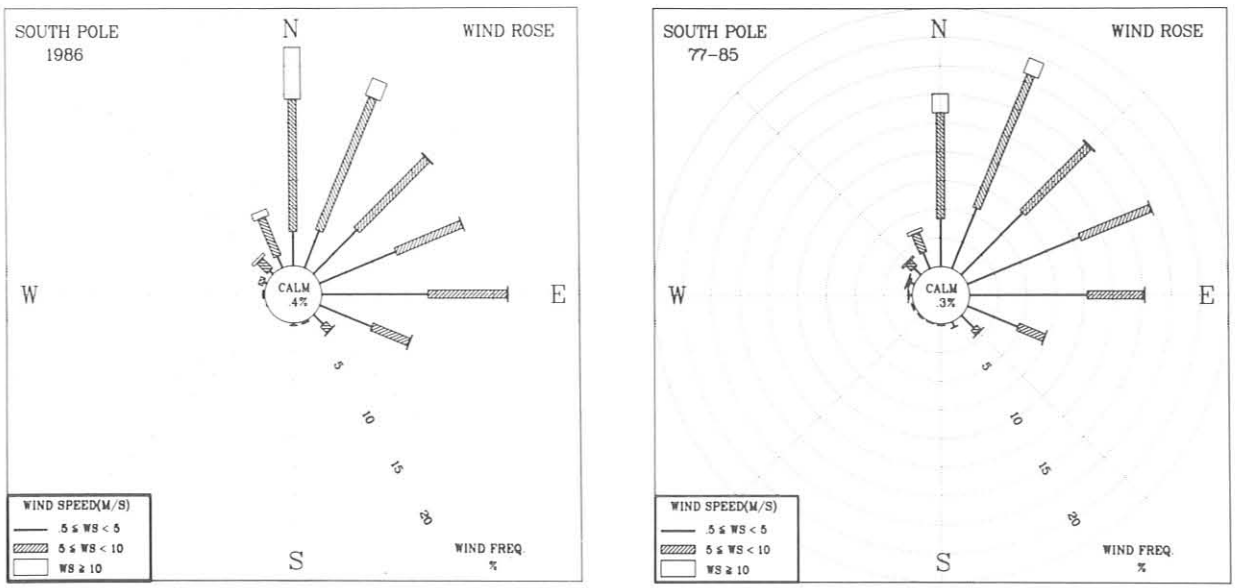

Figure 4.--Wind roses of the surface wind for SPO for 1986 (left) and 1974-1984 (right). The distribution of the resultant wind direction and speed are in units of percent occurrence for the year and 9-yr period, respectively. Wind speed is displayed as a function of direction in three speed classes.

Table 4.--SPO 1986 monthly climate summary*

	Jan	Feb	Mar	Apr	May	Jun	Jul	Aug	Sep	Oct	Nov	Dec	1986
Prevailing wind direction	N	NNE	N	N	E	ESE	E	N	NE	NNE	N	NNE	N
Average wind speed ($m\ s^{-1}$)	6.0	5.9	6.1	5.9	6.5	4.9	6.3	7.4	6.1	6.2	5.7	4.9	6.0
Maximum wind speed† ($m\ s^{-1}$)	13	12	15	13	12	13	14	15	13	12	12	11	15
Direction of max. wind† (deg.)	360	5	5	5	355	350	10	10	20	320	15	35	5
Average station pressure (mb)	690.2	693.4	684.3	680.5	684.4	679.9	673.9	672.0	664.3	672.5	676.6	684.9	679.7
Maximum pressure† (mb)	700	705	701	692	696	705	692	693	678	690	691	698	705
Minimum pressure† (mb)	682	682	667	668	665	657	653	658	647	662	656	677	647
Average air temperature (°C)	-24.7	-34.7	-51.7	-54.9	-61.8	-63.6	-60.0	-58.6	-64.3	-52.8	-37.8	-27.0	-49.7
Maximum temperature† (°C)	-18	-24	-34	-41	-48	-34	-34	-41	-49	-38	-28	-18	-18
Minimum temperature† (°C)	-35	-42	-70	-66	-74	-78	-74	-74	-80	-71	-48	-34	-80
Average dewpont temperature (°C)	-28.0	-38.9	-52.1	--	--	-63.5	--	--	--	--	--	--	--
Maximum dewpoint temperature (°C)	-21	-27	-37	--	--	-60	--	--	--	--	--	--	--
Minimum dewpoint temperature (°C)	-40	-48	-81	--	--	-74	--	--	--	--	--	--	-

*Instrument heights: wind, 12 m; pressure, 2841 m (MSL); air temperature, 2 m. The anemometer and thermometer are located on a tower 100 m grid east-southeast of CAF. Pressure measurements are made inside CAF.
†Maximum and minimum values are hourly averages.

The distribution of the wind direction for June is unique in that it is one of only a very few instances in which the prevailing wind direction has a southerly component. In this particular case, the wind was from the east southeasterly direction 29% of the month.. ESE wind directions in June usually occur about 11% of the time. The average wind speed is usually below average as well.

The average pressure for the year was 679.7 mb, which is 1.6 mb above the long-term average. The average temperature for the year was -49.7°C, less than 1°C above the climatological average. A series of equipment problems limited the amount of reliable frost-point measurements obtained in 1986.

DATA MANAGEMENT

The automated data acquisition system (CAMS) continued operation through 1986 with few problems. Table 5 shows the operations record for CAMS at the four observatories in terms of the number of blocks recorded for each block type. SMO has the most blocks missing, not because of CAMS operations, but because two data cassettes were lost in the mail: an ASR cassette covering the period from DOY 91 to DOY 105 and an MO3 cassette from DOY 69 to DOY 76. To help prevent such losses in the future, a permanent label with GMCC's address was affixed to each new cassette. Not reflected in the number of missing records is the problem that SMO had with the interface between the MO3 CAMS and the Dasibi ozone meter, causing all nines to be recorded in the data field for a significant portion of the year. About a dozen power outages were reported for SMO during the year, while MLO reported over twice that number; BRW's ASR clock board failed and was replaced; at SPO a bad CPU and monitor board were repaired; and MLO had CPU board problems as well that were diagnosed and fixed.

The software for the CO2 CAMS was revised to correct some minor bugs. New PROMs were installed at BRW in April and June, at MLO in June, at SMO in May, and at SPO in June. The software in the other two CAMS is also being upgraded.

Table 5.--GMCC CAMS operations summary, 1986

Block type	Description	Expected no.of blocks/yr*	Blocks recorded and [blocks missing] BRW	MLO	SMO	SPO
A	Hourly aerosol data	2190	2164[26]	2188[2]	2016[174]	2189[2]
H	Daily aerosol data	365	364[2]	365[0]	337[28]	367[0]
S	Hourly solar radiation data	8760	8659[101]	8754[6]	8754[6]	8057[703]
C	Hourly CO_2 data	Variable <8760	8255[171]	8371[43]	7875[553]	8363[13]
D	Daily CO_2 data	365	365[4]	370[0]	347[22]	368[0]
E	Hourly CO_2 calibration data	Variable	331	345	332	376
F	CO_2 calibration report	~52	49	53	50	58
M	Hourly meteorological data	4380	4359[23]	4378[3]	4249[132]	4375[3]
O	Daily ozone data	365	368[0]	366[0]	354[11]	365[0]
W	Daily meteorological data	365	368[0]	366[0]	354[11]	365[0]
I	Meteorological calibration information	365	367[0]	366[0]	357[11]	364[1]

*Discrepancies between the expected number of blocks and (blocks recorded + blocks missing) are due to clock problems or autorestarts.

6.2 Special Projects

ATMOSPHERIC TRAJECTORIES

Descriptions of various atmospheric trajectory programs developed within GMCC have appeared in previous summary reports (Bodhaine and Harris, 1982, pp. 71-74; Harris and Bodhaine, 1983, pp. 67-75; Harris and Nickerson, 1984, pp. 73-80; Nickerson, 1986, pp. 71-75; Schnell and Rosson, 1986, pp. 68-72).

Table 6 lists most of the trajectories computed during 1986. These were provided for atmospheric researchers within GMCC and ARL as well as scientists at numerous universities and research institutes of foreign governments affiliated with GMCC. In all, about 44 station-years of trajectories were computed. Table 7 lists experiments supported.

Table 6.--GMCC trajectories calculated in 1986

Location	Dates
Bermuda	1985
Mediterranean	1985
Katherine, Australia	Jan-Apr 1985
Amsterdam Island	1985
La Réunion Is.	1985
Torres del Paine, Chile	1981-1985
Cape Point, South Africa	1983-1985
Adrigole, Ireland	1980-1985
Charlottesville, VA	1977-1985
Illinois location	July 1979
Norfolk, VA	Feb-Apr 1985
Ohio location	Feb-Apr 1985
Boston	Jan-Feb 1986
Syracuse	Jan 1986
BRW	1980-1985, Mar-Apr 1986
Barter Island	Mar-Apr 1986
Alert, Canada	Mar-Apr 1986
Augustine Island	Mar-Apr 1986
McMurdo	1985
SPO	Jan 1986
MLO	1980-1985
Big Spring, TX	Apr 1984
Cienfuegos, Cuba	1984-1985
Virgin Islands	1985
Lewes, DL	1979-1980

Input data for the Northern Hemisphere model (65 × 65 grid) consists of E-W and N-S wind components from 1975 to the present. Data for the global model (2.5° grid) began 2 years later in 1977 and extended until the present. Data are available on a monthly basis so that trajectories can be produced in a timely manner. Beginning March 1986, the 70- and 50-mb levels were added to the input data set to make 12 mandatory levels of meteorological data (from 1000 to 50 mb) available for trajectory computation.

A visit to NMC was made to investigate the quality of the data, particularly those data used to calculate trajectories over the Antarctic continent. Apparently NMC has had problems producing reliable data over Antarctica. Specifically, prior to 30 May 1986, an error in the code for the default climatology caused spurious ridges over the continent. Often the default climatology differed enough from the real data observations that the real data were rejected. During this time no satellite data were available

over the continent. Beginning 30 May 1986, the error in the default climatology was corrected and rawinsonde and satellite data were accepted; however, at the same time, a computational error affecting data at the 100, 70, and 50 mb levels was introduced. This error was corrected on 11 September 1986. Trajectories computed for dates after 11 September 1986 should be more reliable than earlier ones, although caution is advised when using them because the coverage of meteorological observations is sparse. Over land or ice, the satellite data are useful only at 100, 70, and 50 mb.

Numerous requests for isentropic trajectories have prompted some streamlining of the isentropic model. Improvements made this year allow multiple destinations, both directions, and longer time periods over which trajectories are calculated during one run. There are still some limitations for this model, mostly related to the finite nature of the computer. These include the area over which isentropic trajectories can be calculated (Northern Hemisphere and Antarctica only), the fact that only one surface at a time can be computed, and restrictions on the size of the subgrid. Moreover, finding the correct isentropic surface is quite often an iterative process that is time and computer intensive. Further streamlining is planned to make the isentropic model even more usable.

Table 7.--Experiments supported during 1986

Experiment	Dates	Organization
MV Atlantic cruise	1984-1985	Univ. of Virginia
SS Oceanic cruise	1984-1985	Univ. of Virginia
AGASP-II flights	Mar-Apr 1986	GMCC
RV Polar Duke cruise	Mar-Apr 1986	Univ. of Virginia
Arctic haze flights	Mar-Apr 1986	Univ. of Washington
NOAA R/V Researcher equatorial cruise	Aug 1986	Univ. of Virginia
FIRE flights	Aug 1985	WPL
Gulf cruise	Jul-Aug 1986	ARL

6.3 References

Bodhaine, B. A., and J. M. Harris (eds.), 1982. Geophysical Monitoring for Climatic Change, No. 10: Summary Report 1981. NOAA Environmental Research Laboratories, Boulder, CO, 158 pp.

Chin, J. F. S., H. T. Ellis, B. G. Mendonca, R. P. Pueschel, and H. J. Simpson, 1971. Geophysical monitoring at Mauna Loa Observatory. NOAA Tech. Memo. ERL APCL-13, NOAA Environmental Research Laboratories, Boulder, CO, 34 pp.

DeLuisi, J. J. (ed.), 1981. Geophysical Monitoring for Climatic Change, No. 9: Summary Report 1980. NOAA Environmental Research Laboratories, Boulder, CO, 163 pp.

Harris, J. M., and B. A. Bodhaine (eds.) 1983. Geophysical Monitoring for Climatic Change, No. 11: Summary Report 1982. NOAA Environmental Research Laboratires, Boulder, CO, 160 pp.

Harris, J. M., and E. C. Nickerson (eds.), 1984. Geophysical Monitoring for Climatic Change, No. 12: Summary Report 1983. NOAA Environmental Research Laboratories, Boulder, CO, 184 pp.

Herbert, G. A., E. R. Green, J. M. Harris, G. L. Koenig, and K. W. Thaut, 1986a. Control and monitoring instrumentation for the continuous measurement of atmospheric CO_2 and meteorological variables. Journal of Atmospheric and Oceanic Technology 3:414-421.

Herbert, G. A., E. R. Green, G. L. Koening, and K. W. Thaut, 1986b. Monitoring instrumentation for the continuous measurement and quality assurance of meteorological observations. NOAA Tech. Memo. ERL ARL-148, NOAA Environmental Research Laboratories, Boulder, CO, 44 pp.

Nickerson, E. C. (ed.), 1986. Geophysical Monitoring for Climatic Change, No. 13: Summary Report 1984. NOAA Environmental Research Laboratories, Boulder, CO, 111 pp.

Schnell, R. C., and R. M. Rosson (eds.), 1986. Geophysical Monitoring for Climatic Change, No. 14: Summary Report 1985. NOAA Environmental Research Laboratories, Boulder, CO, 146 pp.

7. AIR QUALITY GROUP

7.1 Continuing Programs

AQG research during 1986 had three objectives: (1) to improve the understanding of the mechanisms responsible for the formation of acidic aerosols; (2) to explain the effects of these aerosols and of trace gases on the formation, colloidal stability, optical properties, and chemical composition of clouds; (3) to supply observational data to validate and improve the acid deposition models now under development. AQG acquired data to satisfy these objectives using the NOAA King Air aircraft. Table 1 summarizes the research flights made by the King Air in support of our activities during 1986.

THE NATIONAL ACID PRECIPITATION ASSESSMENT PROGRAM (NAPAP)

The Interagency Task Force on Acid Precipitation, created by Congress, sponsors NAPAP. This program consists of task groups entitled (A) Natural Sources, (B) Manmade Sources, (C) Atmospheric Processes, and (D) Deposition Monitoring. AQG continued its participation in NAPAP during 1986 by contributing to Task Groups A and C.

The Western Atlantic Ocean Experiment (WATOX)

WATOX, a NAPAP-sponsored project, continued during 1986. Its purpose was to quantify the flux of various trace species, notably sulfur and nitrogen, away from the U.S. east coast. WATOX used the NOAA King Air during January, February, and June 1986 and a NOAA WP-3D during January 1986.

Sulfur dioxide flux measurements over the western Atlantic Ocean. One purpose of WATOX was to determine the eastbound flux of anthropogenic emissions from the North American continent to the Atlantic Ocean atmosphere. Eight air sampling flights carried out between 1 March and 26 March 1985, roughly 100 km east of Newport News, VA, produced valid SO_2 data. Luria et al. (1987) summarized the data obtained in these flights.

They also calculated the SO_2 flux away from the US east coast using the aircraft data. The results of this calculation (fig. 1) show that the flux was nearly constant at 100 $\mu g\ m^{-2}\ s^{-1}$ within the marine boundary layer (top at 1000 m) and that it decayed exponentially above the boundary layer.

This flux estimate was higher than that of Galloway et al. (1984) by a factor of 2.7. However, this estimate was based on samples taken over a period of less than a month and extrapolated for an entire year to compare with the Galloway et al. results. Furthermore, these data were gathered only shortly after the passage of cold fronts. Cold fronts pass along the U.S. east coast often during the winter months; even so, the composition of the air behind cold fronts may have introduced a bias into the sulfur flux estimates.

It is obvious that accurate flux estimates require more measurements, with improved analytical methods, in other seasons, and at different locations along the coast. The work of Luria et al. (1987) showed that an agreement between climatological flux estimates and field observations is possible.

Table 1.--NOAA King Air research flights during 1986

Project	Location	Flight date	Flight time (local time)
WATOX	Boston, MA	860102	1504-1751
		860104	0718-1118 and 1409-1652
		860106	0719-1134
		860108	0744-1028 and 1407-1705
		860109	0909-1446 and 1457-1841
		860206	1754-2153
		860208	1221-1721
		860209	1102-1553 and 1555-1819
		860210	1140-1640
		860212	1359-1805
		860213	0810-1148 and 1409-1744
		860215	1211-1706
		860216	1212-1625
		860220	1116-1452
WATOX	Bermuda	860607	1136-1357
		860608	1230-1613
		860609	1302-1631
		860610	1100-1334
		860612	1112-1255
		860613	0821-1144
PRECP	Syracuse, NY	860117	1330-1639
		860118	1321-1730
		860119	1233-1620
		860120	1311-1709
		860122	1303-1610
		860125	1600-1913
		860127	1358-1751
PRECP	Raleigh, NC	860223	1400-1747
		860224	1418-1717 and 1941-2309
		860226	1424-1755
		860227	1427-1813
		860301	1104-1343
		860303	1218-1556
RITS	Miami, FL	860701	0851-1256
		860916	0906-1217
		861003	0900-1300
		861103	0900-1300
		861203	0900-1300
SAFE	Alaska	860506	0900-1135 and 1315-1600
		860507	0900-1130 and 1300-1540
		860508	0915-1230 and 1500-1815
		860509	0915-1140 and 1330-1605
		860510	0800-1000 and 1100-1400
	Washington	860510	1500-1715
	Montana	860511	0900-1300
	Colorado	860511	1400-1800

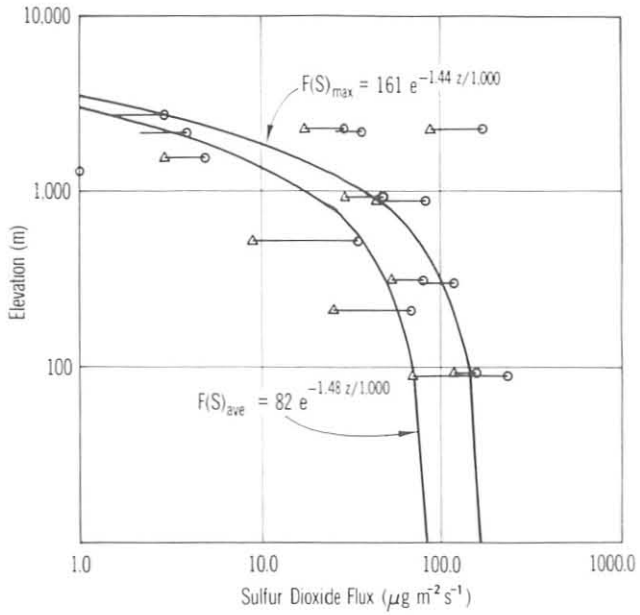

Figure 1.--Elevation profiles of SO_2 flux (after Luria et al., 1987). The circles represent maximum 1-min averages, and the triangles represent the entire flight leg average.

Size distributions of sea-source aerosol particles: a physical explanation of observed differences, near shore vs. open sea. Atmospheric aerosols contribute significantly to the physical process of mass exchange at air-water interfaces and to chemical processing of the elements in the Earth's troposphere. Sea-salt aerosol particles may have a predominant role in this processing during the transport of continental anthropogenic and natural source material over near-shore air environments. WATOX provided an opportunity for the AQG to measure the concentration and size distribution of sea-derived coarse-fraction (diameter, $D \geq 1$ μm) aerosol particles with the externally mounted optical particle counters (Particle Measuring Systems, Boulder, CO) on the NOAA King Air. Lognormal fits to the particle size data provided the opportunity to accurately compare the size distributions of near-shore vs. open-sea particles. Detailed results of this investigation are given by Sievering et al. (1987).

The particle data showed that a bimodal aerosol distribution prevailed throughout WATOX-85 sampling; a coarse-mode fraction predominated for aerosol sizes larger than about 0.8-μm diameter. A lognormal fitting analysis of the probe data was done. A description of the fitting technique was given by Horvath et al. (1988). The number and volume geometric median diameters (VGMD), geometric standard deviations, and total particle number and volume were determined for all representative distributions.

For the near-shore environment, 502 minutes of data were used; for the open sea, 133 minutes of data were used. The fitting showed no significant differences between fine-mode aerosol size distributions, nearshore vs. open sea. The coarse-mode data did exhibit a significant difference. The VGMD was 8.08 ± 1.41 μm for near-shore cases and 5.65 ± 0.78 μm for open-sea cases, at a 99.6% confidence level. This striking difference requires an explanation.

Sievering et al. (1987) discounted several potential explanations, including data base outliers, instrumentation, meteorological differences, and the advection of soils from the continent. The nearshore research flights composing this data set were made under predominantly offshore flow

conditions. Sievering et al. (1987) also investigated this offshore flow as a cause for the observed differences and showed that it was a possible explanation. They found that, during offshore flow, larger sea-derived particles will prevail. The combination of developing ocean waves along with shoreline disturbed conditions produced the effect.

More large, sea-derived aerosol particles occur during offshore flow. This may be of geophysical significance. Also, enhanced cloud growth in nearshore environments during offshore flow periods is possible, and the rate of liquid-phase gas-to-particle conversion (e.g., sulfur dioxide gas to aerosol sulfate) may be different over the open sea from that over nearshore areas.

Dimethyl sulfide over the western Atlantic Ocean. DMS samples were taken with the NOAA King Air during WATOX-86 using the technique of Andreae et al. (1985). Figure 2 shows the DMS data obtained near Boston during January and February 1986. Typical DMS values during the January field operation were in the range 0.5-5 pptv in both the marine layer (ML) and free troposphere (FT). On 9 January the DMS value of 18 pptv was exceptionally high at the lowest flight altitude of 200 m above sea level. In the February measurements the DMS concentrations ranged from 1 to 12 pptv in the ML and 1 to 3 pptv in the FT.

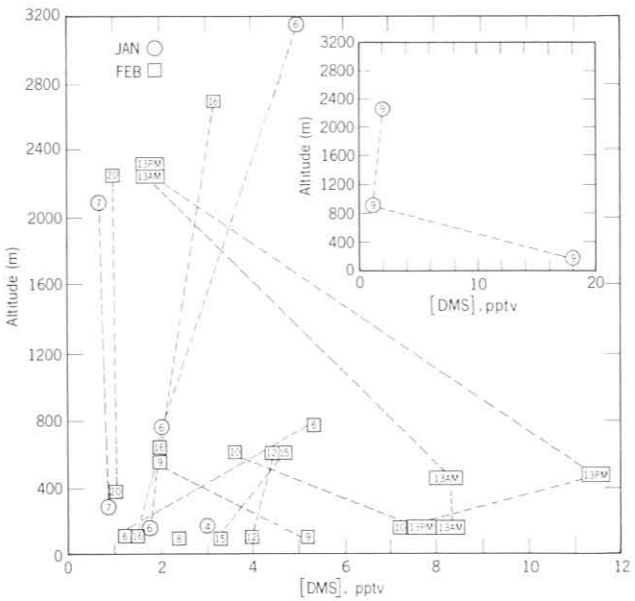

Figure 2.--Dimethyl sulfide concentration as a function of altitude, measured near Boston during January and February 1986 (after Van Valin et al., 1987b). The numbers in the circles or squares indicate the date of that measurement. The dashed lines connect samples from different altitudes during a given flight.

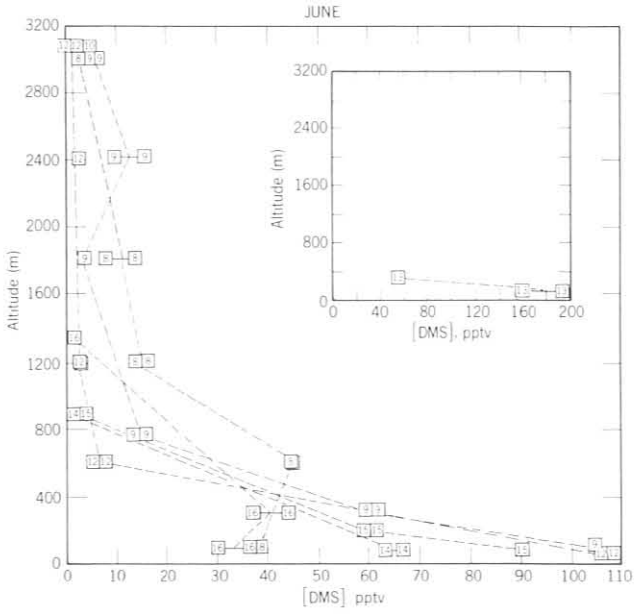

Figure 3.--Dimethyl sulfide concentration as a function of altitude, measured near Bermuda during June 1986 (after Van Valin et al., 1987b). The numbers in the squares indicate the date of that measurement.

Figure 3 presents the DMS data obtained during eight flights near Bermuda in June 1986. The values at the lowest flight level (90 m) were in the range 30-195 pptv. The individual profiles showed a very strong decrease in DMS concentration as the altitude increased, the concentration range being 5-45 pptv in the upper ML (600-1000 m) and <1-17 pptv in the FT (1000-3000 m). Exceptions occurred only on 8 June and 16 June, when the concentrations at 90-m altitude were low. On both of these days the DMS concentrations obtained at both ML flight altitudes were nearly the same, unlike for the profiles obtained on the other five flights. Concurrent SO_2 measurements suggested that SO_2 throughout the sampling period was less than the detection limit of 0.3 ppbv.

DMS average concentrations observed in the ML near Boston during the winter season were lower by a factor of ten than those observed in Bermuda during the summer. DMS concentrations in the ML did not decrease with altitude near Boston. In Bermuda, a strong altitude gradient appeared in five of the seven ML flights. Two major features contributed to the differences between the Boston and Bermuda data sets. The first is active mixing within the ML in the coastal region compared with a more stable atmosphere at Bermuda. The second is the radically different times of transport of the air masses over the ocean. Van Valin et al. (1987b) give a more complete description of this work.

The Processing of Emissions by Clouds and Precipitation Experiment (PRECP)

PRECP, another NAPAP project, provided AQG the opportunity to investigate the complex chemical transformations occurring in and near clouds. PRECP field efforts were completed at Oklahoma City, OK (June 1985), Syracuse, NY (January 1986) and Raleigh, NC (March 1986). The Oklahoma City experiment used the NOAA King Air to examine the chemical and physical processes that occur in large thunderstorms of the high plains. The Syracuse and Raleigh experiments used the NOAA King Air to examine the chemical and physical processes occurring in winter cloud systems.

THE RADIATIVELY IMPORTANT TRACE SPECIES (RITS) PROJECT

GMCC found that concentrations of certain trace gases were increasing at its observatories. This spawned concern that these RITS gases (notably carbon monoxide and methane) would soon become important contributors to the "greenhouse effect" along with carbon dioxide. Therefore, GMCC began to obtain climatologically representative vertical profiles of them to supplement surface measurements. The NOAA King Air made 14 research flights (one flight per month) near Miami, FL, in 1986 to gather these data.

THE SOUTHEAST ALASKA FLUX EXPERIMENT (SAFE)

Nuclear reactor no. 4 at Chernobyl, Soviet Union, exploded on 26 April 1986 at 0123 LT. The NOAA King Air made six research flights to examine the radioactive cloud produced by the accident. The initial goals of the research were to determine the width of the radioactive plume as it reached the North American continent, the radioactive isotopes present, and the concentration of each radioisotope.

The project used two research aircraft, the King Air and the Battelle Pacific Northwest Laboratories DC-3. Measurements were made from Anchorage, AK, to Reno, NV. The radioactive cloud from Chernobyl was first detected over the west coast of North America using gamma-ray spectrometers on 8 May 1986. Later analysis of air filters showed that the leading edge of the cloud just reached the west coast on 6 May 1986. This was in good agreement with trajectory model calculations. A comparison of the reported Soviet discharge concentrations relative to ^{137}Cs showed agreement for the volatile radionuclides ^{131}I and ^{134}Cs collected on the airborne air filters. Agreement was also observed for the nonvolatile ^{140}Ba. Lepel et al. (1987) give a detailed description of the results from the project.

MATERIALS AND METHODS USED IN AIR QUALITY PROGRAMS

The Air Quality Group uses the NOAA King Air aircraft as a data collection platform in its research projects. This platform provides the unique capability to obtain physical and chemical observations of the atmosphere in both the horizontal and vertical dimensions. Its range (2100 km), flight duration (4.5 h), and service ceiling (7.6 km) make it an ideal platform for atmospheric research in the troposphere above North America.

The Use of an Airborne Air Sampling Platform for Regional Air Quality Studies

The use of aircraft is common for studying a wide variety of atmospheric processes on the local, regional, and global scales. Airborne atmospheric chemistry studies expanded during the 1970's with the goal of understanding the various aspects of gas-to-particle conversion in plumes emanating from point sources. Large aircraft (the four-engine Lockheed Electra and WP-3D) were instrumented and used in global-scale atmospheric chemistry studies. The need to investigate regional air quality issues motivated the AQG to develop an airborne platform capable of providing complete air quality information using limited resources, on the one hand, but retaining the flexibility to operate anywhere above the North American continent, on the other hand. Since our objectives called for operation over areas affected by anthropogenic pollution, the analytical instrument package on board used commercially available units. These units are sometimes less sensitive than "experimental" or "developmental" instrumentation but provide a higher degree of reliability.

A LORAN system (Advanced Navigation Inc. model 7000) determines the aircraft position accurately to 0.5 km. A radar altimeter (King, KRA10) aids in maintaining constant altitude at low elevations (<760 m) and enhances flight safety at low altitude.

The air intake system aboard the aircraft has different intakes for different applications. For the WATOX, PRECP, RITS, and SAFE studies, a five-tube stainless steel configuration was employed. Three tubes pointed forward and two pointed vertically. One forward-pointing inlet tube, used for total aerosol sampling, was isokinetic at any flight sampling speed; another had an inner Teflon tube and supplied air for the gas monitors; a third supplied air to a "cyclone" particle separator described by Boatman et al. (1988). Additional air samples, for intermittent sampling devices, were drawn from the vertical tubes and the sextant port at the top center of the fuselage.

A fully computerized data acquisition system digitizes the data from all continuous monitors, aerosol probes, and mass flow meters and records it to magnetic tape. The onboard computer system displays the data during flight. Magnetic tape also records the data from the navigation system (Algo, Inc.). All magnetic tape data are later merged into one file for analysis using an HP-1000 computer system.

An illustration of the aircraft configured for scientific research is given in fig. 4. Wellman et al. (1987) provide a more detailed discussion of the aircraft platform.

In-Flight Intercomparisons of Some Aircraft Meteorological and Chemical Measurement Techniques

The NOAA King Air and one of the two NOAA WP-3D's were flown side by side on 8 January 1986 to compare the scientific measurements being made using the two platforms. The King Air was flown side by side with a Beechcraft Queen Air (Brookhaven National Laboratory) and a Douglas DC-3 (Battelle Pacific Northwest Laboratories) on 1 March 1986. Accuracy limits were established during a comparison of the scientific data collected aboard the four aircraft.

Table 2 summarizes the results found during these comparison flights. Different groups prepared and calibrated the scientific instruments aboard the four research aircraft at different times and in different locations. Instrument preparation and calibration procedures were similar but not identical. The agreement between the various instruments was very good even

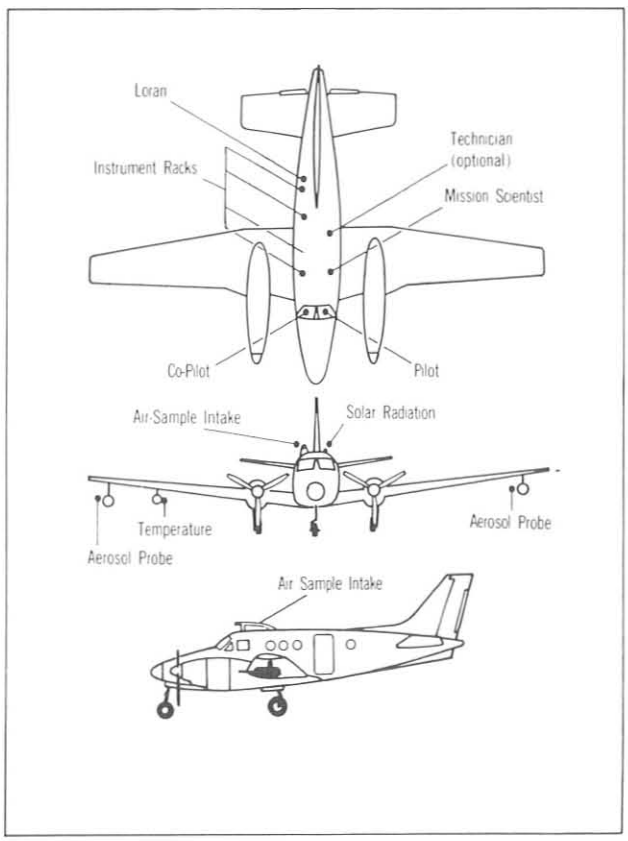

Figure 4.--The NOAA King Air C-90, configured for research.

Table 2.--Results of the aircraft intercomparison flights

Aircraft involved A	Aircraft involved B	Measurements compared	Accuracy A	Accuracy (Unit)	Accuracy B	Response time(s) A	Response time(s) B
King Air	WP-3D	Temperature	1	(°C)	1	1	1
		Dew Point	3	(°C)	3	1	1
		Pressure	1	(mb)	1	0.5	0.5
		Position	0.5	(km)	1	1	1
		Wind speed*	2	(m/s)	2	60	1
		Wind direc.*	10	(deg)	10	60	1
		Ozone	1	(ppbv)	1	30	15
		SO_2 FP-GC	1000	(pptv)	50	10	600
		SO_2 PF-GC	1000	(pptv)	50	60	600
King Air	Queen Air	Temperature	1	(°C)	2	1	1
		Wind speed*	2	(m/s)	2	60	1
		Wind direc.*	10	(deg)	10	60	1
		SO_2 FP-FP**	5	(%)	5	10	10
		SO_2 PF-FP**	5	(%)	5	60	10
		Ozone	1	(ppbv)	1	30	2
King Air	DC-3	Temperature	1	(°C)	1	1	1
		Dew Point	3	(°C)	3	1	1
		Pressure	1	(mb)	1	0.5	0.5
		Wind speed†	2	(m/s)	--	60	--
		Wind direc.	10	(deg)	10	60	1
		Ozone	1	(ppbv)	1	30	30
		SO_2 FP-FP**	5	(%)	5	10	10
		SO_2 PF-FP**	5	(%)	5	60	10

*KA turns unacceptable
**0-30 ppbv
†DC-3 overestimates

under diverse conditions. A detailed discussion of the scientific instruments aboard the King Air is given in Boatman et al. (1988).

7.2 Special Projects

AEROSOL AND CLOUDWATER PROPERTIES AT WHITEFACE MOUNTAIN, NEW YORK

During the summers of 1981, 1982, and 1983 the AQG conducted projects at the Vincent Schaefer Observatory, Whiteface Mountain, NY, in cooperation with SUNYA/ASRC. The purpose was to document some of the physical and chemical characteristics of aerosols and clouds in polluted and nonpolluted air masses, and to relate differences to source areas or meteorology. The characteristics of interest included aerosol and cloud size distributions, the chemical composition of aerosol and water samples, especially the air mass source sectors, the nucleation of cloud, and the incorporation of aerosols in the cloud liquid phase. A detailed description of the results from this study is given by Van Valin et al. (1987a).

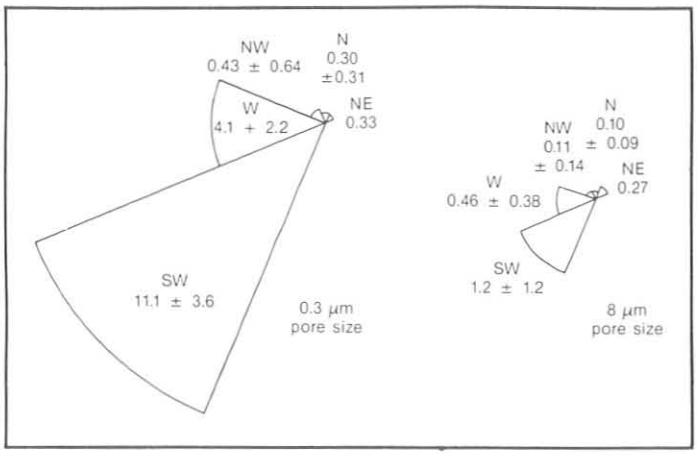

Figure 5. Aerosol S expressed as sulfate ($\mu g\ m^{-3}$), mean and 1-σ standard deviation, during cloud-free sampling times, arranged according to 45° source direction sectors (after Van Valin et al., 1987a). The scale of the right pie graph is expanded by a factor of 2.5 relative to the left graph.

The aerosol S (expressed as sulfate) source sectors, based on air mass trajectories, are shown in fig. 5. The left pie graph represents analyses of 0.3-μm-pore-size filters; the right represents the 8-μm filters (the right-side scale contains a 2.5 enhancement factor compared with the left side). All filter samples from cloud events were excluded. No air masses from the S, SE, or E occurred during the sample collection period. The greatest concentrations of sulfate were in the SW and W sectors. More important, ~90% of the sulfate at Whiteface Mountain is in the accumulation mode.

Water samples collected from clouds formed in air masses with back trajectories to industrial regions southwest of Whiteface Mountain had the highest median concentrations of most of the measured substances. In these samples SO_4^{2-} and NO_3^- were highly correlated to each other and to free H^+, CA^{2+}, Cl^-, Pb, and Ba. Other metallic elements were present in all three trajectory sectors in proportions suggestive of crustal origin, and had stronger correlations to SO_4^{2-} and NO_3^- in the NE than in the SW sector. The formation of a water cloud in a polluted atmosphere resulted in the removal of ~90% of the dry-aerosol sulfate by the time the cloud reached full density.

7.3 References

Andreae, M. O., R. J. Ferek, F. Bermond, K. P. Byrd, R. T. Engstrom, S. Hardin, P. D. Houmere, F. LeMarrec, H. Raemdonck, and R. B. Chatfield, 1985. Dimethyl sulfide in the marine atmosphere. Journal of Geophysical Research 90:12891-12900.

Boatman, J. F., D. L. Wellman, R. C. Schnell, K. M. Busness, M. Luria, and C. Van Valin, 1988. In-flight intercomparisons of some aircraft meteorological and chemical measurement techniques. Global Biogeochemical Cycles (Accepted).

Galloway, J. N., D. M. Whelpdale, and G. T. Wolff, 1984. The flux of S and N eastward from North America. Atmospheric Environment 18:2595-2607.

Horvath, H., R. L. Gunter, and S. W. Wilkison, 1988. Determination of the Coarse Mode of the Atmospheric Aerosol with Optical Counters. Aerosol Science and Technology submitted; (available through Air Quality Group, NOAA/GMCC, 325 Broadway, Boulder, CO).

Lepel, E. A., W. K. Hensley, J. F. Boatman, K. M. Busness, W. E. Davis, D. E. Robertson, and W. G. N. Slinn, 1987. In situ gamma-ray measurements in the Chernobyl plume. Proceedings of the International Conference on Methods and Applications of Radioanalytical Chemistry., April 5-10, 1987, Kona, HI., American Nuclear Society, Richland, WA, 1-19.

Luria, M., C. C. Van Valin, J. F. Boatman, D. L. Wellman, and R. F. Pueschel, 1987. Sulfur dioxide flux measurements over the Western Atlantic Ocean. Atmospheric Environment 21(7):1631-1636.

Sievering, H., J. Boatman, L. Gunter, H. Horvath, D. Wellman, and S. Wilkison, 1987. Sea source of aerosol particle size distributions: A physical explanation of observed differences, nearshore vs. open sea. Journal of Geophysical Research (accepted).

Van Valin, C. C., H. Berresheim, M. O. Andreae, and M. Luria, 1987b. Dimethyl sulfide over the Western Atlantic Ocean. Geophysical Research Letters (accepted).

Veal, D. L., W. A. Cooper, G. Vali, and J. D. Marwitz, 1978. Some aspects of aircraft instrumentation for storm research. American Meteorological Society Monograph 38:237-255.

Wellman, D. L., M. Luria, C. C. Van Valin, and J.F. Boatman, 1987. The use of an airborne air sampling platform for regional air quality studies., Global Biogeochemical Cycles (accepted).

8. NITROUS OXIDE AND HALOCARBONS GROUP

8.1 Continuing Programs

ORGANIZATION

The NOAH Group was created in July 1986 as a result of the reorganization of the Trace Gases Group under the RITS initiative and the arrival of the new group chief in Boulder. The chief is a former NBS employee with expertise in gas standard preparation, EC-GC, and IR spectroscopy. A CIRES research associate joined the group at the same time as leader of special projects (KOROLEV cruise and LEAPS, discussed below).

CONTINUOUS AND FLASK NETWORK (CFN)

Weekly collection of air samples in 0.3 L flasks from BRW, NWR, MLO, and SMO continued as in the past; station personnel at SPO exposed flasks only during January, November, and December 1986. These air samples were analyzed for halocarbons CCl_3F (F-11) and CCl_2F_2 (F-12),and N_2O using EC-GC at the Boulder laboratory. Figure 1 presents the flask data for F-11, F-12, and N_2O from BRW, NWR, MLO, and SMO. Estimated secular trends and standard deviations (at the 95% confidence level, C.L.) are also presented.

The Shimadzu Mini-2 GC at SPO measured N_2O, F-12, and F-11 in situ twice a week. SPO flask data are combined with the in situ GC data in fig. 2. N_2O data for 1986 were excluded from fig. 2, because of excessive drift of the N_2O signal. A new detector and gas sample valve will be sent on the 1987 mid-winter drop to fix this problem.

Latitudinal profiles of F-12 and F-11 using annual mean flask data are presented in fig. 3 for 1977-1986 from the GMCC baseline stations and NWR. The increases in the growth rates of F-11 and F-12 at all stations between 1985 and 1986 are probably the result of switching to a new calibration tank whose calibration is drifting with time. This tank was last calibrated against OGC's scale in 1985. An intercomparsion is planned with OGC in late 1987, which may resolve this change in growth rate.

The new RITS automated GC and data processing system was installed at SMO in June and BRW in October. Representative data for F-12 daily means from the RITS GC at SMO are compared with flask data in fig. 4. It is planned that MLO will receive its system in early 1987 and SPO late next year. Using an HP model no. 5890 GC, Nelson Analytical interface, HP9816 computer, HP9133 hard disk, and printer, the system measures air concentrations of N_2O, F-12, F-11, methyl chloroform (CH_3CCl_3), and carbon tetrachloride (CCl_4) every 2 hours. Commericially prepared calibration gases in 29.5-L aluminum high-pressure cylinders were found to be contaminated with 1,1,2-trichlorotrifluoroethane (F-113), making quantitation of CH_3CCl_3 impossible. Also, low concentrations of CCl_4 (about 30 ppt) were found to be unstable in the untreated aluminum cylinders; CCl_4 completely disappeared after 6 months. Changes will be made in 1987 to correct these problems.

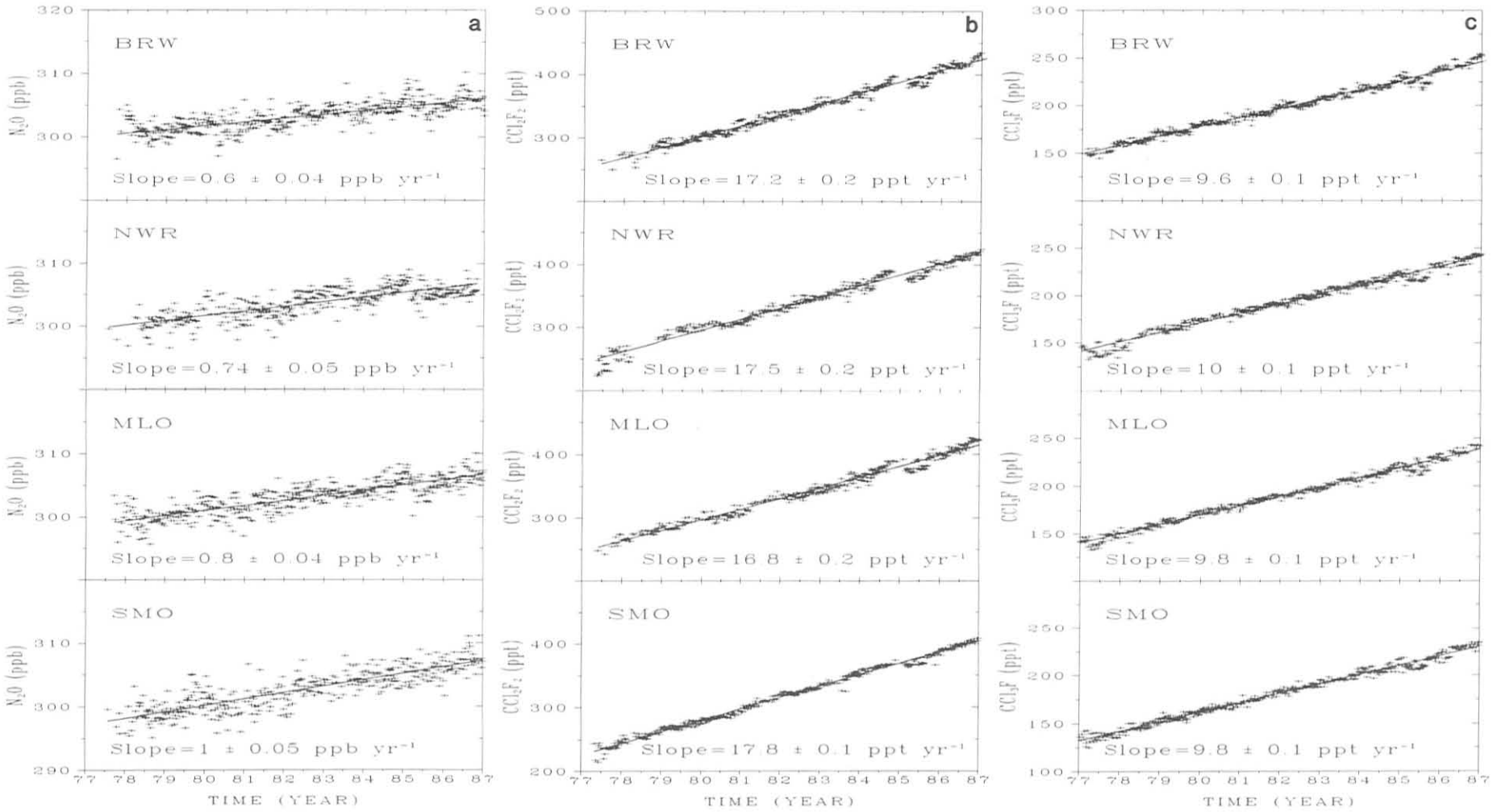

Figure 1.--Growth rates of (a) N_2O, and halocarbons (b) F-12 and (c) F-11 at BRW, NWR, MLO, and SMO for 1977-1986. The growth rates and their standard deviations at the 95% confidence level (C.L.) are also presented.

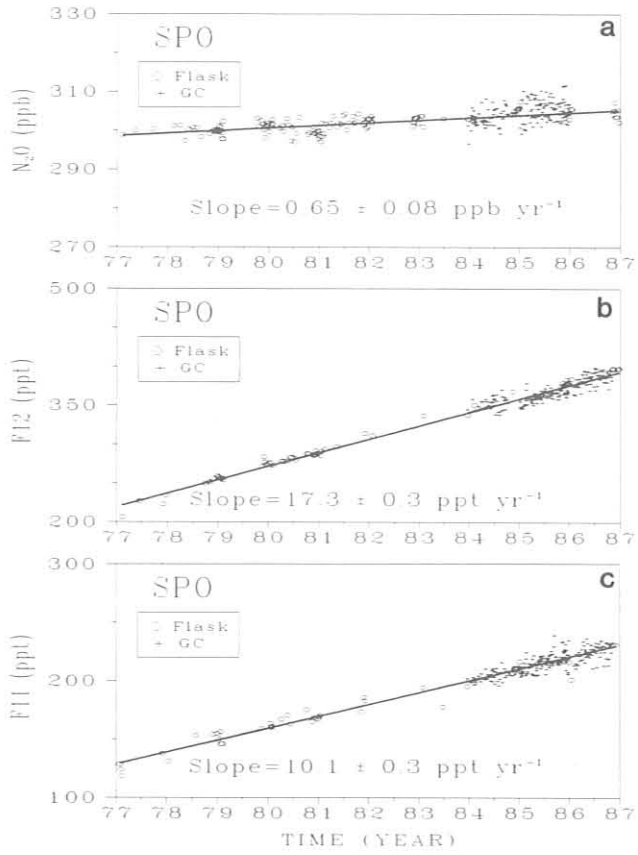

Figure 2.--Growth rates of (a) N_2O, and halocarbons (b) F-12 and (c) F-11 at SPO for 1977-1986. Crosses denote in situ GC results and ovals indicate flask samples analyzed in Boulder. The growth rates and their standard deviations at the 95% C.L. for the combined data sets are also presented.

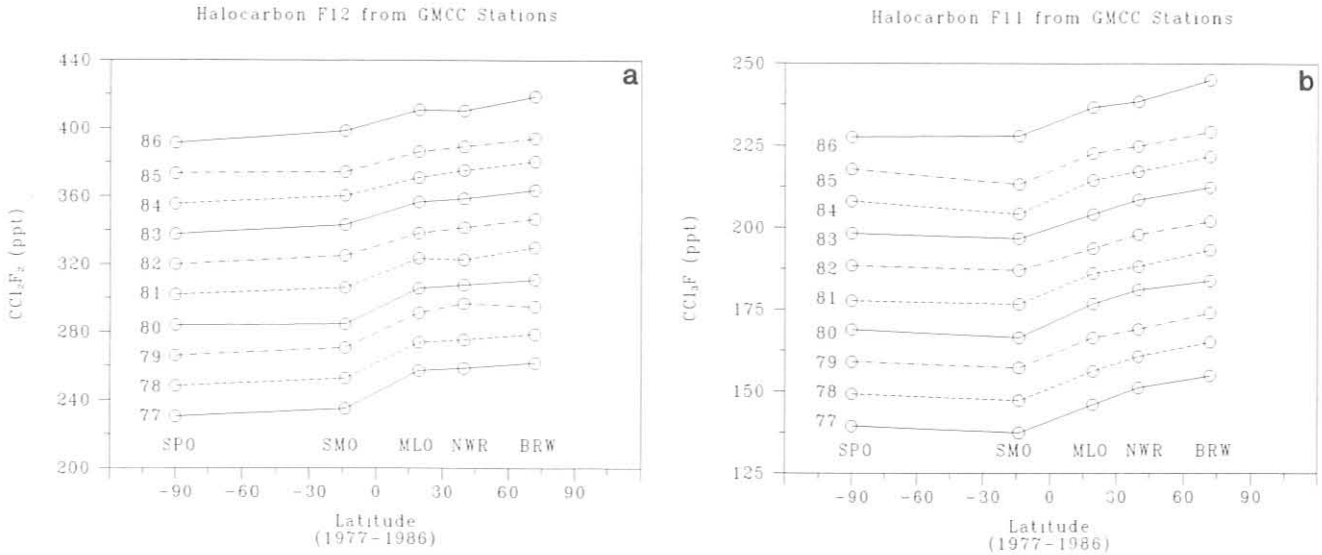

Figure 3.--Latitudinal profiles of (a) F-12 and (b) F-11 using annual mean flask data are presented for 1977-1986 from the GMCC baseline stations and NWR.

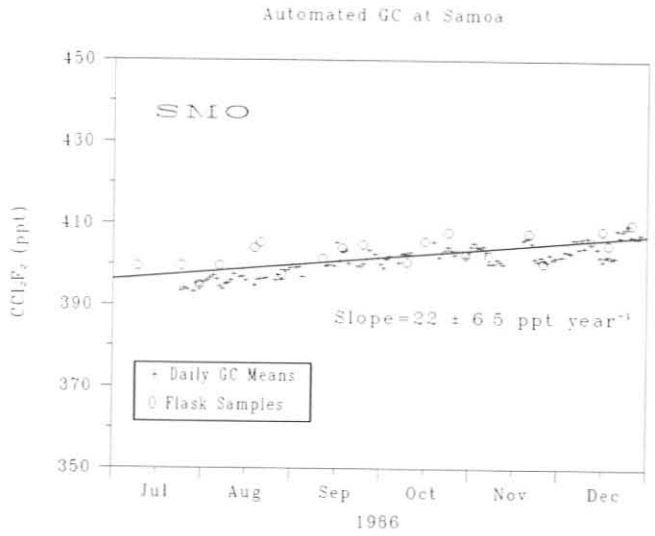

Figure 4.--F-12 daily means (+) from the RITS GC at SMO compared with flask samples (o) that were analyzed in Boulder. The growth rate and its standard deviation at the 95% C.L. for the combined data sets are given.

LOW ELECTRON ATTACHMENT POTENTIAL SPECIES (LEAPS)

The NOAH Group has received incremental RITS funding to begin measuring some of the "minor" atmospheric halocarbons. Specifically, plans are to develop or adapt techniques to investigate F-22 ($CHClF_2$), F-113 (CCl_2F-$CClF_2$), Halon-1211 ($CBrClF_2$), and Halon-1301 ($CBrF_3$). Although currently low in concentration, these halocarbons have been introduced into the atmosphere in much greater quantities in recent years, and their atmospheric lifetimes are long. These gases are involved in the radiative budget of the Earth's atmosphere, and all appear to be increasing in concentration at alarming rates. As with most halocarbons, they also may be important in the chemistry of the stratosphere. This is especially true of the brominated species, as stratospheric bromine is 10 times more effective than chlorine in removing ozone. These gases have been historically difficult to measure by EC-GC techniques because of their low electron affinity, their low atmospheric concentration, or both. Hence, they have been designated as LEAPS gases. Physical data are outlined in table 1. Information for table 1 came from Braker and Mossman (1980), Weast and Ostle (1979), L'Air Liquide (1976), and WMO (1986).

Table 1.--Properties of LEAPS Gases

Halocarbon	Formula	Boiling point (°C)	Atmospheric concentration (ppt)	(year)	Residence time (years)	Annual increase %	Sources*
F-22	$CHClF_2$	-40.8	52	1980	75	11.7-25	1,2,3,6
F-113	CCl_2F-$CClF_2$	47.7	32	1985	90	10	5
Halon-1211	$CBrClF_2$	-4.0	1.5	1984	25	20	4
Halon-1301	CBrF3	-57.8	1.0	1984	110	30	1,2,3,4

*1 = Refrigerant; 2 = freezing; 3 = air conditioning; 4 = fire extinguishing; 5 = solvent; 6 = intermediate in polymer chemistry.

GRAVIMETRIC STANDARDS

NOAH received RITS incremental funding in 1986 to develop an independent scale for the absolute gas calibration of RITS gases using gravimetric techniques. Since there are no standards available for many of the LEAPS gases, NOAH must prepare these standards. A standards laboratory complete with high-accuracy analytical balances will be installed in 1987. The NBS N_2O SRM which was developed and prepared by the Group Chief of NOAH, is currently being used for the absolute calibration of N_2O. NOAA personnel prepared a series of gravimetric standards for CH_4, F-11, F-12, CH_3CCl_3, and CCl_4 at NBS in the spring of 1986. The new CH_4 gravimetric standards compare better than ±1% with the NBS SRM, the most commonly used standard for atmospheric methane studies. The halocarbon standards are being used for our automated RITS GC. However, the OGC scale is still being used for F-11 and F-12 for continuity with the flask program until intercomparsions can be made with other international standards.

8.2 Special Projects

PLANS FOR JOINT U.S.-U.S.S.R. RESEARCH IN 1987

Planning was begun for a joint U.S.-U.S.S.R. research cruise aboard the research vessel AKADEMIK KOROLEV, to take place May-August 1987. The expedition, SAGA II, will involve the measurement of atmospheric and dissolved trace gases along a transect from Hawaii to Kamchatka, then down the 160°E meridian from about 45°N to 45°S, around Australia, up to Singapore, and back along the equator to Hawaii. The work will be conducted in conjunction with the Carbon Cycle Group of GMCC, as well as participants from NOAA/PMEL, OGC, SIO, University of Washington, Washington State University, and University of Hawaii. It is anticipated that GMCC will be able to obtain considerable valuable information on a number of gases along this route. The gases to be measured are N_2O in the atmosphere, in the surface water, and at depth, and F-11, F-12, CO_2, and CH_4 in the atmosphere and surface waters. In addition, we plan to collect flask samples along the 160th meridian for subsequent analysis of CCl_4, CH_3CCl_3, CO_2, CH_4, and perhaps the LEAPS gases as well.

Our objectives are (1) to test our new, highly precise technique for measuring N_2O under rigorous operating conditions, (2) to test a new automated headspace sampler for measuring dissolved N_2O, (3) to compare the latitudinal, atmospheric gradients obtained from these data with those indicated from our station sampling network, (4) to detect any sharp interhemispheric gradients of N_2O, F-11, F-12, CO_2, or CH_4 near the equator, (5) to evaluate the fluxes of these gases from the sea surface to the atmosphere along this transect, and (6) to observe any signals that may be associated with the recent ENSO event. We also hope to intercalibrate some of our measurements with those of the Soviets as well as other US participants on the cruise.

FOURIER TRANSFORM INFRARED ARCHIVE PROGRAM

The total atmospheric content of a strong IR absorbing gas is required to determine the "greenhouse effect" of a particular species. Although ground-based measurements of these species give a reliable temporal indication of the

total atmospheric content, a vertical profile must either be assumed or measured using expensive balloon or aircraft studies in order to calculate the total gas concentration in the atmosphere. It is possible with new computer technology and instrumentation to measure the "column density" or the total concentration above a site using an FT-IR spectrometer at a resolution (0.12 cm^{-1} or better) sufficient to resolve possible overlapping IR absorption lines of interfering species. The measurement of the column density involves tracking the sun, using it as an IR source at various zenith angles, yielding atmospheric path lengths between 10 and 70 km with a ground-based FT-IR spectrometer coupled to a cooled (70 K) IR detector. Many of the RITS gases, including O_3, CO_2, CH_4, CO, N_2O, F-12, and F-11, have been observed using this technique to precisions of a few percent. A great many IR absorbing lines have not been identified in solar spectra, and archiving spectra can be used to establish a baseline for future molecules not analyzed by GMCC (e.g., hydrocarbons, oxides of nitrogen, heavier halocarbons). It is also possible to measure the greenhouse effect directly by observing warming trends on night-time emission of atmospheric IR lines.

A proposal was written by the NOAH, ARM, and Carbon Cycle Groups in GMCC to start this research. This proposal received partial support from the Director's Office of ERL to purchase a used FT-IR spectrometer with a maximum resolution of 0.06 cm^{-1} from NBS in Gaithersburg, MD. Plans are to field test this instrument in an observatory on the roof of RL-3 in Boulder. After successful tests, the plan is to move the instrument to MLO where both the water vapor content and atmospheric pressure broadening are lower.

8.3 References

Braker, W., and A.L. Mossman, 1980. Matheson Gas Data Book, 6th ed. Matheson Gas Products, Secaucus, NJ, 711 pp.

Weast, R.C., and M.J. Astle (eds.), 1979. CRC Handbook of Chemistry and Physics, 59th ed. CRC Press, Inc., West Palm Beach, FL.

L'Air Liquide, 1976. Encyclopedie des Gas. Elsevier/North-Holland, New York, 1150 pp.

WMO (World Meteorological Organization), 1986. Atmospheric ozone 1985. WMO Global Ozone Research and Monitoring Project, Report No. 16. Vols. 1-3, Geneva, Switzerland.

9. DIRECTOR'S OFFICE

9.1 Alkaline Aerosols

DUST EMISSIONS INVENTORY FOR THE UNITED STATES: APPLICATION TO NAPAP NEEDS

Workers in GMCC are estimating emissions of alkaline aerosols that potentially neutralize some acidity in precipitation, specifically, dust emissions by wind action on soils, as part of NOAA's contribution to Task A of the NAPAP. During the past year, a model of dust emissions has been developed. Its validity is being tested in a region of active wind erosion, USDA Major Land Resource Area 77 (MLRA 77), which is roughly located in the panhandles of Texas and Oklahoma.

SHORT DESCRIPTION OF THE MODEL

The model gives the mathematical expectation for wind erosion soil loss and for dust emission, integrated from the threshold velocity for wind erosion to infinity. The model uses 1 month for its basic time period and uses the Weibull distribution as its probability density function for each month. This formalism allows the specification of soil conditions by the month. The soil conditions are entered into the model by threshold velocities, the erosion and dust emission functions, and drag coefficients. The ridge roughness function of the USDA wind erosion equation (WEE) is used along with simplified treatments of the field length effect and vegetative residue.

THRESHOLD VELOCITIES USED IN THE MODEL

Crusting of the soil and cloddiness of the soil are two extremely important factors in determining threshold velocities for wind erosion. Since crusting and cloddiness are greatly affected by precipitation and are critical to the model, we had as a major goal to introduce precipitation climatology into models of the threshold velocity expressed as monthly values. The threshold velocities used in the model follow a previous model developed from observations of threshold velocities for a variety of soil textures, from wind tunnel testing in the field, and from tests of change of threshold velocity as it responds to cultivation, rainfall, and drying.

The threshold velocities were expressed as depending upon cultivation procedures (fall planting, spring planting, fallowing), soil textures, vegetative residue, crops, and five classes of soil moisture corresponding to five climatological classes. The five climatological classes corresponded to (1) below average precipitation 2 years previous to the present and below average precipitation the present year, (2) below-average precipitation by at least 8 inches for the 2 years previous to the present and below-average precipitation the present year, (3) below-normal precipitation for the previous 2 years and above average precipitation by at least 4 inches for the present year, (4) above average precipitation by at least 4 inches for the previous 2 years and less than 4 inches above average precipitation the present year, and (5) above average precipitation by at least 4 inches for the previous 2 years and above average by at least 4 inches for the present year. ARL analyzed the precipitation climatology for MLRA 77 and furnished data that could be organized in the above five classes.

OTHER DATA USED BY THE MODEL

In addition to the precipitation climatology data, the model uses the following data sets:

(1) NRI point sample unit (PSU) data. This data set is an extensive description of soil, cropping, and land use of nonfederal lands. It consists of 841,860 records.

(2) Wind Erosion Coefficients. This data set consists of 259,628 records of ridge roughness, "I" factor, field length, and vegetative residue on agricultural land.

(3) Wind Energy Resource Inventory. This set consists of 1735 blocks of data representing wind records over the entire United States summarized into monthly summaries of hourly means. The period of record is 1948-1978.

TEST OF THE MODEL IN MLRA 77

At this time, the model has been tested only in MLRA 77. The area was chosen because it was the location of several dust storm measurements in the 1970's and because it includes part of the area where the WEE was developed. New estimates from the model should roughly agree with the WEE for this area for the years 1954, 1955, and 1956 because it was during these years that critical measurements were taken for the development of the WEE.

The results for the period 1948-1978 for MLRA 77 for dust emissions are shown for 100 PSU's (a small fraction of the entire area in MLRA 77) in fig. 1. Variability within this period for dust emission is almost 2 orders of magnitude. Model estimates for 100 PSU's of wind erosion for MLRA 77 in 1954-1956 are within a factor of 2 of the WEE estimates for the same period (see table 1).

Table 1.--Total erosion and dust production for MLRA 77 in 1954-1956 (in million tonnes)

Year	Wind erosion		Dust production
	WEE estimate	Model estimate	
1954	349	221	19
1955	349	154	11
1956	349	122	8

Because of the highly nonlinear nature of dust production, it was estimated that production from very large dust storms was practically equal to the entire monthly dust production. Data for dust production, estimated by aircraft sampling, were taken from Gillette et al. (1978). Table 2 gives the results of the measured production and the model-estimated production. Since the measured injection of dust was limited to particle size range smaller than 20 μm, and suspended dust particles produced in these storms were as large as about 100 μm, the measured injections were multiplied by a factor of 3 to compensate. The model monthly injections in table 2 are higher than the

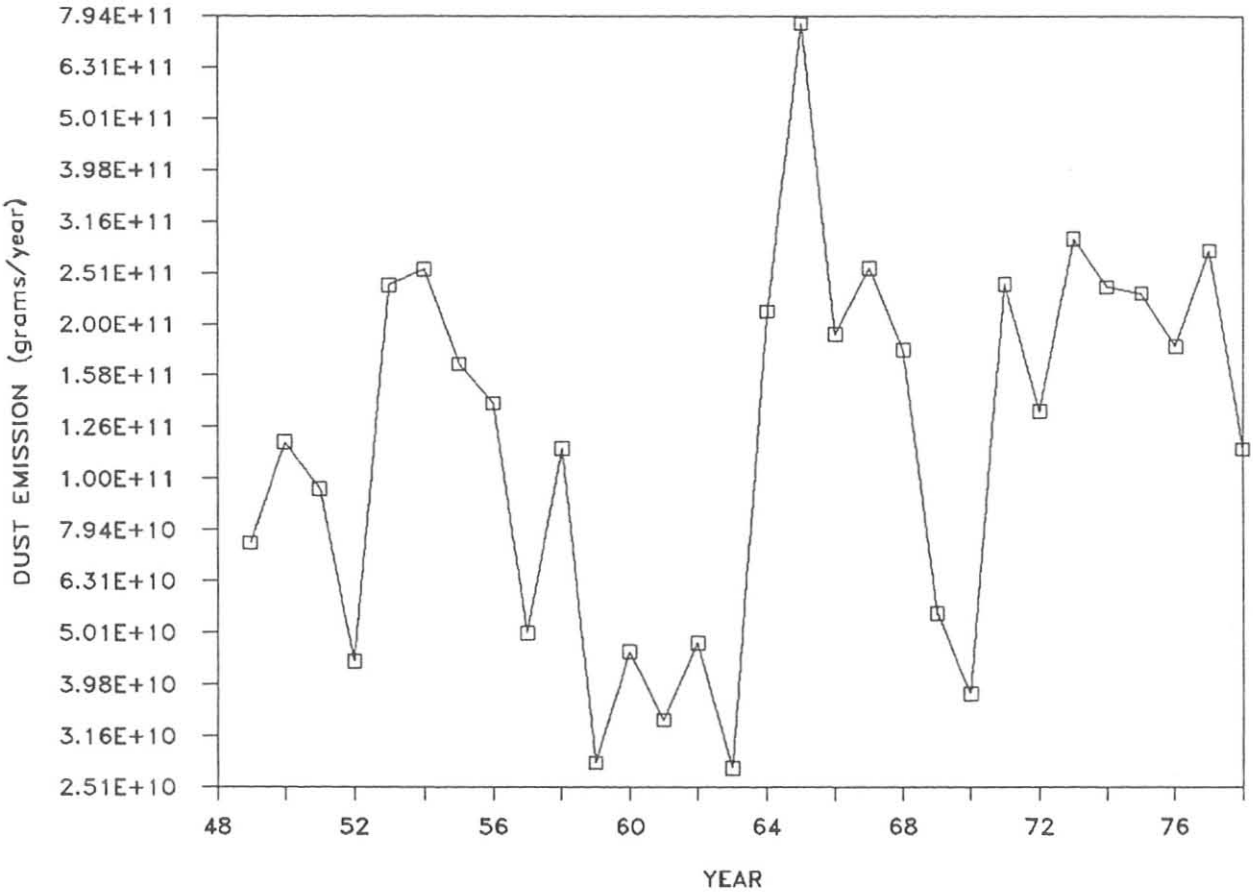

Figure 1.--Dust emission vs. year for 100 PSU's in MLRA 77.

observed, adjusted injections by less than a factor of 2. The difference may be because the model estimates are for the entire month's production, whereas the measurements are for large storm production, or it may be that aircraft measurements of dust concentrations were low because the aircraft did not fly into the most severe and most concentrated parts of the storm.

Table 2.--Monthly total input from individual dust storms (in million tonnes)

Year	Month	Measured and adjusted	Estimated by model
1972	April	2.4	4.9
1973	April	3.6	5.8
1975	April	3.0	4.6

REFERENCES

Gillette, D., R. Clagton, T. Mayeda, and M. L. Jackson, 1978. Tropospheric aerosols from some major dust storms of the southwestern United States. Journal of Geophysical Research 17:832-845.

9.2 Arctic Gas and Aerosol Sampling Program

A "MAJOR" ARCTIC HAZE EVENT NORTH OF POINT BARROW, April 1986

Russell C. Schnell
Cooperative Institute for Research in
Environmental Sciences
University of Colorado, Boulder, CO 80309

INTRODUCTION

The Arctic Gas and Aerosol Sampling Program (AGASP) is a multifaceted cooperative research program designed to determine the distribution, transport, chemistry, aerosol physics, and radiative effects of the polar-wide air pollution phenomenon know as Arctic haze. The research was conceived, organized, and directed by the National Oceanic and Atmospheric Administration (NOAA), and the Cooperative Institute for Research in Environmental Sciences (CIRES), University of Colorado, Boulder. AGASP has involved participants from the United States, Canada, Norway, Sweden, Federal Republic of Germany, and Denmark and has covered two intensive field study periods in March-April 1983 and March-April 1986. The core field research program consists of airborne measurements tied to similar baseline station measurements at Pt. Barrow, Alaska; Alert, Northwest Territories; and Ny Alesund, Spitzbergen. The results of the 1983 program were published in special issues of Geophysical Research Letters (Vol. 11, no. 5, May 1984) and Atmospheric Environment (Vol. 19, no. 12, December 1985).

The second phase of the AGASP (AGASP-II) began in March 1986 with intensive ground-based operations at various locations in the Arctic, followed in April by research flights covering the Arctic from Alaska to Greenland. One component of the airborne operations was flights by an extensively instrumented NOAA WP-3D Orion research aircraft. This aircraft flew three missions to the Alaskan north slope in support of baseline monitoring at Barrow, and three missions in the Canadian Arctic, based at Thule, Greenland. The latter flights were related to the Canadian Baseline Station at Alert, operated by the Atmospheric Environment Service, Canada. They were flown in conjunction with the Twin Otter research aircraft of the National Aeronautical Establishment of Canada and the C-131 research aircraft of the University of Washington.

On the first AGASP-II flight, a haze zone with exceptionally large condensation nuclei (CN), and SO_2 concentrations was encountered 100 km northwest of the Barrow GMCC Baseline Station. The characteristics of the haze and information on its source and transport are presented below.

HAZE DISTRIBUTION

A vertical profile through the edge of the "major haze layer" is shown in fig. 1 for an ascending profile between 0056 and 0126 GMT, April 3, at 72.35°N latitude, 159°W longitude. The haze, as determined by CN concentrations and

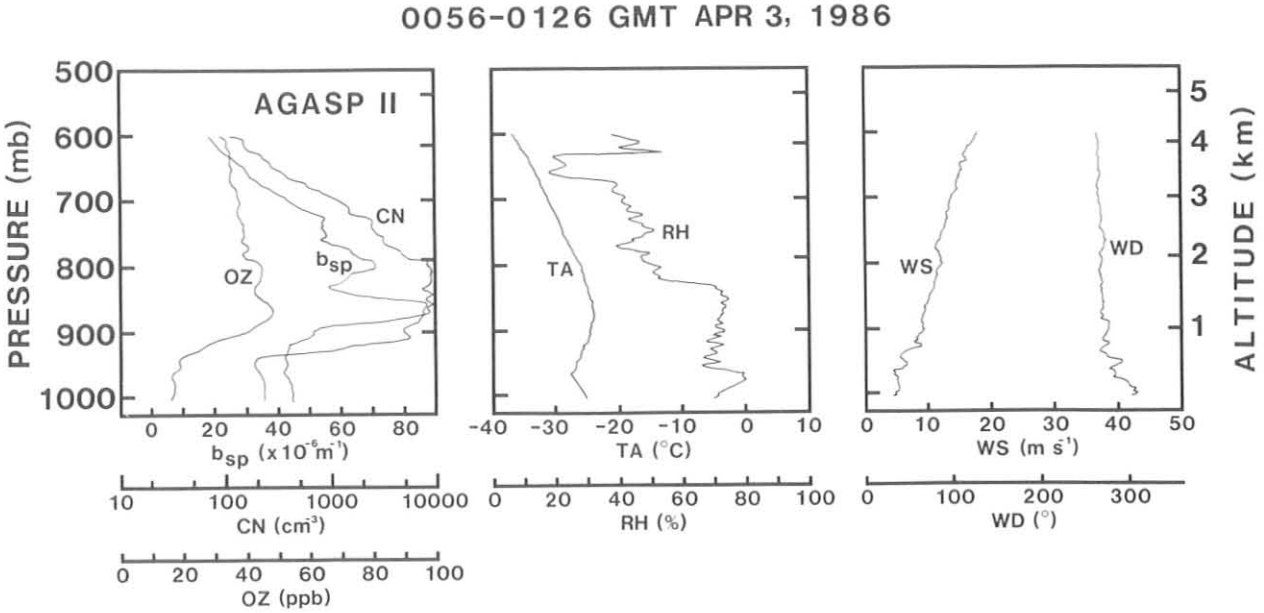

Figure 1.--Vertical profiles of ozone (OZ), b_{sp}, CN concentration, ambient temperature (TA), relative humidity (RH), wind speed (WS), and wind direction (WD) through the major haze layer, 2-3 April 1986.

aerosol light scattering (b_{sp}) had a sharp lower boundary at 950 mb at the top of the surface temperature inversion. The lower portion of the haze layer was associated with relatively moist air and slightly elevated ozone concentrations. The peak in b_{sp} (90×10^{-6} m^{-1}) occurred just below the top of the moist layer at 870 mb. CN concentrations held fairly steady, in the 9,000-10,000 cm^{-3} range, from 880 to 790 mb both within and above the moist layer. SO_2 concentrations within the layer peaked at 15 ppb. The haze and the higher moisture correlate well with the layer of warmer air between 940 and 830 mb. Wind direction throughout the profile was steady from 270°-280°, increasing in speed from 4 m s^{-1} near the surface to 15 m s^{-1} at 600 mb.

This haze zone had been penetrated earlier at 72.28°N, 158.27°W, 2332 GMT, 794 mb, as shown in fig. 2. After flying level for 10 min in the haze, the aircraft reversed track from 188° to 22° and flew out of the side of the haze zone at a point 30 km from the entry point. In fig. 2, an abrupt increase in CN concentration to 70,000 cm^{-3} occurred at the haze boundary coincident with a sharp increase in RH from 50% to 75%. Aerosol b_{sp} increased from 35×10^{-6} m^{-1} at the edge to 60×10^{-6} m^{-1} near where the aircraft reversed direction. The penetrations shown in figs. 1 and 2 were separated by 2.5 h; the data shown in fig. 1 were collected 90 km upwind of the data exhibited in fig. 2. At a haze flow rate of 10 m s^{-1}, these two penetrations occurred about 190 km apart with reference to the flowing haze stream. By comparing figs. 1 and 2, we can observe that b_{sp} at the same level (794 mb) and 36 km in from the edge of the haze at the turning point (thought to be about equivalent to the point where the profile shown in fig. 1 was undertaken) were both in the 55-60) $\times 10^{-6}$ m^{-1} range. CN concentrations were higher in the side penetration (≈16,000 cm^{-3}) compared with the profile (≈10,000 cm^{-3}), but were in agreement 4 min later (14 km ground distance). Ozone was 39 ppb at both locations.

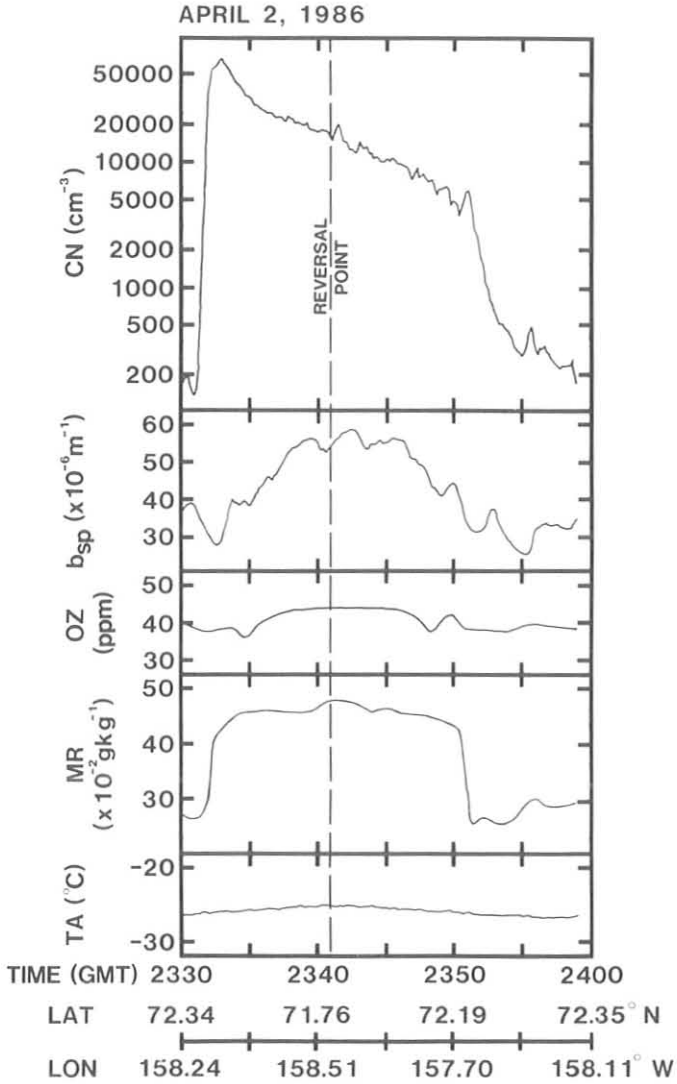

Figure 2.--Time series (top to bottom) of CN concentration, b_{sp}, ozone (OZ), relative humidity, and temperature from 2330 to 2400 GMT when the aircraft encountered the major haze layer (794 mb, 1825 m altitude), 2-3 April 1986. At the reversal point, the aircraft changed direction from 188° to 22° and flew out of the side of the haze layer at 2351 GMT.

HAZE CROSS SECTION

The magnitude of the variation of the haze experienced during a transect 90° to the prevailing wind direction, 190 km upwind of the descent profile is shown in Figure 3. This porpoising segment took 55 minutes to cross the major portion of the plume, thus it offers a relatively quick cross-section look at the haze layer and its surroundings. The plot of b_{sp} shows a maximum of >70 x 10^{-6} m^{-1} at 71.4°N (870 mb), and a minimum at 72°N (815 mb). The values of b_{sp} at the edges of the chart are generally representative of the background. The CN concentrations are generally above background levels throughout the entire segment, and the maximum is >23,000 cm^{-3} at 72°N (820 mb). The minima in CN concentrations at 71.5°N (500 cm^{-3}) correspond to the highest b_{sp} values (>70 x $10^{-6}m^{-1}$).

By comparing the moisture distribution with the b_{sp} and CN distributions, it is observed that high b_{sp} correlates with higher mixing ratio (MR), and high CN correlates with lower MR. It should be emphasized at this point that the feed air to the nephelometer that measures b_{sp} is heated from ambient air temperature to +29-32°C before the b_{sp} measurement. Thus, it is expected that

water droplets and/or ice crystals are not detected in the nephelometer. That this is probably the case is supported by observations that b_{sp} does not change when the aircraft passes through clouds. Thus, we assume that the b_{sp} signals measured on these profiles are for dry aerosols.

These relationships between higher moisture-higher b_{sp} and lower moisture-lower CN might be explained by assuming that the moister air had enhanced particle growth from nucleation mode (CN) aerosols to accumulation mode aerosols measured as b_{sp}. Thus, former CN would now be detected in the aerosol b_{sp} signal. Higher CN concentrations in dry air may indicate recent SO_2 gas-to-particle conversions to H_2SO_4 droplets which have not yet grown to accumulation mode aerosol size. Such growth would be enhanced by greater moisture supplies.

During AGASP-I, Radke et al. (1984) measured high CN concentrations and coincident nucleation mode aerosols in Arctic haze when ambient SO_2 concentrations exceeded 1 ppb. Similar results were observed by Flyger et al. (1976) in the Greenland area where they measured SO_2 concentrations >1 ppb and peak CN concentrations >10,000 cm^{-3}.

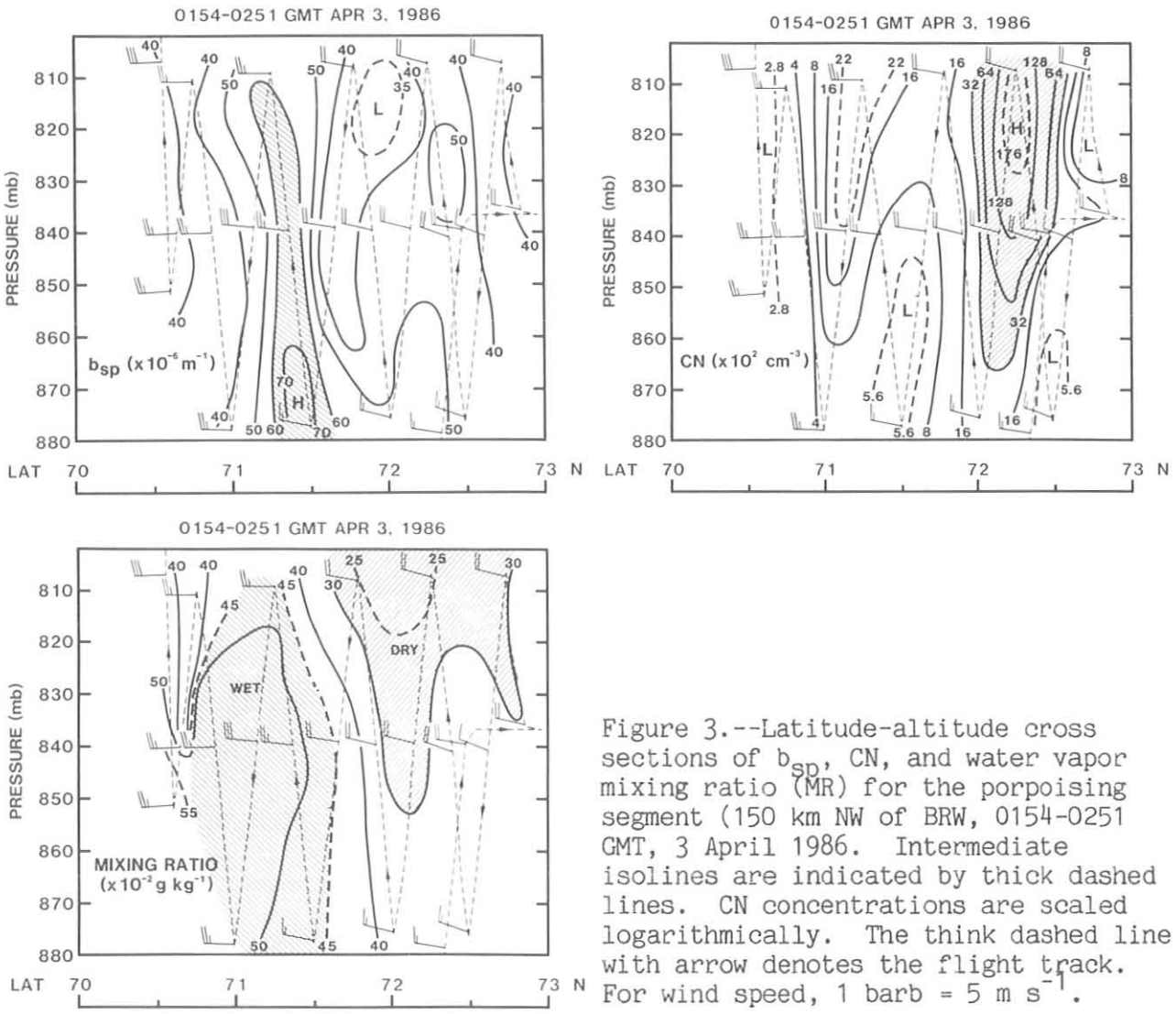

Figure 3.--Latitude-altitude cross sections of b_{sp}, CN, and water vapor mixing ratio (MR) for the porpoising segment (150 km NW of BRW, 0154-0251 GMT, 3 April 1986. Intermediate isolines are indicated by thick dashed lines. CN concentrations are scaled logarithmically. The think dashed line with arrow denotes the flight track. For wind speed, 1 barb = 5 m s^{-1}.

HAZE SOURCE AND TRANSPORT

Back trajectories from the haze zone north of Barrow indicated a path crossing Svalbard and Scandinavia 10 days earlier. Sulphate and SO_2 data from the Norwegian Air Quality Network for March 1986 are shown in fig. 4. From this figure, it may be observed that a major air pollution episode flowed northward across Norway and past Svalbard on the same pathway and timing as suggested by the trajectories and the aircraft penetrations of the haze.

Further extensive forward and back trajectories from the Norwegian stations and meteorological analyses have defined a probable source region for the haze as being industrialized central Europe.

This source region, the centerline of the trajectory, and the meteorologically derived pathway for the haze encountered by the aircraft off Barrow is shown in fig. 5. In this figure, a map of the United States is superimposed on the Arctic to provide a relative scale for the long-range transport of the pollution. For instance, the April 2-3 haze event travelled a distance equivalent to air pollution originating in the Ohio Valley flowing east to New York City then south to Miami before turning to the west and flowing past Houston onto Los Angeles. At Los Angeles, it turns north and flows to Seattle where it turns and heads east and crosses the continent again back to New York.

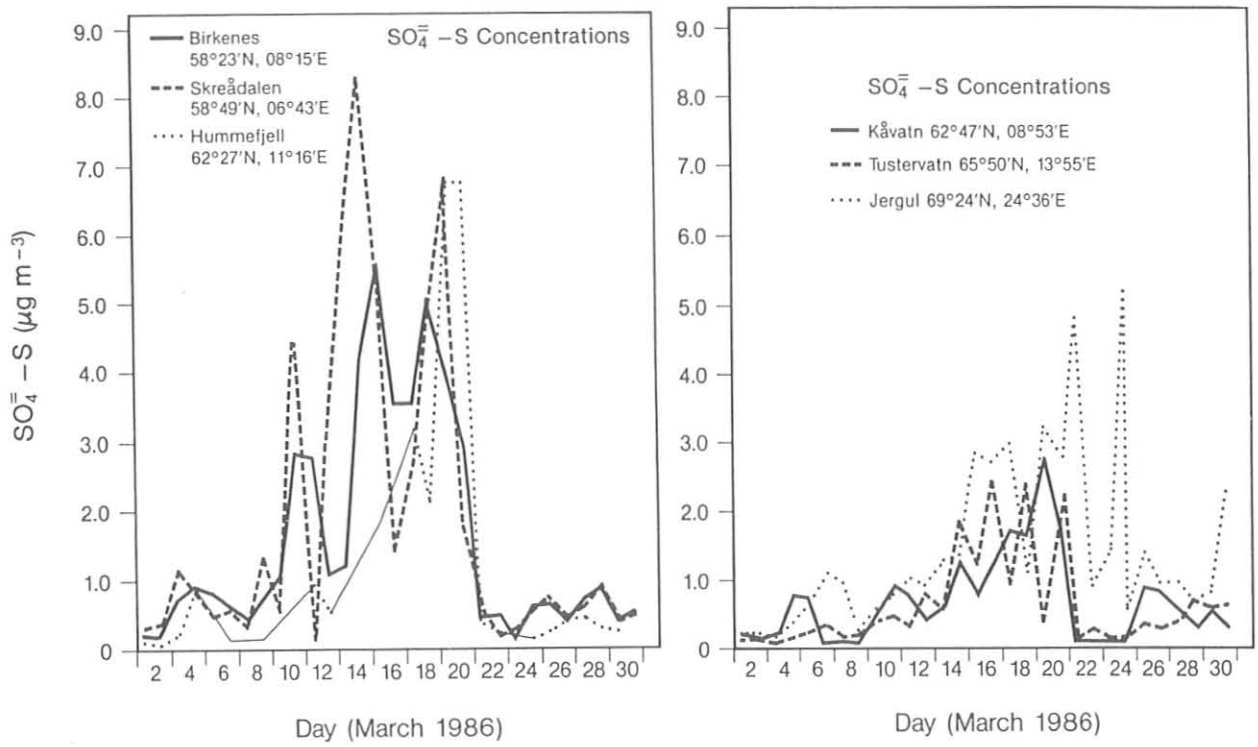

Figure 4.--Daily $SO_4^=$ - S concentrations for March 1986 showing the northbound movement of the pollution over Norway into the Arctic.

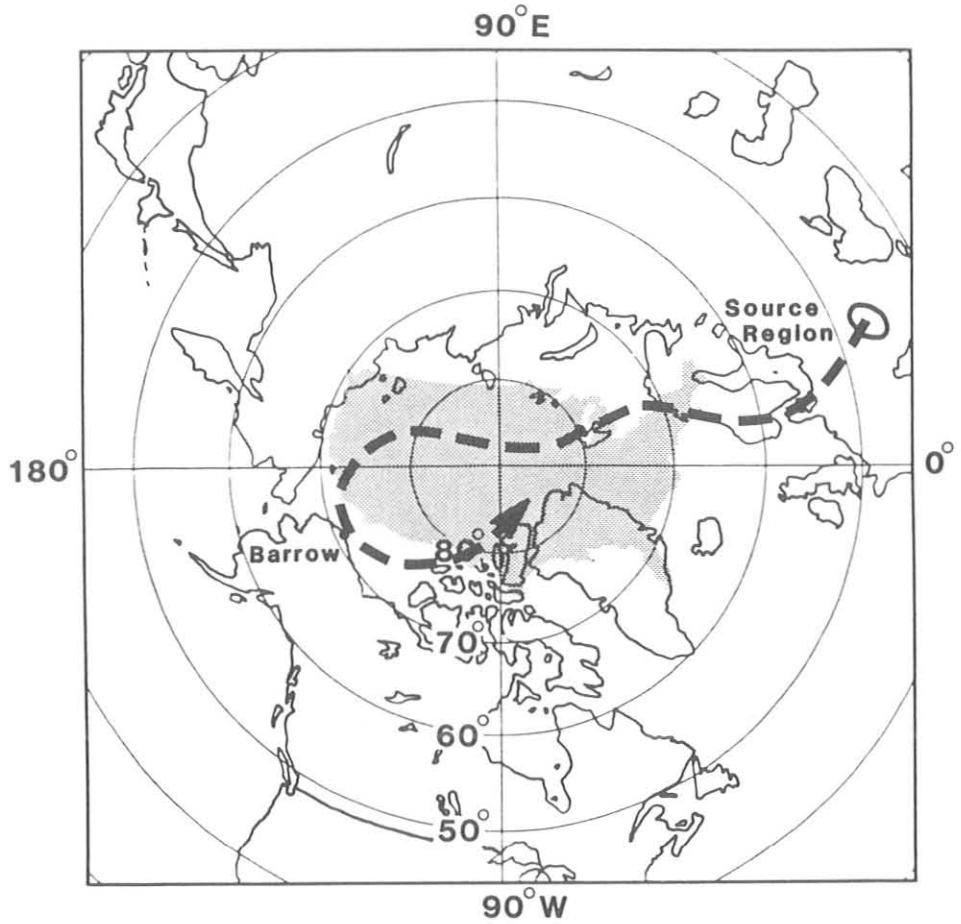

Figure 5.--Overlay of the United States on the Arctic with the track of the major haze event shown by the broken line. This haze traveled ~10,000 km.

After travelling this 10,000 km distance, the April 2-3 haze episode still had SO_2, aerosol black carbon, b_{sp} and CN concentrations in excess of those measured with the same aircraft in air pollution episodes sampled off the east coast of the United States in January of the same year. This suggests that both diffusion and haze removal by precipitation are severely limited in the cold, stable Arctic atmosphere, thus allowing for exceptional long-range transport of anthropogenic pollutants into and across the Arctic basin.

REFERENCES

Flyger, H., Heidam, N. Z., Hanse, K., Megan, W. J., Walther, E. G., and Hogan, A. W., 1976. The background level of the summer tropospheric aerosol, sulphur dioxide and ozone over Greenland and the North Atlantic Ocean, J. Aerosol Sci. 7:103-140.

Radke, L. F., Lyons, J. H., Hegg, D. A., Hobbs, P. V., and Bailey, I. H., 1984. Airborne observations of Arctic aerosols, I: Characteristics of Arctic haze, Geophys. Res. Lett. 11:393-396.

9.3 Cooperative Programs

POTENTIAL FOR ALKALINE DUST SCAVENGING AND DRY DEPOSITION OF SO_2 AND OTHER ACIDIC TRACE GASES

John W. Winchester*
Florida State University
Tallahassee, FL 32306-3048

Dale A. Gillette
NOAA/ARL/GMCC
Boulder, CO 80303

An assessment of the acid-base balance of the natural atmosphere and its perturbation by the emission of acidic air pollutants, including oxides of sulfur and nitrogen, is one of the goals of NAPAP. Natural aerosols formed by the dispersion of soil dust and sea spray are generally alkaline, having the base capacity to neutralize acidic gases that diffuse to particle surfaces or into rainwater that has entrained alkaline particles. To evaluate whether pollutants cause a displacement from the natural acid-base balance, it is important to estimate the magnitudes of fluxes of alkaline particles to the atmosphere and to compare these with the fluxes of acids from pollution and natural sources.

It is also important to determine whether the effects of aerosols that have reacted with acidic pollutants can differ from the effects of acidic pollutants in particle-free air. Whereas alkaline particles could mitigate acid deposition onto aquatic or terrestrial surface areas and their biota, particles coated with sulfates, nitrates, or other soluble pollution-derived compounds deposited onto sensitive tissues could cause localized biological damage that may not have occurred by the uptake of gaseous pollutants directly. It is especially important to determine the consequences for human health of inhaling pollutant-coated particles.

Winchester et al. (1986) proposed that the alkaline capacity of soil dust aerosols that occur commonly in terrestrial areas may be comparable with the concentration of SO_2 expected from anthropogenic emissions. They calculated that the rate of scavenging of acidic gases by basic particles is rapid and may exceed the rate of direct deposition of the gases to the Earth's surface. Thus, the process of dry deposition of the pollution gases may be mediated by heterogeneous reaction with particle surfaces, and the overall rate of deposition to the ground may be limited by deposition rates of aerosol particles rather than of gas molecules to the Earth's surface. Failure to recognize the possibility of reactive gas removal by dust scavenging could lead to an error in estimating the dry-deposition rate of SO_2 and other acidic pollutant gases.

*Visiting scientist at NOAA/ARL/GMCC, Boulder, CO 80303.

We have now evaluated the compositional relationships in soil-derived aerosol particles statistically in order to ascertain if air pollution sulfur uptake has occurred. On the bais of measurements made in China, Japan, and Hawaii, factor analysis (Hopke, 1985) could resolve externally mixed aerosol components, some of which appeared to contain sulfur in association with soil dust but at concentrations much higher than could be attributed to natural soil composition (Wang et al., 1987; Winchester, 1986a, 1986b). In further statistical analysis of more recent data from Japan, using microcomputer software (STSC, 1986), we have compared the composition of resolved aerosol factors with that expected by interactions between alkaline dust and acidic pollution sulfur gases (Winchester, 1987; Winchester et al., 1987).

It is important that sulfur is largely associated statistically with aerosol factors (combination of elements mixed in determined proportions) that also contain soil dust elements in proportions similar to average Earth crust. Moreover, the sulfur loading approaches, but does not greatly exceed, that expected by acid-base neutralization reactions between the gases and dust. These findings imply a mechanism of acid gas scavenging by alkaline dust up to a saturation, or titration, limit beyond which further uptake is inhibited.

Natural silicate particles coated with the reaction products of acidic vapors can be identified by electron microscopy (Marshall, 1987), and in the Denver urban atmosphere a substantial portion of nitrate is found in association with coarse dust (Wolff, 1984). Wind erosion is a source of much of the soil dust found in continental areas, and dust fluxes to the atmosphere can be predicted from wind and soil conditions (Gillette, 1986). Because of the conditions that prevail over much of the United States, throughout the western states and extending at least into the midwest region, the alkalinity flux to the atmosphere is calculated to be comparable with or in excess of the flux of acidic gases from combustion and industrial sources. Consequently the ultimate fates of acidic gases, and their effects, may be determined in part by the presence of alkaline dust.

REFERENCES

Gillette, D. A., 1986. Wind erosion. In Soil Conservation, Assessing the National Resources Inventory, Vol. 2. National Academy Press, Washington, DC, 129-157.

Hopke, P. K., 1985. Receptor Modeling in Environmental Chemistry. Wiley, New York, 155-197.

Marshall, J. R., (ed.), 1987. Clastic Particles, Scanning Electron Microscopy and Shape Analysis of Sedimentary and Volcanic Clasts. Van Nostrand, New York, 341 pp.

STSC, 1986. Statgraphics: Statistical Graphics System by Statistical Graphics Corporation, User's Guide. STSC, Inc., Rockville, MD.

Wang Ming-xing, J. W. Winchester, and Li Shao-meng, 1987. Aerosol composition in the drylands of northwestern China. Nuclear Instruments and Methods in Physics Research, B22:275-282.

Winchester, J. W., 1986a. Aerosol sulfur and terrestrial dust components in the troposphere over eastern Asia and the North Pacific. Paper for discussion at World Meteorological Organization Expert Meeting on the Strategy of BAPMoN SPM Monitoring (Background Air Pollution Monitoring Network for Suspended Particulate Matter), Xiamen (Amoy), China, 13-17 October 1986 (A. Koehler, convenor).

Winchester, J. W., 1986b. Use of PIXE analysis and multielemental statistical analysis for resolving tropospheric aerosol sulfur and terrestrial dust components in eastern Asia and the North Pacific. Paper for discussion at International Atomic Energy Agency Advisory Group Meeting on Nuclear-Related Techniques in Environmental and Occupational Health Studies, Vienna, 15-19 December 1986 (R. M. Parr, convenor).

Winchester, J. W., 1987. Aerosol components resolved by statistical factor analysis: A case study of time sequence concentration measurements by PIXE in samples from Niigata, Japan, May 7-16, 1986. Paper for presentation at annual meeting of American Association for Aerosol Research, Seattle, Washington, 14-17 September 1987.

Winchester, J. W., Li Shao-meng, and D. A. Gillette, 1986. Potential for airborne dust scavenging and dry deposition of SO_2. Technical report for discussion at NAPAP Workshop on Dry Deposition, Harper's Ferry, WV, 25-27 March 1986, (B. B. Hicks, S. E. Lindberg, and M. L. Wesely, co-chairmen).

Winchester, J. W., Y. Hashimoto, and Wang Ming-xing, 1987. Base capacity effects on pollution aerosol sulfur transported over the Pacific. Paper for presentation at 6th CACGP Symposium on Global Atmospheric Chemistry, Peterborough, Ontario, 23-29 August 1987.

Wolff, G. T., 1984. On the nature of nitrate in coarse continental aerosols. Atmospheric Environment 18:977-981. Notes for report and Gillette-Winchester CIRES seminar July 29, 1987.

PRECIPITATION CHEMISTRY

R.S. Artz
Air Resources Laboratory, NOAA
Silver Spring, MD 20910

INTRODUCTION

Routine and special precipitation chemistry measurements continued at the four GMCC sites and at the 14 regional sites. Special studies continued at MLO through the use of the Dionex ion chromatograph and through the continuation of a cooperative project instituted through the University of Virginia designed to measure organic acids in precipitation.

During the summer, a major upgrade in the routine monitoring protocol was planned for SMO and MLO with the goal of implementing most changes by January, 1987. Important changes include the following:

o Halai Hill, 22 Mile, MLO, and SMO GMCC precipitation collections will become daily instead of weekly except for weekends and holidays.

o In order to accommodate the increased sample load, sites at Kauai and Kulani Mauka will be closed. The Cape Kumukahi site will remain closed.

o The QIC and Model 10 Dionex chromatographs will be used to analyze all anions and monovalent cations typically found in precipitation (K^+, Na^+, NH_4^+, NO_3^-, $SO_4^=$, Cl^-). The pH (H^+) and conductivity measurements will continue.

Surface snow collections at BRW and SPO will continue. A Canadian snow bag and bucket system will be mailed to BRW to attempt the collection of precipitating snow, and the suitability of installing a Nipher gauge on a Belfort precipitation collector at BRW will be explored.

BASELINE MEASUREMENTS

The four-site special network on the island of Hawaii and a fifth site on Kauai continued to operate on a weekly schedule. Monitoring ceased on Kauai and at Kulani Mauka at the beginning of September in order to reduce the sampling load on the laboratory and to allow for the preparation of the daily sampling network at the remaining sites.

As seen in Figure 1, high sulfate and hydrogen ion concentrations were observed only sporatically during the months of January, February, March, and October. As noted in past years these observations can be explained by the very low precipitation received at the affected sites (Figure 2) and are probably not due to anthropogenic or volcanic activity. Agreement for sulfate and hydrogen ion concentrations at Halai Hill and Kauai, sites with similiar elevation and orientation to the trade winds, appeared reasonable although a thorough evaluation was not possible due to repeated vandalism at the Halai Hill site and the closing of the Kauai site in September.

In Figure 3 monthly precipitation weighted $SO_4^=$ and H^+ means for the Hawaiian sites are presented. The typical situation of highest sulfate values occurring at low elevation sites was not clearly observed this year except for

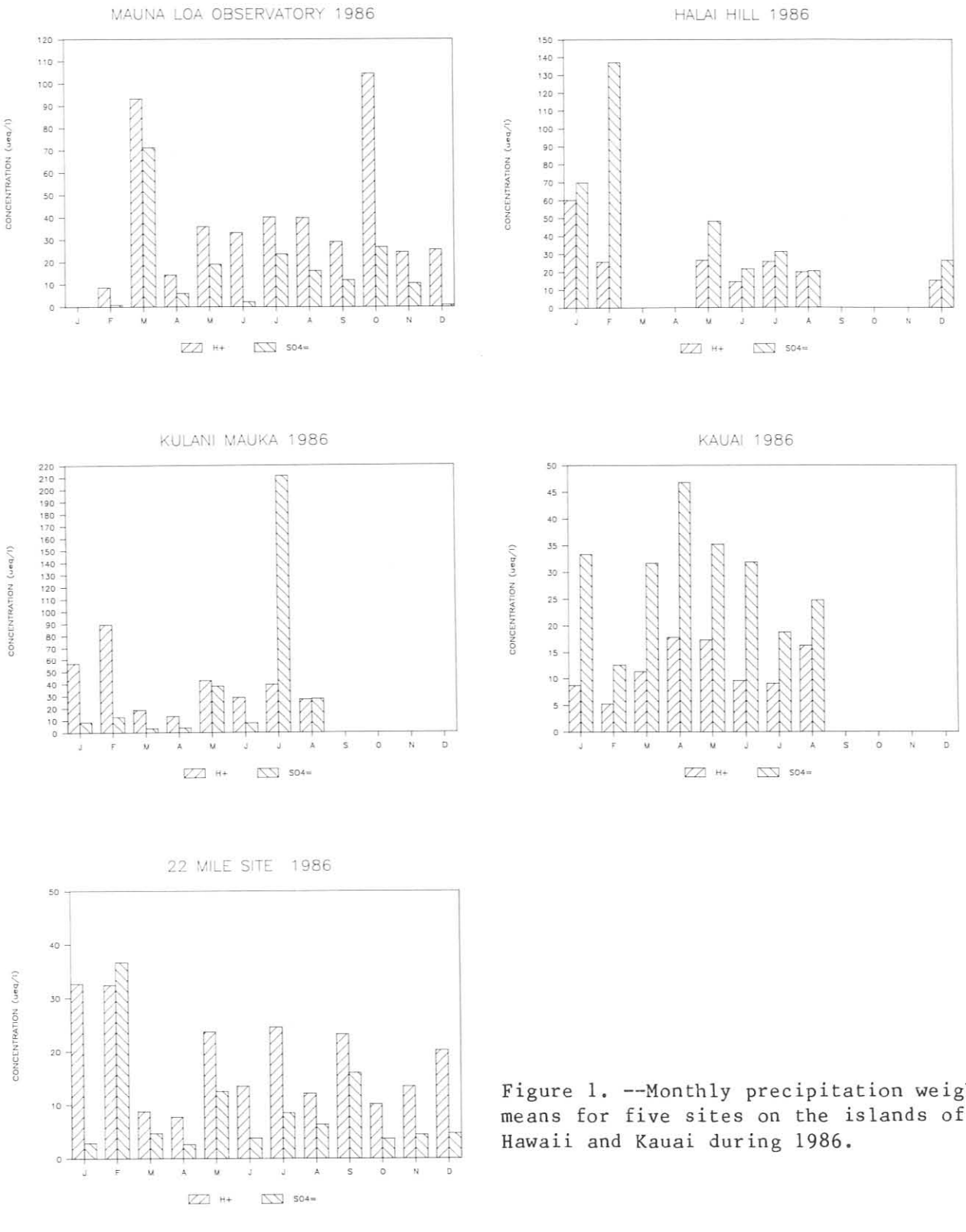

Figure 1. --Monthly precipitation weighted means for five sites on the islands of Hawaii and Kauai during 1986.

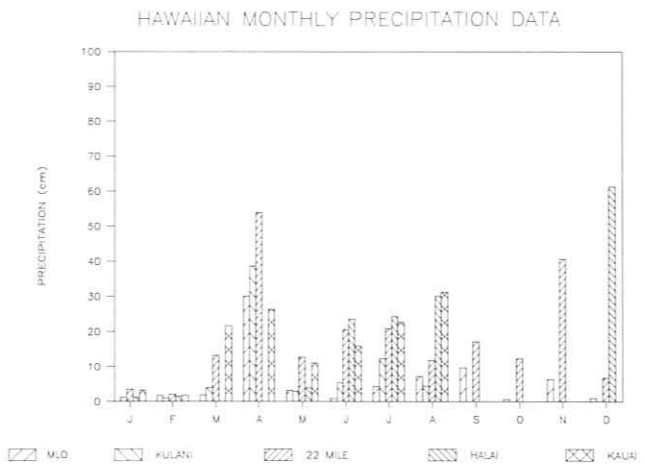

Figure 2. --Monthly precipitation at Hawaiian sites for 1986.

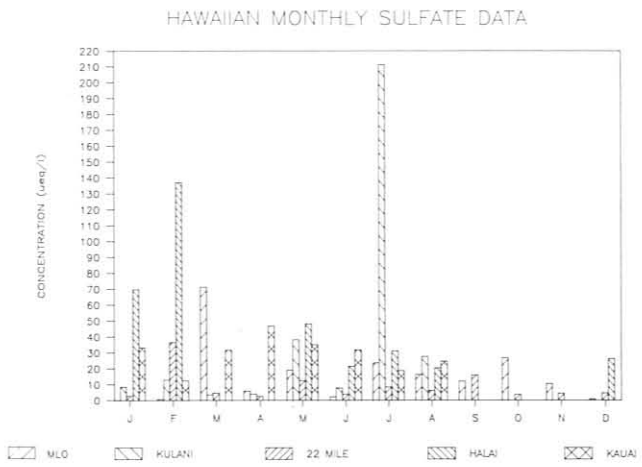

Figure 3a.--Monthly precipitation weighted sulfate means for the Hawaiian network.

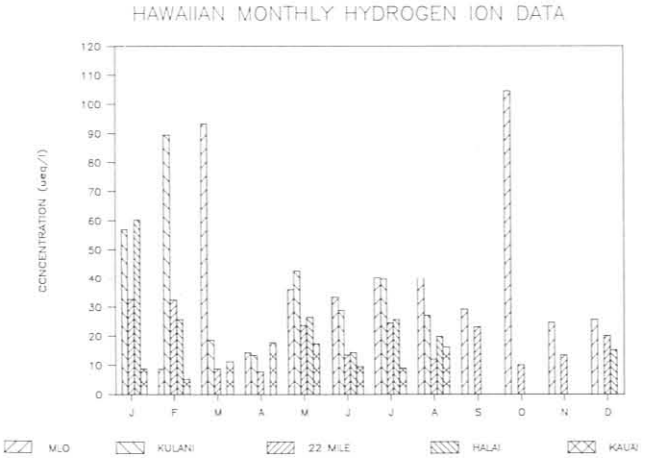

Figure 3b.--Monthly precipitation weighted hydrogen ion means for the Hawaiian network.

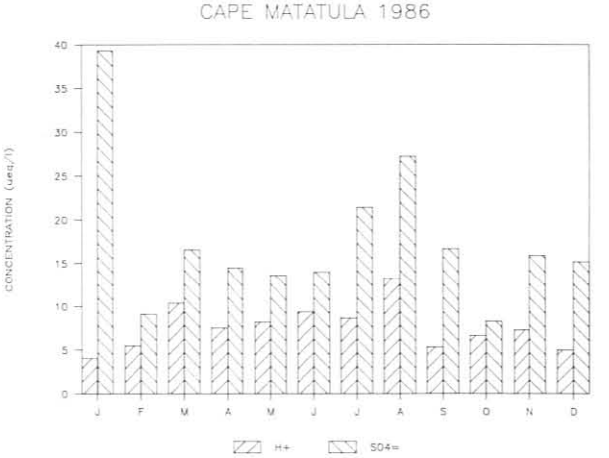

Figure 4. --Monthly precipitation weighted sulfate and hydrogen ion means for Samoa during 1986.

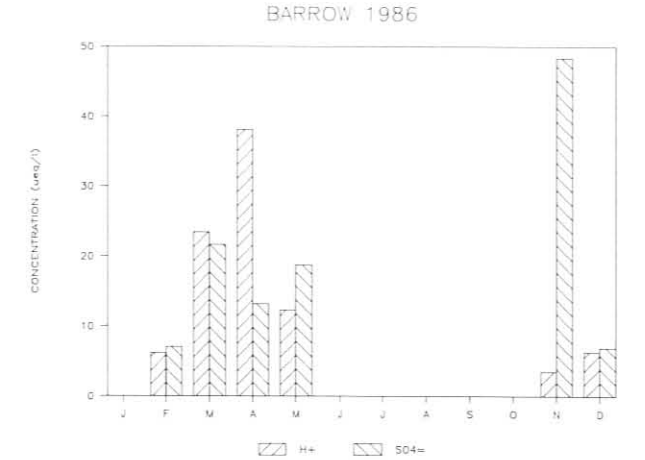

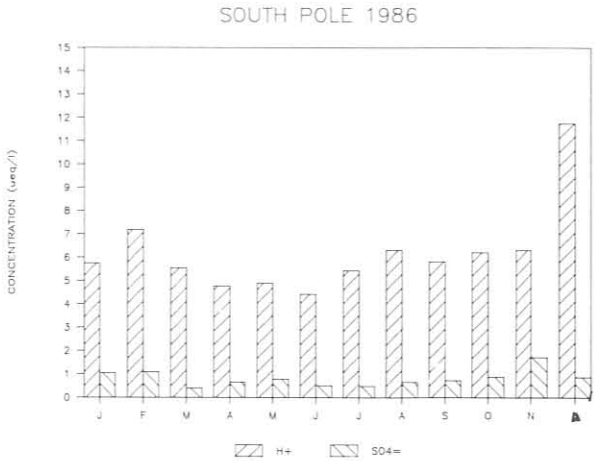

Figure 5. --Monthly average hydrogen ion and sulfate concentrations for snow samples collected in Barrow and at the South Pole for 1986.

July, probably due to the fact that fewer samples were analyzed because of vandalism, site closings, and dry weather. The other trend, increasing H^+ concentrations with elevation, was somewhat more evident.

In Figure 4 Samoa H^+ and $SO_4^=$ monthly precipitation weighted means are presented. With the exception of January, values are nearly constant. The cause of this high value for $SO_4^=$ is not known.

Snow sample data for BRW and SPO are shown in Figure 5. SPO samples, as usual, are exceptionally clean and constant, typically showing concentrations of about 1 μeq/l of $SO_4^=$ and approximately 7 μeq/l of H^+ (except for December). Barrow values remain consistant with measurements from other background sites but are quite variable. Shipping problems continue to result in the loss of measurements.

REGIONAL MEASUREMENTS

All 14 of the existing NOAA NADP/NTN regional precipitation sites remained in operation through 1986. One new site was added to the network at Newton, MS (32°20'N lat, 89°09'W lon, elev. 147 m) during November, in an effort to assess the representativeness of an existing site in Meridian, MS. A paired site intercomparison between Caribou and Presque Isle, Maine and Victoria and Beeville, Texas stations is planned for 1987.

$\delta^{13}C$ IN ATMOSPHERIC CO_2 1982-1987

Irving Friedman, Jim Gleason, Augusta Warden
U.S. Geological Survey
Denver, CO 80225

INTRODUCTION

The bi-monthly sampling of atmospheric CO_2 in 10 ℓ stainless steel flasks at ambient pressure was continued at South Pole, Mauna Loa, Samoa, and Point Barrow. The samples were treated and the separated CO_2 was analyzed for $\delta^{13}C$ in the same manner as previously.

RESULTS

The results from 1981 to October 1987 are shown in fig. 1-4 in which the dates are plotted consecutively beginning with January 1, 1981 as zero. Linear least square solutions to the data were made from 1981 to September 1984, from September 1984 to October 1987, and to the whole data set. September 1984 was chosen because it appeared that a change in slope of δD vs. time occurred at about that date in data sets from several stations. The slopes of the least squares lines are given in the figures as permil ($^0/_{oo}$)/yr. The reason for the change in slopes pre- and post-September 1984 is not known.

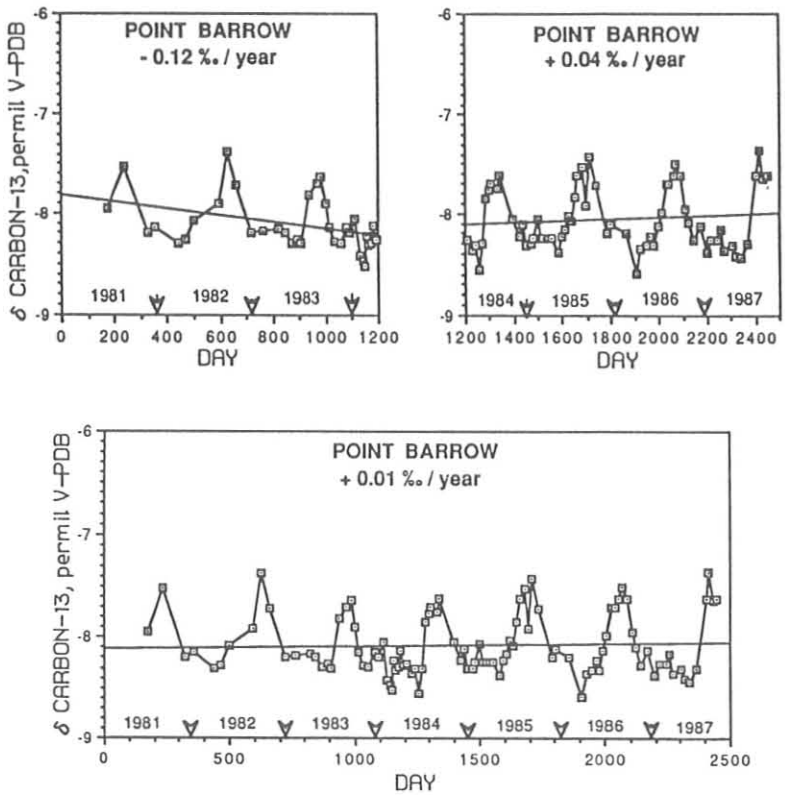

Figure 1.--Bi-monthly $\delta^{13}C$ at Point Barrow from 1981 to mid-1987 showing segments of the record separated at September 1984 and the long-term trend.

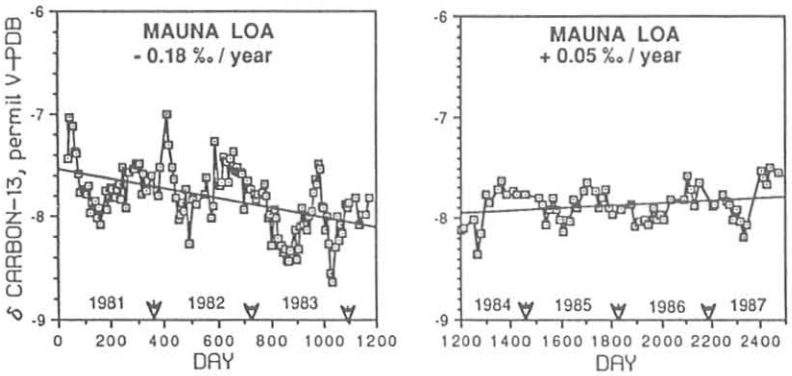

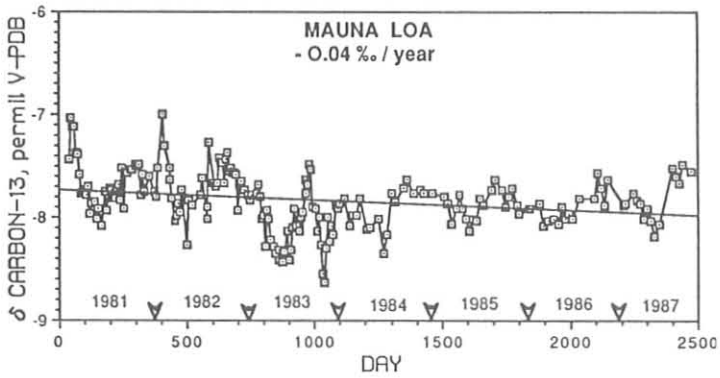

Figure 2.--Bi-monthly $\delta^{13}C$ at Mauna Loa from 1981 to mid-1987 showing segments of the record separated at September 1984 and the long-term trends.

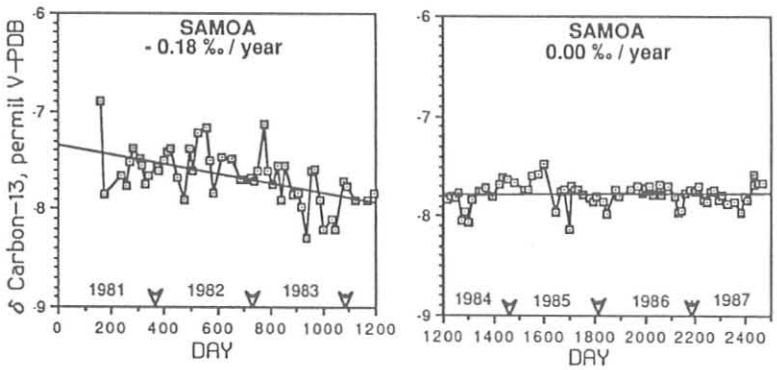

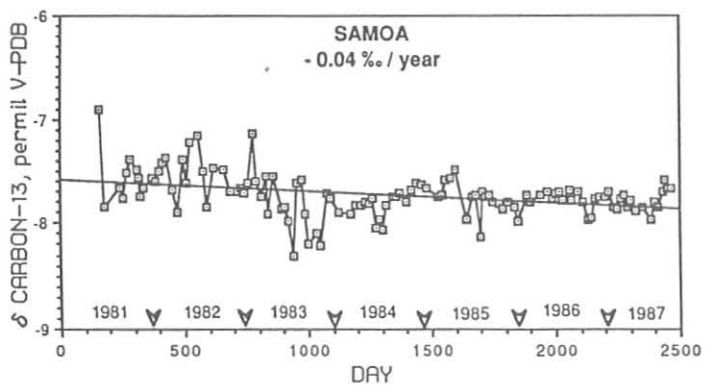

Figure 3.--Bi-monthly $\delta^{13}C$ at Samoa from 1981 to mid-1987 showing segments of the record separated at September 1984 and the long-term trends.

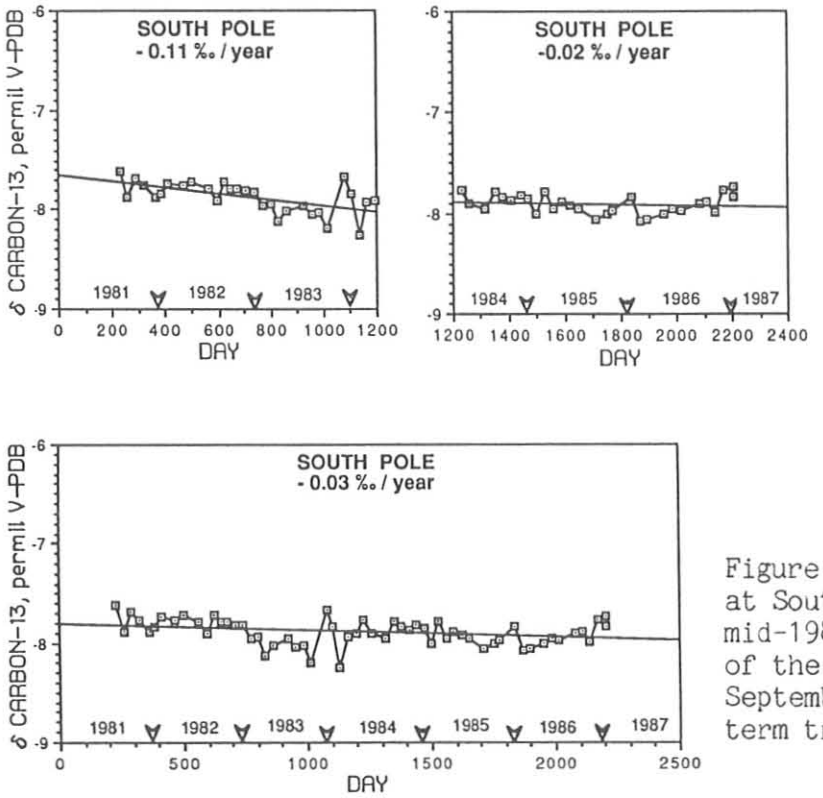

Figure 2.--Bi-monthly $\delta^{13}C$ at South Pole from 1981 to mid-1987 showing segments of the record separated at September 1984 and the long-term trends.

AEROSOL OPTICAL THICKNESS AT MLO

G.M. Shah and W.F.J. Evans
Atmospheric Environment Service
4905 Dufferin Street, Downsview, Ontario, M3H 5T4

INTRODUCTION

Measurements of spectral solar radiation extinction at MLO were continued with a multi-wavelength sunphotometer since the eruption of EL Chichon volcano in Mexico in March and April 1982. These measurements are supported through the cooperative programme of the NOAA GMCC observatory.

This report presents the results of the analysis of aerosol optical thickness calculated from the solar extinction measurements at 380 nm, 500 nm and 862 nm wavelengths for the period April, 1982 to December, 1986.

OBSERVATIONS

The instrument used for taking the extinction measurements is the hand-held Sonotek sunphotometer manufactured by Sonotek limited of Canada. The description of the instrument is reported elsewhere (Shah, 1979). Sonotek Limited of Canada has discontinued manfacturing of sunphotometers. The instruments are now being manufactured by Sci-tec Instruments Inc. of Canada.

The instrument was calibrated by the Langley method at MLO in 1982 and 1984. A substantial change in calibration constant especially at 380 nm wavelength was found. This was taken into account while calculating aerosol optical thickness.

Aerosol optical thicknesses were calculated from the measurements of the solar spectral extinction made during the day. The values reported in this report are the monthly means of the daily averages of aerosol optical thickness. Observations contaminated by local volcanic fumes or high haze are also included in daily averages.

RESULTS AND DISCUSSIONS

Figure 1 presents the plot of monthly means of aerosol optical thickness at 380 nm, 500 nm and 862 nm wavelengths at MLO for the period 1982 to 1986.

It is evident from the figure that the elevated values of aerosol optical thickness at all the three wavelenghts observed after the eruption of EL Chichon volcano in Mexico have continuously declined with time and attained the normal background values by the fall of 1984. The values have remained more or less constant since then.

It is further noted that the aerosol optical thickness becomes a maximum in the spring and a minimum in the winter months.

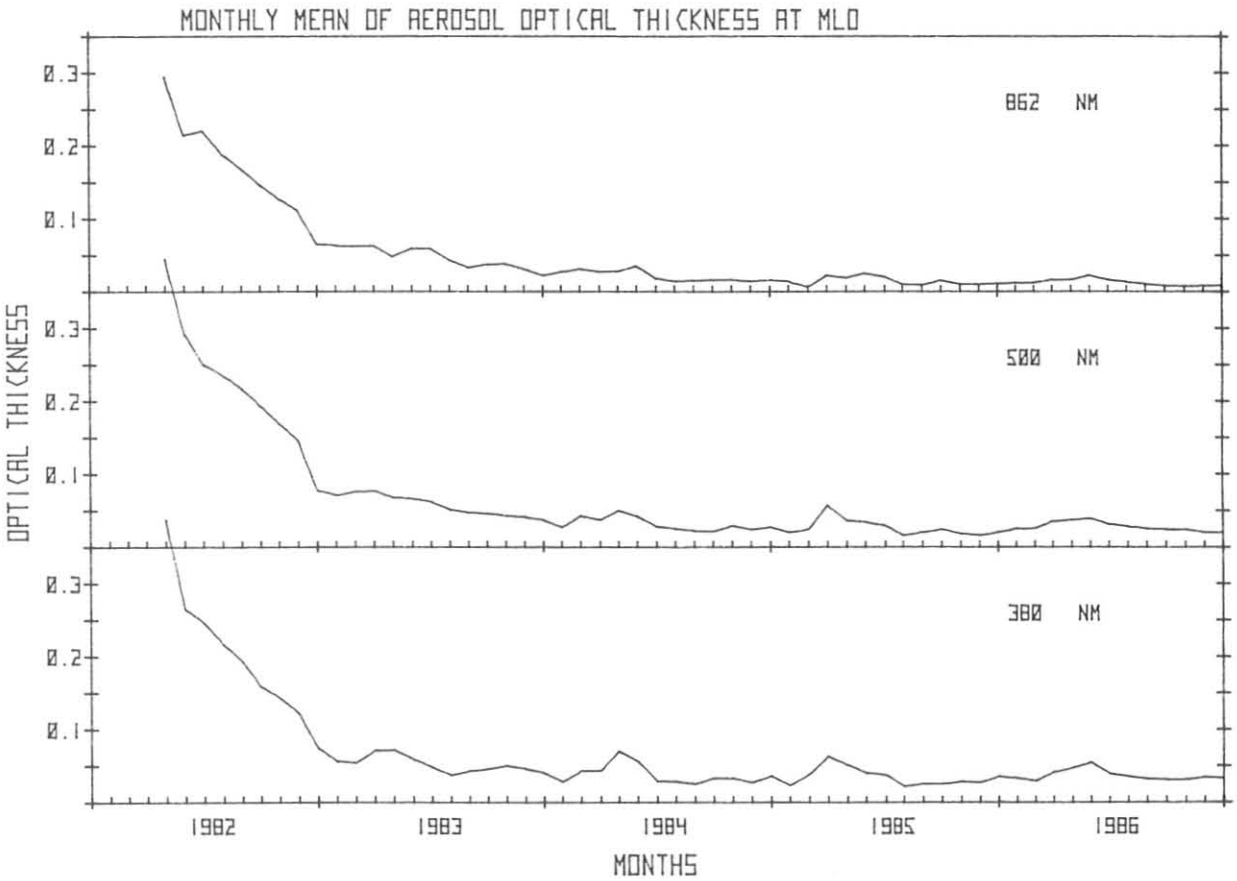

Figure 1.--Monthly means of aerosol optical thickness in the atmosphere at 380 nm, 500 nm and 862 nm wavelengths measured with the sunphotometer at MLO.

The effects of the eruption of the Nevado de Ruiz volcano in Colombia in November 1985 (SEAN 1985) and of the Augustine volcano in Alaska in March 1986 (SEAN 1986) are barely discernable above the measurements in December 1985 and April 1986.

Figures 2 and 3 present the plots of aerosol optical thickness versus wavelengths on a log - log scale graph, in the months of April and December for the years 1982 to 1986.

The variation of aerosol optical thickness with wavelength was essentially flat with occasional inflexion near 500 nm wavelength until September, 1983. Since October 1983 the aerosol optical thickness decreased monotonically with an increase in wavelength.

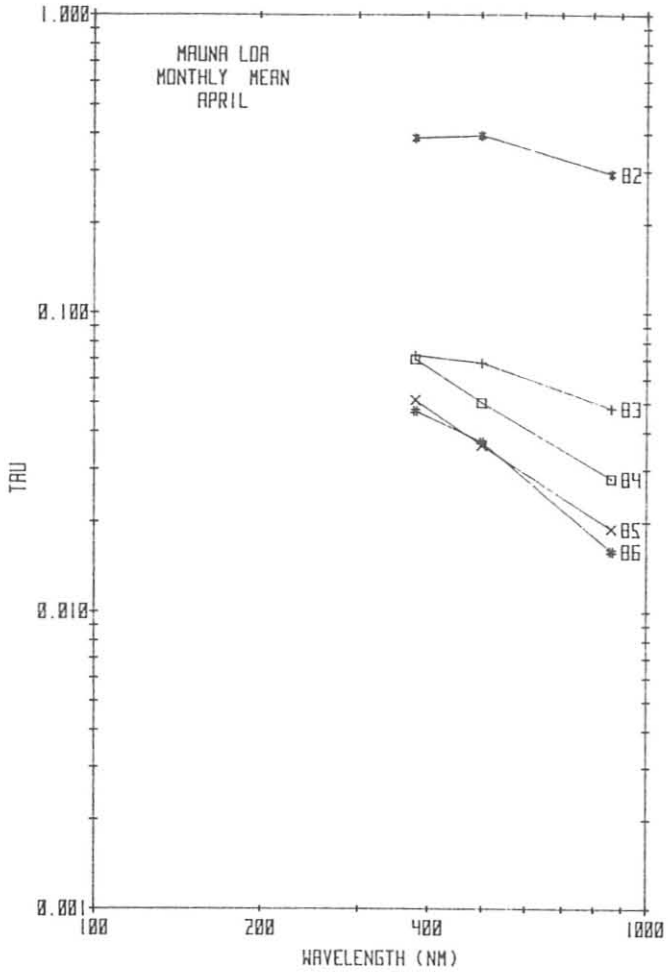

Figure 2.--Wavelength dependence of monthly means of the aerosol optical thickness in the month of April for the years 1982-1986.

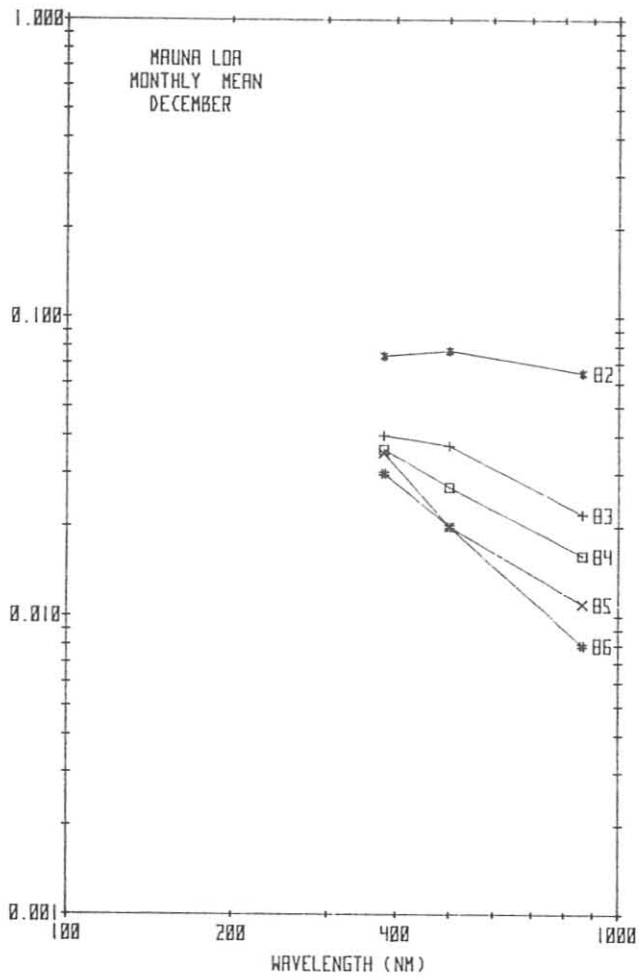

Figure 3.--Wavelength dependence of monthly means of the aerosol optical thickness in the month of December for the years 1982-1986.

ACKNOWLEDGMENT

We acknowledge the important contributions of the NOAA/GMCC staff at MLO observatory in making sunphotometer measurements in this cooperative project.

REFERENCES

SHAH, G.M., A Multiwavelength sunphotometer, AES Internal Report No. ARQA-70-79, Atmospheric Environment Service, 4905 Dufferin Street, Downsview, Ontario, Canada, 22 p, 1979.

Smithsonian Institution, SEAN Bulletin, 10. (11 and 12) Washington, D.C., 1985.

Smithsonian Institution, SEAN Bulletin, 11 (3), Washington, D.C., 1986.

MONITORING FOR SULFUR DIOXIDE AND TOTAL SUSPENDED PARTICULATE AT MAUNA LOA OBSERVATORY

Henry Yee, Wilfred Ching, and Richard Sasaki
Hawaii State Department of Health
Honolulu, HI 96813

INTRODUCTION

Sulfur dioxide (SO_2) and total suspended particulate (TSP) monitoring were reinstituted as a long-term study at MLO by the state of Hawaii at the request of E.P.A. Region IX. The long-term trends in sulfur dioxide and particulate (10 μm diameter and smaller) concentrations will be studied to determine the factors contributing to increases observed in the past. Also, the study will work towards determining the atmospheric lifetime of the particular gases and particulates, and the chemical composition of the other particulates collected at the elevation of MLO.

Table 1 and fig. 1 show the integrated concentrations of 24-hr TSP and SO_2 for samples collected at MLO in 1986.

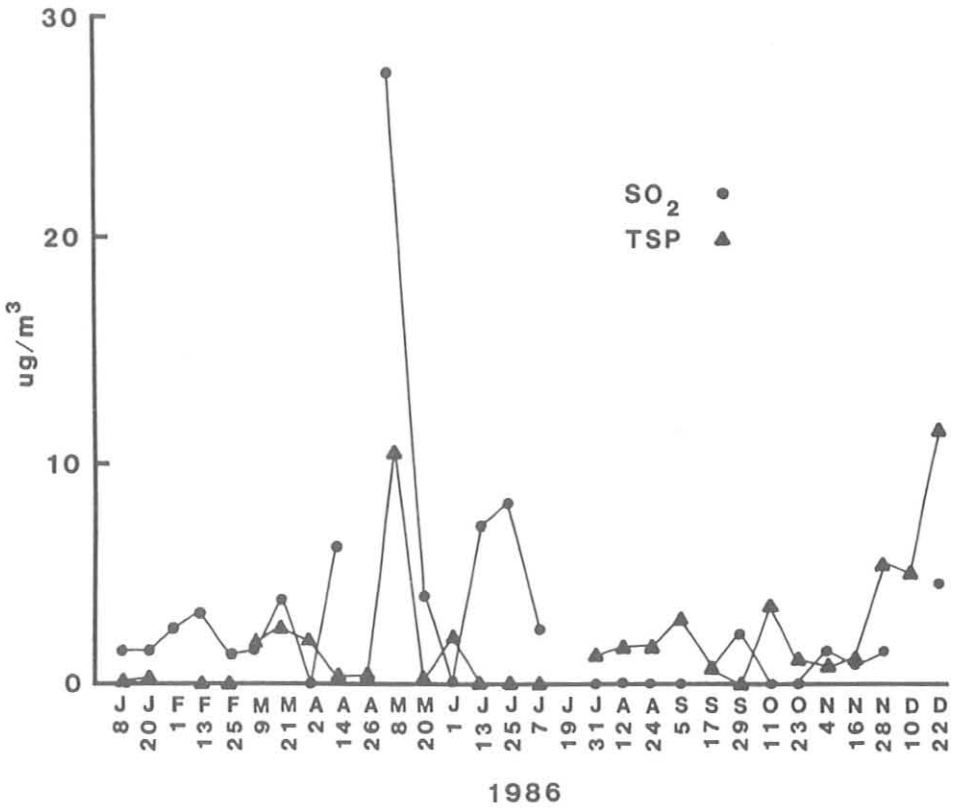

Figure 1.--Twenty-four-hour integrated concentrations of TSP and SO_2 samples collected at MLO for 1986.

Table 1.--Twenty-four-hour concentrations of TSP (hi-vol, gravimetric) and SO_2 (pararosaniline method) at MLO ($\mu g/m^3$)

1986	TSP	SO_2
Jan 08	0	1.5
20	0.4	1.6
Feb 01	-	2.3
13	0	3.1
25	0	1.4
Mar 09	2.1	1.5
21	2.4	3.8
Apr 02	2.1	0
14	0.4	6.2
26	0.4	-
May 08	10.5	26.8
20	0.4	3.9
Jun 01	2.1	0
13	0	7.3
25	0	8.2
Jul 07	0	2.4
19	-	-
31	1.3	0
Aug 12	1.7	0
24	1.6	0
Sep 05	3.1	0
17	1.0	0.8
29	0	2.3
Oct 11	3.5	0
23	1.0	0
Nov 04	0.8	1.5
16	1.3	0.8
28	5.4	1.5

SIZE DISTRIBUTIONS OF VOLATILE AND REFRACTORY ARCTIC HAZE AEROSOL COMPONENTS MEASURED AT BARROW DURING AGASP II, 1986

Antony D. Clarke
Hawaii Institute of Geophysics
University of Hawaii
Honolulu, HI 96822

INTRODUCTION

Thermal and optical techniques were used at Barrow, Alaska during AGASP II (3/20/86-4/7/86) to measure in-situ variability of major aerosol components present in Arctic Haze. The experiment provided continuous data on the concentration, size distribution and relative proportions of sulfate species and refractory aerosol for particle diameters of 0.15 to 5 um. Filter samples were also taken for determination of aerosol optical absorption due to soot (EC-elemental carbon). The measurement system uses a laser optical particle counter, LOPC, (Particle Measurement Systems, Boulder CO.) modified to accomodate a 256 channel pulse height analyser and microcomputer to provide detailed size resolution and extensive software capabilities. First the aerosol is conditioned by 5 environments that alter the size distribution in ways that can be interpreted in terms of aerosol physio-chemical properties. In this Thermo-Optic Aerosol Descriminator (TOAD) ambient aerosol is dried to 30% RH prior to being split into 5 flows. Channel A is heated to 40 C to drive off bound water and low-temperature volatiles. Channels B,C and D are heated to 150 C to volatilize sulfuric acid in the system but leave ammonium sulfate/bisulfate intact. Channel C had RH controlled at 65% since the difference in deliquescence of ammonium sulfate (80% RH) and ammonium bisulfate (33% RH) is used to help identify the latter from an increase in the size distribution (mass) at 65%. Channel D had ammonia added prior to heating in order to convert any sulfuric acid to ammonium sulfate (not volatile at 150 C), such that a return to ambient mass concentrations confirms the presence of sulfuric acid. Channel E is held at 300 C in order to eliminate common volatile species and leave a refractory aerosol. The latter is frequently EC in the fine particle mode (less than 0.5 um diameter) and crustal dust, sea salt or fly ash in the coarse particle mode (generally greater that 0.5 um). Since we have found no significant refractory fine particle mass in the remote cntral Pacific, this aerosol is considered continental and, as shown below, often dominated by EC. An example of typical size distributions obtained from the LOPC-TOAD is shown in Fig 1. for Julian Day 93 at 13.27 GMT for the 5 conditions described above and an ammonium bisulfate calibration curve.

Interpretation of data based upon the light scattering properties of atmospheric aerosol must consider the the real and complex refractive indices for various particles and the combined effects on their integrated light scattering. LOPC calibrations were developed in our laboratory for both dry and wet (65%RH) sulfate aerosol. Comparison of the response characteristics for the LOPC with sulfate and EC aerosol have been published (Garvey and Pinnick, 1984) and is used here with our calibration to provide a LOPC calibration curve for fine particle EC. The dashed line in panel E indicates the reduction in apparent fine mode mass resulting from application of the EC calibration mentioned above. This was applied only to the fine mode aerosol size distribution ($dp<0.42$ um) after being heated to 300 C since EC is both refractory and usually found in this size range when souces are distant. Damage to the RH control circuit during shipping resulted in little information gained from channels C and D, otherwise the LOPC/TOAD performed as intended. The data presented here is for the fine mode only since particle losses occured in this system for particles over 2 um which make quantitative interpretion of these results for the coarse particles more uncertain.

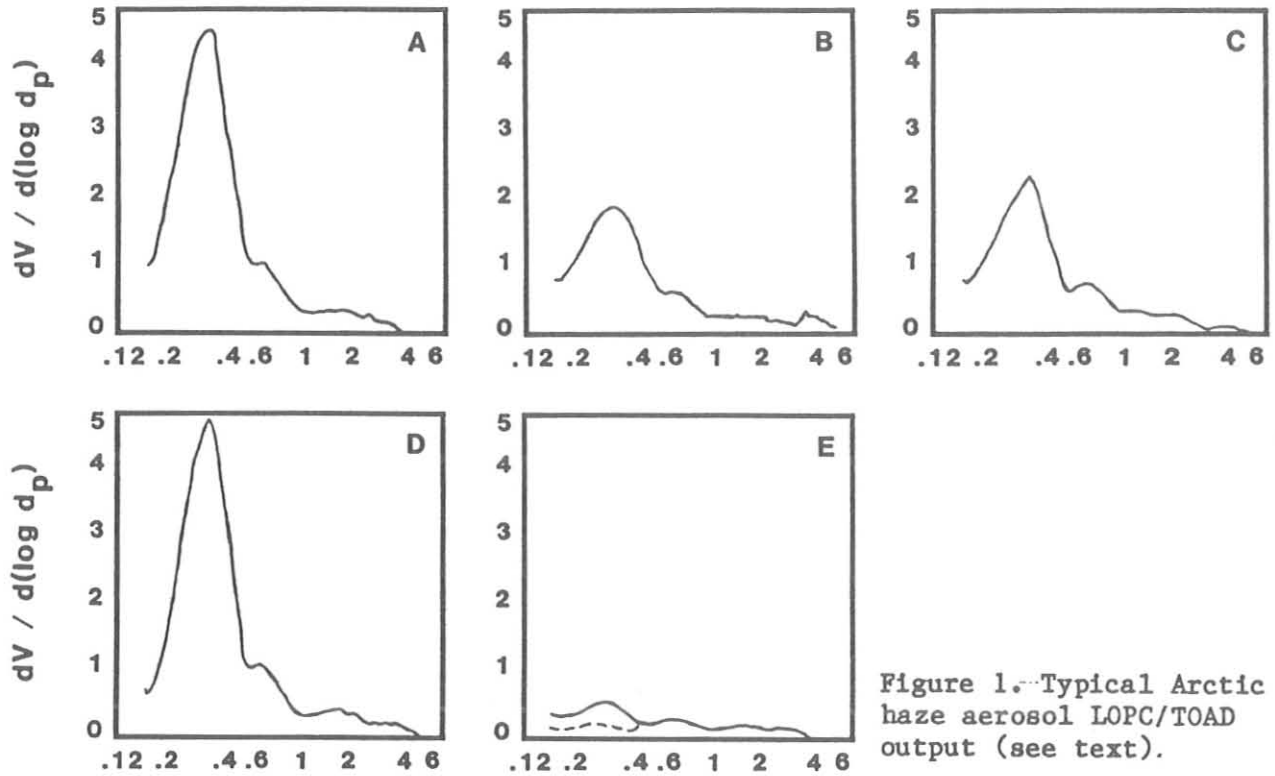

Figure 1. Typical Arctic haze aerosol LOPC/TOAD output (see text).

DISCUSSION AND RESULTS

Size resolved volume distributions of the components mentioned above can be obtained by appropriate differencing of the various size distributions. This was done for about 40% of these data plots and provide a good example of the variability in aerosol composition during this period. Only the mass below 0.5 um is compared here since it is of most interest to us and is generally both physically and chemically distinct from the rest. Figure 2 is a plot of total aerosol mass, sulfuric acid, ammonium sulfate/bisulfate, and refractory EC (soot) obtained as described. Note that a sudden reduction in sulfuric acid and increase in ammoniated sulfate occurs for JD 95-97, a weekend when the NOAA/GMCC staff discovered a disconnected sample tube that resulted in room air being measured. Although room aerosol concentrations remained at or below outdoor levels ammonia present in the station is sufficient to significantly neutralize the ambient aerosol. Otherwise the concentrations of components trend down to a minimum about JD 95 and then increase again by a factor of two. A plot of the ratios of aerosol volatile at 160 C (sulfuric acid) to total mass; the molar ratio of inferred sulfuric acid to inferred ammonium sulfate/bisulfate; and the non-volatile (soot) to volatile (sulfates) are presented in Figure 3 for the same data set. The sulfuric acid appears as a relative constant fraction of the aerosol mass except for the above mentioned contamination period and short periods of local contamination. The relative ratio of "sulfuric acid" to "ammoniated sulfates" ranges from 1 to 2 and suggesting a mixture of sulfuric acid and ammonium bisulfate. The "soot-EC" concentation ranges from about 0.1 to 0.4 ug/m3 and accounts for about 10% of the total fine particle mass. The relatively small excursions in these ratios suggest that the haze during this period was nearly homogeneous in relative constituents and differed by less than a factor of two in concentration. Some short term variations in aerosol perturbed locally can be seen (eg. JD 89, 92).

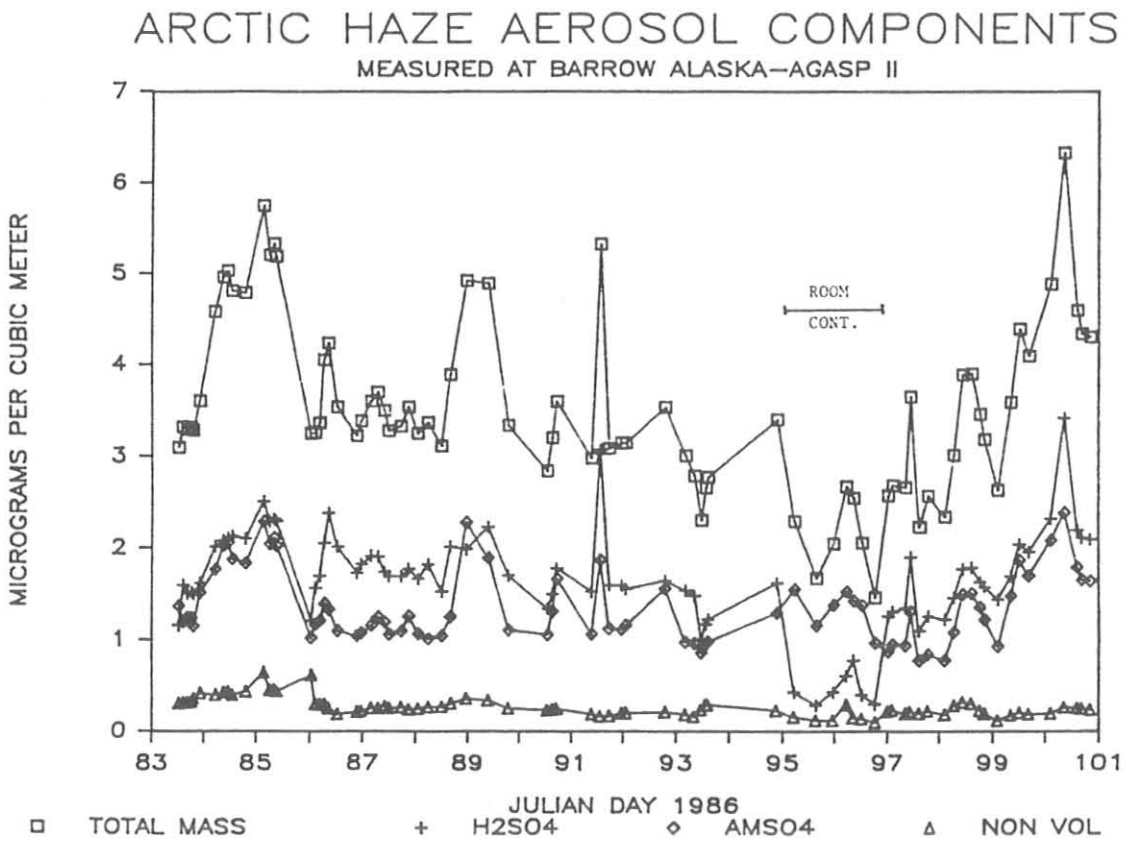

Figure 2.--Arctic haze aerosol from LOPC/TOAD system.

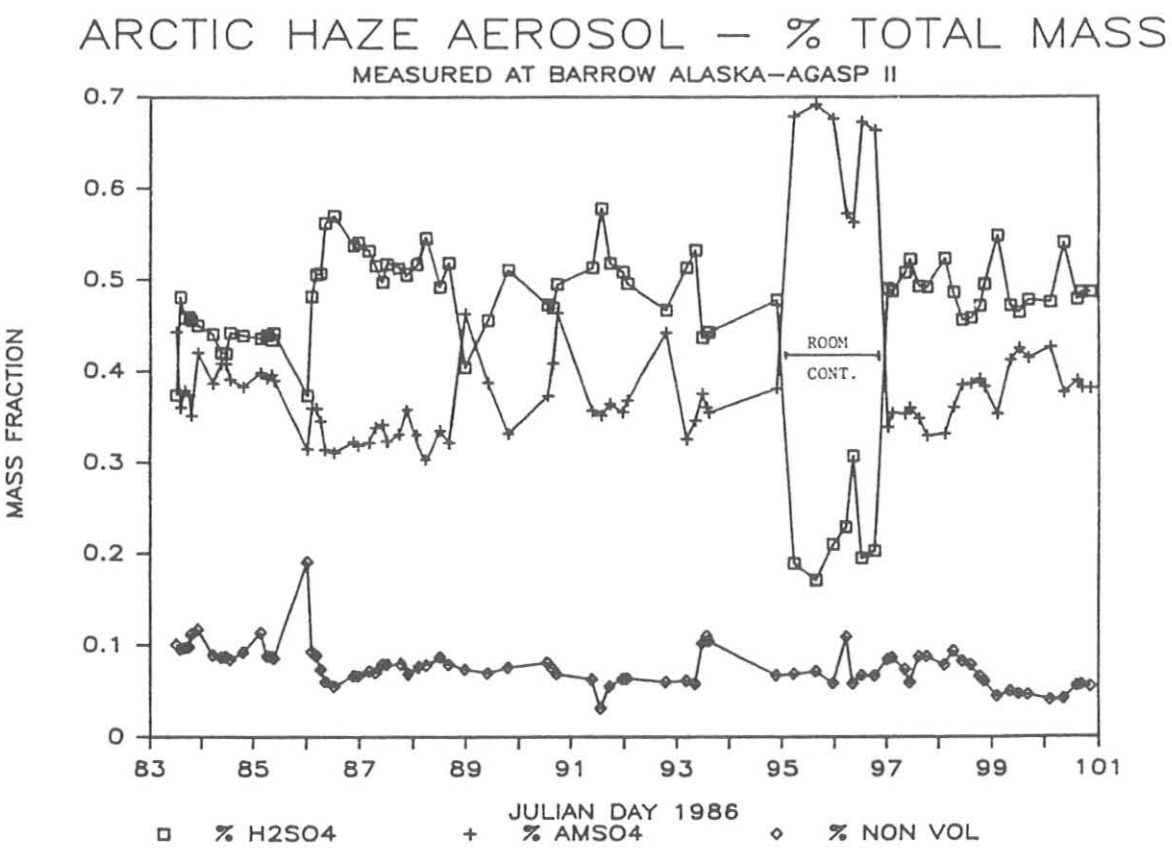

Figure 3.--Mass fractions for aerosol in Figure 1.

The aerosol light absorption coefficient (540 nm) measured on filter samples is plotted in Fig. 4 with the scattering coefficient at 550nm measyred by the NOAA 4- nephelometer. The value of the single scatter albedo (SSA) (x10) derived from them is also shown as nearly constant over the period (exept during possible local pollution) with an average value of 0.86. This is the same mean value observed during our aircraft flights out of Barrow during AGASP I (Clarke, et al., 1984) and supports our earlier contention that this value may be a useful mean for modeling typical Arctic haze optical properties. Figure 5 compares EC concentrations estimated from the light-absorption data (based on a specific absorption for soot of 9.68 m2/g) with the refractory aerosol mass observed by the OPC/TOAD below 0.42 um. Although sample intervals were not always coincident, a remarkable agreement exists between estimates of EC for these entirely different measurement methods. This report presents a limited analysis of a portion of our data collected at Barrow during AGASP II but it illustrates the utility of in-situ thermo-optic analysis. Substantial improvements have since been made in reducing coarse particle losses below 5 um and a more reliable RH controler been added. The curent configuration is optimized for in-situ measurement suitable for future aircraft deployment.

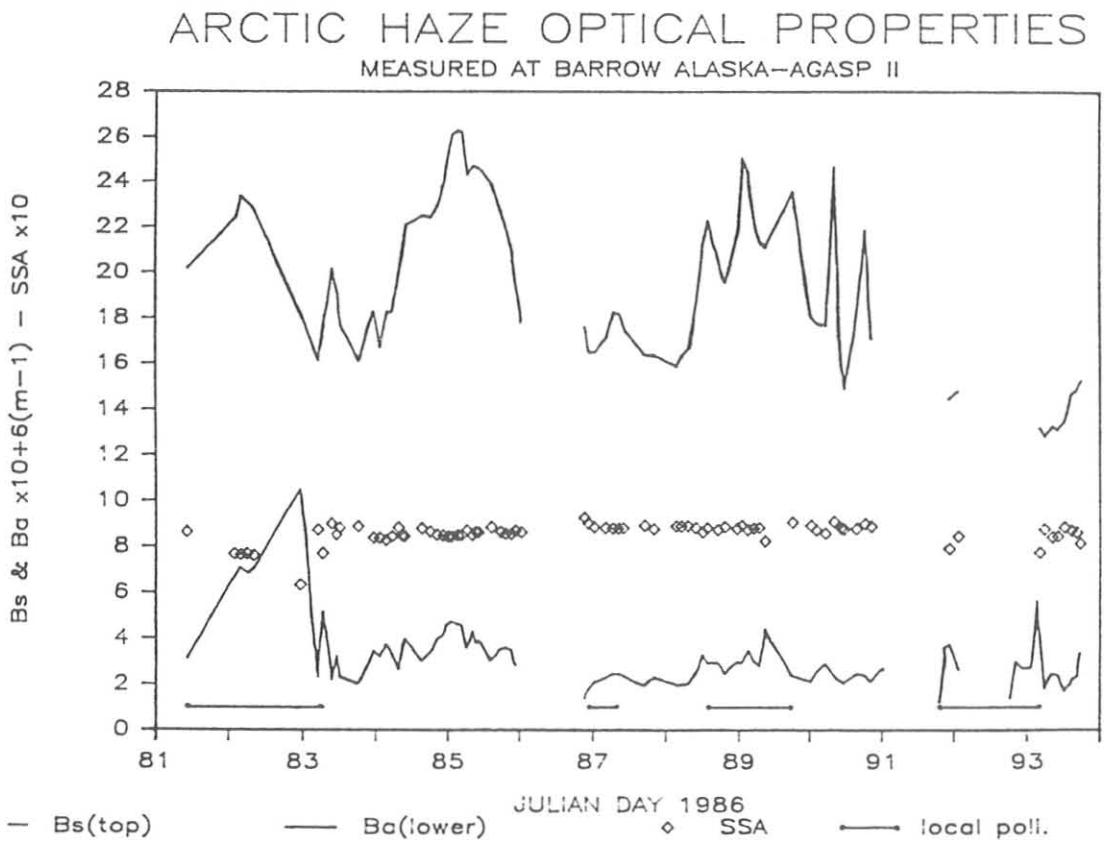

Figure 4.- Scattering and absorption coefficients and single scatter albedo (x10) (see text).

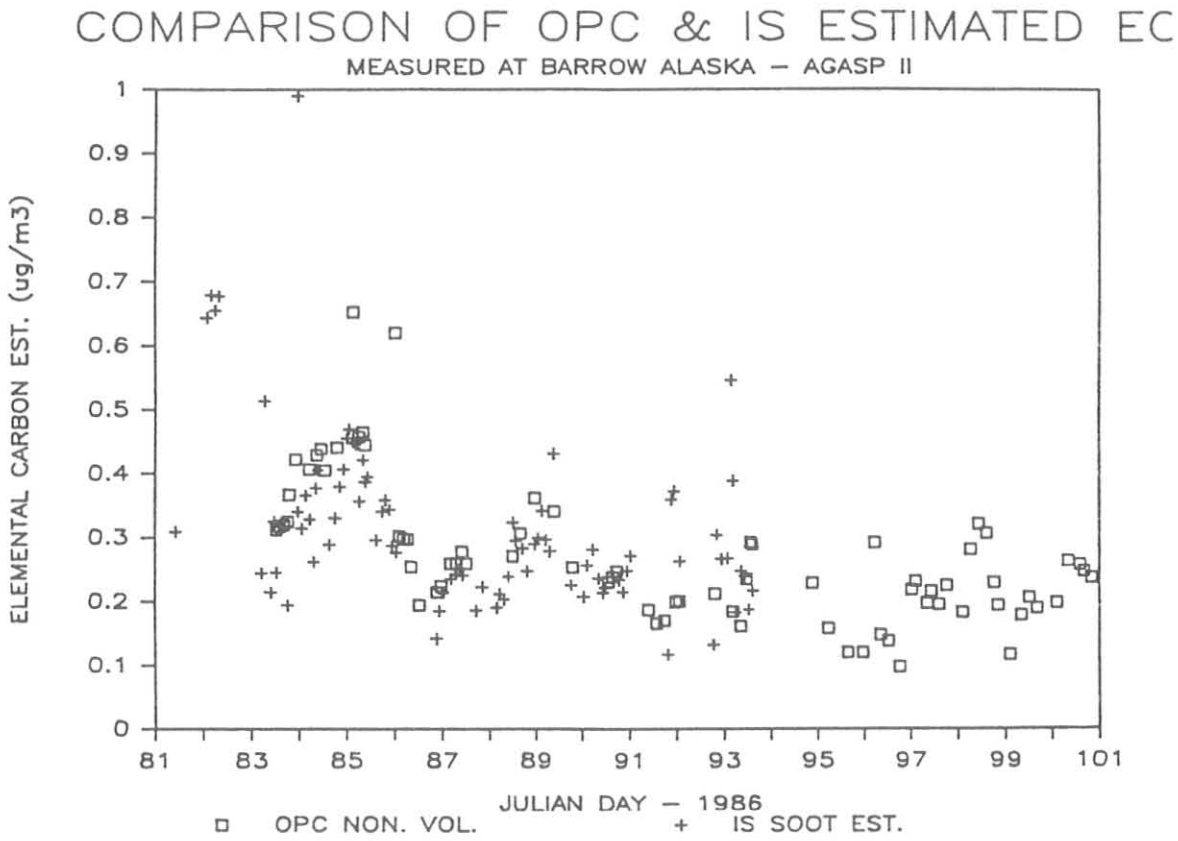

Figure 5. Comparison of estimated EC concentrations from LOPC/TOAD and Integrating Sandwich.

REFERENCES

Clarke, A.D., R.J. Charlson and L.F. Radke, Airborne observations of Arctic aerosol, IV: Optical properties of Arctic haze, Geophysical Research Letters, 5:405-408 (1984)

Garvey, D.M. and R.G. Pinnick, "Response Characteristics of the Particle Measuring Systems Active Scattering Aerosol Spectrometer Aerosol Probe, Aerosl Science and Technology, 2:477-488 (1983)

NITRIC ACID AND AEROSOL NITRATE VARIATIONS AT MAUNA LOA

B. J. Huebert
Graduate School of Oceanography
University of Rhode Island
Narragansett, RI 02882-1197

L. J. Salas
M. A. Baugh
SRI International
333 Ravenswood Ave.
Menlo Park, CA 94025

INTRODUCTION

Much of the NO and NO_2 which is emitted into the atmosphere is converted to nitric acid vapor or aerosol nitrate before it is removed by dry or wet deposition. This conversion to nitrate is largely complete within a few days of the odd-nitrogen's emission, so that in remote areas (such as at the Mauna Loa Observatory) the total nitrate concentration (vapor plus aerosol) represents a fair estimate of the total odd-nitrogen concentration. (It is possible, however, that there may be similar amounts of PAN at high altitudes in clean air, but there are still far too few measurements to say for certain.)

With support from NSF, we measured nitrate concentrations at MLO for several years, to help identify the important sources of odd-nitrogen compounds in remote parts of the globe.

MATERIALS AND METHODS

We use a teflon/nylon filter pack method for collecting atmospheric nitrate. The filter packs are exposed by a sequential sampler during eight-day visits to the site approximately every two months. Filters are returned to the laboratory for extraction and analysis by ion chromatography. Our final data are sorted using three criteria (wind direction, humidity, and CN count) to eliminate those samples which might have been influenced by local sources on the island.

RESULTS AND DISCUSSION

Diurnal Variation

We find a distinct diurnal cycle in nitric acid concentration (see figure), even when we remove the island-influenced samples. Nighttime concentrations are sometimes only half the daytime values. We believe this is the result of the rapid dry-deposition of nitric acid vapor, which is resupplied from the free troposphere more rapidly in the daytime than at night.

Annual Variation

We have observed a sharp maximum in nitric acid and aerosol nitrate concentrations in the late summer (figure). Possible reasons for this peak include reduced loss rates during this time period (which seems unlikely), increased natural sources (such as lightning in the ITCZ, which is closer in summer), and increased transport of anthropogenic material to MLO. One possible anthropogenic source is the North American continent, which is in the general direction from which MLO back trajectories originate.

This is of course a very controversial suggestion, since the MLO is considered to be a pristine sampling site which is largely free of anthropogenic influence. A community-wide discussion has begun as to the origin of the late summer maximum: The best available 10 day back-trajectories do not quite cross the west coast of North America, yet we have found unmistakably anthropogenic material several hundred miles west of California on three separate late summer aircraft sampling programs.

We sincerely hope that this investigation and discussion will lead to improvements in our ability to describe those coastal eddies and diurnal flows which are missed by (relatively coarse) trajectories using input winds from GCM's. The search for an explanation of the maximum is having a stimulating effect on our science.

ONGOING RESEARCH

We are now making measurements both at the surface and on the new tower at MLO, in an attempt to demonstrate whether or not dry deposition is indeed the cause of the observed diurnal variation. We are also continuing our year-round measurements to learn more about the reasons for the observed annual variation. Finally, we are planning to participate in a joint program with numerous other investigators during the spring of 1988 to study the clean troposphere's nitrogen cycle at MLO in much greater detail.

REFERENCES

Galasyn, J.F., K.L Tschudy, and B.J. Huebert, 1987. Seasonal and Diurnal Variability of Nitric Acid Vapor and Ionic Aerosol Species in the Remote Free Troposphere at Mauna Loa, Hawaii. J. Geophys. Res. 92:3105-3113.

Huebert, B.J., J.F. Galasyn, and K.L. Tschudy, in press. Authors' Response to the Comment of Robinson and Harris. J. Geophys. Res.

Robinson, E., and J. Harris, in press. Comment on "Seasonal..." by Galasyn, Tschudy, & Huebert. J. Geophys. Res.

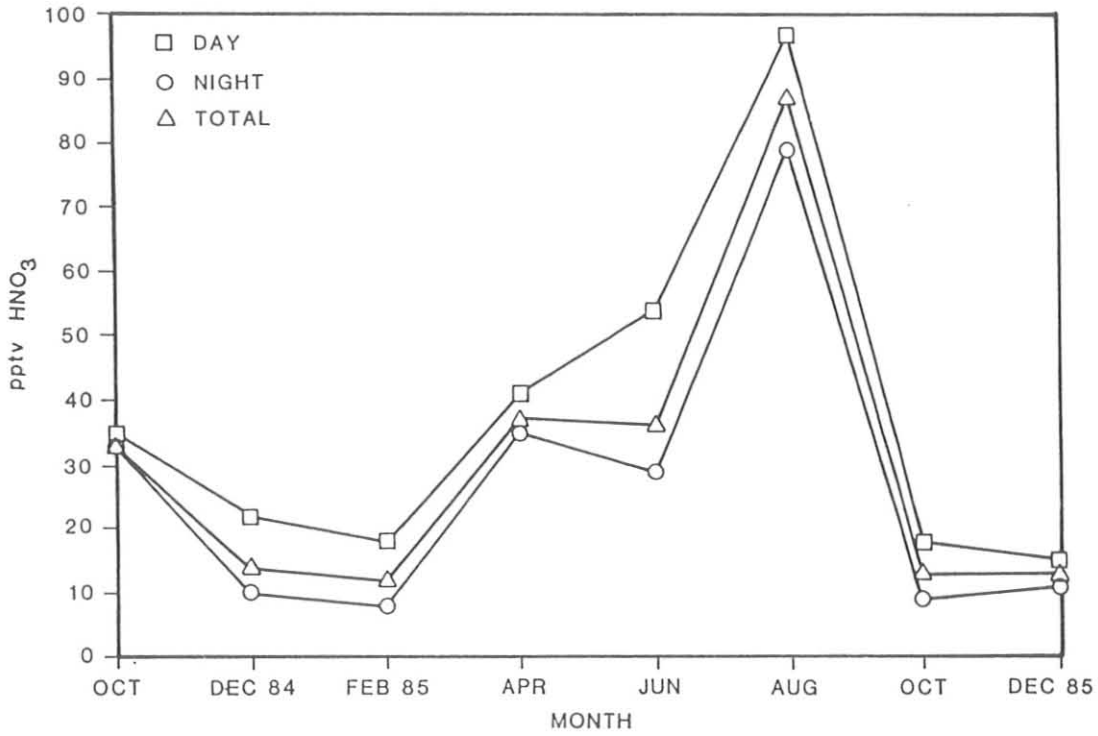

Figure 1.--The diurnal cycle in nitric acid concentration at Mauna Loa.

ATMOSPHERIC BROMINE IN THE POLAR REGIONS

M.A.K.Khalil
R.A.Rasmussen
R.Gunawardena
Institute of Atmospheric Sciences
Oregon Graduate Center, Beaverton, Oregon 97006

INTRODUCTION

In some cases long-lived bromine-containing trace gases can deplete stratospheric ozone more effectively than the chlorofluorocarbons. Furthermore, gases with bromine can act synergistically with chlorine gases to destroy even more ozone than each group would by itself (Wofsy et al., 1975). At present there is very little gaseous bromine in the atmosphere and only a fraction of it is from human activities. However, the levels of the anthropogenic species are increasing. Here we will discuss the concentration of gaseous bromine in the polar regions, specifically at Barrow, Alaska, in the arctic and at the South Pole in the antarctic.

METHODS AND DATA

Air samples collected in stainless steel containers at the two sites were sent to our laboratory for analysis. Samples are collected once a week at Barrow throughout the year and only during the Austral summers at the South Pole. Our data span January 1984 to January 1987 during which time samples were obtained for 29 months from Barrow and 11 months from the South Pole. The samples were analyzed using a Perkin-Elmer gas chromatograph with a capillary column and an electron capture detector. We have described the analytical methods in our earlier paper (Rasmussen & Khalil, 1984).

RESULTS

In all we studied 9 bromine-containing trace gases: $CBrF_3$, $CBrClF_2$, CH_3Br, C_2H_5Br, CH_2BrCl, CH_2Br_2, $CHBr_2Cl$, $C_2H_4Br_2$, and $CHBr_3$. Of these $CBrF_3$ and $CBrClF_2$, which are used in modern fire extinguishers, are probably entirely man-made and their concentrations are increasing at 0.15-0.3 pptv/yr (see Khalil & Rasmussen, 1985). CH_2BrCl, CH_2Br_2, CH_3Br, and $C_2H_4Br_2$ have anthropogenic sources but also have natural origins. Some of these gases are more concentrated in arctic haze, reflecting their anthropogenic origins (Rasmussen & Khalil, 1984). There are indications that CH_3Br and CH_2Br_2 are increasing. The remaining gases probably come from natural sources. Except for $CBrF_3$ and $CBrClF_2$, the concentrations of these gases are quite variable, both from year to year and by seasons.

We calculated the average concentration of each gas between 1/1984 and 1/1987 since in most cases there were no significant trends. For $CBrF_3$ and $CBrClF_2$ we took the average during 1986. These average concentrations are shown in Figure 1. From the data in Figure 1 we estimated the concentration of total bromine in the polar regions both as number of molecules of bromine gases per trillion molecules of air (gas concentration in pptv) and as the number of

bromine atoms per trillion molecules of air (bromine in pptv). The total concentration of bromine-containing gases is only about 17 pptv (or 23 pptv as bromine) at the South Pole and about 42 pptv (or 76 pptv as bromine) in the arctic.

There may be other bromine-containing gases that we have not yet detected, but assuming that their concentrations are small, we calculated the relative abundances of the 9 bromine gases as shown in Figure 2. Methylbromide is more concentrated than any other gas in the Antarctic and second only to bromoform in the arctic. Bromoform is abundant in the arctic and has more bromine atoms per molecule that any other gas. The two fire extinguishing compounds are a greater fraction of the bromine budget in the antarctic (about 20%) than in the arctic (about 9%). This observation is partly a reflection of their long atmospheric lifetimes compared to the other bromine-containing gases, which causes a more even distribution throughout the atmosphere.

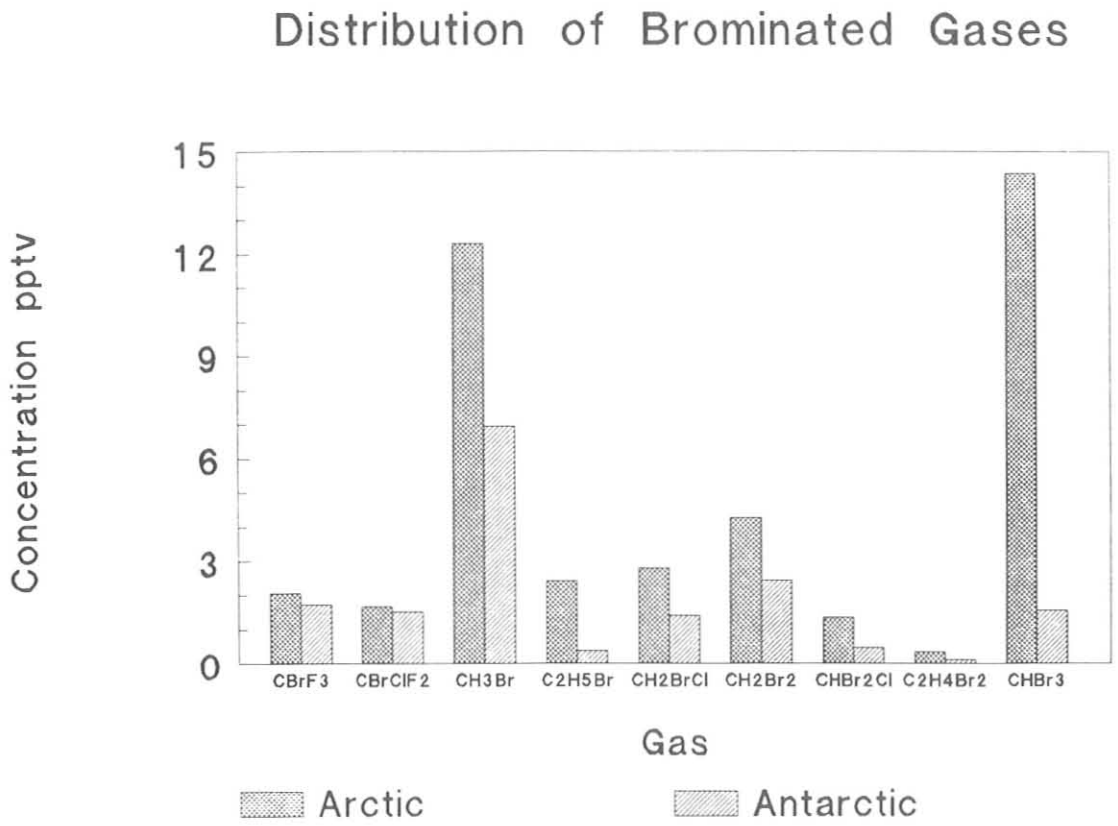

Figure 1.-- The concentrations of bromine-containing trace gases at Barrow, Alaska, and at the South Pole.

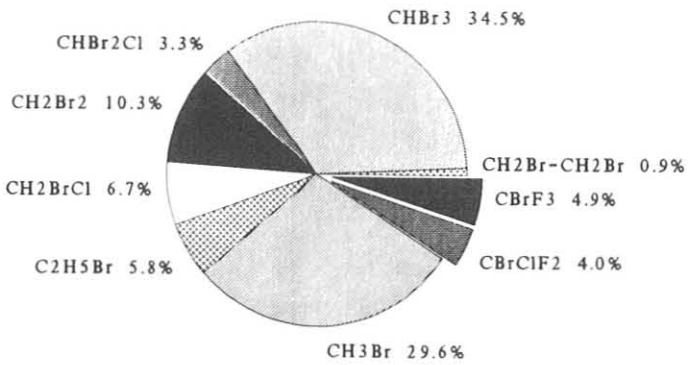

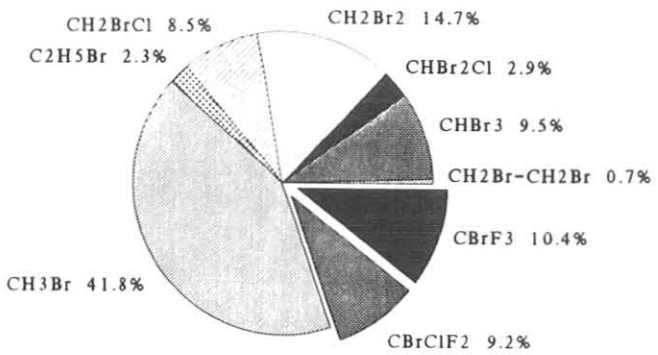

Figure 2.-- The relative abundances in the polar regions expressed as the percent of the total concentration of bromine gases.

REFERENCES

Wofsy, S.C., M.B.McElroy, and Y.L.Yung, 1975. The chemistry of atmospheric bromine. Geophysical Research Letters 2: 215-218.

Rasmussen, R.A., and M.A.K.Khalil, 1984. Gaseous bromine in the arctic and arctic haze. Geophysical Research Letters 11: 433-436.

Khalil, M.A.K., and R.A.Rasmussen, 1985. The trend of bromochlorodifluoromethane and the concentrations of other bromine-containing gases at the south pole. Antarctic Journal of the United States 19:206-207.

SPECTRAL DATA IN THE UVB REGION OF DAYLIGHT FROM THE SOUTH POLE AND MAUNA LOA

Bernard Goldberg
Smithsonian Institution
Washington,D.C. 20560

During the last part of the Austral spring at the South Pole a UVB monitoring unit developed at the Smithsonian Institution was placed in service. The unit started collecting data from late November to mid February The latter data has not as yet arrived from Antarctica. Although there was considerable depletion in the ozone at the pole, by the time the instrument started gathering data the ozone was at normal levels and so was the ultraviolet from 290nm to 325nm.

The data were collected in eight 5nm bands from 290nm to about 325nm at both Mauna Loa and the South Pole. Because the air mass at the South Pole does not vary to any extent during the day and the sun is up for 24 hours,we could calculate the the solar secant at noon for the pole,find the time this occurred at Mauna Loa and use this time to compare data taken simultaneously at these two sites. The data used in the three figures were determined in this way.

The ozone depletion had disappeared by the time these data were obtained. However,in mid to late November,the ozone was at a very high level and declined to a much smaller level in January 1987. The amount of ozone at the South Pole was almost to the values recorded at Mauna Loa. The major data trend shown in figure 1 is due to the change in air mass not changes in ozone. The fluctuations in the data curves are due to variations in ozone,clouds and albedo. The albedo at Mauna Loa is almost zero while the snow field at the pole is very high.

Figure 2 shows the change in the ratio of like bands at the two sites. As stated earlier the high ozone levels in November of 1986 attenuated the 304nm band much more then the 314nm band. Since the ozone at Mauna Loa was fairly constant during the three months under study,the irradiance in both bands at Mauna Loa also remained quite constant. Also from the figure it can clearly be seen that the 314nm band does not track the changes in ozone as well as the shorter wavelength band. To further see how the irradiance varied with ozone at the two sites,the ozone values were multiplied by the air mass used for the day and the values plotted as shown in figure 3. It is readily apparent that the weather was much more constant at Mauna Loa then at the South Pole.

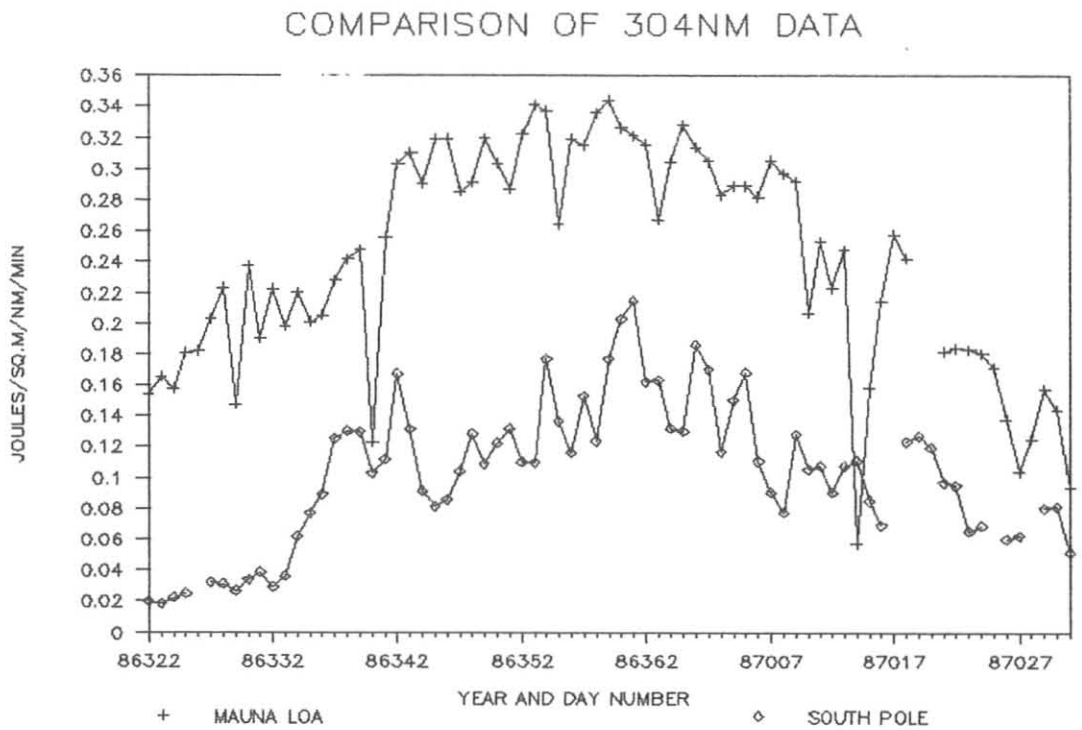

Figure 1.--Measured irradiances at various air masses. The maximum air mass is about 3.1.

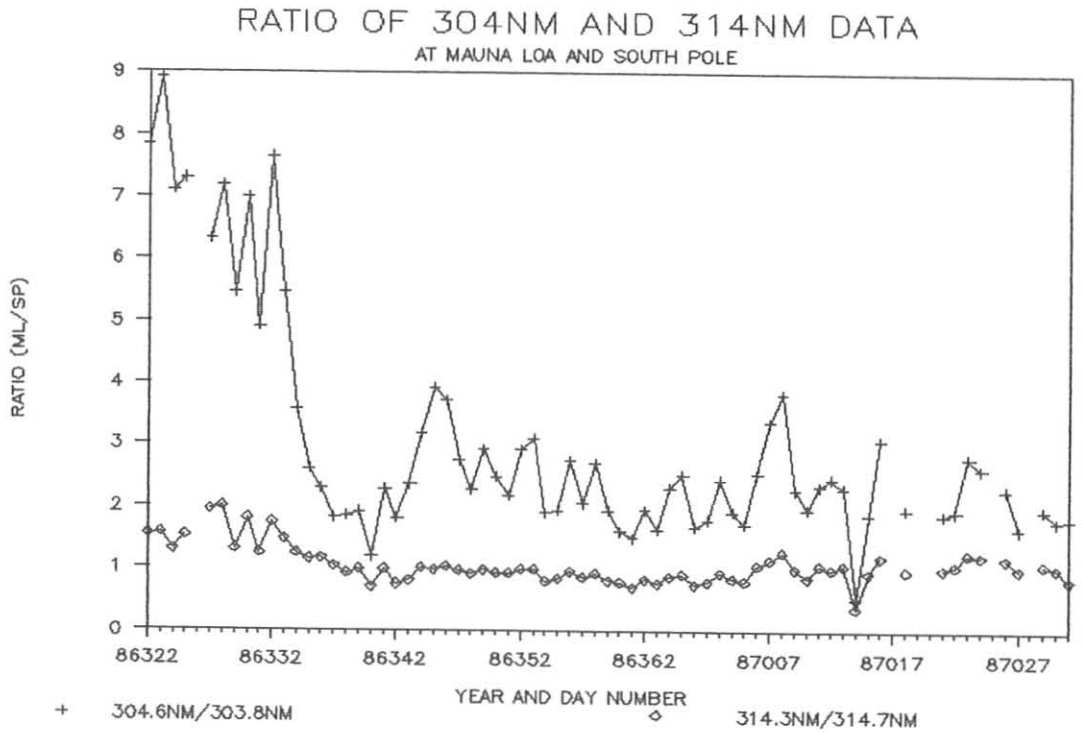

Figure 2.--Ratio of irradiances from Mauna Loa to South Pole. No weather factors were taken into account.

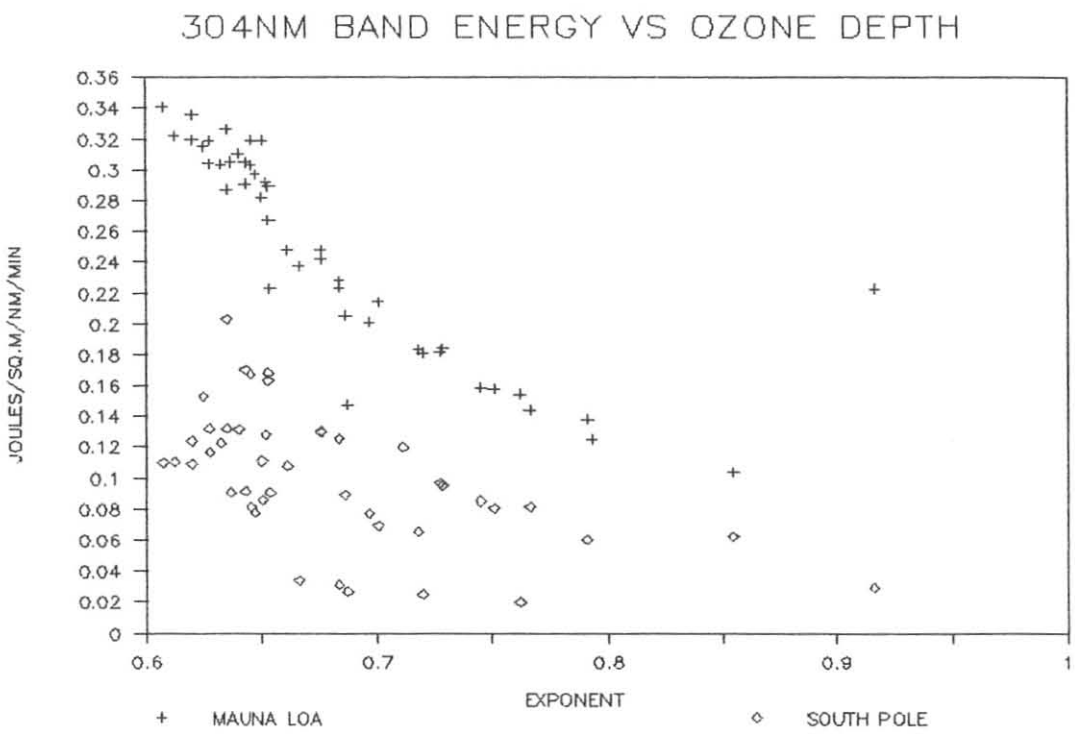

Figure 3.--Irradiance value vs. the exponent term used in normal incidence calculations, exp(O_3*m).

RESOLUTION OF PHYSICAL AND CHEMICAL COMPONENTS OF THE 1982 WINTER AEROSOL AT SOUTH POLE STATION BY FACTOR ANALYSIS

John W. Winchester
Florida State University, Tallahassee, FL 32306-3048;
Visiting Scientist, NOAA GMCC, Boulder, CO 80303

B. A. Bodhaine
GMCC/NOAA Environmental Research Laboratories
Boulder, CO 80303

Bodhaine et al. [1986, 1987] have compared measurements of aerosol extinction coefficients at four wavelengths (σ_{sp}), condensation nucleus (CN) concentration, and the concentrations of aerosol sodium (Na), chlorine (Cl), and sulfur (S) at South Pole Station during calendar year 1982. By trend analysis over the full year and detailed study of correlations among the variables over a 2-mo winter period, August-September, they found correlations that suggest links between the physical properties and chemical composition of aerosol.

Over the year, fluctuations in σ_{sp} were correlated with those in Na and Cl and these three variables rose to highest values in winter. Moreover, in winter the relative σ_{sp} values were skewed to long wavelengths (implying a preponderance of large particles). This observation is supported by calculated air trajectories that indicate frequent winter incursions over the Antarctic continent of coarse aerosol seasalt in which Na and Cl are major constituents. During the two winter months, 8-h mean values of Na concentration were strongly correlated with corresponding σ_{sp} measurements.

Over the year both CN and S generally decreased from highest values in summer to low wintertime values. This observation is consistent with a non-seasalt origin of most of the S, and the parallel seasonal trends of CN and S suggest that non-seasalt S is a fine aerosol constituent most abundant in summer. Except when wintertime seasalt incursions were strong, the ratio Cl/Na tended to be lower than expected from seawater composition, hinting at a volatility loss of HCl from seasalt aerosol by reaction with sulfuric acid (normally a fine aerosol product of the atmospheric oxidation of gaseous SO_2). However, no detailed short-term correlation between variations of S and those of either CN or short wavelength (fine particle) extinction was demonstrated.

These general conclusions, based on correlations and trend analysis, have now been tested statistically by factor analysis of the eight measured variables. The analysis used 166 cases with no missing values of the 61 days of three times daily observations (8-h means) in August-September 1982. A procedure for classical factor analysis with Varimax rotation [Hopke, 1985] contained in the microcomputer package Statgraphics, Version 2.1 [STSC, 1986] was used.

The procedure fits the measured values of the variables to a linear mixing model that computes the composition of each of the factors found and their mixing ratios in the different cases (samples) measured. The

investigator is allowed to decide the number of factors to be retained, always fewer than the number of variables entered into the computation and usually the number needed to account for about 95% of the variance of the data set. In the procedure the variables entered, as well as each of their measured values, are assigned equal weights.

The procedure first transforms each variable by subtracting its mean and dividing by its standard deviation, then computes a matrix of linear correlation coefficients between pairs of variables. The correlation matrix is used to compute an initial set of factors by least squares minimization, followed by an orthogonal "Varimax" rotation of axes to arrive at a new set of factors. The rotation causes each of these to have correlation coefficients ("factor loadings") with each input variable that are either near unity or near zero, rather than intermediate. The investigator can then compare these factors with components he expects to be present in the mixture in an effort to interpret them physically.

In order to test the robustness of the factor analysis, the procedure was applied 15 times to different combinations of the eight measured variables:

N1, N2, N3, N4 - σ_{sp} in 4 nephelometer channels, ordered short to long wavelength (smaller to larger particles)
CN - condensation nucleus concentration by continuous GE counter (fine particles)
Na, Cl, S - element concentrations by PIXE analysis of time sequence filter samples

A selection of the results, expressed as factor loadings (correlation coefficients) with the variables, is presented here.

When all 166 sets of observations of 8 variables are entered into the factor analysis, 4 factors are found with correlations with the variables as shown in table 1. These factors place the σ_{sp} variables together in one (F11), the seasalt in another (F12), CN in a third (F13), and S by itself in a fourth (F14). When just the highest half of the values (cases that include the highest 83 values of N1) are used in the factor analysis, the composition of the four factors is essentially the same, as shown in table 2. CN, Na, and Cl are only weakly correlated with the σ_{sp} factor.

Table 1.--All eight variables, four factors

Variable	F11	F12	F13	F14
N1	.90	.35	.22	.07
N2	.90	.36	.23	.06
N3	.90	.36	.24	.04
N4	.89	.37	.22	.03
CN	.31	.08	.95	-.02
Na	.46	.85	.11	.11
Cl	.56	.75	.06	.22
S	.05	.13	-.01	.99

Table 2.--Highest half (83 cases) of N1 data, all eight variables, four factors

Variable	F21	F22	F23	F24
N1	.93	.28	.11	.13
N2	.94	.30	.09	.14
N3	.94	.30	.04	.14
N4	.92	.32	.02	.13
CN	.21	-.05	-.04	.98
Na	.40	.89	.12	-.01
Cl	.45	.80	.32	-.10
S	.07	.20	.97	-.03

Possibly the redundancy of the four σ_{sp} measurements biases the factor analysis and obscures a significant link to seasalt. Therefore, we can use factor analysis to describe these four variables by two factors, in analogy to conventional treatment of light scattering data by its magnitude and wavelength dependence expressed as the Angstrom coefficient. Table 3 shows that, although one factor (a magnitude) can account for 99.1% of the variance, two factors (F31 and F32) very precisely account for 99.8%. One (F31) is weighted somewhat toward the short wavelength variable N1, whereas the other (F32) is toward the long wavelength N4, being measures of finer and coarser aerosol particles, respectively. The same treatment given to the three element variables, Table 4, clearly separates a seasalt factor (F41) from a non-seasalt S factor (F42).

Table 3.--Only four σ_{sp} variables, two factors. Note: Only one factor can explain 99.1%, but two factors 99.8% of the variance

Variable	F31	F32
N1	.78	.62
N2	.73	.68
N3	.68	.73
N4	.62	.78

Table 4.--Only three element variables, two factors

Variable	F41	F42
Na	.97	.09
Cl	.94	.21
S	.15	.99

Now we can introduce into the factor analysis as σ_{sp} variables the two factors (F31 and F32) that express their essential characteristics, together with the remaining four variables, with results shown in table 5. Seasalt is largely in a factor (F51) that is much more strongly correlated with the coarse σ_{sp} factor (F32). The fine σ_{sp} factor (F31) stands alone (factor F52) without strong correlation with CN or S. Instead, CN and S continue to stand in single factors of their own (F53 and F54). This analysis repeated using a combined Na and Cl factor (F41) as a variable, instead of these two elements separately, gives results nearly the same, as shown in table 5.

Table 5.--Two σ_{sp} factors, CN, and three element variables, four factors

Variable	F51	F52	F53	F54
F31 (fine)	.18	.95	.14	.09
F32 (coarse)	.78	-.41	.36	-.05
CN	.18	.13	.97	-.01
Na	.92	.21	.10	.12
Cl	.89	.30	.09	.20
S	.14	.08	-.01	.99

The independence of CN from the σ_{sp} variables, as well as from S, is a striking feature of all the factor analyses. We can force a test of correlation between CN and the two factors (F31 and F32) that describes the σ_{sp} measurements by performing a factor analysis of these three as variables, without the three element concentrations. The results, shown in table 6, show that CN is about equally (poorly) correlated with each measure of σ_{sp} (F31 and F32); the slightly higher correlation with the fine factor (F31) is probably not significantly better than with the coarse (F32).

Table 6.--Two σ_{sp} factors and CN, two factors

Variable	F61	F62
F31 (fine)	.93	-.09
F32 (coarse)	-.03	.94
CN	.66	.56

We conclude from these results that factor analysis can provide a more sensitive test of the relationship among these several variables than can be achieved by long-term trend analysis or by pairwise correlations between measured variables. The results reaffirm most of the conclusions reached earlier by Bodhaine et al. [1986, 1987], but the independence of measured variance in CN from that in S or in fine σ_{sp} extinction is a new finding.

REFERENCES

Bodhaine B.A., Deluisi J.J., Harris J.M., Houmere P., and Bauman S. (1986). Aerosol measurements at the South Pole. Tellus 38B:223-235.

Bodhaine B.A., Deluisi J.J., Harris J.M., Houmere P., and Bauman S. (1986). PIXE analysis of South Pole aerosol. Nucl. Instrum. Meth. Phys. Res. B22:241-247.

Hopke P.K. (1985). Receptor Modeling in Environmental Chemistry. Wiley, New York, pp. 155-197.

STSC (1986). Statgraphics, Statistical Graphics System by Statistical Graphics Corporation, User's Guide. STSC, Inc., Rockville, MD 20852, USA.

THE GLOBAL PRECIPITATION CHEMISTRY PROJECT

W. C. Keene
J. N. Galloway
Department of Environmental Sciences
University of Virginia, Charlottesville, VA 22903

G. E. Likens
Institute of Ecosystems Studies
Cary Arboretum, Millbrook, NY 12545

J. M. Miller
Air Resources Laboratory
NOAA, Silver Spring, MD 20910

INTRODUCTION

Anthropogenic emissions of SO_2 and NO_x have resulted in widespread acidification of precipitation and subsequent environmental damage in eastern North America and Northern Europe. Of numerous research questions posed by this phenomenon, two are of special interest: (1) What was the composition of precipitation prior to the advent of fossil-fuel combustion; and (2) To what degree does the long-distance transport of sulfur and nitrogen species influence the composition of precipitation in remote regions of the world? The Global Precipitation Chemistry Project (GPCP) was initiated in 1979 to address these questions. Principal objectives are to measure the chemical composition of precipitation in remote areas of the world and to determine major processes controlling measured composition. Earlier reports of the GPCP compare the composition of precipitation in remote and impacted regions (Galloway et al., 1982; 1984), quantify the importance and evaluate sources for organic acids in precipitation (Keene et al., 1983; Keene and Galloway 1984a,b; 1985; 1986), assess the influence of airmass source region on the composition of precipitation at remote locations (Jickells et al., 1982; Church et al., 1982; Galloway and Gaudry, 1984; and Dayan et al., 1985), and present objective methods for differentiating sea-salt and non-sea-salt constituents in marine precipitation and aerosols (Keene et al., 1986). This report summarizes current research and reviews more recent contributions of the project.

MATERIALS AND METHODS

Samples of precipitation are collected by event in scrupulously washed polyethylene containers. Immediately after collection, pH is measured, samples are treated $CHCl_3$ to prevent biological activity and aliquots are subsequently sent to the University of Virginia for analyses for major organic and inorganic chemical constituents. To-date we have analyzed approximately 2035 samples of precipitation collected at 14 land-based sites and during 8 oceanic cruises.

RESULTS AND DISCUSSION

The Chemistry of Precipitation at Katherine, Australia

Wet-only rain samples were collected during 1980-1984 at Katherine, Australia and analyzed for major chemical constituents (Likens et al., 1987). During this period rainfall averaged 104 cm/yr and ranged from 74.6 to 135.7

cm/yr. The volume-weighted concentration of total cations was about 29 ueq/1. The volume-weighted mean H^+ expressed as pH was 4.73 with 64% of the free acidity contributed by formic acid (HCOOH) and acetic acid (CH_3COOH). The pH associated with strong mineral acids only was 5.08. Air-mass trajectories during the wet season (September to April) were predominately from the northeast (51%), and this source region was most important in terms of deposition. Although there is a high frequency of lightning during the wet season, no evidence was found that it contributed significantly to the nitrate concentration in rain. Because concentrations decreased markedly with amount of precipitation, total deposition of dissolved substances was not correlated directly with amount of rain.

Acid Rain: China, United States, and a Remote Area

The composition of precipitation in China is highly influenced by fossil fuel combustion and agricultural and cultural practices (Galloway et al., 1987). Compared to the eastern United States, precipitation in China generally has higher concentrations of sulfate, ammonium, and calcium. Wet deposition rates of sulfur in China are 7 to 130 times higher than those in a remote area of the Southern Hemisphere. In many areas of the world, significant ecological changes have occurred in ecosystems receiving lower rates of acidic deposition than those currently existing in China.

Intercomparison of Measurement Systems for Atmospheric Organic Acids

During June 1986, nine measurement systems for vapor phase, and five for particulate phase, concentrations of HCOOH and CH_3COOH were intercompared in central Virginia. Gases were sampled by condensate, mist, Chromosorb 103 GC resin, NaOH coated annular denuders, NaOH, K_2CO_3 and Na_2CO_3 impregnated quartz and cellulose filters, and nylasorb filters. Particles were sampled on teflon filters by both hi-vol and lo-vol systems. Samples were collected during 31 discrete day and night intervals over a four day period. Measured gaseous HCOOH and CH_3COOH ranged from 13-266 nmol/m^3 and from <22 to 198 nmol/m^3, respectively, with highest concentrations during the day and lowest concentrations during the night. Particulate concentrations were 1-2 orders of magnitude lower than those for vapor phase species. The generation and destruction of organic acids in sampling media subsequent to collection resulted in significant bias between most data sets.

Ongoing Research

Research efforts currently underway within the GPCP include:

- Assessment of airmass back trajectories using cluster analysis and non-parametric statistics to reevaluate processes controlling precipitation composition on Bermuda and on Amsterdam Island.
- Measurement and interpretation of organic acid concentrations in cloudwater.

REFERENCES

Church, T. M., J. N. Galloway, T. D. Jickells, and A. H. Knap, 1982. The chemistry of western Atlantic precipitation at the mid-Atlantic coast and on Bermuda. Journal of Geophysical Research 87: 11013-11018.

Dayan, U., J. M. Miller, W. C. Keene, and J. N. Galloway, 1985. A meteorological analysis of precipitation chemistry from Alaska. Atmospheric Environment 19: 651-657.

Galloway, J. N. and A. Gaudry, 1984. The chemistry of precipitation on Amsterdam Island, Indian Ocean. Atmospheric Environment 18: 2649-2656.

Galloway, J. N., G. E. Likens, and M. E. Hawley, 1984. Acid precipitation: Natural versus anthropogenic components. Science 226: 829-830.

Galloway, J. N., G. E. Likens, W. C. Keene, and J. M. Miller, 1982. The composition of precipitation in remote areas of the world. Journal of Geophysical Research 87: 8771-8786.

Galloway, J. N., D. Zhao, J. Xiong, and G. E. Likens, 1987. Acid rain: China, United States, and remote area. Science 236: 1559-1562.

Jickells, T. C., A. H. Knap, T. M. Church, J. N. Galloway, and J. M. Miller, 1982. Acid precipitation on Bermuda. Nature 297: 55-56.

Keene, W. C., and J. N. Galloway, 1984a. A note on acid rain in an Amazon rainforest. Tellus 36: 137-138.

Keene, W. C. and J. N. Galloway, 1984b. Organic acidity in precipitation of North America. Atmospheric Environment 18: 2491-2497.

Keene, W. C., and J. N. Galloway, 1985. Gran's titrations: Inherent errors in in measuring the acidity of precipitation. Atmospheric Environment 19: 199-202.

Keene, W. C. and J. N. Galloway, 1986. Considerations regarding sources for formic and acetic acids in the troposphere. Journal of Geophysical Research 91: 14,466-14,474.

Keene, W. C., J. N. Galloway and D. H. Holden, Jr., 1983. Measurement of weak organic acidity in precipitation from remote areas of the world. Journal of Geophysical Research 88: 5122-5130.

Keene, W. C., A. A. P. Pszenny, J. N. Galloway and M. E. Hawley, 1986. Sea-salt corrections and interpretation of constituent ratios in marine precipitation. Journal of Geophysical Research 91: 6647-6658.

Keene, W. C., R. W. Talbot, M. O. Andreae, K. Beecher, H. Berresheim, J. C. Farmer, J. N. Galloway, M. R. Hoffman, S.-M. Li, J. R. Maben, J. W. Munger, R. B. Norton, A. A. P. Pszenny, H. Puxbaum, H. Westberg and W. Winiwarter, 1987. An intercomparison of measurement systems for vapor and particulate phase concentrations of formic and acetic acids (unpublished manuscript). 32 pp.

Likens, G. E., W. C. Keene, J. M. Miller and J. N. Galloway, 1987. The chemistry of precipitation from a remote terrestrial site in Australia. Journal of Geophysical Research (in press).

MAUNA LOA AEROSOL BACKSCATTER INTERCOMPARISON EXPERIMENT (MABIE)

David A. Bowdle
Johnson Research Center
University of Alabama/Huntsville, Huntsville, AL 35899

William D. Jones
Guidance, Control, and Optical Systems Division
NASA/Marshall Space Flight Center, Huntsville, AL 35812

Antony D. Clarke
Hawaii Institute of Geophysics
University of Hawaii, Honolulu, HI 96822

Stanley A. Johnson
Chemical Technology Division
Argonne National Laboratories, Argonne, IL 60439

Daniel E. Fitzjarrald
Earth Science and Applications Division
NASA/Marshall Space Flight Center, Huntsville, AL 35812

INTRODUCTION

The Mauna Loa Aerosol Backscatter Intercomparison Experiment (MABIE) was conducted at Mauna Loa Observatory (MLO) on August 1-9, 1986, as part of NASA's GLObal Backscatter Experiment (GLOBE) to develop a global-scale aerosol backscatter data base for the background free troposphere (Bowdle, 1986). MABIE focused on direct backscatter measurements at CO_2 wavelengths. Concurrent GMCC measurements of visible wavelength aerosol scattering coefficients were used to derive empirical scaling relationships between the short and long wavelength aerosol scattering properties, and thereby to incorporate the long-term MLO aerosol climatology (Bodhaine, 1983) into the GLOBE backscatter data base. Measurements of aerosol size distributions, size-segregated aerosol chemistry, and aerosol infrared absorption spectra were also obtained for Mie computations of scattering properties at the various wavelengths. GMCC measurements of surface meteorological quantities and condensation nuclei concentrations were used for airmass classification and contamination screening.

EXPERIMENT DESIGN

MLO was selected for this activity because its nocturnal downslope flow pattern frequently allows extended ground-based sampling of free tropospheric aerosols (Bodhaine, 1983). MABIE took place in mid summer to avoid weather extremes of the winter season, without encountering aerosol concentrations markedly higher than typical winter values. During MABIE, nocturnal sample runs with all instruments lasted from about 2000 to 0800 Local Time.

MABIE instruments sampled from the MLO Camera Building about 50 m W of the main MLO instrument building, well removed from other GMCC facilities. During steady downslope flow, anthropogenic contamination from local upwind sources should not have been significant at this location. However, during light and variable wind conditions, with local stagnation and recirculation,

anthropogenic contamination may have affected MABIE measurements. To avoid local contamination, activity near the equipment shed was minimized.

INSTRUMENTATION

Measurements of aerosol backscatter coefficients were obtained from a focused, monostatic, continuous wave (CW), CO_2 lidar with coherent detection, operating at 10.6 micrometers wavelength (Jones et al, 1983). The lidar had a dual signal processor, with a photometric (volume backscattering) mode for high aerosol concentrations and a single particle backscattering mode for low concentrations. During MABIE, the lidar was directed along the axis of a thin-walled, stainless steel vacuum cleaner extension tube (approximately 1 m long and 3 cm inside diameter), attached to a home vacuum cleaner. The tube was leveled about 1 m above the rough lava surface, 10 m from the lidar, with its axis nearly normal to the prevailing downslope wind. The lidar focal volume was located near the tube midpoint. The nominal axial velocity in the tube was set at about 25 m s^{-1}, well above the 5-10 m s^{-1} ambient values, while still maintaining laminar flow with small velocity variance in the focal volume. The center frequency of the lidar receiver passband was locked to the sample velocity, and the receiver bandwidth was set to encompass the backscatter signal. This simple configuration provided a well-defined sample volume, with negligible sampling losses at the ambient wind speeds encountered during MABIE. To establish a noise floor, the beam was diverted a few deg from the aspirator axis, where it encountered only particles with velocities well outside the passband. The lidar controller automatically cycled between 60 s aerosol samples and 60 s noise samples for several h. System alignment remained stable during these long runs, even in brisk winds.

Concurrent measurements of size-segregated aerosol composition and particle size distributions were obtained with a high-resolution Laser Optical Particle Counter (LOPC) with thermal, relative humidity, and ammoniation preconditioning (Clarke, personal communication). The LOPC data were available in real time. Measurements of aerosol bulk composition and of infrared absorption spectra between 2.5 and 40 micrometers were obtained with an Attenuated Total Reflection (ATR) impactor (Johnson et al, 1983), in conjuction with a Perkin Elmer dispersive infrared spectrophotometer. These measurements were usually available within a few hours after sample collection.

RESULTS

Four nocturnal experiments were conducted during MABIE, with aerosol concentrations near climatological averages on three nights. In addition, the LOPC and ATR operated nearly continuously during most of the experimental period. All of the aerosol instrumentation worked remarkably well. Initial processing of the entire MABIE data set has been completed. Analysis and detailed intercomparison of the individual lidar, ATR, and LOPC data sets is in progress. The results show that measurements of aerosol backscatter coefficients at CO_2 wavelengths can be obtained at MLO with sample times of 1 h or less, even in very clean airmass conditions, as can measurements of size-segregated aerosol composition with the LOPC and measurements of aerosol composition and infrared aerosol absorption spectra with the ATR.

Preliminary analyses from the LOPC and ATR measurements suggest that sulfate compounds dominated background aerosol optical properties at CO_2 wavelengths between 9 and 10 micrometers. In many samples, the sulfate was present as sulfuric acid in the sub-micrometer range, sometimes possibly mixed with ammonium sulfate or ammonium bisulfate. Occasionally, sulfate was also present in micrometer-sized particles. It is possible that the sulfate detected by the LOPC and the ATR may have been partially neutralized before sampling by residual ammonia around the MABIE equipment shed, since both instruments sampled from low stacks (only a few m above the roof of the shed). Additional neutralization could have occurred in some of the ATR samples between the time they were collected and analyzed. Micrometer-sized refractory material, possibly crustal, was apparently present in some of the LOPC data. However, preliminary analysis of the ATR spectra showed no positive indications of crustal silicate absorption bands. Resolution of this discrepancy will require careful comparison of the relative sampling efficiencies of the OPC and the ATR for micrometer-sized crustal particles.

Aerosol concentrations for all downslope flow conditions were low enough for the lidar data to be analyzed in the single particle mode. Particle count rates with the lidar appeared to be consistent with count rates from the OPC.

ACKNOWLEDGEMENTS

We gratefully acknowledge the assistance of the Geophysical Monitoring for Climatic Change program of the National Oceanic and Atmospheric Administration, particularly Bernard Mendonca, Barry Bodhaine, and Elmer Robinson. This work was supported in part by the University of Alabama / Huntsville under NASA contract NAS8-36279.

REFERENCES

Bodhaine, B. A., 1983. Aerosol measurements at four background sites. Journal of Geophysical Research, 88:10,753-10,768.

Bowdle, D. A., 1986. A global-scale model of aerosol backscatter at CO_2 wavelengths for satellite-based lidar sensors. Preprints, Second Conference on Satellite Meteorology / Remote Sensing, Williamsburg, Virginia, May 13-16, 1986. American Meteorological Society, Boston, Massachusetts, 303-306.

Johnson, S. A., R. Kumar, and P. T. Cunningham, 1983: Airborne detection of acidic sulfate aerosol using an ATR impactor. Aerosol Science and Technology, 2:401-405.

Jones, W. D., L. Z. Kennedy, J. W. Bilbro, and H. B. Jeffreys, 1984. Coherent focal volume mapping of a cw CO_2 Doppler lidar. Applied Optics, 23:730-733.

AEROSOL BLACK CARBON MEASUREMENTS AT BARROW, ALASKA, DURING AGASP-II

A.D.A. Hansen and T. Novakov
Applied Science Division, Lawrence Berkeley Laboratory
University of California, Berkeley, CA 94720

B. A. Bodhaine
GMCC/NOAA Environmental Research Laboratories
Boulder, CO 80303

INTRODUCTION

The main global source of energy production is the combustion of solid liquid, or gaseous carbonaceous fuels. This results in the discharge to the atmosphere of the major species carbon dioxide and water vapor and of minor and trace effluents. These latter species include emissions of both gaseous and particulate pollutants that are strongly dependent on the nature of the fuel, the quality of the combustion, and the extent and efficiency of emission controls. One combustion byproduct is graphitic or "black" particulate carbon emitted as aerosol particles of submicron size. This material is a good tracer for combustion emissions: it cannot be produced by secondary mechanisms from precursors in the atmosphere. It can have a long atmospheric lifetime, resulting in its transport to and detection at all parts of the globe.

In winter months, favorable meteorological conditions may transport emissions from certain northern hemisphere regions to all parts of the Arctic Basin. The Arctic haze has been documented for many years at numerous locations in the western hemisphere and appears to contain carbonaceous, silicaceous, and sulfate components, all of which could be related to combustion emissions. The fuel consumption within the region is insufficient to account for the observed concentrations of these species, and therefore long-range transport from intermediate latitudes to the Arctic is indicated.

During March and April, 1986, we installed and operated an aethalometer at the NOAA/GMCC observatory at Barrow, Alaska. This instrument collects the ambient aerosol on a filter and responds in real time to the concentration of particulate black carbon. The data were taken every six minutes and integrated over 1-h periods. The filter in the instrument was changed every day, and the accumulated deposit was analyzed for total black carbon content. These totals represented the 24-h integrals of the real-time data and agreed well with the instrument's calibration.

RESULTS AND DISCUSSION

Hourly mean concentrations of aerosol black carbon and condensation nuclei (CN) are shown in Fig. 1. Carbon concentrations ranged from minima of approximately 50 ng m^{-3} to occasional spikes exceeding 500 ng m^{-3}. The large events that occurred during DOY 89-94 were correlated with winds not from the clean sector and were most likely caused by emissions from vehicle use, space heating, and other burning in the nearby town. These local contamination

events also resulted in excursions in the measurements of other combustion effluents, for example CN (shown in the figure), methane, and carbon dioxide.

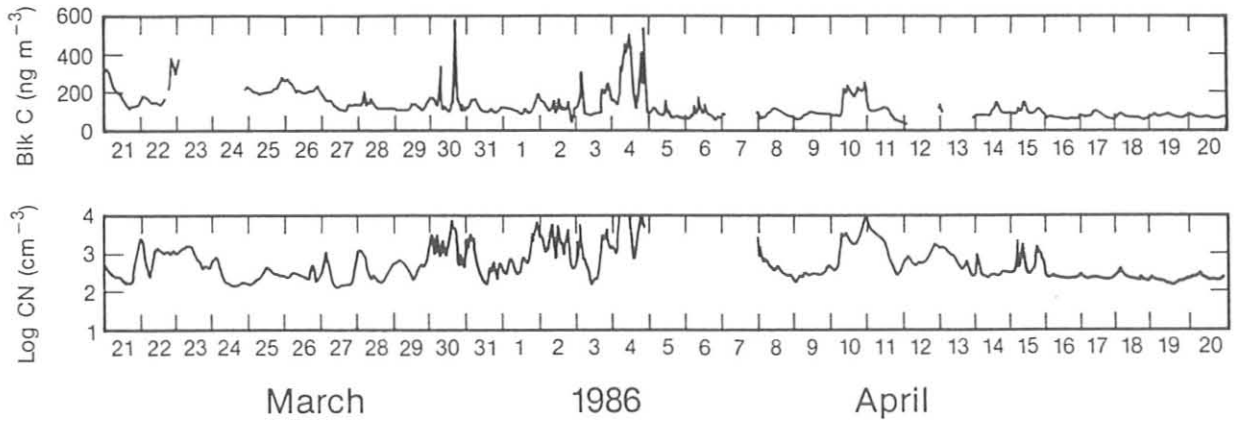

Figure 1.-- Hourly mean (GMT) CN and aerosol carbon concentration at the Barrow GMCC Observatory.

A more interesting type of event takes the form of a smooth fluctuation in aerosol black carbon lasting 1 or 2 days. Such events may be seen clearly during the time period DOY 100-105. It has been found that these events consist of highly correlated variations of the combustion-derived species CO_2, CH_4, and aerosol black carbon, and occur with steady winds blowing from the clean sector. Seven such events were identified during the period of operation of the aethalometer and are characterized by ratios of the increments of these species that are similar to those expected from combustion effluent plumes. A detailed study of these events (Hansen et al., 1988) discusses whether they may represent the passage over the Barrow observatory of compositionally preserved plumes from distant regions of substantial fuel combustion.

The data in Fig. 1 show that the CN and carbon concentrations are strongly correlated, suggesting that carbon is associated with particles in the small or Aitken particle size range. Bodhaine et al. (1988) have shown using diffusion battery data that the event on DOY 100-101 was primarily a small particle event and that the DOY 105 events were composed primarily of large particles. Furthermore, during DOY 89-94, the aerosol particles were primarily in the small size range and were clearly pollution particles produced from local combustion sources.

CONCLUSIONS

Aethalometer measurements during the springtime Arctic haze season of 1986 at Barrow, AK, showed evidence suggesting both local combustion impacts and passage over the station of plumes from distant sources. Aerosol black carbon concentrations for nonlocal source wind directions ranged from 50 to 300 ng m^{-3} and correlated well with other measurements.

Events in the aerosol black carbon data appear better correlated with the CN events than with aerosol scattering extinction events (Bodhaine et al., 1988), suggesting that aerosol black carbon is more likely to be associated with particles in the small particle size range. Diffusion battery data also show that CN and carbon events tend to be small particle events.

These aerosol black carbon data represent the first continuous carbon measurements made at Barrow. Because of the success of this experiment and the demonstration that the aethalometer is a suitable instrument for these measurements, it is hoped to make aethalometer measurements a permanent part of the aerosol monitoring program at Barrow.

REFERENCES

Bodhaine, B A , E. G. Dutton, J. J. DeLuisi G A. Herbert, G. E. Shaw and A. D. A. Hansen, 1988. Surface aerosol measurements at Barrow during AGASP II. J. Atmos. Chem., submitted

Hansen, A. D. A., T. Novakov, B. A. Bodhaine, T. Conway, L. P. Steele, P. Tans, and K. W. Thoning, 1988. The correlation of combustion effluent species in local and distant plume impacts at Barrow, Alaska. J. Atmos. Chem., submitted.

ATMOSPHERIC SUBMICRON PARTICLE COLLECTION AT THE SPO

R. E. Witkowski and W. A. Cassidy
University of Pittsburgh
Pittsburgh, PA 15260

G. W. Penney
Carnegie-Mellon University
Pittsburgh, PA 15213

INTRODUCTION

More than 20,000 hours of operation have been logged on an electrostatic precipitation (ESP) particle collector operating in the clean air sector at the South Pole Observatory (SPO). At the end of the 1986 season (January, 1987), the particle collector was shut down, packaged in a sealed polyethylene bag and returned to the University of Pittsburgh. Our particle collection program at the Clean Air Facility (CAF) has been completed.

The purpose for which we designed this device was to collect delicate submicron-size particles from the atmosphere in an undamaged state and preserve them as individual grains (Cassidy and Witkowski, 1984); the collector fulfilled these requirements.

A few of the particles we collected may be of extraterrestrial origin (Witkowski, et al., 1985). These include single-element or single-compound particles whose simple compositions may represent sublimates generated in the solar nebula or in the stratosphere by condensation of vapor species from volatilized infalling micrometeoroids. Single-particle characterization continues (Witkowski, et al., 1987) via scanning transmission electron microscopy (STEM) coupled with energy dispersive spectrometry (EDS) and selected area electron diffraction (SAED) measurements.

RESULTS AND DISCUSSION

To date, we have identified one particle as extraterrestrial: it contains the elements Mg, Al, Si, Ca, Fe, S(?) and Ni(?) (see Figure 1) in proportions matching the larger chondritic interplanetary dust particles (IDP) that have been collected in the stratosphere by high flying aircraft. Another particle shows a Mg single-element EDS signature. It may be of cosmic origin: Mg is about as abundant as Si and Fe in the solar system. In addition, ionized clouds of Mg have been detected high in the ionosphere (Swenson and Mende, 1985). This, combined with the difficulty of explaining a pure Mg or MgO terrestrial contaminant suggests that this particle is more likely to be extraterrestrial in origin. A collection of very tiny (0.08 μm) agglomerated "fume-type" particles of Al (with a trace of Fe) have also been collected: these also may be of extraterrestrial origin. These particles are not dimensionally similar to the large 10-20 μm aluminum oxide spheres (AOS) produced by solid fuel rocket exhausts; they may be similar to the amorphous products produced experimentally in the laboratory to simulate stellar condensation processes (Nuth and Donn, 1983).

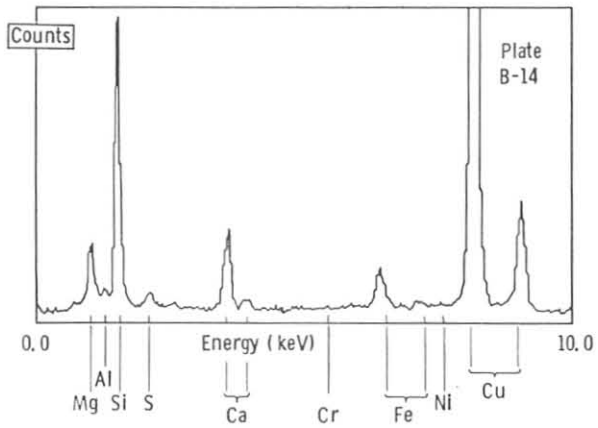

Figure 1.--The energy dispersive spectrometry (EDS) spectrum of a submicron-size particle showing a chondritic elemental signature. The Cu peaks are from the collector sampling grid.

FUTURE PROGRAM

For this ESP collector, any large particles (>5 μm) entering the system would have been trapped in the charging section of the device. A search for these particles will be made; the collector will be disassembled and carefully inspected. If large particles are found, they will be removed and studied; it is felt that Scanning Electron Microscopy (SEM) sampling handling techniques and methods will be adequate for this initial inspection.

ACKNOWLEDGMENTS

This continuing effort is part of the University of Pittsburgh Antarctic Search for Meteorites Project and is made possible through NSF Grant DPP 83 14496. We gratefully acknowledge the assistance of the SPO CAF station staff who maintained this experiment throughout the 1986 winter season.

REFERENCES

Cassidy, W. A., and R. E. Witkowski 1984. Atmospheric submicron particle collection at the South Pole Station, 1983-84. Antarctic Journal of the United States 19 (5):207-209.

Nuth, J. A., and B. Donn 1983. Laboratory studies of the condensation and properties of amorphous silicate smokes. Journal of Geophysical Research Supplement 88:A847-A852.

Swenson, G. R., and S. B. Mende 1985. Ionized Mg clouds in the high ionosphere taken in the ultraviolet (2800 A). EOS 66 (12): Cover Story.

Witkowski, R. E., W. A. Cassidy, and G. W. Penney 1985. Atmospheric submicron particle collection at the South Pole Observatory (Abstract). Meteoritics 20:786.

Witkowski, R. E., W. A. Cassidy, and G. W. Penney 1987. A search for submicron size cosmic dust particles at the South Pole Observatory (unpublished manuscript). 47 pp.

10. INTERNATIONAL ACTIVITIES

The World Lidar Network has been providing stratospheric aerosol profile data to GMCC and to the WODC at Toronto. These data will be permanently archived in the "Redbook" issued by WODC. The data will be used by GMCC to calculate errors to ozone profiles deduced from Umkehr measurements. The organization of the network is spearheaded by GMCC. In 1986 a new lidar site, Aberystwyth College in Wales, was added to the network. The network organization is beginning to be more formal, and a meeting of participants is planned for the XIV International Laser Radar Conference, which will be held 20-24 June 1988, at Innichen-San Candido, Italy.

In May 1986, J. DeLuisi was a student participant in a NATO-sponsored course on physically based modeling and simulation of climate and climate change. The course was given at Erice, Sicily. After completion of the course, DeLuisi met with G. Giocco and F. Congeduti in Rome, Italy, to assess progress with their collaborative work on El Chichon lidar observations, and future activities of the World Lidar Network.

During July-August 1986, 24 flask samples were collected aboard the Mexican research vessel H-02 during a joint U.S.-Mexico cruise in the Gulf of Mexico. These samples were collected in support of the more extensive measurement program of the Environmental Sciences Group of ERL. The samples were analyzed for CO_2 and CH_4 concentration. The results showed background levels of these gases that are consistent with the GMCC flask network, but with some concentrations that tended to be high and variable due to the proximity of local anthropogenic sources.

Flask sample pairs were collected monthly during 1986 at the Japanese Antarctic Research Program site at Syowa Station (69.0°S, 39.6°E). The collection project, conducted in cooperation with T. Nakazawa of the Upper Atmosphere and Space Research Laboratory, Tohoku University, Sendai, Japan, will allow for a comparison of GMCC CO_2 data with the data from Japanese in situ and flask measurement programs at Syowa.

As part of ongoing operations of the CO_2 flask sampling network, cooperative flask sampling continued with Norway (Station M); France (Amsterdam Is.); the United Kingdom (Halley Bay, South Georgia Is.); Canada (Alert, Mould Bay); and Australia (Cape Grim). The cooperative programs with France, Canada, and Australia also include exchanges of data which enable comparisons of flask and in-situ measurements and provide information on the comparability of the CO_2 measurements made by different countries.

A WMO-sponsored CO_2 measurement intercomparison was successfully completed in 1986. Three cylinders containing CO_2-in-air, provided by NBS were analyzed by groups in Canada (IOS, C.S. Wong; AES, N. Trivett); New Zealand (DSIR, M. Manning); Australia (CSIRO, G. Pearman); and the United States (NBS, GMCC). The results were sent to J. Peterson, Director, GMCC, and will be included in a forthcoming WMO report.

In February, P. Steele visited the CSIRO Division of Atmospheric Research for consultation with P. Fraser and other members of the Division on collaborative programs. In April, P. Steele acted as examiner for a Ph.D. thesis submitted to the Australian National University, Canberra, Australia.

W. Komhyr, R. Grass, R. Evans, and K. Leonard participated in the intercomparison of total ozone measuring instruments at Arosa, Switzerland, in August 1986. See Sec. 8. of this report for additional details. This was the laragest intercomparison ever undertaken between total ozone measuring instruments, including Brewer and Dobson spectrophotometers. Participants included both eastern- and western-block scientists from 13 nations.

Cooperative Umkehr observation programs with automated Dobson ozone spectrophotometers continued in 1986 at Observatory Haute Provence, France; Perth, Australia; and Huancayo, Peru.

S. Oltmans visited the DSIR Observatory at Lauder, New Zealand, to install ground tracking and receiving equipment and initiate operation of an ozonesonde program.

As part of a cooperative program with INPE in Natal, Brazil, Dobson ozone instrument No. 93 was revamped and recalibrated.

As a participant in AGASP-II, G. Herbert accompanied the NOAA WP-3D aircraft to Thule, Greenland, during the period 13-16 April 1986. G. Herbert also attended the AGASP-II data workshop held in Fenelon Falls, Ontario, Canada, during September 1986 to discuss meteorological conditions experienced during the six Arctic flights.

The Air Quality Group participated in SAFE from 6-10 May 1986. A portion of the SAFE flights was made along the west coast of Canada. Data collected during SAFE were shared with the Canadian government.

The Air Quality Group also participated in WATOX on the island of Bermuda on 7-13 June 1986. The Bermuda Biological Station was host to the experiment, providing housing and laboratory facilities. In return, the Air Quality Group collected trace chemical species using a special sampler provided by the Bermuda Biological Station.

H. Sievering and M. Luria representated the Air Quality Group at a WATOX data analysis meeting held in Fenelon Falls, Ontario, Canada, during September 1986. Preliminary results from the WATOX study were presented by various researchers.

D. Gillette worked with P. R. Owen of the Imperial College (University of London) on experimentation for dust flux as a function of wind stress. D. Gillette also presented experimental results and interacted in a panel discussion at the 17th Annual Binghamton Geomorphology Symposium, September 1986 at Guelph, Ontario.

Two Soviet scientists, V. Koropolov and V. Yegorov visited Boulder during November 1986 under the U.S.-U.S.S.R. bilateral agreement, Working Group VIII. The purpose of the meeting was to discuss the proposed schedule of the Soviet oceanographic ship Akademic Korolev in the Pacific during spring 1987. GMCC scientists were invited to participate in trace gas measurements in the air and ocean. Koropolov and Yegorov described U.S.S.R. plans to establish a site for long-term monitoring of halocarbons, and learned about

U.S. gas chromatographic techniques for such measurements. They also participated in an ECC ozonesonde launch and in filling standard gas tanks at Niwot Ridge.

J. Peterson attended the First Annual Meeting of the Australian Baseline Monitoring Program held at Aspendale, Australia, 5-7 November 1986. He gave a pesentation on recent highlights of the GMCC program and discussed issues of mutual interest with Australian baseline project leaders.

In March and April, R. Schnell directed the AGASP-II flight program that flew NOAA WP-3D missions covering the Arctic from Alaska to Greenland. From Thule, Greenland, the NOAA WP-3D flew a joint mission with the Canadian National Aeronautical Establishment Twin Otter, upwind and above the Canadian AES baseline station at Alert, NWT.

In September, H. Bridgman and R. Schnell attended WATOX and AGASP-II workshops in Fenelon Falls, Ontario. The AGASP-II workshop was jointly organized by R. Schnell and N. Trivett of AES, and was attended by 40 participants. From the two programs, a total of 60 reviewed publications are in press bearing authorship representing eight countries.

11. PUBLICATIONS AND PRESENTATIONS BY GMCC STAFF, 1986

Boatman, J., and D. Henderson, 1986. Grand Canyon wind study aids in smoke management. Park Sci. 6(4):18-19.

Boatman, J., M. Luria, C. C. Van Valin, and D. L. Wellman, 1986. Continuous atmospheric SO_2 measurements at various altitudes: A comparison between the flame photometric and fluorescence methods. Paper A52-10 presented at the AGU Fall Meeting, 8-12 December 1986, San Francisco, CA. EOS 67(44):903.

Bodhaine, B. A., 1986. The Barrow aerosol record. In Arctic Air Pollution. B. Stonehouse (Ed.), Cambridge University Press, United Kingdom, 159-173.

Bodhaine, B. A., E. G. Dutton, J. J. DeLuisi, G. E. Shaw, and A. D. A. Hansen, 1986. Surface aerosol measurements at Barrow during AGASP-II. Paper A51-03 presented at the AGU Fall Meeting, 8-12 December 1986, San Francisco, CA. EOS 67(44):900.

Bodhaine, B. A., J. J. DeLuisi, J. M. Harris, P. Houmere, and S. Bauman, 1986. Aerosol measurements at the South Pole. Tellus 38:223-235.

Bodhaine, B. A., J. J. DeLuisi, J. M. Harris, P. Houmere, and S. Bauman, 1986. PIXE analysis of South Pole aerosol. Paper presented at the Fourth International Conference on Particle Induced X-ray Emission and Its Analytical Applications, 9-13 June, Tallahassee, FL.

Bodhaine, B. A., J. J. DeLuisi, J. M. Harris, R. A. Castillo, and R. A. Castillo, 1986. Light scattering, condensation nuclei, and air mass trajectories at Whiteface Mountain: Summers of 1983 and 1985. NOAA Data Rep. ERL ARL-8, Air Resources Laboratory, Silver Spring, MD, 82 pp.

Bridgman, H. A., and R. C. Schnell, 1986. Vertical cross sections of condensation nuclei over the Western Atlantic during WATOX January 4-10, 1986. Paper presented at the AGU Fall Meeting, 8-12 December 1986, San Francisco, CA. EOS 67(44):902.

Butler, J. H., and L. I. Gordon, 1986. Hydroxylamine and nitrous oxide in the Cariaco Trench. Invited poster presented at the AGU Fall Meeting, 8-12 December 1986, San Francisco, CA. EOS, 67(44):1067.

Butler, J. H., and L. I. Gordon, 1986. Rates of nitrous oxide production in the oxidation of hydroxylamine by iron (III). Inor. Chem.. 25(25):4573-4577.

Butler, J. H., R. D. Jones, J. E. Pequegnat, and L. I. Gordon, 1986. Cycling of methane and carbon monoxide in a meromictic, coastal lagoon. Paper 041E-04 presented at the AGU Fall Meeting, 8-12 December 8-12 1986, San Francisco, CA. EOS 67(44):1051.

Butler, J.H., and L. I. Gordon, 1986. An improved gas chromatographic method for the measurement of hydroxylamine in marine and fresh waters. Mar. Chem. 19:4573-4577.

Codispoti, L. A., G. E. Friederich, T. T. Packard, H. E. Glover, P. J. Kelly, R. W. Spinrad, R. T. Barber, J. W. Elkins, B. B. Ward, F. Lipschultz, and N. Lostaunau, 1986. High nitrite levels off northern Peru: A signal of instability in the marine denitrification rate. Science 233:1200-1202.

Conway, T. J., and L. P. Steele, 1986. Vertical profiles of CO_2 and CH_4 in the Arctic. Paper A51-09 presented at the AGU Fall Meeting, 8-12 December 1986, San Francisco, CA. EOS 67(44):901.

DeLuisi, J. J., T. DeFoor, and D. Longenecker, 1986. Lidar observations of stratospheric aerosol over Mauna Loa Observatory: 1984-1985. NOAA Data Rep. ERL ARL-9, Air Resources Laboratory, Boulder, CO, 66 pp.

DeLuisi, J. J., E. Dutton, and D. Longenecker, 1986. An analysis of diffuse-direct solar radiation measurement of El Chichon aerosols. Paper presented at AMS Sixth Conference of Atmospheric Radiation, May 13-16, Williamsburg, Virginia.

Dickerson, R. R., G. J. Huffman, W. T. Luke, L. J. Nunnermacker, K. E. Pickering, A. C. D. Leslie, C. G. Lindsey, W. G. N. Slinn, T. J. Kelly, P. H. Daum, A. C. Delany, J. P. Greenberg, P. R. Zimmerman, J. F. Boatman, J. D. Ray, and D. H. Stedman, 1986. Thunderstorms: An important mechanism in the transport of air pollutants., Science 235:460-465.

Dutton, E. G, 1986. Airborne measurements of Arctic aerosol optical thickness during AGASP-II. Paper A51-14 presented at the Fall AGU Meeting, 8-12 December 1986, San Francisco, CA. EOS 67(44):901.

Dutton, E. G., and J. J. DeLuisi, 1986. Cloud information contained in global-sky solar flux measurements at four remote sites. Extended Abstracts, Sixth Conference on Atmospheric Radiation, 13-16 May 1986, Williamsburg, VA. American Meteorological Society, Boston, MA, 149-152.

Elkins, J. W., F. Lipschultz, S. C. Wofsy, M. B. McElroy, L. A. Codispoti, and G. Friederich, 1986. Dissolved N_2O and the appearance of two N_2O minima in Peruvian waters during NITROP-85. Paper 92B-10 presented at the AGU Ocean Sciences Meeting, 13-17 January 1986. EOS, 66(51):1320.

Elkins, J. W., R. L. Sams, and J. Wen, 1986. Temperature dependence on the infrared band strengths and shapes for halocarbons F-11 and F-12. Paper A32C-13 presented at the AGU Spring Meeting, 19-22 May 1986. EOS 67(16):254.

Gammon, R. H., W. D. Komhyr, and J. T. Peterson, 1986. The global atmospheric CO_2 distribution 1968-1983: Interpretations of the results of the NOAA/GMCC measurement program. In The Changing Carbon Cycle A Global Analysis. J. Trabalka and D. Reichle (Eds.), Springer-Verlag, New York, 1-15.

Gillette, D. A., 1986.Wind Erosion. In Soil Conservation Assessing the National Resources Inventory, Committee on Conservation Needs and Opportunities, Board on Agriculture, National Research Council (Ed.), National Academy Press, Washington, DC, 129-158.

Gillette, D. A., and E. O. Box, 1986. Modeling seasonal changes of atmospheric carbon dioxide and carbon 13. J. Geophys. Res. 91:5287-5304.

Gillette, D. A., and P. H. Stockton, 1986. Mass, momentum, and kinetic energy fluxes of saltating particles. In Aeolian Geomorphology. W. G. Nickling (Ed.), Allen and Unwin, Boston, 35-56.

Hansen, A. D. A., B. A. Bodhaine, and T. Novakov, 1986. Ground-level measurements of aerosol black carbon at GMCC-Barrow, Alaska, during the AGASP-II program. Paper A51-18 presented at the AGU Fall Meeting, 8-12 December 1986, San Francisco, CA. EOS 67(44):901.

Herbert, G. A., E. R. Green, G. L. Koening, and K. W. Thaut, 1986. Monitoring instrumentation for the continuous measurement and quality assurance of meteorological observations. NOAA Tech. Memo ERL ARL-148, NOAA Air Resources Laboratories, Boulder, CO, 44 pp.

Herbert, G. A., E. R. Green, J. M. Harris, G. L. Koening, S. J. Roughton, and K. W. Thaut, 1986. Control and monitoring instrumentation for the continuous measurement of atmospheric CO_2 and meteorological variables. J. Atmos. Ocean. Technol. 3(3):414-421.

Herbert, G. A., J. M. Harris, B. A. Bodhaine, and R. C. Schnell, 1986. Meteorological conditions and air mass transport during AGASP-II. Paper A51-02 presented at the AGU Fall Meeting, 8-12 December 1986, San Francisco, CA. EOS 67(44):900.

Hilsenrath, E., W. Attmannspacher, A. Bass, W. Evans, R. Hagemeyer, R. A. Barnes, W. Komhyr, K. Mauersberger, J. Mentall, M. Proffitt, D. Robbins, S. Taylor, A. Torres, and E. Weinstock, 1986. Results from the Balloon Ozone Intercomparison Campaign (BOIC). J. Geophys. Res. 91:13137-13152.

Komhyr, W. D., 1986. Operations handbook -- Ozone measurements to 40-km altitude with model 4A electrochemical concentration cell (ECC) ozonesondes (used with 1680-Mhz radiosondes). NOAA Tech. Memo. ERL ARL-149, NOAA Air Resources Laboratory, Boulder, CO, 49 pp.

Komhyr, W. D., R. D. Grass, and R. K. Leonard, 1986. Total ozone decrease at South Pole, Antarctica, 1964-1985. Geophys. Res. Lett. 13:1248-1251.

Luria, M., C. C. Van Valin, D. L. Wellman, and R. F. Pueschel, 1986. Contribution of Gulf area natural sulfur to the North American sulfur budget. Environ. Sci. Technol. 20:91-95.

Luria, M., C. C. Van Valin, and J. F. Meagher, 1986. Boundary layer transport over the western Atlantic Ocean. Paper A52-13 presented at the AGU Fall Meeting, 8-12 December 1986, San Francisco, CA. EOS 67(44):903.

Oltmans, S. J., 1986. Water vapor profiles for Washington, DC; Palestine, TX; Laramie, WY; and Fairbanks, AK during the period 1974 to 1985. NOAA Data Report ERL ARL-7, NOAA Environmental Research Laboratories, Boulder, CO, 360 pp.

Oltmans, S. J., and W. D. Komhyr, 1986. Surface ozone distributions and variations from 1973-1984 measurements at the NOAA Geophysical Monitoring for Climatic Change baseline observatories. J. Geophys. Res. 91:5229-5239.

Owen, P. R., and D. Gillette, 1986. Wind tunnel constraint on saltation. In Proceedings of International Workshop on the Physics of Blown Sand. B. Willetts (Ed.). Memoirs No. 8, 1985, Department of Theoretical Statistics, Institute of Mathematics, University of Aarhus, 253-269.

Peterson, J. T, W. D. Komhyr, L. S. Waterman, R. H. Gammon, K. W. Thoning, and T. J. Conway, 1986. Atmospheric CO_2 variations at Barrow, Alaska, 1973-1982. Atmos. Chem. 4:491-510.

Porch, W. M., J. E. Penner, and D. A. Gillette, 1986. Parametric study of wind generated super-μm particle effects in large fires. Atmos. Environ. 20:919-929.

Pueschel R. F., C. C. Van Valin, R. A. Castillo, J. J. Kadlecek, and E. Ganor, 1986. Aerosols in polluted vs. non-polluted airmass: Long-range transport and effects on clouds. J. Clim. Appl. Meteorol. 25:1908-1917.

Quakenbush, T. K., and B. A. Bodhaine, 1986. Surface aerosols at the Barrow GMCC observatory: Data from 1976 through 1985. NOAA Data Rep. ERL ARL-10, Air Resources Laboratory, Silver Spring, MD, 230 pp.

Schnell, R. C., 1986. Bacteria ice nuclei, frost, and precipitation: A regulatory wild card. Paper presented at BIOTECH-86, 18-20 November 1986, San Franciso, CA.

Schnell, R. C., 1986. The international Arctic Gas and Aerosol Sampling Program. In Arctic Air Pollution. B. Stonehouse (Ed.), Cambridge University Press, United Kingdom, 135-142.

Schnell, R. C., and R. M. Rosson (Eds.), 1986. Geophysical Monitoring for Climatic Change, No. 14: Summary Report 1986. NOAA Environmental Research Laboratories, Boulder, CO, 146 pp.

Schnell, R. C., W. E. Raatz, and J. T. Peterson, 1986. Arctic Gas and Aerosol Sampling Program (AGASP). Paper presented at the 15th Annual Arctic Workshop, Boulder, 24-26 April 1986, University of Colorado.

Schnell, R. C., and P. J. Sheridan, 1986. Lower stratosphere in-situ airborne gas and aerosol measurements in the Arctic: Spring 1986. Paper presented at the Upper Atmosphere Theory and Data Analysis Program Meeting, 23-27 June 1986, Seattle, WA.

Shapiro, M. A., and R. C. Schnell, 1986. Lower stratosphere in-situ airborne gas and aerosol measurements in the Arctic: Spring 1983. Paper presented at the Upper Atmosphere Theory and Data Analysis Program Meeting, 23-27 June 1986, Seattle, WA.

Sievering, H., 1986. Gradient measurements of sulfur and soil mass dry deposition rates under clean air and high-wind-speed conditions. Atmos. Environ. 20(2):341-345.

Sievering, H., 1986. Sea source aerosol measurements during WATOX: Differences between nearshore and open sea size distributions. Paper A52-11 presented at the AGU Fall Meeing, 8-12 December 1986, San Francisco, CA. EOS 67(44):903.

Stearns, L. P., R. F. Pueschel, D. L. Wellman, 1986. Anthropogenic haze in upstate New York: Impact on the physical and optical state of the atmosphere. Paper presented at the 7th World Clean Air Congress, 24-27 August 1986, Sydney, Australia.

Tiao, G. C., G. C. Reinsel, J. H. Pedrick, G. M. Allenby, C. L. Mateer, A. J. Miller, and J. J. DeLuisi, 1986. A statistical trend analysis of ozonesonde data. J. Geophys. Res. 91:13121-13136.

Van Valin, C. C., M. Luria, H. Berresheim, and M. O. Andreae, 1986. DMS measurements over the western Atlantic Ocean. Paper A52-12 presented at the AGU Fall Meeting, 8-12 December, 1986, San Francisco, CA. EOS 67(44):903.

Weinreb, M. P., L. D. Johnson, P. A. Bridges, M. L. Hill, I. Chang, S. Oltmans, A. Sanyal, and W. A. Morgan, 1986. Balloon-based occultation measurements of stratospheric constituent profiles. Paper presented at American Meteorological Society 2nd Conference on Satellite Remote Sensing and Applications, 13-16 May 1986, Williamsburg, VA.

Wellman, D.L., M. Luria, C. C. Van Valin, and J. F. Boatman, 1986. The use of an airborne air sampling platform for regional air quality studies. Poster presented at the AGU Fall Meeting, 8-12 December 1987, San Francisco, CA. EOS 67(44):885.

12. ACRONYMS AND ABBREVIATIONS

ADN	Automated Dobson Network
AES	Atmospheric Environment Service, Canada
AGASP	Arctic Gas and Aerosol Sampling Program
AH	Arctic haze
ALE	Atmospheric Lifetime Experiment
AOS	Aluminum oxide sphere
ARL	Air Resources Laboratory, Silver Spring, MD (ERL)
ARM	Aerosols and Radiation Monitoring Group, Boulder, CO (GMCC)
ASCS	Alaska Soil Conservation Service
ASR	Aerosols and Solar Radiation
ASRC	Atmospheric Sciences Research Center, Albany, NY
ATS	Applications Technology Satellite
AQG	Air Quality Group, Boulder, CO (GMCC)
BAPMoN	Background Air Pollution Monitoring Network
BAO	Boulder Atmospheric Observatory
BBS	Bulletin Board System
BRAM	battery random access memory
BRW	Barrow Observatory, Barrow, Alaska (GMCC)
BUV	biologically-active ultraviolet
CAF	Clean Air Facility
CAMS	Control and Monitoring System
CFC	chlorofluorcarbon
CFN	Continuous and Flask Network
CIRES	Cooperative Institute for Research in Environmental Sciences, University of Colorado, Boulder, CO
C.L.	confidence level
CMA	Chemical Manufacturers Association
CN	condensation nuclei
CNC	condensation nucleus counter
CSIRO	Commonwealth Scientific and Industrial Research Organization, Australia
CSU	Colorado State University
DEC	Digital Equipment Corporation
DEW	distant early warning
DMS	dimethyl sulfide
DOE	Department of Energy
DSIR	Department of Scientific and Industrial Research, New Zealand
DOY	day of year, Julian
D.U.	Dobson unit
DWR	Daily Weather Report
EC	elemental carbon
EC-GC	electron capture gas chromatography
ECC	electrochemical concentration cell
EDS	Energy Dispersive Spectrometry
EKTO	(A commercial name for a prefabricated building)
EML	Environmental Measurements Laboratory (DOE)
ENSO	El Nino Southern Oscillation
EPA	Environmental Protection Agency
EPOCS	Equatorial Pacific Ocean Climate Studies
ERL	Environmental Research Laboratories, Boulder, CO (NOAA)
ESG	Environmental Sciences Group, Boulder, CO (ERL)
ESP	electrostatic precipitation

FIRE	First ISCCP Regional Experiment
FT	Fourier transform
GC	gas chromatograph
G.E.	General Electric
GMCC	Geophysical Monitoring for Climatic Change, Boulder, CO (ARL)
GMT	Greenwich mean time
GPCP	Global Precipitation Chemistry Project
GSA	General Services Administration
HASL	Health and Safety Laboratory (EPA)
HP	Hewlett-Packard
IBM	International Business Machines
IDP	interplanetary dust particles
INPE	Instituto de Pesquisas Espaciais, Brazil
IOS	Institute of Ocean Sciences, Canada
IPC	International Pyrheliometer Comparison
IR	infrared
ISCCP	International Satellite Cloud Climatology Program
ISWS	Illinois State Water Survey
LBL	Lawrence Berkeley Laboratory (DOE)
LOPC	laser optical particle counter
LST	local standard time
LEAPS	low electron attachment potential species
LORAN	long-range aid to navigation
MLO	Mauna Loa Observatory, Hawaii (GMCC)
MO3	meteorology and ozone (CAMS unit)
MLRA	Major Land Resources Area
MSL	mean sea level
MUSIC	Multiple Species Intercomparison (a software package)
NADP	National Atmospheric Deposition Program
NAPAP	National Acid Precipitation Assessment Program
NASA	National Aeronautics and Space Administration
NBS	National Bureau of Standards
NCAR	National Center for Atmospheric Research, Boulder, CO
NCDC	National Climatic Data Center, Asheville, NC
NESDIS	National Environmental Satellite, Data, and Information Service
NIP	normal incidence pyrheliometer
NMC	National Meteorological Center, Suitland, MD
NOAA	National Oceanic and Atmospheric Administration
NOAH	Nitrous Oxide And Halocarbons Group, Boulder, CO (GMCC)
NRI	National Resource Inventory
NRIP	New River Intercomparison of Pyrheliometers
NSF	National Science Foundation
NWR	Niwot Ridge, CO
NWS	National Weather Service
NWT	Northwest Territories, Canada
NZARP	New Zealand Antarctic Research Program
OGC	Oregon Graduate Center, Beaverton, OR
ppb	parts per billion
ppt	parts per trillion
PC	personal computer
PMEL	Pacific Marine Environmental Laboratory, Seattle, WA (ERL)
PRECP	Processing of Emissions by Clouds and Precipitation Experiment
PROM	programmable read-only memory
PSU	point sample unit

P^3	Portable Pressurizer Pack (air sampler)
RITS	Radiatively Important Trace Species
RL-3	Research Laboratory No. 3, Boulder, CO (GMCC)
SAED	selected area electron diffraction
SAGA	Soviet-American Gas and Aerosol Experiment
SAGE	Stratospheric Aerosol and Gas Experiment
SBUV	solar backscattered ultraviolet (satellite ozone instrument)
SEASPAN	SEAREX South Pacific Aerosol Network
SEAREX	Sea-Air Exchange Program
SEM	scanning electron microscopy
SERI	Solar Energy Research Institute
SIO	Scripps Institution of Oceanography, La Jolla, CA
SMO	Samoa Observatory, American Samoa (GMCC)
SUNYA	State University of New York at Albany
SPO	South Pole Observatory, Antarctica (GMCC)
SRF	Solar Research Facility
SRM	standard reference material
STEM	scanning transmission electron microscopy
TOAD	thermal optic aerosol descriminator
TSI	Thermo Systems Incorporated
URI	University of Rhode Island, Kingston, RI
USDA	United States Department of Agriculture
USGS	United States Geological Survey
UV	ultraviolet
UPS	uninterruptible power supply
WATOX	Western Atlantic Ocean Experiment
WEE	wind erosion equation
WODC	World Ozone Data Center
WMO	World Meteorological Organization, Geneva, Switzerland
ZRAM	"Z" random access memory

☆ U.S. GOVERNMENT PRINTING OFFICE:1988-573-002/80514